

**Disulfide Bond Formation and Methionine Sulfoxide Reduction in  
*Streptococcus gordonii***

by

Naif A. Jalal

Submitted in partial fulfilment of the requirements  
for the degree of Doctor of Philosophy

at

Dalhousie University

Halifax, Nova Scotia

August 2019

© Copyright by Naif A. Jalal, 2019

## Table of Contents

List of Tables .....	vi
List of Figures .....	vii
Abstract .....	ix
List of Abbreviations .....	x
Acknowledgments .....	xii
<b>Chapter 1. Introduction.....</b>	<b>1</b>
<b>1.1 Disulfide Bonds.....</b>	<b>1</b>
<b>1.2 Disulfide Bond Formation in Eukaryotic Cells .....</b>	<b>1</b>
<b>1.3 Disulfide Bond Formation in Bacteria .....</b>	<b>3</b>
<b>1.3.1 Disulfide Bond Formation in Gram-Negative Bacteria .....</b>	<b>4</b>
<b>1.3.1.1 The Oxidation Pathway in <i>E. coli</i> .....</b>	<b>4</b>
<b>1.3.1.2 The Isomerization and Reduction Pathways in <i>E. coli</i> .....</b>	<b>7</b>
1.3.1.2.1 The Isomerization Pathway .....	8
1.3.1.2.2 The Reduction Pathway .....	11
<b>1.3.1.3 Disulfide Bond Formation in Other Gram-Negative Bacteria.....</b>	<b>15</b>
<b>1.3.2 Disulfide Bond Formation in Gram-Positive Bacteria.....</b>	<b>17</b>
<b>1.3.2.1 The Oxidation Pathway .....</b>	<b>18</b>
1.3.2.1.1 Actinobacteria .....	18
1.3.2.1.2 Firmicutes.....	22
1.3.2.1.2.1 <i>Streptococcus gordonii</i> .....	25
1.3.2.1.2.1.1 Disulfide Bond Forming Enzyme in <i>S. gordonii</i> .....	27
1.3.2.1.2.1.2 Other TDORs in <i>S. gordonii</i> .....	30
<b>1.3.2.2 The Reduction Pathway .....</b>	<b>30</b>
<b>1.4 Rationale, Hypothesis, and Objectives of this Study .....</b>	<b>37</b>
<b>Chapter 2. Materials and Methods.....</b>	<b>39</b>
<b>2.1 Bacterial Strains and Growth Conditions.....</b>	<b>39</b>
<b>2.2 Genetic Manipulation of <i>E. coli</i> .....</b>	<b>44</b>
<b>2.2.1 Isolation of Plasmid DNA from <i>E. coli</i> .....</b>	<b>44</b>
<b>2.2.2 Transformation of <i>E. coli</i>.....</b>	<b>44</b>

<b>2.3 Genetic Manipulation of <i>S. gordonii</i></b> .....	<b>45</b>
<b>2.3.1 Isolation of Genomic DNA from <i>S. gordonii</i></b> .....	<b>45</b>
<b>2.3.2 Transformation of <i>S. gordonii</i></b> .....	<b>46</b>
<b>2.3.3 Polymerase Chain Reaction (PCR)</b> .....	<b>46</b>
<b>2.3.4 Construction of Knockout Mutants</b> .....	<b>47</b>
<b>2.3.5 Construction of Complemented Strains</b> .....	<b>47</b>
<b>2.4 Site Directed Mutagenesis</b> .....	<b>53</b>
<b>2.4.1 SdbA</b> .....	<b>53</b>
<b>2.4.2 SdbB</b> .....	<b>54</b>
<b>2.5 Reverse-Transcription PCR</b> .....	<b>54</b>
<b>2.6 Phenotypic Assays</b> .....	<b>55</b>
<b>2.6.1 Extracellular (e)DNA Release</b> .....	<b>55</b>
<b>2.6.2 Bacteriocin Activity</b> .....	<b>56</b>
<b>2.6.3 Genetic Competence</b> .....	<b>56</b>
<b>2.6.4 Autolysis</b> .....	<b>57</b>
<b>2.6.5 Zymographic Analysis</b> .....	<b>57</b>
<b>2.6.6 H<sub>2</sub>O<sub>2</sub> Sensitivity Assay</b> .....	<b>58</b>
<b>2.6.7 Methionine Sulfoxide Sensitivity Assay</b> .....	<b>58</b>
<b>2.6.8 Copper Sensitivity Assay</b> .....	<b>58</b>
<b>2.6.9 Level of MsrAB, SdbB, and Sgo_1177 in Response to Aeration and in         Biofilms</b> .....	<b>59</b>
<b>2.7 SDS-PAGE and Western Immunoblotting</b> .....	<b>59</b>
<b>2.8 Protein Alkylation</b> .....	<b>60</b>
<b>2.8.1 AtIS</b> .....	<b>60</b>
<b>2.8.2 Anti-CR1 scFv</b> .....	<b>61</b>
<b>2.8.3 SdbA</b> .....	<b>62</b>
<b>2.9 DNA Cloning, Protein Expression, and Isolation of Recombinant Proteins</b> ....	<b>62</b>
<b>2.9.1 SdbA, SdbB, Sgo_1177, MsrAB, Trx-2, and TrxB</b> .....	<b>62</b>
<b>2.9.2 CcdA1 and CcdA2</b> .....	<b>63</b>
<b>2.9.3 DsbC</b> .....	<b>64</b>

2.10	Antibody Production and Purification .....	64
2.11	Preparation of Oxidized and Reduced Recombinant Proteins.....	65
2.12	DTNB Assay .....	66
2.13	Enzyme Assays .....	66
2.13.1	Oxidase Assay .....	66
2.13.2	Reductase Assay .....	67
2.13.3	Isomerase Assay .....	68
2.13.4	Methionine Sulfoxide Reductase Assay.....	68
2.14	Enzyme Kinetics.....	69
2.14.1	SdbA .....	69
2.14.2	MsrAB .....	69
2.15	Disulfide Exchange Reactions.....	70
2.16	SdbA-SdbB Complex Formation in <i>S. gordonii</i> and Immunoprecipitation ...	71
2.17	<i>In vitro</i> SdbA-SdbB Complex Formation .....	72
2.18	Sequence Analysis .....	72
2.19	Statistical Analysis .....	73
Chapter 3.	Results .....	74
3.1	Identification and Characterization of Redox Partners of the Thiol- Disulfide Oxidoreductase SdbA in <i>S. gordonii</i> .....	74
3.1.1	Identification and Genetic Organization of SdbA Redox Partners .....	74
3.1.2	Confirmation of the Knockout and Complemented Mutant Strains.....	79
3.1.3	The <i>sdbBccdA2</i> Double-Gene Mutant Exhibits a Pleiotropic Mutant Phenotype Identical to the <i>sdbA</i> Mutant .....	83
3.1.4	AtIS in <i>sdbBccdA2</i> Mutant Lacks Activity and a Disulfide Bond .....	87
3.1.5	SdbB and CcdA2 Possess Oxidase Activities .....	89
3.1.6	SdbA is in a Reduced State in the <i>sdbBccdA2</i> Mutant.....	94
3.1.7	SdbA <sub>C89A</sub> Variant Forms Mixed Disulfide with SdbB <i>In vivo</i> .....	94
3.1.8	SdbBCcdA2 Homologs Exist in Other Gram-Positive Bacteria .....	97
3.1.9	Summary .....	102
3.2	Identification and Characterization of a Reducing Pathway in <i>S. gordonii</i> ...	102

3.2.1 The Genetic Locus of MsrAB in <i>S. gordonii</i> .....	103
3.2.2 MsrAB, SdbB, Sgo_1177, and CcdA Proteins are Involved in Oxidative Stress Resistance.....	105
3.2.3 MsrAB, SdbB, and Sgo_1177 Production are Induced by Aeration .....	108
3.2.4 SdbB and Sgo_1177 are Able to Reduce MsrAB.....	111
3.2.5 Methionine Sulfoxide Reductase Activity of MsrAB with SdbB and Sgo_1177 as Partners .....	114
3.2.6 Summary .....	117
3.3 SdbB is a Putative Disulfide Bond Isomerase in <i>S. gordonii</i> .....	118
3.3.1 SdbB Exhibits Reductase and Isomerase Activities .....	118
3.3.2 SdbBCcdA2 are Required for the Production of Anti-CR1 scFv .....	120
3.3.3 Anti-CR1 is Oxidized and Misfolded in <i>sdbBccdA2</i> Mutant .....	124
3.3.4 SdbB and CcdA2 are Involved in Copper Resistance in <i>S. gordonii</i> .....	126
3.3.5 Summary .....	126
3.4 Preliminary Investigations of Structure and Function of SdbA.....	128
3.4.1 Role of the Active-Site Cysteines in SdbA-SdbB Interaction .....	128
3.4.2 Role of Surface-Exposed Amino Acid Residues in SdbA Enzyme Kinetics .....	131
3.4.3 Role of Surface-Exposed Amino Acid Residues in SdbA-SdbB Interaction .....	137
Chapter 4. Discussion .....	139
4.1 Oxidative Protein-Folding Pathway in <i>S. gordonii</i> .....	139
4.2 The Reducing Pathway in <i>S. gordonii</i> .....	143
4.3 Disulfide Bond Isomerization Pathway in <i>S. gordonii</i> .....	148
4.4 Structural Determinants of SdbA Protein and Evidence of SdbA-SdbB Interaction Through their Active Site Cysteines.....	151
4.5 General Conclusion.....	155
4.6 Future Direction .....	157
Reference .....	160
Appendix: Copyright Release for Published Material.....	177

## List of Tables

Table 1.1 TDORs in other Gram-negative bacteria.....	16
Table 2.1 Bacterial strains and plasmids used in this study .....	40
Table 2.2 PCR conditions .....	48
Table 2.3 Primers used in this study.....	49
Table 3.1 Kinetic parameters of parent SdbA and SdbA point mutants.....	136

## List of Figures

Figure 1.1 The DsbA/DsbB disulfide bond formation pathway in <i>E. coli</i> . .....	6
Figure 1.2 The DsbC/DsbD disulfide bond isomerization pathway in <i>E. coli</i> . .....	10
Figure 1.3 The reducing pathway in <i>E. coli</i> . .....	12
Figure 1.4 Disulfide bond formation pathways in <i>Mycobacterium</i> and <i>Actinomyces</i> . .....	20
Figure 1.5 Disulfide bond formation in <i>Bacillus</i> and <i>Staphylococcus</i> . .....	23
Figure 1.6 Disulfide bond formation in <i>S. gordonii</i> . .....	28
Figure 1.7 The reducing pathways in Gram-positive bacteria. ....	32
Figure 3.1 Genetic organization and amino acid sequences analysis for redox partners of SdbA in <i>S. gordonii</i> . .....	76
Figure 3.2 Reverse Transcription (RT)-PCR analysis of <i>sgo_1177ccdA1</i> and <i>sdbBccdA2</i> operons in <i>S. gordonii</i> . .....	78
Figure 3.3 PCR and RT-PCR confirmation of <i>ccdA</i> mutants. ....	80
Figure 3.4 Immunoblot analysis of SdbB, Sgo_1177, and MsrAB in the parent, knock-out mutant, and complemented mutant strains. ....	81
Figure 3.5 Immunoblot analysis of SdbB, Sgo_1177, and MsrAB in the parent and <i>ccdA</i> mutant strains. ....	82
Figure 3.6 Phenotypic analysis of single- and double-gene mutants of <i>S. gordonii</i> . .....	84
Figure 3.7 RT-PCR confirmation of <i>sdbBccdA1</i> and <i>sdbBccdA2</i> mutants. ....	86
Figure 3.8 The major autolysin AtlS is inactive in the <i>sdbBccdA2</i> and <i>sdbBccdA2degP</i> mutants. ....	88
Figure 3.9 The major autolysin AtlS lacks a disulfide bond in the <i>sdbBccdA2</i> and <i>sdbBccdA2degP</i> mutants. ....	90
Figure 3.10 SdbB and CcdA2 exhibit oxidase activity. ....	92
Figure 3.11 Oxidation of SdbA by oxidized SdbB or CcdA2. ....	93
Figure 3.12 The redox state of SdbA in <i>S. gordonii</i> parent and mutant strains. ....	95
Figure 3.13 SdbB forms a disulfide-linked complex with SdbA <sub>C89A</sub> in <i>S. gordonii</i> . .....	98
Figure 3.14 SdbBCcdA2 and Sgo_1177CcdA1 homologs are present in other Gram- positive bacteria that possess SdbA homolog. ....	99

Figure 3.15 Sequence alignment of <i>S. gordonii</i> MsrA, MsrAB, and <i>S. pneumoniae</i> MsrAB2. ....	104
Figure 3.16 Sensitivity to H <sub>2</sub> O <sub>2</sub> and methionine sulfoxide by <i>S. gordonii</i> .....	106
Figure 3.17 Immunoblot analysis of the level of MsrAB, SdbB, and Sgo_1177 in <i>S. gordonii</i> .....	109
Figure 3.18 Disulfide exchange between MsrAB, SdbB, Sgo_1177, CcdA1, and CcdA2. ....	112
Figure 3.19 Enzymatic activities of MsrAB. ....	115
Figure 3.20 SdbB exhibits isomerase activity. ....	119
Figure 3.21 SdbB and CcdA2 are required for the production of anti-CR1 scFv protein in <i>S. gordonii</i> . ....	122
Figure 3.22 SdbB and CcdA2 are required for the proper folding of anti-CR1 scFv in <i>S. gordonii</i> . ....	125
Figure 3.23 Growth of <i>S. gordonii</i> strains in the presence of CuSO <sub>4</sub> .....	127
Figure 3.24 Reactivity of SdbB cysteines with DTNB. ....	129
Figure 3.25 SdbA-SdbB complex formation. ....	130
Figure 3.26 Crystal structure and sequence alignment of SdbA and ResA.....	132
Figure 3.27 Oxidation of parent SdbA and SdbA variants by SdbB. ....	138
Figure 4.1 A proposed model for oxidative protein-folding pathway in <i>S. gordonii</i> . ....	144
Figure 4.2 A proposed model for the reducing pathway in <i>S. gordonii</i> . ....	149
Figure 4.3 A proposed model for the disulfide bond isomerase pathway in <i>S. gordonii</i> .....	152
Figure 4.4 A proposed model for SdbA reoxidation by SdbB. ....	154
Figure 4.5 A proposed model for the oxidation, reduction, and isomerization pathways in <i>S. gordonii</i> . ....	156



## Abstract

Disulfide bonds are important for proper folding and activity of extracytoplasmic proteins. These bonds are formed, reduced, and isomerized by thiol-disulfide oxidoreductases (TDORs). TDORs also catalyze the reduction of methionine sulfoxide to repair oxidatively damaged proteins. A TDOR, named SdbA, which catalyzes disulfide bonds in *Streptococcus gordonii*, was previously identified. The objectives of this study were to identify the redox partners of SdbA, characterize the methionine sulfoxide reduction pathway, and identify the disulfide bond isomerization pathway in *S. gordonii*.

Using mutational, phenotypic, and biochemical approaches, SdbB and CcdA2 were identified as the redox partners of SdbA. *sdbBccdA2* mutants recapitulated the *sdbA* mutant phenotype and produced inactive AtIS, the natural substrate of SdbA, which lacked a disulfide bond. SdbA was found in a reduced state in the *sdbBccdA2* mutant. In *S. gordonii*, SdbB formed a disulfide-linked complex with SdbA. Using SdbA and SdbB active site variants, we showed that SdbA-SdbB interacts through their N-terminal cysteines.

MsrAB was identified as a key enzyme in the methionine sulfoxide reduction pathway with SdbB and another TDOR, Sgo\_1177, as immediate redox partners and two membrane proteins, CcdA1 and CcdA2, as downstream partners. The CcdA proteins likely played a role in relaying electrons from the cytoplasm to the pathway. In the cells, MsrAB, SdbB, Sgo\_1177, CcdA1, and CcdA2, are needed for protection against oxidative stress.

Lastly, SdbB was identified as a potential disulfide bond isomerase with CcdA2 as its redox partner. Both SdbB and CcdA2 are required for the stability and production of a protein with two disulfide bonds and protection against copper stress in *S. gordonii*.

In conclusion, this study advances the understanding of disulfide bond formation and methionine sulfoxide reduction in Gram-positive bacteria. This study gives the first example of a complex oxidative protein-folding pathway in Gram-positive bacteria that consists of an enzyme that uses multiple redox partners to function. It also provides an insight into the extracytoplasmic methionine sulfoxide reduction pathway in *S. gordonii*. Finally, to the best of my knowledge, this study presents the first evidence that Gram-positive bacteria have a disulfide bond isomerization pathway.

## List of Abbreviations

BHI	Brain heart infusion
CcdA	Cytochrome <i>c</i> biogenesis protein A
CSP	Competence-stimulating peptide
cCMP	Cytidine 2':3'-cyclic monophosphate monosodium salt
DEAE	Diethylaminoethyl
DEPC	Diethyl pyrocarbonate
DPC	N-dodecylphosphocholine
Dsb	Disulfide bond
DTNB	5,5'-dithio-bis(2-nitrobenzoic acid)
DTT	Dithiothreitol
eDNA	Extracellular DNA
EDTA	Ethylenediaminetetraacetic acid
FMN	Flavin mononucleotide
HEPES	4-(2-hydroxyethyl)-1-piperazineethanesulfonic acid
IPTG	Isopropyl $\beta$ -D-1-thiogalactopyranoside
LB	Luria-Bertani
Mal	Maleimide
Met	Methionine
MetO	Methionine sulfoxide
MOPS	3-(N-morpholino) propanesulfonic acid
Msr	Methionine sulfoxide reductase
NADP <sup>+</sup>	Nicotinamide adenine dinucleotide phosphate
NADPH	Reduced form of NADP <sup>+</sup>
PBS	Phosphate buffered saline
PBST	Phosphate buffered saline Tween 20
PCR	Polymerase chain reaction
PDI	Protein disulfide isomerase

PEG	Polyethylene glycol
rdRNase A	Reduced and denaturated RNase A
RNase A	Ribonuclease A
ROS	Reactive oxygen species
RT-PCR	Reverse transcription PCR
scFv	Single chain variable fragment
SdbA	<i>Streptococcus</i> disulfide bond protein A
SdbB	<i>Streptococcus</i> disulfide bond protein B
SDS	Sodium dodecyl sulfate
sRNase A	Scrambled RNase A
TAE	Tris-acetate and EDTA
TCA	Trichloroacetic acid
TDOR	Thiol-disulfide oxidoreductase
TE	Tris-EDTA
Tris	Tris (hydroxymethyl) aminomethane
Trx	Thioredoxins
TrxR	Thioredoxin reductase
VKOR	Vitamin K epoxide reductase

## Acknowledgments

First, I would like to express my deep respect and sincere gratitude to my supervisor and mentor Dr. Song Lee for his continuous support, patience, and motivation throughout the different phases of this work. His help and encouragement were, indeed, the main support to me throughout this work. A very special sincere thanks to my committee members: Dr. Nikhil Thomas, Dr. John Rodhe, and Dr. Neale Ridgeway for their great advice and valuable feedback. I am very grateful to Dr. Scott Halperin for his advice and feedback throughout this work. Thank you to our collaborators, Dr. Alexi Shevchenko, and Peter Stogios. Very special gratitude goes to my external examiner Dr. Hung Ton-That (University of California). A special thanks to my external advisor Dr. Jason Leblanc. I would also like to thank all the current and past members of Dr. Lee's lab for their support with a special thanks to Lauren Davey for her valuable remarks and advice throughout this work.

Also, I would like to express my greatest appreciation to my sponsor, The Ministry of Higher Education represented by the Saudi Cultural Bureau in Canada and Umm Al-Qura University in Saudi Arabia, for giving me the opportunity to continue my postgraduate study. Many thanks also to my friends in Umm Al-Qura University, Department of Medical Microbiology, for their support, cooperation, and encouragement. A special thanks to the Natural Sciences and Engineering Research Council of Canada (NSERC) for funding this work.

Lastly, I would like to give special thanks to my lovely parents, my parents-in-law, my brother, and my sister in Saudi Arabia for their support and encouragement. A very special sincere thanks to my soulmate, Abrar Alem, who had to live with this work from the beginning, for her support, encouragement, love, and patience. Finally, I would like to give special thanks and love to my children (Yusof, Ayah, Ibrahim, and Israa) for making my life important.

## **Chapter 1. Introduction**

### **1.1 Disulfide Bonds**

Proper protein folding is essential for functions and crucial for all living organisms (Hatahet and Ruddock, 2009; Landeta *et al.*, 2018). Both prokaryotic and eukaryotic cells use a group of enzymes named thiol-disulfide oxidoreductases (TDOR) to catalyze the formation, reduction, and isomerization of disulfide bonds (Hatahet and Ruddock, 2009; Landeta *et al.*, 2018).

In bacteria, disulfide bond formation takes place in the periplasmic space or the cell envelope (Davey *et al.*, 2016b; Landeta *et al.*, 2018), while in eukaryotic cells, oxidative protein folding occurs in the endoplasmic reticulum (Hatahet and Ruddock, 2009). The exception to the above is in some thermophilic archaea where disulfide bonds can be formed in the cytoplasm (Mallick *et al.*, 2002). These intracellular disulfide bonds are thought to help in protein-stabilization in these thermophilic archaea to assist their survival in the harsh environment (Beeby *et al.*, 2005).

The cytoplasm in both bacteria and eukaryotes is a reducing environment. Cells maintain this reducing environment using two major anti-oxidant systems, the glutathione and the thioredoxin anti-oxidant system (Fernandes and Holmgren, 2004; Lu and Holmgren, 2014). This reducing environment is important for cells to protect their proteins and other macromolecules against oxidative stress and assist in several cellular processes such as DNA synthesis and DNA repair (Sengupta and Holmgren, 2014).

Below, the current understanding of disulfide bond formation, reduction, and isomerization are discussed.

### **1.2 Disulfide Bond Formation in Eukaryotic Cells**

In 1963, Anfinsen and colleagues reported the first disulfide bond formation catalyst, named protein disulfide isomerase (PDI), in a microsomal component of rat liver

(Goldberger *et al.*, 1963). Since then, multiple studies indicate that oxidative protein folding takes place in several compartments, including the endoplasmic reticulum (ER) (Ohba *et al.*, 1977), the mitochondrial intermembrane space (i.e., IMS) (Mesecke *et al.*, 2005), and plant chloroplasts (Feng *et al.*, 2011).

In the ER, PDI is the primary TDOR that catalyzes disulfide bond formation and isomerization. PDI is a thioredoxin family protein consist of 4 domains (a, b, b', and a'), a highly acidic C-terminal extension “c” (possesses ER retention sequence KDEL), and an x-linker sequence between the b' and a' domains (Alanen *et al.*, 2003; Darby *et al.*, 1996). PDI has two catalytic active CGHC sites, one in the “a” domain and the other in the “a'” domain (Darby and Creighton, 1995). Interestingly, the a and a' domains each possesses oxidase activity similar to the whole PDI, but the two domains have very low isomerase activity (Darby and Creighton, 1995).

*In vivo*, PDI occurs as a mixture of oxidized and reduced forms (Appenzeller-Herzog and Ellgaard, 2008). Oxidized PDI catalyzes disulfide bond formation in nascent polypeptides in the ER lumen. The initial reaction is the formation of a mixed disulfide bond between the active site of PDI and the reduced substrate. The substrate then folds into a “near-native” state, followed by the resolution of the mixed disulfide leading to the formation of a disulfide bond in the substrate (Kosuri *et al.*, 2012). In contrast, disulfide isomerization requires PDI in a reduced form. The results from experiments using active site cysteine point mutants suggest two possible mechanisms for disulfide isomerization (Walker *et al.*, 1996; Walker and Gilbert, 1997). The first mechanism involves the N-terminal cysteine in the active site of PDI attacking the substrate disulfide bond. This is followed by an intramolecular rearrangement of the disulfide bond within the substrate itself. The second mechanism involves the completed reduction of the substrate, followed by the reoxidation of the substrate by the mixed reduced/oxidized PDI (Walker *et al.*, 1996; Walker and Gilbert, 1997).

To maintain a portion of PDI in an oxidized state, PDI needs to be recharged after oxidation of the substrates. Ero1, an integral membrane flavoprotein, is the main redox partner of PDI *in vivo* (Mezghrani *et al.*, 2001). During the reoxidation of PDI, electrons are transferred from PDI to Ero1 via disulfide exchange reactions. Ero1 utilizes O<sub>2</sub> as the

final electron acceptor to oxidize its active site in a reaction that generates  $H_2O_2$  as a by-product (Gross *et al.*, 2006).  $H_2O_2$  produced by Ero1 can be utilized by peroxiredoxin 4 (Prx4) and glutathione peroxidases 7 and 8 (GPx7/8) to reoxidize PDI (Wang *et al.*, 2014; Zito *et al.*, 2010). In addition, oxidized glutathione and vitamin K epoxide reductase (VKOR) can reoxidize PDI by direct interaction with its active site cysteines (Lappi and Ruddock, 2011; Rutkevich and Williams, 2012).

In addition to the ER, oxidative protein folding takes place in the mitochondrial intermembrane space (i.e., IMS). In IMS, Mia40 is the TDOR involved in disulfide bond formation (Mesecke *et al.*, 2005). Mia40 is a non-thioredoxin TDOR that contains a hydrophobic substrate binding groove and a CPC active site motif (Banci *et al.*, 2009). Once it introduces a disulfide bond into the substrate, Mia40 transfers electrons to its redox partner Erv1 (Rissler *et al.*, 2005). Erv1 shuttles electrons directly into the respiratory chain by reducing cytochrome *c*, and thus avoids the production of  $H_2O_2$  (Bihlmaier *et al.*, 2007). Similar to PDI, Mia40 has both oxidase and isomerase activity; however, the isomerase activity of Mia40 is restricted to its natural substrates. For example, when scrambled RNase A was used as a substrate, Mia40 showed minimal isomerase activity, but when Mia40 natural substrate Cox17 (a mitochondrial copper-binding protein with 2 disulfide bonds) was used, Mia40 was able to rescue scrambled (mis-disulfide bonded) Cox17 (Hudson and Thorpe, 2015; Koch and Schmid, 2014).

### **1.3 Disulfide Bond Formation in Bacteria**

Bacteria also use TDOR to accelerate the process of protein folding. However, TDOR in bacteria are more diverse, possibly due to the differences in the structure of the bacterial cell envelope where oxidative protein folding occurs (Davey *et al.*, 2016b; Landeta *et al.*, 2018). In both Gram-negative and Gram-positive bacteria, disulfide bond forming systems are important for cell physiology and virulence. In addition, disulfide bond forming systems play essential role in biotechnology by enhancing recombinant protein production (Heras *et al.*, 2009; Kouwen and van Dijl, 2009a). Therefore, understanding the TDOR systems in bacteria has the potential to allow the development

of new anti-virulence agents or enhance recombinant protein production (Kouwen and van Dijk, 2009a; Smith *et al.*, 2016).

### 1.3.1 Disulfide Bond Formation in Gram-Negative Bacteria

Disulfide bond formation in Gram-negative bacteria occurs in the periplasmic space. In this compartment, enzymes involved in disulfide bond formation, reduction, and isomerization cooperate to allow proper folding of the newly translocated proteins (Landeta *et al.*, 2018). Among these enzymes, the *Escherichia coli* Dsb system is the best-characterized.

#### 1.3.1.1 The Oxidation Pathway in *E. coli*

DsbA was the first disulfide bond-forming enzyme discovered in bacteria. In 1991, Jon Beckwith's laboratory described DsbA as a periplasmic protein with a C<sub>30</sub>P<sub>31</sub>H<sub>32</sub>C<sub>33</sub> motif that catalyzes disulfide bond formation in *E. coli* (Bardwell *et al.*, 1991). Two years later, a membrane protein DsbB was identified as the DsbA redox partner (Bardwell *et al.*, 1993).

DsbA is a 21-kDa, monomeric oxidase, with a redox potential of -120 mV (Kadokura *et al.*, 2003). In the periplasm of *E. coli*, DsbA exists in an oxidized state and the reduced state can only be detected in the *dsbB* mutant (Kishigami *et al.*, 1995a). The structure of DsbA shows the presence of a thioredoxin fold containing the active site C<sub>30</sub>P<sub>31</sub>H<sub>32</sub>C<sub>33</sub> motif with an  $\alpha$ -helical domain that occurs at the middle of the thioredoxin fold. In addition, the structure shows a hydrophobic groove flanking the active site of the enzyme and a conserved *cis* proline<sub>151</sub> residue in a loop at the end of a long helix, which links the  $\alpha$ -helical domain and the thioredoxin domain (Martin *et al.*, 1993; Schirra *et al.*, 1998). The N-terminal C<sub>30</sub> of the active site has a low pK<sub>a</sub> value of 3.5, and therefore, it will be in a thiolate anion state (RS<sup>-</sup>) under physiological conditions. This makes the oxidized form of DsbA less stable and more reactive than the reduced form (Nelson and Creighton, 1994).



*E. coli* produces more than 300 periplasmic proteins that contain at least two cysteines and thus are potential substrates of the DsbAB system (Kadokura and Beckwith, 2010). Since the discovery of the DsbAB system, more than 30 periplasmic proteins have been identified as natural substrates of this system. *dsbAB* mutants displayed pleiotropic phenotypes (Depuydt *et al.*, 2011). For example, inactivation of *dsbA* or *dsbB* resulted in a non-motile phenotype due to a defect in flagellar assembly. This defect was due to the inability to form a disulfide bond in the flagellar P-ring motor protein FlgI (Dailey and Berg, 1993). Many of the DsbA substrates were identified using the *cis* P<sub>151</sub> point mutant. P<sub>151</sub>T point mutant slowed down the resolution of DsbA-substrate, which caused accumulation of DsbA-substrate complexes in the cell that can be detected. Interestingly, only the P<sub>151</sub>T mutation resulted in the accumulation of DsbA-substrate complexes. Other proline point mutations, such as proline to serine or histidine, resulted in accumulation of DsbA-DsbB complex (Kadokura *et al.*, 2004; Kadokura *et al.*, 2005).

The crystal structure of DsbA in complex with a peptide derived from its natural substrate, the autotransporter protein SigA, sheds light on how DsbA interacts with its substrate. The structure shows that the substrate interacts with surface residues at the interface between the  $\alpha$ -helical domain and the thioredoxin domain of DsbA. These residues include V<sub>150</sub> and R<sub>148</sub> that are located within the *cis* P<sub>151</sub> loop and P<sub>31</sub>, H<sub>32</sub>, and Q<sub>35</sub> (Paxman *et al.*, 2009).

The interaction between DsbA and its substrate is initiated by the attack of the first cysteine of the substrate to C<sub>30</sub> of the oxidized DsbA. This results in the formation of a mixed disulfide between the substrate and DsbA. Next, the second cysteine of the substrate attacks the first cysteine of the substrate. The result is the generation of a disulfide-bonded substrate and the release of DsbA, which is now in a reduced form (Figure 1.1) (Depuydt *et al.*, 2011; Kadokura and Beckwith, 2009).

To perform another round of reaction, the reduced DsbA needs to be reoxidized, and this is achieved by donating electrons to its redox-partner DsbB, which then transfers the electrons to the electron transport chain (Depuydt *et al.*, 2011). DsbB is a 20-kDa cytoplasmic membrane protein with four-transmembrane  $\alpha$ -helices, and two periplasmic loops each contains a redox active site, namely C<sub>41</sub>XXC<sub>44</sub> and C<sub>104</sub>-C<sub>130</sub>, respectively.

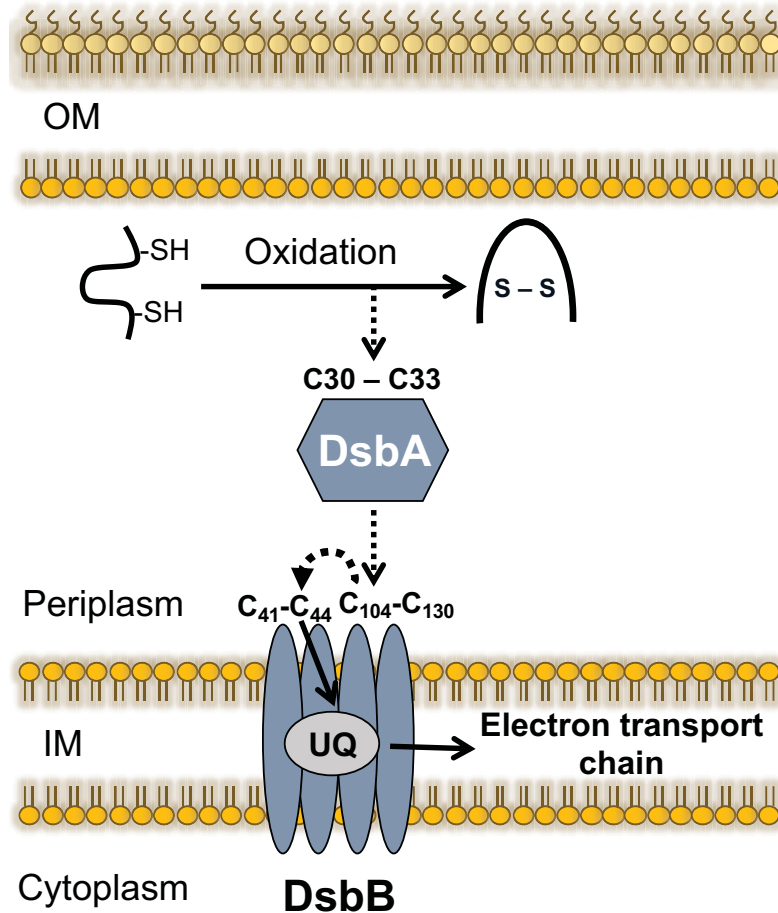


**Figure 1.1 The DsbA/DsbB disulfide bond formation pathway in *E. coli*.**

DsbA is a periplasmic oxidase that forms disulfide bonds in substrate proteins using its active site (C<sub>30</sub>P<sub>31</sub>H<sub>32</sub>C<sub>33</sub>). Following substrate oxidation, DsbA is reoxidized by the membrane protein DsbB. DsbB then transfers the electrons to the electron transport chain. Arrows indicate the flow of electrons; IM: inner membrane; OM: outer membrane; UQ: ubiquinones. Adapted from Landeta *et al.* (2018) and Inaba *et al.* (2006).

DsbB also possesses a quinone-binding site located in a groove between transmembrane helices 1 and 4 and close to the  $C_{41}XXC_{44}$  active site (Bader *et al.*, 1999). Interestingly, the crystal structure of the DsbA-DsbB complex showed that DsbB binds to the hydrophobic groove of DsbA, which is different from the substrate binding site (Inaba *et al.*, 2006).

Structural studies of DsbB and DsbB-DsbA complex proposed a mechanism of how DsbB reoxidizes DsbA. Briefly,  $C_{30}$  of the reduced DsbA attacks  $C_{104}$  of the  $C_{104}$ - $C_{130}$  disulfide bond of DsbB (Kishigami *et al.*, 1995b; Zhou *et al.*, 2008). This results in a mixed disulfide complex between DsbA and DsbB. This is followed by a rapid disulfide rearrangement within the DsbB, in which DsbB  $C_{130}$  attacks  $C_{41}$ , which is disulfide bonded to  $C_{44}$ . This results in the formation of  $C_{130}$ - $C_{41}$  disulfide bond. This disulfide rearrangement within the DsbB prevents the backward resolution of the DsbA $C_{30}$ -DsbB $C_{104}$  complex. Finally,  $C_{33}$  of DsbA attacks the DsbA $C_{30}$ -DsbB $C_{104}$  disulfide bond. This results in the release of DsbA, which is now reoxidized (Figure 1.1) (Inaba *et al.*, 2006; Zhou *et al.*, 2008).

DsbB is regenerated by transferring two electrons to a quinone. Under aerobic conditions, DsbB transfers electrons to ubiquinone, which will then transfer the electrons to the respiratory chain via cytochromes and ultimately to oxygen as the final electron acceptor. Under anaerobic conditions, DsbB reduces menaquinone and uses alternative electron acceptors, such as fumarate or nitrate reductase (Figure 1.1) (Bader *et al.*, 1999).

### **1.3.1.2 The Isomerization and Reduction Pathways in *E. coli***

DsbA is a powerful oxidant and it introduces disulfide bonds indiscriminately, resulting in non-native disulfide bonds in substrates that have more than two cysteines. This occurs because DsbA can bind to its substrate during protein translocation across the membrane. Consequently, disulfide bonds will be formed in the substrate as cysteines appear sequentially, resulting in non-native disulfide bonds (Kadokura and Beckwith, 2009).

In addition, H<sub>2</sub>O<sub>2</sub> and other reactive oxygen species (ROS) can react with proteins, causing damage (Ezraty *et al.*, 2017). Specifically, cysteine and methionine are susceptible to oxidation by ROS. In the case of cysteine, the thiol (-SH) is oxidized to highly reactive sulfenic acid (-SOH). Sulfenic acid can react with another cysteine residue to form a native or non-native disulfide bond (Ezraty *et al.*, 2017). ROS can also oxidize the sulfur atom in methionine giving methionine sulfoxide (MetO), which if it is not repaired, can lead to protein inactivation and degradation. Oxidation of methionine results in two diastereomeric forms of MetO, Met-*R*-O, and Met-*S*-O. MetO can be further oxidized to the irreversible methionine sulfone (Met-O<sub>2</sub>) (Cho and Collet, 2013; Ezraty *et al.*, 2005a).

To correct the non-native disulfide bonds, *E. coli* possesses a disulfide bond isomerization system that consists of DsbC and DsbD, where DsbC functions as an isomerase and DsbD as a redox partner (Denoncin and Collet, 2013). In addition, the periplasmic reductases (DsbG and CcmG) and the methionine sulfoxide reductase (Msr) protect cysteine and methionine residues from oxidation, respectively (Cho and Collet, 2013).

### 1.3.1.2.1 The Isomerization Pathway

DsbC is also a periplasmic TDOR involved in disulfide bond formation (Missiakas *et al.*, 1994; Shevchik *et al.*, 1994). It is a 23-kDa protein with a C<sub>98</sub>G<sub>99</sub>Y<sub>100</sub>C<sub>101</sub> active site and a thioredoxin domain (Zapun *et al.*, 1995). The protein forms a V-shaped homodimer. The crystal structure of DsbC shows that the thioredoxin domains are linked through hinged linker  $\alpha$ -helices to an N-terminal dimerization domain (McCarthy *et al.*, 2000). This dimerization is essential for DsbC isomerization activity. DsbC mutants that failed to form dimers were oxidized by DsbB. These DsbC monomers will act as an oxidase and can complement *dsbA* mutation (Bader *et al.*, 2001).

In the cell, the active site of DsbC is maintained in the reduced state, which is needed for the interaction with mis-disulfide bonded proteins. *In vivo*, DsbC is reduced by DsbD, which receives electrons from the cytoplasmic thioredoxin (Joly and Swartz, 1997;

Rietsch *et al.*, 1997). Two mechanisms have been proposed for the isomerase activity of DsbC (Kadokura and Beckwith, 2010). In both mechanisms, C<sub>98</sub> of the reduced DsbC attacks the incorrect disulfide bond in the substrate. This results in a mixed-disulfide bond between DsbC and the substrate that can be resolved by two mechanisms. In the first mechanism, a second cysteine in the substrate attacks the mixed-disulfide bond. This will result in the formation of the correct disulfide bond in the substrate and the release of reduced DsbC. The second proposed mechanism is that C<sub>101</sub> in DsbC attacks the mixed-disulfide bond. This will result in the release of a reduced substrate and an oxidized DsbC. In this case, DsbC acts as a reductase to give the substrate another chance to be oxidized by DsbA. The latter mechanism is supported by the finding that a thioredoxin-like protein with only reductase activity can complement *dsbC* mutant in *E. coli* (Shouldice *et al.*, 2010). In both mechanisms, DsbC must be maintained in a reduced state and this is achieved by acquiring electrons from its redox partner DsbD (Rietsch *et al.*, 1997).

DsbD is a 59-kDa cytoplasmic membrane protein, which consists of three domains: DsbD $\alpha$  (N-terminal periplasmic domain with an immunoglobulin-like fold), DsbD $\beta$  (eight transmembrane segments), and DsbD $\gamma$  (C-terminal periplasmic domain with a thioredoxin fold). Each domain contains a pair of cysteines (DsbD $\alpha$ <sub>C109-C103</sub>, DsbD $\beta$ <sub>C163-C285</sub>, DsbD $\gamma$ <sub>C461-C644</sub>) that are essential for DsbD activity (Chung *et al.*, 2000; Missiakas *et al.*, 1995; Stewart *et al.*, 1999). The reduction of periplasmic proteins by DsbD involves the transfer of electrons from the thioredoxin system [thioredoxin, thioredoxin reductase, and nicotinamide adenine dinucleotide phosphate (NADPH)] in the cytoplasm. In this process, the cytoplasmic thioredoxin transfers electrons to DsbD $\beta$ <sub>C163-C285</sub>. The result is DsbD $\beta$ <sub>C163-C285</sub> becomes reduced. Electrons are then transferred from DsbD $\beta$ <sub>C163-C285</sub> to DsbD $\gamma$ <sub>C461-C644</sub> and from there to DsbD $\alpha$ <sub>C109-C103</sub>. DsbD $\alpha$ <sub>C109-C103</sub> then donates the electrons to DsbC in the periplasm resulting in the reduction of DsbC (Figure 1.2) (Katzen and Beckwith, 2000; Krupp *et al.*, 2001).

Oxidized thioredoxin generated from the above reactions is then reduced by thioredoxin reductase (TrxR) in a NADPH-dependent manner. The thioredoxin system in *E. coli* has one thioredoxin reductase encoded by *trxB* and two thioredoxins, Trx1 and

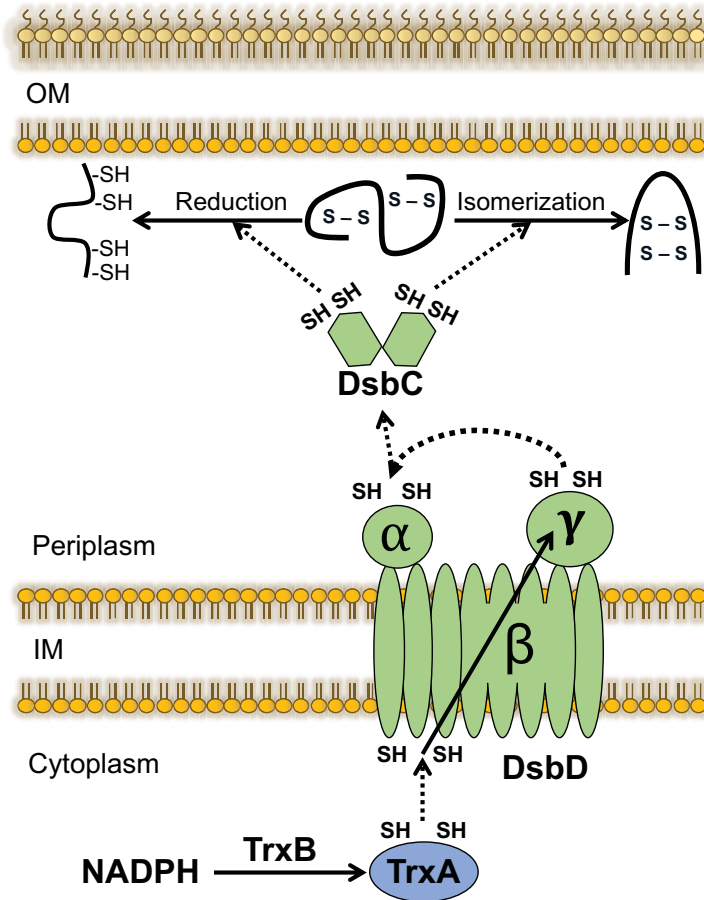


**Figure 1.2 The DsbC/DsbD disulfide bond isomerization pathway in *E. coli*.**

DsbC is a homodimeric periplasmic isomerase that catalyzes disulfide bond rearrangement in mis-disulfide bonded substrates. DsbC is maintained in its active, reduced form by the membrane protein DsbD. Electrons are transferred from thioredoxin in the cytoplasm to the  $\beta$  domain and then to the  $\gamma$  domain and finally to the  $\alpha$  domain in DsbD. Arrows indicate the flow of electrons; IM: inner membrane; OM: outer membrane; TrxA: thioredoxin; TrxB: thioredoxin reductase. Adapted from Cho and Collet (2013) and Ezraty *et al.* (2017).

Trx2 encoded by *trxA* and *trxC*, respectively (Lu and Holmgren, 2014; Potamitou *et al.*, 2002). Although both Trx1 and Trx2 are able to reduce DsbD, Trx1 is more efficient. In addition to DsbD, thioredoxin also reduces cytoplasmic methionine sulfoxide reductase, ribonucleotide reductase, and 3'-phosphoadenosyl sulfate (PAPS) (Rietsch *et al.*, 1997; Ritz *et al.*, 2000).

### 1.3.1.2.2 The Reduction Pathway

In addition to DsbC, *E. coli* possesses two other DsbD-dependent periplasmic reductases, DsbG and CcmG (DsbE) (Cho and Collet, 2013). Similar to DsbC, DsbG (26-kDa) is a homodimeric V-shaped soluble periplasmic protein with a C<sub>109</sub>P<sub>110</sub>Y<sub>111</sub>C<sub>112</sub> active site. The two-thioredoxin domains on the dimer are linked through linker helix to an N-terminal dimerization domain (Heras *et al.*, 2004). In the cell, the active site of DsbG is maintained in a reduced state by DsbD (Bessette *et al.*, 1999). Although overexpression of *dsbG* can complement *dsbC* mutant (Bessette *et al.*, 1999), the main function of DsbG in *E. coli* is to protect single cysteine residues from oxidation in the periplasm. YbiS, ErfK, and YnhG are substrates of DsbG and belong to the family of L,D-transpeptidases that catalyze the crosslinking of the outer membrane lipoprotein to the peptidoglycan. YbiS, ErfK, and YnhG each possess a single cysteine that can be oxidized to sulfenic acid in the absence of DsbG (Figure 1.3A) (Depuydt *et al.*, 2009).

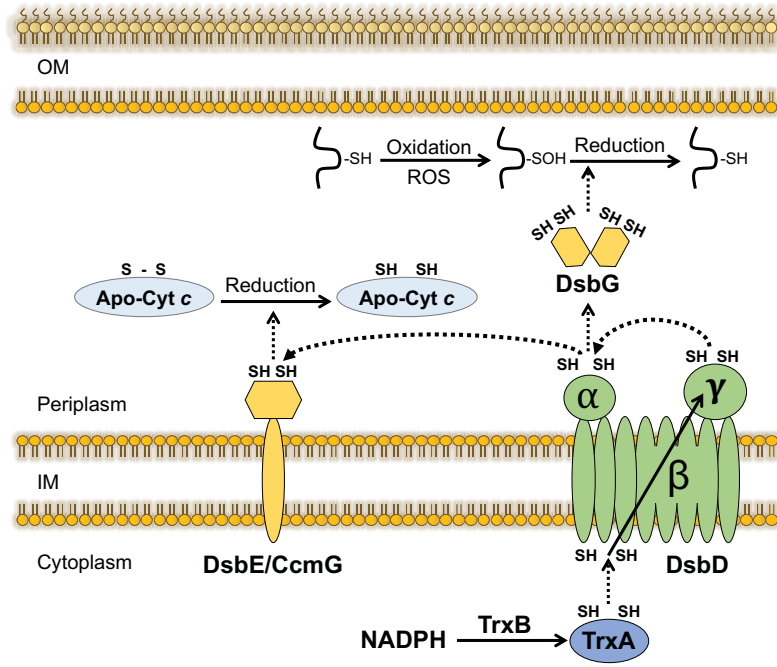
CcmG (DsbE) is a membrane-bound thioredoxin-like protein with a conserved active site C<sub>80</sub>P<sub>81</sub>T<sub>82</sub>C<sub>83</sub> motif. CcmG has disulfide reductase activity, which is essential for cytochrome *c* maturation (Throne-Holst *et al.*, 1997). To form a mature cytochrome *c*, heme needs to be ligated to the reduced thiols of the CXXC motif of apocytochrome. Interestingly, DsbA forms a disulfide bond in the apocytochrome, presumably to prevent irreversible cysteine oxidation by reactive oxygen species (ROS) (Stirnemann *et al.*, 2005). CcmG reduces the disulfide bond in apocytochrome. *ccmG* deletion mutants and cysteine active site mutants were defective in cytochrome *c* maturation (Fabianek *et al.*, 1998; Throne-Holst *et al.*, 1997). DsbD maintains CcmG in a reduced state, which allows CcmG to act as a reductase (Figure 1.3A) (Reid *et al.*, 2001; Stirnemann *et al.*, 2005).

**Figure 1.3 The reducing pathway in *E. coli*.**

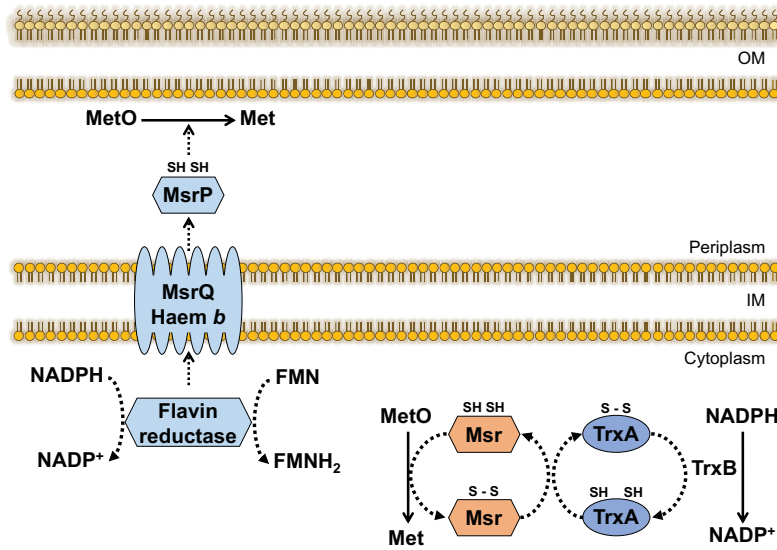
**A.** DsbE/DsbD and DsbG/DsbD disulfide bond reduction pathway. DsbE (CcmG) is a disulfide bond reductase that specifically reduces disulfide bond in apocytochrome. DsbG is a homodimeric periplasmic disulfide bond reductase that protects single cysteine residues from oxidation. Both DsbE and DsbG are maintained in the reduced form by DsbD. **B.** Methionine sulfoxide reductases and their regeneration systems. Cytoplasmic Msr involves in the reduction of MetO. Oxidized Msr is then reduced by the thioredoxin system in the cytoplasm. MsrP/MsrQ system repairs methionine sulfoxide in *E. coli* periplasm. MsrP is a periplasmic Msr that reduces MetO. MsrP is maintained in its active, reduced form by the membrane protein MsrQ, a *b*-type heme-containing membrane protein. Arrows indicate the flow of electrons; IM: inner membrane; OM: outer membrane; TrxA: thioredoxin; TrxB: thioredoxin reductase; Apo-Cyt *c*: apocytochrome *c*; ROS: reactive oxygen species; MetO: methionine sulfoxide; Met: methionine; FMN: flavin mononucleotide. Adapted from Cho and Collet (2013) and Ezraty *et al.* (2017).



A.



B.



In addition to the above-mentioned periplasmic TDORs that protect the periplasmic proteins from oxidative damage, the thioredoxin system in *E. coli* also reduces cytoplasmic enzymes such as methionine sulfoxide reductase (Msr). In the cells, Msr can reduce MetO to Met (Brot *et al.*, 1981). Two classes of Msrs have been described, MsrA and MsrB, which are specific for the Met-*S*-O and Met-*R*-O, respectively.

Because MsrA and MsrB have strict stereospecificity, cells need both MsrA and MsrB (Ezraty *et al.*, 2005a). In general, MsrA and MsrB use a three-step catalytic mechanism to reduce MetO to Met. First, a nucleophilic cysteine residue in MsrA or MsrB attacks the MetO residue in the substrate. This leads to the formation of a sulfenic acid (–SOH) on the catalytic cysteine of MsrA/B and MetO is reduced in the substrate. The sulfenic acid containing cysteine attacks a second catalytic cysteine of MsrA/B leading to the formation of an intramolecular disulfide bond, which is then reduced by thioredoxins. Msr enzyme is regenerated at the end of these reactions (Boschi-Muller *et al.*, 2000).

*E. coli* encodes four cytoplasmic Msrs: MsrA, biotin sulfoxide reductase BisC, MsrB, and fRMsr (MsrC). MsrA reduces both free and protein-bound Met-*S*-O, BisC reduces free Met-*S*-O, MsrB reduces protein-bound Met-*R*-O, and fRMsr (MsrC) reduces free Met-*R*-O (Figure 1.3B) (Brot *et al.*, 1981; Etienne *et al.*, 2003; Ezraty *et al.*, 2005b; Grimaud *et al.*, 2001). *msrA* was induced during the stationary phase of growth and in biofilm cells but not in the presence of exogenous H<sub>2</sub>O<sub>2</sub>. Inactivation of *msrA* led to an increase in sensitivity to H<sub>2</sub>O<sub>2</sub>, and reduction in type I fimbriae-mediated binding to eukaryotic cell receptors (Moskovitz *et al.*, 1995; Wizemann *et al.*, 1996). The expression of *msrB* is regulated by the small non-coding RNA (sRNA) RyhB, which controls the expression of more than 50 genes in response to iron limitation. Under iron-limiting conditions, RyhB represses *msrB* expression, suggesting that MsrB is not needed under this condition (Bos *et al.*, 2013).

An exception to the stereospecificity and thiol-dependent MetO reduction mechanisms has been identified recently in *E. coli*. MsrP, a periplasmic Msr, is able to reduce both diastereoisomer forms of MetO. MsrP uses molybdopterin-based reactions to

reduce MetO. MsrP acquires electrons from its redox partner MsrQ, a *b*-type heme-containing membrane protein (Gennaris *et al.*, 2015). MsrQ acquires electrons from the cytosolic flavin reductase, which uses NADPH to reduce FMN and transfers electrons to MsrQ (Figure 1.3B) (Juillan-Binard *et al.*, 2017).

### 1.3.1.3 Disulfide Bond Formation in Other Gram-Negative Bacteria

Homologs of DsbAB and DsbCD have been identified in other Gram-negative bacteria. Some variations in substrate specificity and the number of copies of TDORs were found (Dutton *et al.*, 2008). For example, *Salmonella enterica* serovar Typhimurium encodes a homolog of DsbAB named DsbLI. *dsbLI* form an operon with its natural substrate *assT*, which encodes the periplasmic arylsulfate sulfotransferase (AssT) that catalyzes the transfer of sulfate group between phenolic compounds. DsbL forms a disulfide bond in AssT that is essential for activity (Lin *et al.*, 2009). In addition to DsbLI, *S. enterica* serovar Typhimurium also has two additional disulfide oxidases, DsbA and SrgA. Although both DsbA and SrgA catalyze disulfide bond formation in SpiA (SsaC), an outer membrane protein and structural component of type III secretion system (Miki *et al.*, 2004), only SrgA catalyzes disulfide bond formation in PefA, a major structural protein subunit of the adhesion fimbriae (Table 1.1) (Bouwman *et al.*, 2003). This substrate specificity explains the need for more than one TDOR in *S. enterica* serovar Typhimurium.

In addition to the difference in substrate specificity, DsbA homologs in Gram-negative bacteria also differ in cellular location. For instance, one of the three DsbA homologs of *Neisseria meningitidis* is located in the periplasm (DsbA3) while two of them are lipoproteins anchored to the inner membrane (DsbA1 and DsbA2) (Tinsley *et al.*, 2004). Interestingly, inactivation of all three DsbA homologs is required to give a defect in growth at 37 °C, suggesting that they can complement each other. Only DsbA1 and DsbA2 are involved in type IV pili biogenesis by catalyzing the proper folding of the outer-membrane secretin PilQ (Sinha *et al.*, 2008; Tinsley *et al.*, 2004). Although it

**Table 1.1 TDORs in other Gram-negative bacteria**

Bacterial species	TDOR	Redox partner	Substrate	Substrate(s) function	Reference
<i>S. enterica</i> serovar Typhimurium	DsbL	DsbI	AssT	Catalyses the transfer of a sulfate group among phenolic compounds	(Lin <i>et al.</i> , 2009)
	DsbA	DsbB	SpiA (SsaC)	Outer membrane protein and structural component of T3SS	(Miki <i>et al.</i> , 2004; Bouwman <i>et al.</i> , 2003)
	SrgA	DsbB	SpiA (SsaC)		
			PefA	Major structural subunit of the adhesion fimbriae	(Bouwman <i>et al.</i> , 2003)
<i>N. meningitidis</i>	DsbA1	DsbB	PilQ	Outer-membrane secretin of type IV pili	(Lafaye <i>et al.</i> , 2009; Tinsley <i>et al.</i> , 2004; Sinha <i>et al.</i> , 2008)
	DsbA2	DsbB			
	DsbA3	DsbB	?	?	(Lafaye <i>et al.</i> , 2009)
	PilB	DsbD	MetO (Undefined substrate)	?	(Olry <i>et al.</i> , 2002; Quintern <i>et al.</i> , 2009)
<i>L. pneumophila</i>	DsbA2	DsbB1 DsbB2 DsbD1 DsbD2	DotG DotC	Components of the Dot/Icm T4SS	(Jameson-Lee <i>et al.</i> , 2011; Kpadeh <i>et al.</i> , 2015)
<i>H. pylori</i>	DsbK	DsbI	HcpE	Protein involved in the modulation of the <i>H. pylori</i> interaction with its host	(Lester <i>et al.</i> , 2015; Bocian-Ostrzycka <i>et al.</i> , 2015)

possesses three DsbA homologs, *N. meningitidis* has only one DsbB, one DsbD, and one DsbC (Table 1.1) (Tinsley *et al.*, 2004).

*N. meningitidis* also has a periplasmic methionine sulfoxide reductase PilB. PilB consists of three domains, an N-terminal thioredoxin-like domain, a central MsrA domain, and a C-terminal MsrB domain. PilB is regenerated by acquiring electrons from DsbD. The electrons originated from the cytoplasmic thioredoxin system (Table 1.1) (Quintern *et al.*, 2009; Olry *et al.*, 2002). Interestingly, the inactivation of *dsbD* in *N. meningitidis* can only be achieved in the *dsbA1A2* double mutant or the *dsbA1A2A3* triple mutant, suggesting a connection between the oxidation and reduction/isomerization pathway (Kumar *et al.*, 2011).

Another variation among DsbA homologs in Gram-negative bacteria is the enzyme activity. For example, *Legionella pneumophila* has a dimeric DsbA named DsbA2 that possesses both disulfide oxidase and isomerase activity. DsbA2 is maintained in a mixture of reduced and oxidized form by DsbB1/DsbB2 and DsbD1/DsbD2. DsbA2 is essential for *L. pneumophila*, and DsbA2<sub>P198T</sub> point mutant resulted in a loss of intracellular multiplication and loss of functional Dot/Icm Type IV secretion system (Jameson-Lee *et al.*, 2011; Kpadeh *et al.*, 2015). A similar bi-functional DsbA was found in a number of Gram-negative bacteria that lack DsbC homolog such as *Brucella*, *Coxiella*, and *Rickettsiae* (Kpadeh *et al.*, 2015). Not all homodimeric DsbA possesses oxidase and isomerase activity. For example, *Helicobacter pylori* DsbK, a homodimeric DsbA homolog, possesses oxidase but not isomerase activity (Bocian-Ostrzycka *et al.*, 2015). DsbK contributes to virulence and colonization to gastric mucosa in *H. pylori* (Table 1.1) (Zhong *et al.*, 2016).

### **1.3.2 Disulfide Bond Formation in Gram-Positive Bacteria**

Disulfide bond formation in Gram-positive bacteria has not been investigated to the same extent as in Gram-negative bacteria (Davey *et al.*, 2016b; Reardon-Robinson and Ton-That, 2015). This is due to the lack of prototypical DsbA homolog in many Gram-positive bacteria. In addition, Gram-positive bacteria lack the periplasmic space,

which represents a defined and enclosed compartment for oxidative protein folding to occur, and thus disulfide bond formation, reduction, and isomerization is catalyzed at the cell wall using cell membrane-anchored TDOR instead of soluble TDOR. (Daniels *et al.*, 2010; Davey *et al.*, 2016b; Landeta *et al.*, 2018). Nonetheless, evidence indicate that disulfide bonds exist, and are important in numerous virulence factors in Gram-positive bacteria, including toxins produced by *Clostridium botulinum* (neurotoxin botulinum) (Simpson *et al.*, 2004), *Clostridium tetani* (tetanospasmin) (Schiavo *et al.*, 1990), and *Corynebacterium diphtheriae* (diphtheria toxin) (Reardon-Robinson *et al.*, 2015b). A few Gram-positive TDOR enzymes have now been identified in the last ten years (Davey *et al.*, 2013; Dumoulin *et al.*, 2005; Ke *et al.*, 2018; Reardon-Robinson *et al.*, 2015a). Many of these are disulfide bond oxidases, and some are disulfide bond reductases, but no disulfide bond isomerase has been identified to date (Daniels *et al.*, 2010; Davey *et al.*, 2013).

### 1.3.2.1 The Oxidation Pathway

#### 1.3.2.1.1 Actinobacteria

Several disulfide bond-forming enzymes have been identified and characterized in *Mycobacterium*, *Actinomyces*, and *Corynebacterium*. *Mycobacterium tuberculosis* produces five extracytoplasmic TDOR and some are essential for growth. It was predicted that *M. tuberculosis* produces more than 160 secreted proteins and more than 60% of them may contain disulfide bonds (Goulding *et al.*, 2004; Chim *et al.*, 2010).

The first TDOR identified in *M. tuberculosis* was DsbE. The crystal structure of *MtbDsbE* shows that it has a typical thioredoxin-like domain with the conserved active site C<sub>36</sub>P<sub>37</sub>F<sub>38</sub>C<sub>39</sub>. The N-terminal cysteine (C<sub>36</sub>) is exposed on the protein surface, whereas the C-terminal cysteine (C<sub>39</sub>) is buried. Interestingly, unlike *E. coli* DsbE, *MtbDsbE* is an oxidase with a redox potential of  $-128 \pm 12$  mV. *MtbDsbE* is able to refold reduced hirudin (Goulding *et al.*, 2004). The second TDOR identified in *M. tuberculosis*

was DsbF. Similar to *MtbDsbE*, the crystal structure of *MtbDsbF* reveals the presence of a conserved thioredoxin-like domain and an active site C<sub>81</sub>P<sub>82</sub>T<sub>83</sub>C<sub>84</sub>. *MtbDsbF* is also an oxidase able to refold reduced hirudin. *MtbDsbF* has a redox potential of  $-89 \pm 9$  mV (Chim *et al.*, 2010).

The third TDOR identified in *M. tuberculosis* was DsbA. *MtbDsbA* is required for optimal growth. An *in vitro* oxidation assay using a fluorescently labeled peptide as a substrate showed that *MtbDsbA* has oxidase activity. *MtbDsbA* has a redox potential of -99 mV (Premkumar *et al.*, 2013). *MtbDsbA* was unable to refold the reduced hirudin or rdRNase A (reduced and denatured RNase A) and showed no reductase activity in the insulin precipitation assay (Wang *et al.*, 2013; Premkumar *et al.*, 2013; Chim *et al.*, 2013). The crystal structure of *MtbDsbA* reveals the presence of two domains: a conserved thioredoxin-like domain with a typical active site C<sub>89</sub>P<sub>90</sub>A<sub>91</sub>C<sub>92</sub>, and an  $\alpha$ -helical domain containing a second pair of cysteines (C<sub>140</sub> - C<sub>192</sub>) that form a structural disulfide bond required for stability of *MtbDsbA* (Wang *et al.*, 2013; Premkumar *et al.*, 2013; Chim *et al.*, 2013).

*MtbDsbA* uses VKOR as the redox partner (Ke *et al.*, 2018). *vkor* mutants showed a severe growth defect. The growth of *M. tuberculosis* was also inhibited by warfarin, an anticoagulant that targets human VKOR (Dutton *et al.*, 2010). *MtbVKOR* is a cytoplasmic membrane protein with five-transmembrane  $\alpha$ -helices, and two extracytoplasmic loops and each loop contains a redox active site (C<sub>57</sub>-C<sub>65</sub> and C<sub>139</sub>-C<sub>142</sub>) (Wang *et al.*, 2011). When *MtbVKOR* and *MtbDsbA* were co-expressed in the *E. coli dsbAB* mutant, they were able to restore motility, a phenotype that is dependent on a functional disulfide bond formation pathway (Genevaux *et al.*, 1999; Dailey and Berg, 1993; Hiniker and Bardwell, 2004; Ke *et al.*, 2018). The oxidation of *MtbDsbA* in the *E. coli dsbAB* mutant was found to be dependent on the presence of *MtbVKOR*. The co-expression of *MtbDsbA* and *MtbVKOR*<sub>C65A</sub> in the *E. coli dsbAB* mutant resulted in a *MtbVKOR*-*MtbDsbA* complex formation, supporting the notion that specific interaction occurred between *MtbVKOR* and *MtbDsbA* (Figure 1.4A) (Ke *et al.*, 2018).

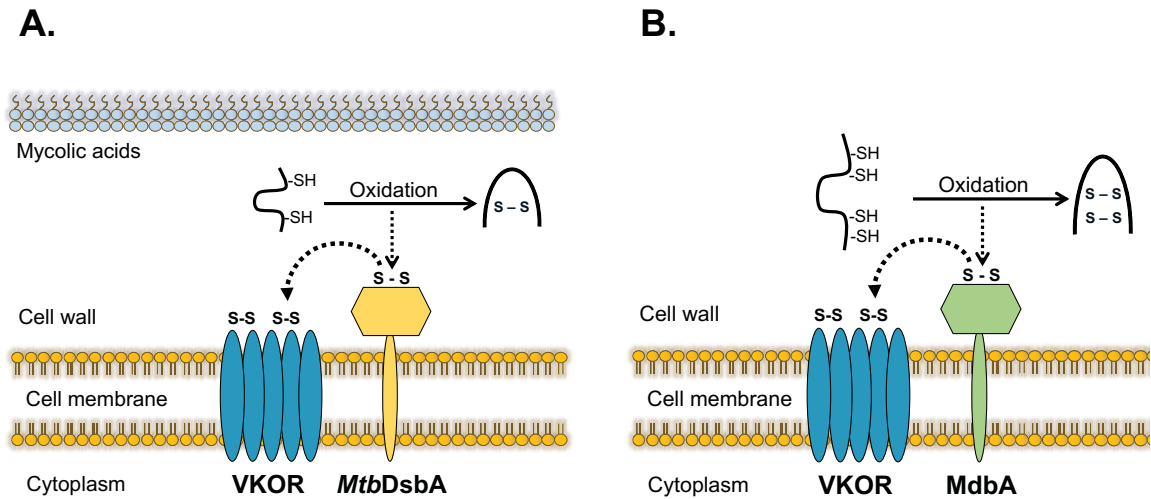


**Figure 1.4 Disulfide bond formation pathways in *Mycobacterium* and *Actinomyces*.**

**A.** Disulfide bond formation pathway in *M. tuberculosis*. Three TDORs were identified in *M. tuberculosis* *MtbDsbA*, *MtbDsbE*, and *MtbDsbF*. Both *MtbDsbE* and *MtbDsbF* have oxidase activity *in vitro*, but no phenotypes were identified yet. *MtbDsbA* is a membrane-associated TDOR that catalyzes disulfide bond formation and uses VKOR as its redox partner. **B.** Disulfide bond formation pathway in *A. oris*. MdbA is a membrane-associated TDOR that catalyzes disulfide bond formation in multiple substrates. MdbA is reoxidized by VKOR. Arrows indicate the flow of electrons. Adapted from Landeta *et al.* (2018) and Reardon-Robinson and Ton-That (2015).



The disulfide bond-forming enzyme has also been identified in *Actinomyces oris*. In this bacterium, MdbA (monoderm disulfide bond-forming protein A) is a TDOR that cooperates with its redox partner, VKOR, to form disulfide bonds in the pilus shaft proteins, FimP and FimA, of types 1 and 2 fimbriae, respectively. FimP and FimA contain two disulfide bonds, which are essential for pilus assembly, biofilm formation, and coaggregation with *Streptococcus oralis* (Reardon-Robinson *et al.*, 2015a; Persson *et al.*, 2012). The deletion of either *vkor* or *mdbA* resulted in a defect in pilus formation and coaggregation with *S. oralis*. The crystal structure of *A. oris* MdbA shows the presence of a thioredoxin-like domain with a typical active site C<sub>139</sub>S<sub>140</sub>H<sub>141</sub>C<sub>142</sub>, and an extended  $\alpha$ -helical domain. *A. oris* MdbA structure also shows the presence of the conserved *cis*-Proline (P<sub>286</sub>) (Reardon-Robinson *et al.*, 2015a). *A. oris* VKOR is a cytoplasmic membrane protein with five-transmembrane  $\alpha$ -helices and two extracytoplasmic loops; each loop contains a redox active site, C<sub>93</sub>XXC<sub>101</sub> and C<sub>175</sub>XXC<sub>178</sub>. Mutation of any of these cysteine residues to alanine abolishes pilus formation and coaggregation with *S. oralis*. Interestingly, C<sub>101</sub>A mutation resulted in VKOR-MdbA complex formation (Luong *et al.*, 2017). The reoxidation of MdbA by VKOR in *A. oris* was linked to the electron transport chain (Figure 1.4B) (Sanchez *et al.*, 2017).

*Corynebacterium diphtheriae* has multiple TDOR, including MdbA, DsbF, and DIP0397. *CdMdbA* plays an essential role in cell division, pilus assembly, and diphtheria toxin production (Reardon-Robinson *et al.*, 2015b). The pilus shaft protein SpaA contains a disulfide bond between C<sub>383</sub> and C<sub>443</sub> (Kang *et al.*, 2009). This disulfide bond is essential for pilus assembly (Reardon-Robinson *et al.*, 2015b). Diphtheria toxin contains two disulfide bonds (C<sub>186</sub> - C<sub>201</sub> and C<sub>461</sub> - C<sub>471</sub>). While the first disulfide bond connects the active domain A to the binding domain B, the second disulfide bond is located within the domain B (Choe *et al.*, 1992; Reardon-Robinson *et al.*, 2015b).

*CdMdbA* has a thioredoxin-like domain with a typical active site C<sub>91</sub>P<sub>92</sub>H<sub>93</sub>C<sub>94</sub>, and an extended  $\alpha$ -helical domain. The thioredoxin domain consists of 6-strand  $\beta$ -sheet and 2 flanking  $\alpha$  helices. *CdMdbA* structure also possesses a conserved *cis*-Pro loop (P<sub>222</sub>) (Reardon-Robinson *et al.*, 2015b). The redox partner(s) of *CdMdbA* has not been identified yet.

*C. diphtheriae* also possesses a second TDOR termed *CdDsbF*. The enzymatic activity and biological functions of *CdDsbF* have not been investigated. Nevertheless, the crystal structure of a *CdDsbF* reveals the presence of a thioredoxin-like domain with a typical C<sub>84</sub>XXC<sub>87</sub> active site (Um *et al.*, 2014).

### 1.3.2.1.2 Firmicutes

Unlike Actinobacteria, Firmicutes are predicted to exclude cysteines from extracytoplasmic proteins (Daniels *et al.*, 2010). Nevertheless, disulfide bond-forming enzymes have been identified in *Bacillus subtilis*, *Staphylococcus*, and *Streptococcus* (Davey *et al.*, 2016b; Reardon-Robinson and Ton-That, 2015).

*B. subtilis* BdbD-BdbC, homologs of DsbA-DsbB, are needed for the stability and secretion of proteins containing disulfide bonds, such as the *E. coli* alkaline phosphatase PhoA (contains two disulfide bonds) and  $\beta$ -lactamase (contains one disulfide bond) (Bolhuis *et al.*, 1999). In *B. subtilis*, induction of PhoA production causes secretion stress. Accordingly, deletion of *bdbC* causes an increase in the secretion stress in *B. subtilis* (Darmon *et al.*, 2006). BdbD-BdbC also catalyzes the formation of disulfide bonds in the competence protein, pseudopilin ComGC, and the DNA translocation channel ComEC. Cells lacking BdbD-BdbC produced a lower amount of ComGC and ComEC, leading to a defect in genetic competence development (Figure 1.5A) (Bolhuis *et al.*, 1999; Meima *et al.*, 2002).

The results of a proteomic study revealed that 15 membrane-associated proteins required BdbD-BdbC for their stability and production. One of them was the osmoprotection membrane protein ProA, which contains two disulfide bonds and requires BdbD-BdbC for stability. Consistent with the defect in the stability of ProA, the *bdbCD* mutant was sensitive to osmotic shock (Goosens *et al.*, 2013).

BdbC is an integral membrane protein, whereas BdbD is a membrane-associated protein (Bolhuis *et al.*, 1999; Crow *et al.*, 2009a). The crystal structure of BdbD shows that it is similar to *E. coli* DsbA, with a thioredoxin domain containing the active site C<sub>69</sub>P<sub>70</sub>S<sub>71</sub>C<sub>72</sub>, and an inserted  $\alpha$ -helical domain.

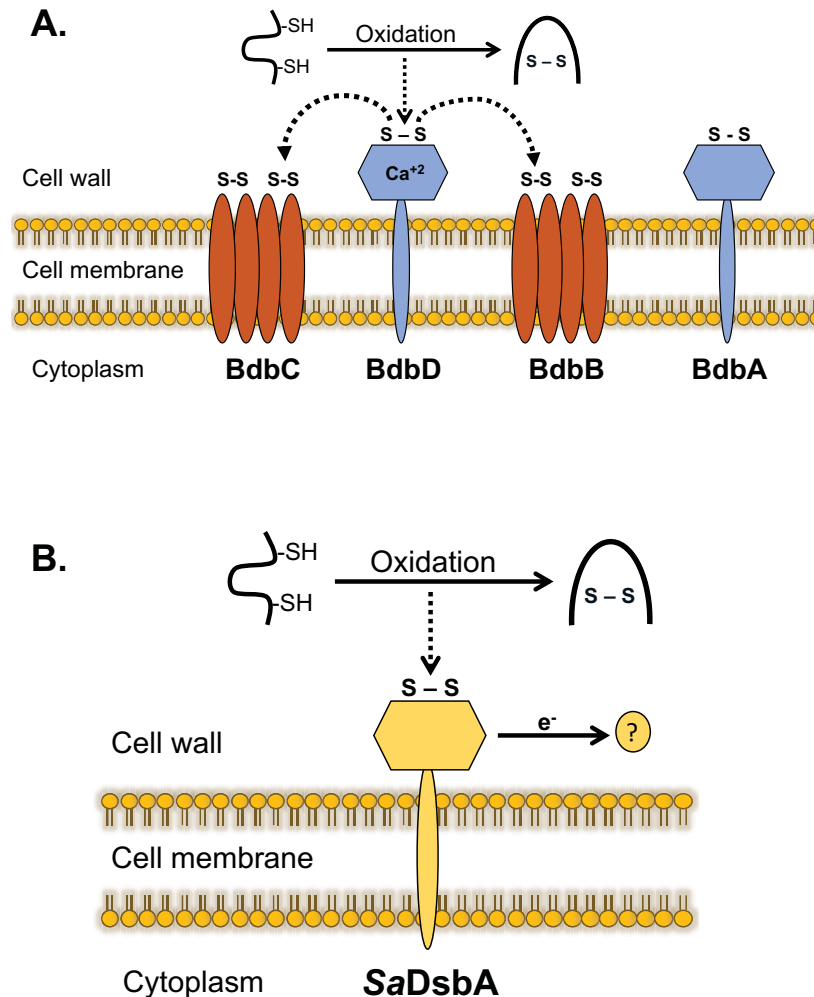


**Figure 1.5 Disulfide bond formation in *Bacillus* and *Staphylococcus*.**

**A.** Disulfide bond forming pathway in *B. subtilis*. BdbD is membrane-associated TDOR with a Ca<sup>2+</sup> binding site. BdbD together with two membrane proteins BdbC and BdbB catalyzes disulfide bond formation. BdbA is membrane-associated TDOR with unknown function. **B.** Disulfide bond forming pathway in *S. aureus*. SaDsbA is a membrane-bound lipoprotein that catalyzes disulfide bond formation in *S. aureus*. SaDsbA seems to depend only on redox-active medium components for reoxidation. Arrows indicate the flow of electrons. Adapted from Landeta *et al.* (2018) and Davey *et al.* (2016b).

Unlike DsbA, BdbD has a Ca<sup>2+</sup> binding site located between the thioredoxin and helical domains. This Ca<sup>2+</sup> binding site is not required for BdbD folding as revealed by the crystal structure of Ca<sup>2+</sup>-depleted BdbD. However, Ca<sup>2+</sup> was found to affect the redox potential of BdbD, with a shift from - 75 ± 5 mV for the Ca<sup>2+</sup>-containing protein to - 95 ± 5 mV for the Ca<sup>2+</sup>-depleted protein, indicating that Ca<sup>2+</sup> may act to enhance the oxidizing power of BdbD (Crow *et al.*, 2009a).

*B. subtilis* also possesses two other TDOR, termed BdbA and BdbB (Bolhuis *et al.*, 1999). BdbB is an integral membrane protein and is required for the stability of PhoA (Bolhuis *et al.*, 1999). BdbA and BdbB form an operon with genes encoding for the bacteriocin, sublancin 168, and the ABC (ATP-binding cassette) transporter SunT. Sublancin 168 contains two disulfide bonds and requires BdbB and BdbC for its production. The natural substrate and enzymatic activity of BdbA have not been investigated (Figure 1.5A) (Dorenbos *et al.*, 2002).

For *S. aureus*, the disulfide bond formation pathway has not been well-investigated. So far, only one TDOR has been identified in *S. aureus*. It is called SaDsbA (Figure 1.5B). SaDsbA is a membrane-bound lipoprotein, which can functionally replace BdbD-BdbC for PhoA production, sublancin 168 production, and competence development in *B. subtilis* (Kouwen *et al.*, 2007). *B. subtilis* expressing SaDsbA showed a 2-fold increase in the secretion of the disulfide bond-containing protein PhoA (Kouwen *et al.*, 2008). When SaDsbA was expressed in the *E. coli dsbA* mutant, it restored the motility phenotype (Dumoulin *et al.*, 2005). This complementation of the *E. coli dsbA* mutant by SaDsbA is independent of EcDsbB, and biochemical assays show that SaDsbA does not interact with EcDsbB (Heras *et al.*, 2008). SaDsbA is an oxidase with a redox potential of -131 mV (Dumoulin *et al.*, 2005).

SaDsbA is unable to reduce insulin and shows no isomerase activity in the scrambled RNase A refolding assay (Heras *et al.*, 2008). The crystal structure of SaDsbA reveals the presence of two domains: a thioredoxin domain with a typical active site C<sub>26</sub>P<sub>27</sub>Y<sub>28</sub>C<sub>29</sub> located at the N terminus of the first helix in the thioredoxin fold, and an extended α-helical domain (Heras *et al.*, 2008; Heras *et al.*, 2007). However, unlike oxidized EcDsbA that has an unstable disulfide bond, the oxidized and reduced forms of

*SaDsbA* show identical stabilities. This suggests that the reoxidation of the *SaDsbA* can be carried out by extracellular oxidants and a redox partner is not required (Heras *et al.*, 2008). Similar to *B. subtilis*, *SaDsbA* catalyzes the formation of a disulfide bond in the pseudopilin ComGC. Consistent with this, *S. aureus dsbA* mutants produce a reduced amount of ComGC (van der Kooi-Pol *et al.*, 2012).

Unlike *Bacillus* and *Staphylococcus*, streptococci lack *EcDsbA* homologs and their disulfide bond forming catalysts are not known. The one TDOR identified in *Streptococcus thermophilus* LMD-9 is BlpG<sub>st</sub>, which is needed for the production of thermophiline 9, a multipetide bacteriocin. BlpG<sub>st</sub> was able to restore the motility phenotype of the *E. coli dsbA* mutant (Fontaine and Hols, 2008). However, the enzymatic activity of BlpG<sub>st</sub> has not been tested, and direct interaction with thermophiline 9 has not been shown.

Recently, our laboratory identified a TDOR in *Streptococcus gordonii* named SdbA (*Streptococcus* disulfide bond protein A) that forms disulfide bonds in substrate proteins and affects multiple cellular processes (Davey *et al.*, 2013).

#### 1.3.2.1.2.1 *Streptococcus gordonii*

*S. gordonii* is a facultative anaerobic bacterium. It inhabits the human oral cavity and is a pioneer colonizer of the tooth surface (Gross *et al.*, 2010). *S. gordonii* produces multiple cell surface-associated proteins, which allows it to interact with the host and other oral bacteria during biofilm formation and colonization (Jakubovics *et al.*, 2005; Nobbs *et al.*, 2007; Jakubovics *et al.*, 2009; Rogers *et al.*, 2001). In the oral cavity, *S. gordonii* plays a key role in the formation of dental plaque, a multispecies biofilm community (Kuramitsu *et al.*, 2007). In this complex community, *S. gordonii* competes with other bacterial species by producing H<sub>2</sub>O<sub>2</sub> as a by-product during the conversion of pyruvate to acetyl phosphate under aerobic growth condition (Barnard and Stinson, 1999).

In addition to H<sub>2</sub>O<sub>2</sub>, *S. gordonii* produces two bacteriocins, Sth1 and Sth2, that are secreted by the ComAB transporter and inhibit the growth of other oral bacteria, such as

*Streptococcus mitis* and *Streptococcus oralis* (Heng *et al.*, 2007). These factors play important roles in the interspecies competition, where *S. gordonii* antagonizes the growth of other oral bacteria (Kreth *et al.*, 2008).

In *S. gordonii*, the production of Sth1 and Sth2 is under the control of the competence regulon (Heng *et al.*, 2007). During genetic competence, *S. gordonii* produces a small autoinducer termed competence-stimulating peptide (CSP), which is secreted by ComAB (Vickerman *et al.*, 2007; Heng *et al.*, 2007). Natural transformation is activated by the two-component system ComDE (ComD is a histidine kinase and ComE is a response regulator) when the extracellular level of CSP reaches the threshold level (Heng *et al.*, 2006). ComDE induces the expression of two alternative sigma factor, *comR1* and *comR2*, which activate the expression of over 100 genes, including those encoding for the DNA uptake machinery and bacteriocin production (Heng *et al.*, 2006; Heng *et al.*, 2007; Vickerman *et al.*, 2007).

In addition to DNA uptake, *S. gordonii* also releases DNA into the surrounding environment. The process of extracellular DNA (eDNA) release is thought to be important for biofilm formation and DNA exchange. eDNA release is independent of cell lysis; however, it depends on H<sub>2</sub>O<sub>2</sub> release and the activity of the murein hydrolase LytF (Xu and Kreth, 2013; Kreth *et al.*, 2009). The mechanism of H<sub>2</sub>O<sub>2</sub>-induced eDNA release depends on chromosomal DNA damage, which is thought to act as an intrinsic signal for the eDNA release. In *S. gordonii*, the process of eDNA release is coupled to the induction of natural transformation and thus facilitates horizontal gene transfer that can lead to the acquisition of new traits such as antibiotic resistance (Itzek *et al.*, 2011).

In addition to exogenous H<sub>2</sub>O<sub>2</sub> and LytF, effective eDNA release in *S. gordonii* also required the presence of the major autolysin AtlS (Liu and Burne, 2011). AtlS is a 130-kDa protein with a  $\beta$ 1,4-N-acetylmuramidase domain. The expression of *atlS* increased when the bacterium enters the stationary phase of growth (Liu and Burne, 2011).

### 1.3.2.1.2.1.1 Disulfide Bond Forming Enzyme in *S. gordonii*

Recently, a TDOR named SdbA was discovered in *S. gordonii*. In contrast to other Gram-positive TDORs, SdbA affects multiple cellular processes. *sdbA* mutants display a pleiotropic phenotype, namely enhanced biofilm formation (thick, multilayered biofilm), loss of eDNA release, absence of autolytic activity, defective bacteriocin production, and impaired genetic competence (Figure 1.6) (Davey *et al.*, 2013). Interestingly, the finding that *sdbA* mutant showed a defect in eDNA release but enhanced biofilm formation suggest that eDNA release is not essential for biofilm formation in *S. gordonii* (Davey *et al.*, 2013; Kreth *et al.*, 2009).

The major autolysin AtlS is the natural substrate of SdbA. AtlS has two cysteines (C<sub>1048</sub> – C<sub>1069</sub>) that form a single intramolecular disulfide bond, which is essential for activity. In *sdbA* mutants, AtlS lacks the intramolecular disulfide bond. Accordingly, AtlS isolated from *sdbA* mutants is enzymatically inactive. In *S. gordonii*, SdbA-AtlS complex was detected in the SdbA<sub>C89A</sub> point mutant indicating a direct interaction between SdbA and its natural substrate AtlS (Davey *et al.*, 2013; Davey *et al.*, 2015a).

SdbA is also needed for the production of anti-CR1 scFv, a single chain variable fragment antibody that requires two disulfide bonds for its stability. Inactivation of *sdbA* results in the production of reduced and misfolded anti-CR1 scFv that rapidly degraded by the extracellular serine protease DegP (Davey *et al.*, 2013; Davey *et al.*, 2015a).

Although AtlS is a natural substrate of SdbA, AtlS alone cannot explain all the phenotypic changes associated with *sdbA* inactivation. Recent studies showed that inactivation of *sdbA* causes a general stress response in *S. gordonii* (Davey *et al.*, 2016a; Davey *et al.*, 2015b). This response causes an upregulation of the CiaRH two-component regulatory system, which leads to the repression of the Com pathway and subsequently the bacteriocin gene. Thus, *sdbA* mutant showed no bacteriocin activity. The addition of synthetic CSP to *sdbA* mutant cultures or inactivation of *ciaRH* restores the bacteriocin activity of the *sdbA* mutant (Davey *et al.*, 2015b).

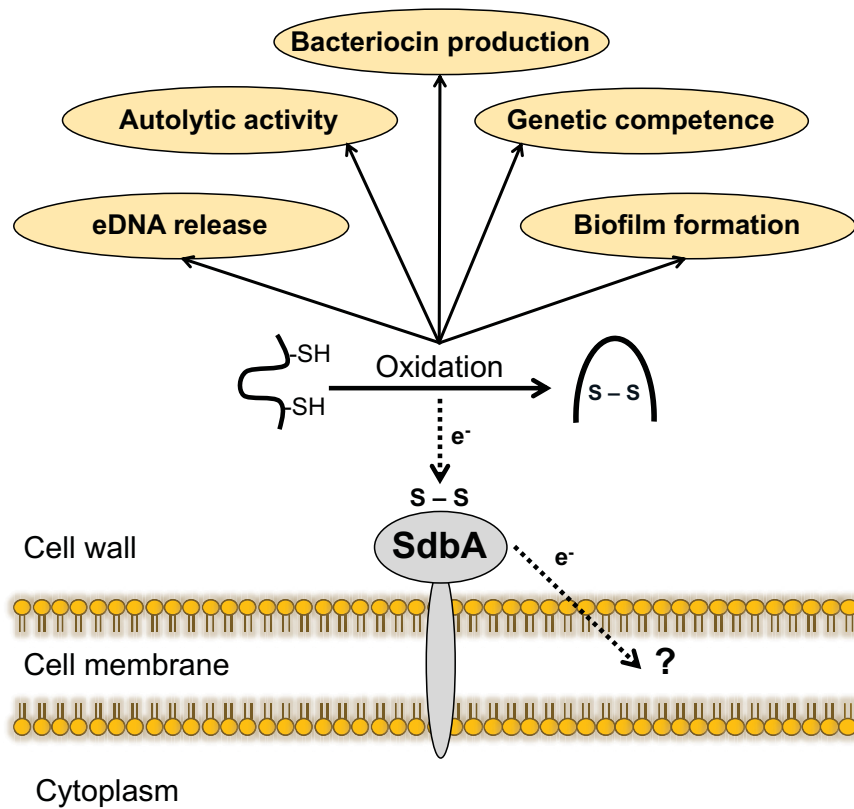


**Figure 1.6 Disulfide bond formation in *S. gordonii*.**

SdbA is an oxidase that catalyzes disulfide bond formation in *S. gordonii*. Inactivation of *sdbA* affects multiple phenotypes including, autolytic activity, eDNA release, genetic competence, bacteriocin production, and biofilm formation. Arrows indicate the flow of electrons. Question mark indicated unknown redox partner(s). Adapted from Davey *et al.* (2016b).



The upregulation of the CiaRH system in the *sdbA* mutant also plays a role in the enhanced biofilm formation phenotype. The addition of synthetic CSP or the inactivation of *ciaRH* reverses the biofilm phenotype (Davey *et al.*, 2016a). Although the mechanism by which the CiaRH system modulates the biofilm formation remain unclear, these findings suggest cooperation between the CiaRH system and the Com system in modulating biofilm formation, especially under stress conditions in *S. gordonii*. This enhanced biofilm phenotype of the *sdbA* mutant is paralleled with increased oral colonization in mice in which the *sdbA* mutant outcompeted the parent strain when tested in a competitive assay (Davey *et al.*, 2016a).

SdbA contains a C<sub>86</sub>PDC<sub>89</sub> active site motif and a conserved *cis*-proline (P<sub>156</sub>) residue. However, SdbA shares little sequence homology to *EcDsbA* and BdbD. SdbA is an oxidase able to refold reduced, denatured RNase A (Davey *et al.*, 2013). The crystal structure of SdbA revealed that the N-terminal cysteine (C<sub>86</sub>) is solvent exposed and the C-terminal cysteine (C<sub>89</sub>) is buried (Davey *et al.*, 2015a; Stogios and Savchenko, 2015). SdbA<sub>C86P/C89A</sub> mutants showed a pleiotropic phenotype identical to the *sdbA*-knockout mutants. SdbA<sub>C86P/C89A</sub> showed no enzymatic activity when tested in the RNase A refolding assay (Davey *et al.*, 2015a).

Interestingly, SdbA single cysteine point mutant (SdbA<sub>C86P</sub> or SdbA<sub>C89A</sub>) exhibited oxidase activity. The activity of SdbA single cysteine point mutant depends on the presence of glutathione, suggesting that both single cysteine variants can use low molecular weight thiols to catalyze disulfide bond formation (Davey *et al.*, 2015a). A similar observation was reported previously in *EcDsbA*, in which the single N-terminal cysteine of *EcDsbA* can catalyze disulfide bond formation *in vitro* using low molecular weight thiols. Unlike SdbA, the C-terminal cysteine of *EcDsbA* was inactive even in the presence of low molecular weight thiols (Walker and Gilbert, 1997). In *S. gordonii*, only SdbA<sub>C86P</sub> can introduce a disulfide bond into AtIS and complement the *sdbA* mutant phenotypes. These findings further suggest that SdbA is quite different from *EcDsbA*. SdbA<sub>C89A</sub> forms multiple mixed disulfide complexes with cellular proteins. SdbA<sub>C89A</sub> was only active *in vivo* when the endogenous H<sub>2</sub>O<sub>2</sub> production was eliminated by inactivation the pyruvate oxidase gene *spxB* (Davey *et al.*, 2015a).

Homologs of SdbA appear to be present in a range of Gram-positive bacteria that lack DsbA, including *C. tetani*, *S. pneumoniae*, *S. pyogenes*, *S. sanguinis*, *S. mutans*, and *S. mitis*, suggesting that this enzyme could be responsible for disulfide bond formation in this group of bacteria (Davey *et al.*, 2013).

#### **1.3.2.1.2.1.2 Other TDORs in *S. gordonii***

In addition to SdbA, *S. gordonii* possesses four other putative TDORs, namely Sgo\_1171, Sgo\_1177, Sgo\_1216, and Sgo\_1267 (Davey *et al.*, 2013; Vickerman *et al.*, 2007). These proteins contain the characteristic CXXC active site motif and the conserved *cis*-proline residue. Sgo\_1171, Sgo\_1177, and Sgo\_1267 are SdbA homolog, whereas Sgo\_1216 is predicted to be homologous to BlpG<sub>st</sub> from *S. thermophilus* LMD-9.

Previous investigations did not find any phenotype associated with these four TDORs except for *sgo\_1216* and *sgo\_1267* that showed a moderate defect in autolysis compared to the parent. Although Sgo\_1216 is annotated as a bacteriocin transporter accessory protein, inactivation of *sgo\_1216* did not affect bacteriocin activity in *S. gordonii* (Davey *et al.*, 2013). However, the level of Sgo\_1216 increased significantly when *S. gordonii* was grown in a mixed culture with *Porphyromonas gingivalis* or *Fusobacterium nucleatum* (Hendrickson *et al.*, 2012). It is possible that Sgo\_1216 affects the production of a new and unidentified bacteriocin that inhibits different strains of bacteria.

It is worth noting that *sgo\_1177* is located in an operon with genes for a methionine sulfoxide reductase (*msrAB*), cytochrome *c* biogenesis protein A (*ccdA1*), and a two-component system (*sgo\_1180* and *sgo\_1181*) (Haase *et al.*, 2015).

### **1.3.2.2 The Reduction Pathway**

There is evidence that Gram-positive bacteria also possess a reducing pathway important for cell physiology and pathogenesis (Kouwen and van Dijl, 2009b; Davey *et al.*, 2016b). For example, *C. diphtheriae* has a DsbA homolog (*CdDsbA*) that acts as a

disulfide bond reductase (Um *et al.*, 2015). The crystal structure of *CdDsbA* shows that it is a monomeric TDOR with a typical thioredoxin fold, an inserted  $\alpha$ -helical region, and unique N-terminal extended region. *CdDsbA* has a typical C<sub>126</sub>PFC<sub>129</sub> active site with the conserved *cis*-Proline (P<sub>249</sub>). *CdDsbA* maintains CueP (copper-binding protein) in the reduced, active form in *C. diphtheriae* (Figure 1.7A) (Um *et al.*, 2015).

To deal with methionine oxidation, *C. diphtheriae* uses a cytoplasmic *CdMsrA* to reduce methionine sulfoxide (Tossounian *et al.*, 2015). A unique feature of *CdMsrA* is its flexible ability to receive electrons from two independent pathways, the thioredoxin and the mycothiol pathways (Figure 1.7A). After MetO reduction, *CdMsrA* is regenerated by one of two pathways. In the thioredoxin pathway, the second cysteine in *CdMsrA* (either C<sub>206</sub> or C<sub>215</sub>) attacks C<sub>52</sub> forming an intramolecular disulfide bond between C<sub>52</sub> - and C<sub>206</sub> or C<sub>215</sub>. The third cysteine (either C<sub>206</sub> or C<sub>215</sub>) attacks the intramolecular disulfide bond regenerating C<sub>52</sub> and forming a C<sub>206</sub> - C<sub>215</sub> intramolecular disulfide bond. This disulfide bond is then reduced by the thioredoxin system.

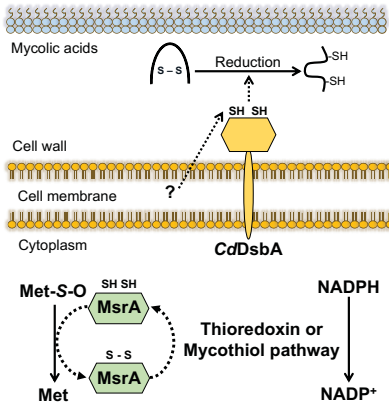
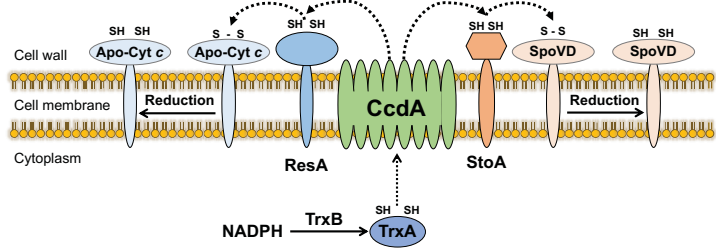
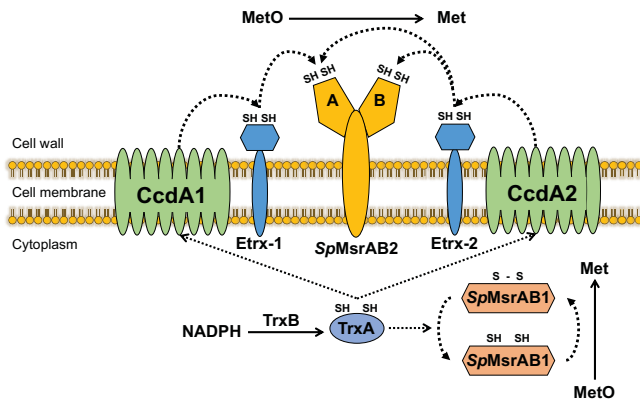
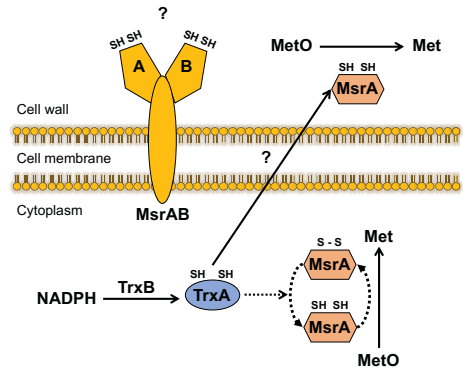
In the mycothiol pathway, mycothiol attacks the sulfenic acid of C<sub>52</sub> and forms a mixed disulfide (C<sub>52</sub> - mycothiol). Next, C<sub>215</sub> attacks the C<sub>52</sub> - mycothiol complex, regenerating C<sub>52</sub> and forming a C<sub>215</sub> – mycothiol complex. Mycothiol is then transferred to C<sub>206</sub> before it is released from *CdMsrA* by the mycothiol /mycoredoxin-1/mycothione reductase pathway (Tossounian *et al.*, 2015).

Similar to *C. diphtheriae*, *Corynebacterium glutamicum* MsrA also uses both thioredoxin and mycothiol pathways for its regeneration (Si *et al.*, 2015). Unlike MsrA, *C. glutamicum* MsrB utilized the thioredoxin system only for regeneration and showed a limited role in oxidative stress resistance (Si *et al.*, 2017).

In *B. subtilis*, the reducing pathway consists of an integral membrane protein CcdA (cytochrome *c* defective protein A), and two extracytoplasmic TDORs, StoA and ResA. CcdA is homologous to the membrane portion ( $\beta$ -domain) of the *E. coli* DsbD, but it lacks the  $\alpha$  and  $\gamma$  domains of DsbD. CcdA is a 26-kDa integral membrane protein that was first identified as a protein required for cytochrome *c* synthesis in *B. subtilis* (Schiott *et al.*, 1997a; Schiott *et al.*, 1997b). A few years later, CcdA was also found to play a role in spore synthesis (Schiott and Hederstedt, 2000).

**Figure 1.7 The reducing pathways in Gram-positive bacteria.**

**A.** The reducing pathway in *C. diphtheriae*. *CdDsbA* is a reductase that reduces CueP. Question mark indicates unidentified redox partner(s) (Um *et al.*, 2015). Reduction of Met-S-O by cytoplasmic MsrA. The oxidized MsrA is reduced by the thioredoxin or mycothiol pathways in the cytoplasm (Tossounian *et al.*, 2015). **B.** The reducing pathway in *B. subtilis*. *CcdA* transfers electrons from the thioredoxin system in the cytoplasm to the extracytoplasmic reductase, ResA and StoA. ResA and StoA are membrane-associated TDORs involved in cytochrome *c* maturation and sporulation by reducing apo-cytochrome *c* and the membrane-bound penicillin-binding protein SpoVD, respectively. Adapted from Kouwen and van Dijl (2009b). **C.** The reducing pathway in *S. pneumoniae*. Extracytoplasmic *SpMsrAB2* involves in the reduction of MetO. *SpMsrAB2* is regenerated by two thioredoxin-like lipoproteins Etrx1 and Etrx2 that receive electrons from *CcdA1* and *CcdA2*. Cytoplasmic *SpMsrAB1* involves in the reduction of MetO. Adapted from Saleh *et al.* (2013) and Kim *et al.* (2009). **D.** The reducing pathway in *S. gordonii*. MsrA reduces Met-S-O in the cytoplasm and cell envelope. Question mark indicated unidentified MsrA redox partner(s). *S. gordonii* also processes MsrAB, but its role in MetO reduction is unknown. Arrows indicate the flow of electrons.

**A.****B.****C.****D.**

Unlike *B. subtilis*, *Bacillus anthracis* possesses two CcdA proteins, CcdA1 and CcdA2. While both are involved in cytochrome *c* maturation and virulence regulation, only CcdA2 is required for sporulation (Han and Wilson, 2013).

CcdA was found to cooperate with ResA in cytochrome *c* maturation (Figure 1.7B). ResA is involved in the reduction of the apo-cytochrome *c*, which counteracts the oxidation of apo-cytochrome *c* by BdbCD (Erlendsson and Hederstedt, 2002; Erlendsson *et al.*, 2003; Le Brun *et al.*, 2000). ResA is an extracytoplasmic, membrane associated, TDOR in *B. subtilis*. The crystal structure of ResA shows that it is a monomeric TDOR with a thioredoxin domain containing the active site C<sub>74</sub>E<sub>75</sub>P<sub>76</sub>C<sub>77</sub>. ResA is a reductase with a very low redox potential of -256 mV, and it preferentially reduces an oxidized CXXCH motif within apo-cytochrome *c* (Lewin *et al.*, 2008; Crow *et al.*, 2004).

An interesting feature of ResA is that it undergoes a redox-dependent conformational change between its oxidized and reduced states. Reduced ResA assumes a surface cavity near the active site that recognizes the oxidized apo-cytochrome *c*. This confirmation requires the movement of multiple amino acids. For example, E<sub>80</sub> residue is buried in the oxidized ResA, but surface exposed in the reduced protein. In addition to E<sub>80</sub>, other amino acids such as E<sub>75</sub>, K<sub>79</sub>, D<sub>136</sub>, P<sub>139</sub>, L<sub>140</sub>, P<sub>141</sub>, and T<sub>159</sub> also rearranged during ResA reduction (Crow *et al.*, 2004; Hodson *et al.*, 2008; Lewin *et al.*, 2006).

CcdA also cooperates with StoA (sporulation thiol-disulfide oxidoreductase A) in endospore production in *B. subtilis* (Figure 1.7B) (Schiott and Hederstedt, 2000; Erlendsson *et al.*, 2004). StoA is a 17-kDa, extracytoplasmic, and membrane-associated TDOR. StoA has reductase activity with a low redox potential -248 mV (Tanaka *et al.*, 2004; Crow *et al.*, 2009b). The crystal structure of StoA shows a typical thioredoxin fold with the active site C<sub>65</sub>P<sub>66</sub>P<sub>67</sub>C<sub>68</sub> motif. Both cysteines in the active site are needed for the activity of StoA. Unlike ResA, the reduction of StoA did not result in a rearrangement of the protein structure (Crow *et al.*, 2009b). StoA also counteracts the oxidation effect of BdbD on extracytoplasmic proteins. Thus, inactivation of *bdbD* suppresses the sporulation defect of *stoA* mutant (Erlendsson *et al.*, 2004).

Recently, it has been shown that StoA reduces a disulfide bond in the membrane-bound penicillin-binding protein SpoVD, which is required for endospore cortex

synthesis in *B. subtilis* (Liu *et al.*, 2010; Bukowska-Faniband and Hederstedt, 2017). Oxidized SpoVD contains a disulfide bond (C<sub>332</sub> - C<sub>351</sub>) closed to the active site of the penicillin-binding domain. This disulfide bond is formed by BdbD. The disulfide bond blocks the function of SpoVD in cortex synthesis. Thus, the reduction and formation of this disulfide bond in SpoVD act as an on/off switch that regulates SpoVD activity in *B. subtilis*. The SpoVDC<sub>332D</sub> variant was able to suppress the effect of *ccdA* or *stoA* mutants on spore cortex synthesis (Liu *et al.*, 2010; Bukowska-Faniband and Hederstedt, 2017).

Another example of reducing pathways in Gram-positive bacteria is the reduction of methionine sulfoxide in *Streptococcus pneumoniae*. *S. pneumoniae* has both intracellular and extracellular methionine sulfoxide reductases, *SpMsrAB1* and *SpMsrAB2*, respectively (Figure 1.7C). Both proteins contain the MsrA and MsrB domains allowing the reduction of the two isoforms of Met-O (Saleh *et al.*, 2013; Kim *et al.*, 2009; Andisi *et al.*, 2012). The crystal structure of *SpMsrAB1* shows that it consists of an N-terminal MsrA domain, a C-terminal MsrB domain, and a linker region. Interestingly, the  $K_m$  of *SpMsrAB1* for Met-S-O is 20-fold higher than that for Met-R-O, suggesting that the MsrB domain has a much higher affinity for the substrate than the MsrA domain (Kim *et al.*, 2009).

Unlike intracellular methionine sulfoxide reductases that can be reduced directly by thioredoxin, the extracytoplasmic *SpMsrAB2* is regenerated by two surface-exposed thioredoxin-like lipoproteins Etrx1 and Etrx2. Etrx1 can reduce MsrA domain of *SpMsrAB2*, whereas Etrx2 is capable of reducing both domains (Figure 1.7C). Crystal structures of Etrx1 and Etrx2 are quite similar with a thioredoxin-like fold containing the active site CXXC motif (C<sub>84</sub>SIC<sub>87</sub> in Etrx1 and C<sub>81</sub>GPC<sub>84</sub> in Etrx2), and a conserved *cis*-proline residue (P<sub>156</sub> in Etrx1 and P<sub>153</sub> in Etrx2), which is located near the active site. Some of the key differences between Etrx1 and Etrx2 structures including the presence of eight extra residues forming a coil at the C-terminus of Etrx2, and the hydrophobic cavity close to the active site observed in Etrx2 but not Etrx1. The redox potentials of Etrx1 and Etrx2 were  $-191 \pm 6\text{mV}$  and  $-282 \pm 16.5\text{mV}$ , respectively (Saleh *et al.*, 2013).

Etrx1 and Etrx2 acquire electrons from CcdA1 and CcdA2, which receive the electrons from the cytoplasmic thioredoxins (Figure 1.7C). This reducing pathway is required for virulence and oxidative stress resistance in *S. pneumoniae*. Loss of either *SpMsrAB2* or both Etrx1 and Etrx2 accelerated phagocytosis and killing of *S. pneumoniae* (Saleh *et al.*, 2013; Andisi *et al.*, 2012).

*S. gordonii* produces more than 1 mM of H<sub>2</sub>O<sub>2</sub> and it lacks catalase (Zheng *et al.*, 2011), but does have a superoxide dismutase and a methionine sulfoxide reductase (Msr) (Jakubovics *et al.*, 2002; Lei *et al.*, 2011). The genome of *S. gordonii* contains two *msr* genes, *msrA* and *msrAB*. MsrA, a 36-kDa protein, was found mostly in the cytoplasm and only a trace amount was detected on the cell surface (Lei *et al.*, 2011). MsrA protects cellular proteins by converting MetO back to Met (Figure 1.7D) (Lei *et al.*, 2011). *msrA* mutants showed increased sensitivity to H<sub>2</sub>O<sub>2</sub>, and a defect in biofilm formation in the presence of exogenous H<sub>2</sub>O<sub>2</sub> (Lei *et al.*, 2011; Vriesema *et al.*, 2000). In contrast, the role of MsrAB in oxidative stress resistance in *S. gordonii* has not been investigated (Figure 1.7D).



## 1.4 Rationale, Hypothesis, and Objectives of this Study

Bacterial disulfide oxidases are known to require redox partners for regeneration (Rietsch and Beckwith, 1998; Landeta *et al.*, 2018). The recent discovery of SdbA in *S. gordonii* provided an important first step to understand the mechanism of disulfide bond formation in this organism (Davey *et al.*, 2013). However, there are questions that remain unanswered, including how SdbA is reoxidized after it introduces a disulfide bond into its substrate.

**Hypothesis:** SdbA uses a redox partner for regeneration.

### **Objectives:**

- Identify the potential redox partner(s) of SdbA in *S. gordonii*.
- Investigate the effects of inactivation of these redox partners on *sdbA*-associated phenotypes in *S. gordonii*.
- Investigate the enzymatic activity of these redox partners and their roles in SdbA reoxidation.
- Investigate the mechanisms of SdbA interaction with its redox partner and its substrate.

*S. gordonii* is constantly exposed to H<sub>2</sub>O<sub>2</sub>, which can oxidize and damage proteins (Barnard and Stinson, 1999; Zhu and Kreth, 2012; Ezraty *et al.*, 2017). How *S. gordonii* deal with this problem is not well studied. The genome of *S. gordonii* has two *msr* genes, *msrA* and *msrAB* (Vickerman *et al.*, 2007). Previous work showed that MsrA is required for oxidative stress resistance (Lei *et al.*, 2011). However, the role of MsrAB in oxidative stress resistance has not been investigated. In addition, the pathway that regenerates MsrAB is unknown.

**Hypothesis:** MsrAB is part of a reducing pathway that protects *S. gordonii* from oxidative stress.

**Objectives:**

- Investigate the role of MsrAB in protection against oxidative stress.
- Investigate the enzymatic activity of MsrAB.
- Identify the redox partners of MsrAB and examine the role of MsrAB redox partner in oxidative stress resistance and MsrAB regeneration.

Both prokaryotic and eukaryotic cells use disulfide bond isomerase to correct the non-native disulfide bonds and protect proteins from oxidative damage. To date, no disulfide bond isomerization pathway has been identified in Gram-Positive organisms (Gleiter and Bardwell, 2008; Depuydt *et al.*, 2011; Cho and Collet, 2013). Thus, the last goal of this work is to use *S. gordonii* as a model organism to investigate the disulfide bond isomerization pathway.

**Hypothesis:** *S. gordonii* has a disulfide bond isomerization pathway.

**Objectives:**

- Identify the disulfide bond isomerases and its redox partner in *S. gordonii*.
- Investigate the enzymatic activity of the disulfide bond isomerase.
- Examine the role of the disulfide bond isomerization pathway in the production and redox state of anti-CR1 single chain antibody, a protein with two disulfide bonds.
- Investigate the role of the disulfide bond isomerization pathway in protection against copper-induced oxidative stress in *S. gordonii*.

## Chapter 2. Materials and Methods

### 2.1 Bacterial Strains and Growth Conditions

Bacterial strains and plasmids used in this study are listed in Table 2.1. *S. gordonii* SecCR1 was used as the parent strain (Knight *et al.*, 2008). Unless otherwise indicated, *S. gordonii* strains were grown at 37°C, 5% CO<sub>2</sub> in HTVG (per ml: 5 mg of glucose, 35 mg of tryptone, 0.04 µg of *p*-aminobenzoic acid, 0.2 µg of thiamine-HCl, 1 µg of nicotinamide, and 0.2 µg of riboflavin, 100 mM HEPES, pH 7.6) (Burne *et al.*, 1999). For bacteriocin production, *S. gordonii* and *S. mitis* I18 strains were grown in brain heart infusion (BHI, WISENT) with 5% heat-inactivated calf serum (Invitrogen). *S. gordonii* strains were also grown in BHI with 5% heat-inactivated calf serum for genetic competence assays and in tryptic soy broth (TSB, WISENT) for methionine sulfoxide sensitivity assay. For H<sub>2</sub>O<sub>2</sub> sensitivity assay, *S. gordonii* strains were plated on TYG agar (per 100 ml: 1 g of tryptone, 0.5 g of yeast extract, 0.2 g of glucose, 0.3 g of K<sub>2</sub>HPO<sub>4</sub>).

For biofilm formation, *S. gordonii* was grown in biofilm medium containing 58 mM K<sub>2</sub>HPO<sub>4</sub>, 15 mM KH<sub>2</sub>PO<sub>4</sub>, 10 mM (NH<sub>4</sub>)<sub>2</sub>SO<sub>4</sub>, 35 mM NaCl, 0.8% (wt/vol) glucose, 0.2% (wt/vol) casamino acids, and 10 µM MgCl<sub>2</sub> (pH 7.4). The biofilm medium was made fresh and supplemented with vitamins (0.04 mM nicotinic acid, 0.1 mM pyridoxine HCl, 0.01 mM pantothenic acid, 1 µM riboflavin, 0.3 µM thiamin HCl, and 0.05 µM D-biotin), and amino acids (4 mM L-glutamic acid, 1 mM L-arginine HCl, 1.3 mM L-cysteine HCl, and 0.1 mM L-tryptophan), and 2 mM MgSO<sub>4</sub>·7H<sub>2</sub>O) and filter-sterilized (Loo *et al.*, 2000). *Escherichia coli* was grown at 37°C in Luria-Bertani broth (per 100 ml: 1 g tryptone, 1 g NaCl, 0.5 g yeast extract) with shaking (180 rpm).

When needed, antibiotics (BioShop) were used at the following concentrations: for *S. gordonii*, spectinomycin (250 µg/ml); kanamycin (250 µg/ml); tetracycline (10 µg/ml); erythromycin (10 µg/ml); chloramphenicol (5 µg/ml); rifampin (100 µg/ml); and for *E. coli*, ampicillin (100 µg/ml); kanamycin (50 µg/ml); chloramphenicol (25 µg/ml); and tetracycline (10 µg/ml).

**Table 2.1 Bacterial strains and plasmids used in this study**

Strains/plasmids	Relevant characteristics	Source
<i>Streptococcus gordonii</i>		
SecCR1	Challis DL-1, <i>hppG::tet</i> , secretes anti-CR1 scFv, Tet <sup>R</sup> , Spec <sup>R</sup>	(Knight <i>et al.</i> , 2008)
<i>degP</i>	SecCR1, <i>degP::ermAM</i> , Tet <sup>R</sup> , Spec <sup>R</sup> , Erm <sup>R</sup>	(Davey <i>et al.</i> , 2016a)
<i>sdbA</i>	SecCR1, <i>sdbA::ermAM</i> , Tet <sup>R</sup> , Spec <sup>R</sup> , Erm <sup>R</sup>	(Davey <i>et al.</i> , 2013)
<i>sdbAdegP</i>	SecCR1, <i>sdbA::ermAM</i> , <i>degP::aphA3</i> , Tet <sup>R</sup> , Spec <sup>R</sup> , Erm <sup>R</sup> , Kan <sup>R</sup>	(Davey <i>et al.</i> , 2016a)
<i>ccdA1</i>	SecCR1, <i>ccdA1::aphA3</i> , Tet <sup>R</sup> , Spec <sup>R</sup> , Kan <sup>R</sup>	This study
<i>ccdA2</i>	SecCR1, <i>ccdA2::ermAM</i> , Tet <sup>R</sup> , Spec <sup>R</sup> , Erm <sup>R</sup>	This study
<i>ccdA2degP</i>	SecCR1, <i>ccdA2::ermAM</i> , <i>degP::aphA3</i> , Tet <sup>R</sup> , Spec <sup>R</sup> , Erm <sup>R</sup> , Kan <sup>R</sup>	This study
<i>sdbB</i>	SecCR1, <i>sgo_1171::ermAM</i> , Tet <sup>R</sup> , Spec <sup>R</sup> , Erm <sup>R</sup>	(Davey <i>et al.</i> , 2013)
<i>sdbB</i>	SecCR1, <i>sgo_1171::aphA3</i> , Tet <sup>R</sup> , Spec <sup>R</sup> , Kan <sup>R</sup>	This study
<i>sdbBdegP</i>	SecCR1, <i>sgo_1171::ermAM</i> , <i>degP::aphA3</i> , Tet <sup>R</sup> , Spec <sup>R</sup> , Erm <sup>R</sup> , Kan <sup>R</sup>	This study
<i>sgo_1177</i>	SecCR1, <i>sgo_1177::ermAM</i> , Tet <sup>R</sup> , Spec <sup>R</sup> , Erm <sup>R</sup>	(Davey <i>et al.</i> , 2013)
<i>msrAB</i>	SecCR1, <i>sgo_1176::ermAM</i> , Tet <sup>R</sup> , Spec <sup>R</sup> , Erm <sup>R</sup>	This study
<i>sgo_1177ccdA1</i>	SecCR1, <i>sgo_1177::ermAM</i> , <i>ccdA1::aphA3</i> , Tet <sup>R</sup> , Spec <sup>R</sup> , Kan <sup>R</sup> , Erm <sup>R</sup>	This study
<i>sgo_1177ccdA1 complement</i>	SecCR1, <i>ccdA1sgo_1177</i> complemented on the chromosome, Tet <sup>R</sup> , Spec <sup>R</sup> , Cm <sup>R</sup>	This study
<i>sdbBccdA2</i>	SecCR1, <i>sgo_1171::aphA3</i> , <i>ccdA2::ermAM</i> , Tet <sup>R</sup> , Spec <sup>R</sup> , Kan <sup>R</sup> , Erm <sup>R</sup>	This study
<i>sdbBccdA2degP</i>	SecCR1, <i>sgo_1171::aphA3</i> , <i>ccdA2::ermAM</i> , <i>degP::cat</i> Tet <sup>R</sup> , Spec <sup>R</sup> , Kan <sup>R</sup> , Erm <sup>R</sup> , Cat <sup>R</sup>	This study
<i>sdbBccdA2 complement</i>	SecCR1, <i>ccdA2sgo_1171</i> complemented on the chromosome, Tet <sup>R</sup> , Spec <sup>R</sup> , Cm <sup>R</sup>	This study
<i>sdbBccdA1</i>	SecCR1, <i>sgo_1171::ermAM</i> , <i>ccdA1::aphA3</i> , Tet <sup>R</sup> , Spec <sup>R</sup> , Kan <sup>R</sup> , Erm <sup>R</sup>	This study
<i>sgo_1177ccdA2</i>	SecCR1, <i>sgo_1177::aphA3</i> , <i>ccdA2::ermAM</i> , Tet <sup>R</sup> , Spec <sup>R</sup> , Kan <sup>R</sup> , Erm <sup>R</sup>	This study
<i>ccdA1ccdA2</i>	SecCR1, <i>ccdA1::aphA3</i> , <i>ccdA2::ermAM</i> , Tet <sup>R</sup> , Spec <sup>R</sup> , Kan <sup>R</sup> , Erm <sup>R</sup>	This study

Strains/plasmids	Relevant characteristics	Source
<i>sdhA<sub>C89A</sub>degP</i>	SecCR1, <i>sdhA<sub>C89A</sub>::aphA3</i> , <i>degP::ermAM</i> , Tet <sup>R</sup> , Spec <sup>R</sup> , Erm <sup>R</sup> , Kan <sup>R</sup>	(Davey <i>et al.</i> , 2016a)
<i>Streptococcus gordonii</i> Wicky WK1	<i>S. gordonii</i> Wicky, Rif <sup>R</sup> , source of gDNA for genetic competence assay	(Lunsford and London, 1996)
<i>Streptococcus mitis</i> I18	Indicator strain for bacteriocin activity	(Heng <i>et al.</i> , 2007)
<b><i>Escherichia coli</i></b>		
M15	Protein expression host, pRE4, Kan <sup>R</sup>	Qiagen
SdbB	M15 carrying pQE-30- <i>sdbB</i> , Kan <sup>R</sup> , Amp <sup>R</sup>	This study
Sgo_1177	M15 carrying pQE-30- <i>sgo_1177</i> , Kan <sup>R</sup> , Amp <sup>R</sup>	This study
XL-1 Blue	Cloning host, Tet <sup>R</sup>	Stratagene
SdbA	XL-1 Blue carrying pQE-30- <i>sdbA</i> , Tet <sup>R</sup> , Amp <sup>R</sup>	(Davey <i>et al.</i> , 2013)
CcdA1	XL-1 Blue carrying pQE-30- <i>ccdA1</i> , Tet <sup>R</sup> , Amp <sup>R</sup>	This study
CcdA2	XL-1 Blue carrying pQE-30- <i>ccdA2</i> , Tet <sup>R</sup> , Amp <sup>R</sup>	This study
MsrAB	XL-1 Blue carrying pQE-30- <i>msrAB</i> , Tet <sup>R</sup> , Amp <sup>R</sup>	This study
Trx-2	XL-1 Blue carrying pQE-30- <i>trx-2</i> , Tet <sup>R</sup> , Amp <sup>R</sup>	(Lee <i>et al.</i> , Unpublished)
TrxB	XL-1 Blue carrying pQE-30- <i>trxB</i> , Tet <sup>R</sup> , Amp <sup>R</sup>	(Lee <i>et al.</i> , Unpublished)
SdbB <sub>C81A</sub>	XL-1 Blue carrying pQE-30- <i>SdbB<sub>C81A</sub></i> , Tet <sup>R</sup> , Amp <sup>R</sup>	This study
SdbB <sub>C84A</sub>	XL-1 Blue carrying pQE-30- <i>SdbB<sub>C84A</sub></i> , Tet <sup>R</sup> , Amp <sup>R</sup>	This study
SdbA <sub>C86A</sub>	XL-1 Blue carrying pQE-30- <i>SdbA<sub>C86A</sub></i> , Tet <sup>R</sup> , Amp <sup>R</sup>	(Davey <i>et al.</i> , 2016a)
SdbA <sub>C89A</sub>	XL-1 Blue carrying pQE-30- <i>SdbA<sub>C89A</sub></i> , Tet <sup>R</sup> , Amp <sup>R</sup>	(Davey <i>et al.</i> , 2016a)
SdbA <sub>K91E</sub>	XL-1 Blue carrying pQE-30- <i>SdbA<sub>K91E</sub></i> , Tet <sup>R</sup> , Amp <sup>R</sup>	(Lee <i>et al.</i> , Unpublished)
SdbA <sub>R119E</sub>	XL-1 Blue carrying pQE-30- <i>SdbA<sub>R119E</sub></i> , Tet <sup>R</sup> , Amp <sup>R</sup>	(Lee <i>et al.</i> , Unpublished)
SdbA <sub>V152A</sub>	XL-1 Blue carrying pQE-30- <i>SdbA<sub>V152A</sub></i> , Tet <sup>R</sup> , Amp <sup>R</sup>	(Lee <i>et al.</i> , Unpublished)

Strains/plasmids	Relevant characteristics	Source
SdbA <sub>P156T</sub>	XL-1 Blue carrying pQE-30-SdbA <sub>P156T</sub> , Tet <sup>R</sup> , Amp <sup>R</sup>	(Lee <i>et al.</i> , Unpublished)
SdbA <sub>T172E</sub>	XL-1 Blue carrying pQE-30-SdbA <sub>T172E</sub> , Tet <sup>R</sup> , Amp <sup>R</sup>	(Lee <i>et al.</i> , Unpublished)
SdbA <sub>S154E</sub>	XL-1 Blue carrying pQE-30-SdbA <sub>S154E</sub> , Tet <sup>R</sup> , Amp <sup>R</sup>	(Lee <i>et al.</i> , Unpublished)
SdbA <sub>F174E</sub>	XL-1 Blue carrying pQE-30-SdbA <sub>F174E</sub> , Tet <sup>R</sup> , Amp <sup>R</sup>	(Lee <i>et al.</i> , Unpublished)
SdbA <sub>Q92A</sub>	XL-1 Blue carrying pQE-30-SdbA <sub>Q92A</sub> , Tet <sup>R</sup> , Amp <sup>R</sup>	This study
SdbA <sub>Q92E</sub>	XL-1 Blue carrying pQE-30-SdbA <sub>Q92E</sub> , Tet <sup>R</sup> , Amp <sup>R</sup>	This study
SdbA <sub>Q92A/S154E</sub>	XL-1 Blue carrying pQE-30-SdbA <sub>Q92A/S154E</sub> , Tet <sup>R</sup> , Amp <sup>R</sup>	This study
SdbA <sub>Q92E/S154E</sub>	XL-1 Blue carrying pQE-30-SdbA <sub>Q92E/S154E</sub> , Tet <sup>R</sup> , Amp <sup>R</sup>	This study
JM83/pDsbC	<i>E. coli</i> JM83 carrying pTrc99a- <i>dsbC</i> , Amp <sup>R</sup>	(Maskos <i>et al.</i> , 2003)
<b>Plasmids</b>		
pQE-30-SdbA	pQE-30:: <i>sdbA</i> , His <sub>6</sub> -tag, Amp <sup>R</sup>	(Davey <i>et al.</i> , 2013)
pQE-30-SdbB	pQE-30:: <i>sdbB</i> , His <sub>6</sub> -tag, Amp <sup>R</sup>	This study
pQE-30-Sgo_1177	pQE-30:: <i>sgo_1177</i> , His <sub>6</sub> -tag, Amp <sup>R</sup>	This study
pQE-30-CcdA1	pQE-30:: <i>ccdA1</i> , N- and C-terminal His <sub>6</sub> and C-terminal HA-tag, Amp <sup>R</sup>	This study
pQE-30-CcdA2	pQE-30:: <i>ccdA2</i> , N- and C-terminal His <sub>6</sub> and C-terminal HA-tag, Amp <sup>R</sup>	This study
pQE-30-MsrAB	pQE-30:: <i>msrAB</i> , His <sub>6</sub> -tag, Amp <sup>R</sup>	This study
pQE-30-Trx-2	pQE-30:: <i>trx-2</i> , His <sub>6</sub> -tag, Amp <sup>R</sup> thioredoxin gene from <i>Streptococcus pyogenes</i> M18	(Lee <i>et al.</i> , Unpublished)
pQE-30-TrxB	pQE-30:: <i>trxB</i> , His <sub>6</sub> -tag, Amp <sup>R</sup> thioredoxin reductase gene from <i>Streptococcus pyogenes</i> M18	(Lee <i>et al.</i> , Unpublished)
pQE-30-SdbA <sub>C86A</sub>	pQE-30:: <i>sdbA</i> <sub>C86A</sub> , His <sub>6</sub> -tag, Amp <sup>R</sup>	(Davey <i>et al.</i> , 2016a)
pQE-30-SdbA <sub>C89A</sub>	pQE-30:: <i>sdbA</i> <sub>C89A</sub> , His <sub>6</sub> -tag, Amp <sup>R</sup>	(Davey <i>et al.</i> , 2016a)
pQE-30-SdbB <sub>C81A</sub>	pQE-30:: <i>sdbB</i> <sub>C81A</sub> , His <sub>6</sub> -tag, Amp <sup>R</sup>	This study
pQE-30-SdbB <sub>C84A</sub>	pQE-30:: <i>sdbB</i> <sub>C84A</sub> , His <sub>6</sub> -tag, Amp <sup>R</sup>	This study
pQE-30-SdbA <sub>K91E</sub>	pQE-30:: <i>sdbA</i> <sub>K91E</sub> , His <sub>6</sub> -tag, Amp <sup>R</sup>	(Lee <i>et al.</i> , Unpublished)

<b>Strains/plasmids</b>	<b>Relevant characteristics</b>	<b>Source</b>
pQE-30-SdbA <sub>R119E</sub>	pQE-30:: <i>sdbA</i> <sub>R119E</sub> , His <sub>6</sub> -tag, Amp <sup>R</sup>	(Lee <i>et al.</i> , Unpublished)
pQE-30-SdbA <sub>V152A</sub>	pQE-30:: <i>sdbA</i> <sub>V152A</sub> , His <sub>6</sub> -tag, Amp <sup>R</sup>	(Lee <i>et al.</i> , Unpublished)
pQE-30-SdbA <sub>P156T</sub>	pQE-30:: <i>sdbA</i> <sub>P156T</sub> , His <sub>6</sub> -tag, Amp <sup>R</sup>	(Lee <i>et al.</i> , Unpublished)
pQE-30-SdbA <sub>T172E</sub>	pQE-30:: <i>sdbA</i> <sub>T172E</sub> , His <sub>6</sub> -tag, Amp <sup>R</sup>	(Lee <i>et al.</i> , Unpublished)
pQE-30-SdbA <sub>S154E</sub>	pQE-30:: <i>sdbA</i> <sub>S154E</sub> , His <sub>6</sub> -tag, Amp <sup>R</sup>	(Lee <i>et al.</i> , Unpublished)
pQE-30-SdbA <sub>F174E</sub>	pQE-30:: <i>sdbA</i> <sub>F174E</sub> , His <sub>6</sub> -tag, Amp <sup>R</sup>	(Lee <i>et al.</i> , Unpublished)
pQE-30-SdbA <sub>Q92A</sub>	pQE-30:: <i>sdbA</i> <sub>Q92A</sub> , His <sub>6</sub> -tag, Amp <sup>R</sup>	This study
pQE-30-SdbA <sub>Q92E</sub>	pQE-30:: <i>sdbA</i> <sub>Q92E</sub> , His <sub>6</sub> -tag, Amp <sup>R</sup>	This study
pQE-30-SdbA <sub>Q92A/S154E</sub>	pQE-30:: <i>sdbA</i> <sub>Q92A/S154E</sub> , His <sub>6</sub> -tag, Amp <sup>R</sup>	This study
pQE-30-SdbA <sub>Q92E/S154E</sub>	pQE-30:: <i>sdbA</i> <sub>Q92E/S154E</sub> , His <sub>6</sub> -tag, Amp <sup>R</sup>	This study

## **2.2 Genetic Manipulation of *E. coli***

### **2.2.1 Isolation of Plasmid DNA from *E. coli***

Plasmids were isolated from *E. coli* by the alkaline lysis method (Birnboim and Doly, 1979). A 1.5 ml culture of *E. coli* was centrifuged (12 000 x g, 5 min). The pellet was resuspended in 100 µl of GTE buffer (50 mM glucose, 10 mM EDTA, 25 mM Tris-HCl, pH 8.0), 186 µl *Milli-Q* water, and 2 µl RNase A (10 mg/ml). Cells lysis were then achieved by the addition of 10 µl 20% (w/v) sodium dodecyl sulfate (SDS) and 4 µl 10 M NaOH followed by gentle inversions and incubation for 5 min at room temperature. The lysate was then neutralized with 150 µl of cold potassium acetate solution [60% (v/v) 5 M potassium acetate, 28.5% (v/v) *Milli-Q* water and 11.5% (v/v) glacial acetic acid] followed by incubation on ice for 10 minutes. Precipitates were removed by centrifugation (14 000 x g, 10 min, 4°C). The supernatant was transferred to a new 1.5 ml tube and extracted with chloroform. The aqueous layer was transferred to a new tube, and the plasmid DNA was precipitated with ice cold ethanol. The resulting pellets were resuspended in 15 µl of TE buffer (10 mM Tris, 10 mM EDTA, pH 8.0).

For sequencing, plasmids were isolated from 5 ml cultures using the QIAprep Spin miniprep kit (QIAGEN, Mississauga, Ontario, Canada) according to the manufacturer's instructions. Agarose gel electrophoresis (see PCR section below) was used to estimate the concentration of isolated plasmid by comparing the intensity of the plasmid band to the intensity of the DNA markers using ImageJ.

### **2.2.2 Transformation of *E. coli***

Plasmid DNA was transformed into competent *E. coli* cells using the protocol described by Sambrook *et al.* (1989). Competent *E. coli* cells were prepared by inoculating 99 ml of LB with 1 ml of overnight culture and incubated until OD<sub>600</sub> reached 0.3. The cells were harvested by centrifugation (10 000 x g, 10 minutes, 4°C). The cell pellet was washed with 100 ml of cold transformation buffer 1 (10 mM Tris, 150 mM



NaCl, pH 7.5) and then gently resuspended in 100 ml of cold transformation buffer 2 (50 mM CaCl<sub>2</sub>) and incubated on ice for 45 minutes. The cells were collected by centrifugation and resuspended in 10 ml of cold transformation buffer 2 containing 20% (v/v) glycerol. The competent cells were stored in aliquots at -80 °C.

For transformation, 200 µl of competent cells were thawed on ice for 10 minutes and an aliquot of DNA and 100 µl transformation buffer 3 (10 mM Tris, 50 mM CaCl<sub>2</sub>, and 10 mM, MgSO<sub>4</sub>, pH 7.5) were added. The cell suspension was gently mixed and incubated on ice for 45 minutes. The cells were then heated at 37°C for 2 minutes and then incubated at room temperature for 10 minutes. Then, 500 µl of LB was added to the cell suspension and incubated for 60 minutes at 37°C. The culture was then plated on LB agar plates containing the appropriate antibiotics and incubated for 24 h.

## **2.3 Genetic Manipulation of *S. gordonii***

### **2.3.1 Isolation of Genomic DNA from *S. gordonii***

To isolate the genomic DNA from *S. gordonii*, 1.5 ml of overnight culture was centrifuged at 12 000 x g for 5 minutes. The pellet was re-suspended in 100 µl TE buffer, 100 µl chloroform, and 200 mg glass beads (500 µm, VWR International). The suspension was vortexed vigorously for 1 minute and then centrifuged. The aqueous layer was transferred to a new tube, and 1 µl was used as DNA template for polymerase chain reaction (PCR).

For experiments to assess transformation frequency, the genomic DNA was isolated from *S. gordonii* Wicky WK1 (Lunsford and London, 1996). A 100 ml of overnight culture was added to 100 ml of fresh BHI and the culture was grown for 2 h. The cells were harvested by centrifugation and re-suspended in 1 ml of TE buffer containing 1% (w/v) lysozyme (Sigma), 20 U/ml mutanolysin (Sigma), and 10 µl of 10 mg/ml RNase A (Sigma). The cell suspension was incubated for 60 minutes at 37°C and 2% (w/v) SDS (BioShop) was added. The mixture was incubated at 37°C for 30 minutes to lyse the cells. The lysate was vortexed and then centrifuged at 14 000 x g for 10

minutes. The supernatant containing the DNA was extracted with two volumes of chloroform. The aqueous layer was transferred to a new tube and the DNA was precipitated by incubation with 95% ethanol containing 2.5 % potassium acetate for 1 hour at -80°C. The DNA was washed with 70% ethanol, air-dried and dissolved in 3 ml TE buffer and stored in 200 µl-aliquots at -20°C.

### **2.3.2 Transformation of *S. gordonii***

Genetic transformation of *S. gordonii* was performed as described previously with modifications (Perry and Kuramitsu, 1981). Briefly, 100 µl of an overnight culture was sub-cultured into 4 ml of pre-warmed BHI containing 5% (v/v) heat-inactivated calf serum (BHIS). The culture was incubated for 1 to 2 hours ( $OD_{600} \approx 0.15$ ). DNA was then added to 750 µl of the culture and further incubated for 30 minutes. A fresh 750 µl of pre-warmed BHIS was then added and the culture was incubated for an additional 90 minutes. The culture was centrifuged at 10 000 x g for 2 minutes and 1 ml of the supernatant was discarded. The cell pellet was re-suspended in the remaining 0.5 ml liquid and aliquots (100 µl) were plated on BHI agar containing the appropriate antibiotics. The agar plates were incubated for 48 h.

### **2.3.3 Polymerase Chain Reaction (PCR)**

Primers used in this study were designed based on the sequenced genome of *S. gordonii* Challis (Vickerman *et al.*, 2007). Primers were synthesized by Alpha DNA (Montreal) and diluted into 10 µM working concentration in *Milli-Q* water. A typical PCR reaction was a 50 µl reaction mixture containing 1 µl template DNA (50 ng/µl), 1 µl 10 µM forward primer, 1 µl 10 µM reverse primer, 5 µl 10 x PCR buffer (New England Biolabs, NEB), 1 µl 10 mM dNTP (10 mM dATP, 10 mM dGTP, 10 mM dCTP, 10 mM dTTP) (Green BioResearch), and 0.25 µl 5 U/µl Taq DNA polymerase (NEB). To generate a blunt-ended PCR product, phusion-HF (High Fidelity) DNA polymerase (NEB) was used. PCR were carried out in an Eppendorf Mastercycler EP S thermo-module

(Eppendorf) with conditions described in Table 2.2. Electrophoresis was used to analyze the PCR products in agarose gels (0.8 %, w/v) prepared in TAE (0.04 M Tris-acetate and 0.001 M EDTA) buffer. Electrophoresis was performed at 110 volts in TAE buffer containing 0.5 µg/ml ethidium bromide.

### **2.3.4 Construction of Knockout Mutants**

The single- and double-gene knockout mutants of *S. gordonii* were constructed by insertional inactivation using the erythromycin resistance cassette (*ermAM*) (Claverys *et al.*, 1995), the kanamycin resistance cassette (*aphA3*) (Dunny *et al.*, 1991), or the chloramphenicol resistance cassette (*cat*) (Vats and Lee, 2001). The antibiotic resistance cassette and the upstream and downstream regions of the target gene were separately amplified by PCR using primers listed in Table 2.3. PCR products were digested with the appropriate restriction enzymes. The digested DNA was electrophoresed on an agarose gel and purified using the DNA Fragment Extraction Kit (DNALand Scientific) according to the manufacturer's instructions. The DNA fragments were ligated using T4 DNA ligase (New England Biolabs). The ligated products were amplified using the outside primers, and the resulting PCR products were used to transform *S. gordonii* SecCR1. The insertion of the *aphA3*, *ermAM*, or *cat* cassette was confirmed by PCR.

### **2.3.5 Construction of Complemented Strains**

To construct the *sdbBccdA2*-complemented mutant, a functional copy of *sdbB* and *ccdA2* genes was introduced back into the chromosome of the *sdbBccdA2* mutant. To achieve this, the *sdbBccdA2* operon plus a portion of the upstream gene (*sgo\_1174*) was amplified using primers SL1061/SL1235 and the PCR product was digested with SphI. A downstream fragment carrying a portion of *sdbB* and *sgo\_1170* was amplified using primers SL869/SL1226 and digested with BamHI. Next, the *cat* resistance cassette was cut from pCopCAT/pUC18 using SphI and BamHI (Vats and Lee, 2001).

**Table 2.2 PCR conditions**

<b>Steps</b>	<b>Temperature</b>	<b>Time</b>
<b>Taq DNA polymerase</b>		
Initial denaturation 35 cycles	95°C	1 minute
Denaturation	94°C	20 seconds
Annealing	48-50°C	20 seconds
Extension	72°C	1 minute/kb
Final extension	72°C	5 minutes
Hold	4°C	
<b>Phusion DNA polymerase</b>		
Initial denaturation 35 cycles	98°C	1 minute
Denaturation	98°C	10 seconds
Annealing	48-55°C	15 seconds
Extension	72°C	30 seconds/kb
Final extension	72°C	5 minutes
Hold	4°C	

**Table 2.3 Primers used in this study**

<b>Primer</b>	<b>Gene</b>	<b>Description*</b>		<b>Sequence</b>
SL609	<i>ermAM</i>	For	Erythromycin	EcoRV TGAGATATCCCGGGCCCA AAATTTGTTTGAT
SL729	<i>ermAM</i>	Rev	Erythromycin	BamHI TACGGATCCAGCGACTCA TAGAATTATTT
SL801	<i>aphA3</i>	For	Kanamycin	BamHI TACGGATCCGCAAGGAAC AGTGAATTGGA
SL823	<i>aphA3</i>	Rev	Kanamycin	KpnI TACGGTACCCAGTTGCGG ATGTA <del>CT</del> CAG
SL1050	<i>ccdA1</i>	For	Knockout	TAAATCTTGGTGTGGGAA AG
SL1051	<i>ccdA1</i>	For	Knockout	KpnI TACGGTACCTCAATATCC AACAACTGCAA
SL1052	<i>ccdA1</i>	Rev	Knockout	TGATTTTTGATTAGAGCA GG
SL1053	<i>ccdA2</i>	For	Knockout	AGAACAGTAGGACTCTCT G
SL1054	<i>ccdA2</i>	Rev	Knockout	EcoRV TACGATATCTCGTTGCGT TACTATCTTT
SL1055	<i>ccdA2</i>	For	Knockout	BamHI TACGGATCCCTCAGCATT TGTATTGGGAA
SL1056	<i>ccdA2</i>	Rev	Knockout	AGTAAAAAACTGCAGC TA
SL1061	<i>sgo_1174</i>	For	Complementation	TGACATATAGTCGGGACA T
SL1235	<i>sdbB</i>	Rev	Complementation	SphI TGAGCATGCTTACTTCAT TTCTTTAAAGG
SL666	<i>pUC19</i> <i>MCs</i>	For	Complementation	SphI ACGCCAAGCTTG <del>CATGCC</del> TGC
SL869	<i>sdbB</i>	For	Complementation	BamHI TACGGATCCGAAAGAAA GACCGCGATTTTC
SL1226	<i>sgo_1170</i>	Rev	RT-PCR/ complementation	GGAACATCACGTGCCCAA G
SL1227	<i>sgo_1170</i>	For	RT-PCR	GTTTTCCACAATCCAAGT C
SL1151	<i>sdbB</i>	For	RT-PCR	GCCAGAACTAATAGAATT G
SL1152	<i>sdbB</i>	Rev	RT-PCR	CTTCGTTGCTGATAGCTC C
SL1065	<i>ccdA2</i>	For	RT-PCR	TCTCTCCCGCTATTTTTCC CT
SL1072	<i>ccdA2</i>	Rev	RT-PCR	CAAATGCTGAGAGAAACT CGT
SL1153	<i>sgo_1177</i>	For	RT-PCR	GAAGGGAAAGACTATGTT G
SL1094	<i>ccdA1</i>	For	RT-PCR	GATTCGGATTTTTGGGAG

<b>Primer</b>	<b>Gene</b>	<b>Description*</b>		<b>Sequence</b>
SL1095	<i>ccdA1</i>	Rev	RT-PCR	GATATTGATAAGTCCCATC
SL1224	<i>sgo_1174</i>	For	RT-PCR	GCTCAGAATCAAGAAAGC A
SL1225	<i>sgo_1174</i>	Rev	RT-PCR	CACCAAGATTCTGCCCTG
SL697	<i>16S rRNA</i>	For	RT-PCR	ATTTATTGGGCGTAAAGCG AGCGC
SL525	<i>16S rRNA</i>	Rev	RT-PCR	GAATTAAACCACATGCTCC ACCGC
SL1157	<i>sdbB</i>	For	Expression	BamHI TGAGGATCCGAAACAAAA AGCAGTAGC
SL1158	<i>sdbB</i>	Rev	Expression	HindIII TGAAAGCTTTTACTTCATTT CTTTAAAGG
SL1159	<i>sgo_1177</i>	For	Expression	BamHI TGAGGATCCTCCACTAACG ATAAAAGCAG
SL1160	<i>sgo_1177</i>	Rev	Expression/ RT-PCR	HindIII TGAAAGCTTTTACTTAATT TCTTTCAGTG
SL1096	<i>ccdA2</i>	For	Expression	BamHI TAGGATCCGAAAGCTTACT TTTCTCAG
SL1295	<i>ccdA2</i>	Rev	Expression	SpeI TAGACTAGTTCCAAATAGC CCCGACAAG
SL334	<i>ccdA2</i>	Rev	Expression	EcoRI CGGAATTCGTTAAGAAGC GTAGTCCGGAACGTC
SL1307	<i>ccdA1</i>	For	Expression	BglII TACAGATCTGCAACAAGTT TTTTGTTCTTTA
SL1308	<i>ccdA1</i>	Rev	Expression	SpeI TACACTAGTTCCGAATAAT GATGCTAAAGC
SL1316	<i>msrAB</i>	For	Expression	BamHI TACGGATCCCGGGTAATCT ATCTGGC
SL1319	<i>msrAB</i>	Rev	Expression	HindIII TACAAGCTTTTAAACATAA TCCAAAAGATAAC
SL1322	<i>sdbB<sub>C81A</sub></i>	For	Expression	TGGGCTTCTTGGGCTGGGC CATGTAAG
SL1323	<i>sdbB<sub>C81A</sub></i>	Rev	Expression	CCCCAAGAAGCCCATTACA TGGCCCAG
SL1324	<i>sdbB<sub>C84A</sub></i>	For	Expression	TGGTGTGGGCCAGCTAAGA AAAGTATG
SL1325	<i>sdbB<sub>C84A</sub></i>	Rev	Expression	CATACTTTTCTTAGCTGGC CCACACCA
SL764	<i>sdbA</i>	For	Expression	BamHI TACGGATCCTCAGCTGTAG AACATGAGCTG
SL1331	<i>sdbA<sub>Q92A</sub></i>	Rev	Expression	TCTGGTAATGCTTTTTGAC AATC
SL1330	<i>sdbA<sub>Q92A</sub></i>	For	Expression	GATTGTCAAAAAGCATTAC CAGA

<b>Primer</b>	<b>Gene</b>	<b>Description*</b>			<b>Sequence</b>
SL763	<i>sdbA</i>	Rev	Expression	HindIII	TACAAGCTTAAGCTCTCCC TTCTCTTTCTTT
SL1328	<i>sdbA<sub>Q92E</sub></i>	For	Expression		GATTGTCAAAAAGAGTTAC CAG
SL1329	<i>sdbA<sub>Q92E</sub></i>	Rev	Expression		CTGGTAACTCTTTTTGACA ATC
SL1146	<i>msrAB</i>	For	Knockout		GACACATATTGGCTACATG
SL1147	<i>msrAB</i>	For	Knockout	BamHI	TACGGATCCGAAGTACGAT AAACCTCTAG
SL1148	<i>msrAB</i>	Rev	Knockout		CAGATACTCATCCTCTAC

\* For: Forward primer, Rev: Revers primer

The three fragments were then ligated using T4 DNA ligase, and the ligation product was amplified using the outside primers SL1061/SL1226. The resulting PCR product was used to transform the *sdbBccdA2* mutant. Transformation resulted in replacing the *ermAM* and *aphA3* cassettes by the functional *sdbBccdA2* genes and the *cat* cassette. Transformants were selected on BHI agar containing chloramphenicol and replica-plated to identify kanamycin- and erythromycin-sensitive colonies. The reintroduction of the *sdbBccdA2* genes was verified by PCR.

*sgo\_1177ccdA1*-complemented mutant was constructed using a similar strategy. First, the downstream fragment of *ccdA1sgo\_1177msrAB* operon carrying a portion of *msrAB* and *sgo\_1175* was amplified using primers SL1147/SL1148 and digested with BamHI. The *cat* resistance cassette was cut from pCopCAT/pUC18 using SphI and BamHI. The downstream fragment was then ligated to the *cat* resistance cassette and the ligation product was amplified using phusion DNA polymerase and the outside primers SL666/SL1148. The PCR product of the *cat*-downstream fragment was then digested with HindIII. Next, the *msrAB* entire gene was amplified using primers SL1319/SL1146 and digested with HindIII. The *cat*-downstream and *msrAB* entire gene were ligated together using T4 DNA ligase. The ligation product was amplified using phusion DNA polymerase and the outside primers SL1146/SL1148 and digested with XbaI, a unique restriction site within *msrAB* gene. Next, the *sgo\_1180ccdA1sgo\_1177msrAB* operon was amplified using primers SL1050/SL1319 and digested with XbaI. Following gel purification, the *sgo\_1180ccdA1sgo\_1177msrAB* operon was ligated with *msrAB-cat*-downstream fragment using T4 DNA ligase, and the ligation product was amplified using SL1050/SL1148. The PCR product was transformed into the *sgo\_1177ccdA1* mutant, and the transformants were selected on BHI agar containing chloramphenicol and replica-plated to identify kanamycin- and erythromycin-sensitive colonies and confirmed by PCR.



## 2.4 Site Directed Mutagenesis

Single amino acid substitution mutants were generated using overlapping PCR with the primers indicated in Table 2.3. The K91E, R119E, V152E, P156T, T172E, S154E, and F174E *sdmA* point mutants were kindly provided by our collaborators at the University of Toronto/Calgary (Savchenko and Stogios), which were subsequently sub-cloned into pQE30 (Lee *et al.*, unpublished). The *sdmA* point mutants Q92A, Q92E, Q92A/S154E, and Q92E/S154E were constructed in this study. All point mutations were confirmed by DNA sequencing (The McGill University and Génome Québec Innovation Centre).

### 2.4.1 SdbA

Based on the crystal structure of SdbA (Stogios and Savchenko, 2015), a number of surface-exposed amino acids were identified, and single amino acid substitution mutants were constructed. For example, *SdbA*<sub>Q92A</sub> was constructed by introducing a mutation to replace the codon for glutamine at position 92 (CAG) to alanine (GCA). To achieve this, the upstream and downstream regions of *sdmA* were amplified from the *S. gordonii* SecCR1 genome using primer pairs (SL764/SL1331 and SL1330/SL763) respectively. Primers SL1331 and SL1330 carried the mutated codon. The upstream and downstream fragments for *SdbA*<sub>Q92A</sub> were combined as the template for a second PCR using the outside primers SL763/SL764 to generate *SdbA*<sub>Q92A</sub> DNA fragment. The resulting PCR product was cloned into the BamHI and HindIII sites of pQE30. The plasmid was transformed into *E. coli* XL-1. A similar approach was used to construct *sdmA*<sub>Q92E</sub> point mutant. To construct a double point mutant (*SdbA*<sub>Q92A/S154E</sub>), *SdbA*<sub>S154E</sub> DNA was used as the template to amplify the upstream and downstream regions of *sdmA* using primer pairs for *SdbA*<sub>Q92A</sub> as described above. The PCR product was similarly cloned into a pQE30 plasmid as described above. A similar approach was used to construct *sdmA*<sub>Q92E/S154E</sub> point mutant.

## 2.4.2 SdbB

Overlapping PCR was also used to construct cysteine point mutants in the active site (CGPC) of SdbB. First, *sdbB*<sub>C81A</sub> was constructed by replacing the codon for cysteine at position 81 (TGT) to alanine (GCT). To achieve this, the upstream and downstream regions of *sdbB* were first amplified with the primer pairs SL1157/SL1323 and SL1322/SL1158, respectively. Next, the two fragments were combined and used as a template for an overlapping PCR and amplified with the outside primers SL1157/SL1158 to generate *sdbB*<sub>C81A</sub> DNA fragment. The resulting PCR product was cloned into pQE30 plasmid via the BamHI and HindIII sites. A similar approach was used to construct *sdbB*<sub>C84A</sub> cysteine point mutant.

## 2.5 Reverse-Transcription PCR

Total RNA was extracted from *S. gordonii* using the hot acid phenol method (Tremblay *et al.*, 2009). Overnight cultures of *S. gordonii* (15 ml) were added to 100 ml of pre-warmed TYG and incubated until the cultures reached mid-exponential phase of growth (OD<sub>600</sub>= 0.6). Cells were collected by centrifugation (10 000 x g, 10 minutes, 4°C) and resuspended in 500 µl diethyl pyrocarbonate (DEPC) treated-water and 1.5 ml of pre-warmed phenol, which contained 0.1% (w/v) SDS and saturated with citric acid buffer (0.05 M sodium citrate and 0.05 M citric acid, pH 4.3). The cell suspension was boiled for 10 minutes and cooled on ice for 3 minutes. The aqueous phase (500 µl) containing the RNA was then separated by centrifugation (5000 x g, 10 minutes) and extracted once with citric acid-phenol (500 µl) and chloroform (500 µl), followed by two volumes of chloroform. The RNA was precipitated with 2 volumes of isopropyl alcohol containing 0.3 M sodium acetate and incubation on ice for 30 minutes. The precipitated RNA was pelleted by centrifugation (15,000 x g, 20 minutes), washed with 75 % ethanol, and dissolved in 50 µl DEPC-treated water. RNA concentrations were estimated by measuring the A<sub>260</sub> of 1:500 diluted RNA samples in DEPC-treated water and calculated using the following equation: RNA concentration = A<sub>260</sub> reading × 500 (dilution factor) ×

40 µg/ml ( $A_{260}$  of 1 corresponds to 40 µg of RNA per ml). To remove contaminating DNA, 1 µg of RNA was treated with 1 µl of amplification-grade DNase I (Life Technologies) in 10 µl of DNase I buffer for 15 minutes at room temperature. Following incubation, 1 µl of 25 mM EDTA was added and DNase I was inactivated at 65°C for 10 minutes.

The removal of DNA in the RNA samples was assessed by PCR using primers specific for the *S. gordonii* 16S rRNA gene (SL525/SL697). The lack of PCR products observed by agarose gel electrophoresis was considered as DNA-free RNA samples and were used for complementary DNA (cDNA) synthesis using random primers and SuperScript II reverse transcriptase (Life Technologies) according to the manufacturer's instructions. Briefly, 1 µg of RNA was mixed with 1 µl of dNTPs (10 µM) and 1 µl of random primers (5 µM) in a 15 µl reaction volume. The sample was incubated at 65°C for 5 minutes, followed by 2 minutes on ice. After incubation, 4 µl of FS buffer (5X) was added and the sample was incubated at 25°C for 2 minutes and Superscript ssRT enzyme (1 µl) was then added. The reaction mixture was incubated for 10 minutes at 25°C, 50 minutes at 42°C, 15 minutes at 70°C to synthesize cDNA. The resulting cDNA (2 µl) was used as the template for the amplification of *sgo\_1170*, *sdbB*, *ccdA2*, *sgo\_1174*, *sgo\_1177*, and *ccdA1* using primers listed in Table 2.3. In addition, reverse transcription PCR (RT-PCR) was used to determine if *ccdA2* and *sdbB* form an operon using cross-gene primers SL867/SL868.

## 2.6 Phenotypic Assays

### 2.6.1 Extracellular (e)DNA Release

Extracellular (e)DNA release was assayed as described previously with modifications (Kreth *et al.*, 2009). Stationary phase cultures (24 h) grown in HTVG were standardized to an  $OD_{600}$  of 1.0, and 1 ml volumes were centrifuged (13,000 x g, 5 minutes, 4 °C). The supernatant containing the eDNA (750 µl) was mixed with an equal volume of cold acetone and incubated on the ice. The next day, the precipitated eDNA

was pelleted (14 000 x g, 10 minutes) and dissolved in 50 µl of TE buffer. The samples were analyzed on 0.8% agarose gels.

## 2.6.2 Bacteriocin Activity

Bacteriocin activity was tested using a liquid culture method as described previously (Heng *et al.*, 2007; Tompkins *et al.*, 1997). Briefly, 50 µl of overnight cultures of *S. gordonii* were inoculated to 5 ml pre-warmed BHIS without antibiotics. Cultures were incubated to an OD<sub>600</sub> of 0.2, and the cells were pelleted by centrifugation (14 000 x g, 5 minutes). The supernatant was filter-sterilized (0.2 µm) and 1 ml of the filtrate was added to 1 ml of fresh pre-warmed BHIS. After 15 minutes at 37°C, the medium was inoculated with 20 µl of an overnight culture of the indicator strain *S. mitis* I18. The culture was incubated for 10 h and OD<sub>600</sub> was read using a spectrophotometer (Shimadzu UV-1700, Kyoto, Japan). Cultures that displayed growth of the indicator strain (OD<sub>600</sub> > 1.0) following incubation were considered as having a defect in bacteriocin activity.

## 2.6.3 Genetic Competence

Genetic competence of *S. gordonii* strains was assessed using the genomic DNA (gDNA) of *S. gordonii* Wicky WK1, which contains a mutation in the β-subunit of RNA polymerase conferring resistance to rifampin (Davey *et al.*, 2013; Lunsford and London, 1996). Briefly, 300 µl of overnight cultures of *S. gordonii* grown in BHIS were added to 12 ml of pre-warmed BHIS and incubated. When the OD<sub>600</sub> reached 0.2, DNA (1 µg) was added to 750 µl aliquots of the cultures. Cultures were incubated for 30 minutes, then 750 µl fresh pre-warmed BHIS was added and further incubated at 37°C. After 90 minutes of incubation, the cultures were serially diluted and plated on BHI agar with and without 100 µg/ml rifampin. The plates were incubated for 48 hours and colonies counted. Transformation frequency was calculated as the percentage of rifampin-resistant colonies divided by the total CFU/ml.

## 2.6.4 Autolysis

Autolysis was performed as described previously with modifications (Ahn and Burne, 2007). One ml of an overnight culture of *S. gordonii* was added to 10 ml of pre-warmed HTVG and grown to an OD<sub>600</sub> of 1.0. The cells were harvested by centrifugation (3 000 x g, 10 minutes) and resuspended in pre-warmed (44°C) autolysis buffer (20 mM potassium phosphate buffer, pH 6.5, 1 M KCl, 1 mM CaCl<sub>2</sub>, 1 mM MgCl<sub>2</sub>, 0.4% (w/v) sodium azide and 0.2% (v/v) Triton X-100). The cell suspensions were incubated at 44°C in a water bath and autolysis was monitored by measuring the OD<sub>600</sub> every hour for four hours.

## 2.6.5 Zymographic Analysis

Zymogram analysis of autolysin was performed as described previously (Liu and Burne, 2011). Overnight cultures of *S. gordonii* were diluted 1:5 in 50 ml pre-warmed HTVG and grown to an OD<sub>600</sub> of 1.0. The cells were harvested by centrifugation (10 000 x g, 10 minutes, 4°C), resuspended in 0.5 ml of 4% SDS, and incubated at room temperature. After 1 hour, the cells were removed by centrifugation (15 000 x g, 15 minutes), and the supernatant mixed with an equal volume with 50 mM Tris buffer (pH 6.5) containing 10% glycerol and served as the autolysin sample.

To prepare the substrate for the zymogram, cells from 800 ml of an overnight culture of *S. gordonii* SecCR1 grown in BHI was collected by centrifugation (5 000 x g, 10 minutes) and washed four times with *Milli-Q* water. The cells were then resuspended in 60 ml of 4% SDS, boiled for 30 min, and then washed five times with *Milli-Q* water. The heat-killed cells (zymogram substrate) were then resuspended in 5 ml of *Milli-Q* water and stored as 1 ml aliquots at -80°C. The heat-killed cells (1% wet weight) was incorporated into 10% SDS-PAGE gels. Following electrophoresis, the gel was washed twice with *Milli-Q* water and then incubated for 12 h at room temperature in 200 mM sodium phosphate buffer (pH 7.0) to allow for the renaturation of the autolysin and

development of the autolytic bands. Gels were scanned with an EPSON Expression 1680 scanner and the zymogram was presented as an inverted image of the scan.

### **2.6.6 H<sub>2</sub>O<sub>2</sub> Sensitivity Assay**

The H<sub>2</sub>O<sub>2</sub> sensitivity assay was performed as described previously (Saleh *et al.*, 2013). *S. gordonii* strains were grown in HTVG. Next day, the cultures were diluted 1:40 in 4 ml of pre-warmed HTVG and grown to OD<sub>600</sub> = 0.2. The cultures were then treated with 10 mM H<sub>2</sub>O<sub>2</sub> (Sigma) at 37°C, 5% CO<sub>2</sub>. Cultures not treated with H<sub>2</sub>O<sub>2</sub> were included as controls to determine the total number of CFU. After 30 minutes, the cultures were serially diluted and drop-plated in triplicates onto TYG agar. CFU was determined after 24 h incubation. The percentage of survival was calculated as follow: (CFU of H<sub>2</sub>O<sub>2</sub> treated sample / CFU of untreated sample) x 100.

### **2.6.7 Methionine Sulfoxide Sensitivity Assay**

Overnight cultures were diluted 1:20 into 5 ml of pre-warmed TSB and grown to OD<sub>600</sub> = 0.1. Aliquots (4 µl) of the culture were added to 200 µl of pre-warmed TSB containing DL-methionine sulfoxide (Sigma) in a 96-well flat bottom plate (Corning Costar, Fisher Scientific, Ontario, Canada). Wells without methionine sulfoxide were included as controls. Cultures were incubated at 37°C, 5% CO<sub>2</sub> and OD<sub>600</sub> was recorded using a microplate reader after 24 h incubation (Synergy HT; BioTeK, USA).

### **2.6.8 Copper Sensitivity Assay**

Overnight cultures were diluted 1:5 into 5 ml of pre-warmed BHI and grown to OD<sub>600</sub> = 1.0. Cultures were 10-fold diluted and 20 µl aliquots were drop-plated onto BHI plates with or without CuSO<sub>4</sub>. The plates were incubated for 48 hours at 37°C, 5% CO<sub>2</sub>.

### **2.6.9 Level of MsrAB, SdbB, and Sgo\_1177 in Response to Aeration and in Biofilms**

One ml of an overnight culture of *S. gordonii* SecCR1 grown stationary in HTVG under anaerobic conditions (GasPak, anaerobic gas generating system, BD) was added to 9 ml of pre-warmed HTVG and incubated at 37°C under anaerobic conditions. A second overnight culture of *S. gordonii* SecCR1 grown stationary in HTVG in a CO<sub>2</sub> incubator was added to 9 ml of pre-warmed HTVG and incubated in ambient atmosphere on a shaker (20 rpm). When the cultures reached OD<sub>600</sub> = 0.8, cells were harvested by centrifugation and analyzed by western blotting for MsrAB, SdbB, and Sgo\_1177.

To examine the level of MsrAB, SdbB, and Sgo\_1177 in biofilm and planktonic cells, overnight cultures of *S. gordonii* SecCR1 grown in HTVG were centrifuged (3000 x g for 10 min). The cells were resuspended in biofilm medium to an OD<sub>600</sub> = 0.25. The cell suspensions (1 ml/well) were added to 24-well flat bottom plates (Costar). The plates were incubated for 24 h at 37 °C, 5% CO<sub>2</sub>. The next day, 1 ml of the liquid above the biofilm was collected as planktonic cells. The wells were then washed once with 1 ml of phosphate-buffered saline (PBS) to remove loosely attached cells. One ml of biofilm medium was added to the well and the biofilm cells were resuspended by vigorous pipetting. The planktonic and biofilm cell suspensions were adjusted to an OD<sub>600</sub> of 0.8 and cells were then harvested by centrifugation and analyzed by western blotting.

## **2.7 SDS-PAGE and Western Immunoblotting**

Cells from overnight cultures (1 ml of *E. coli* or 3 ml of *S. gordonii*) were pelleted by centrifugation (13 000 x g, 5 minutes, 4°C) and resuspended in 50 µl of 1 x sample buffer (250 mM Tris-HCl, pH 6.8, 2% sodium dodecyl sulfate, 10% glycerol, 0.01% bromophenol blue) containing 5% 2-mercaptoethanol. A second sample was prepared in sample buffer without 2-mercaptoethanol. The suspensions were boiled for 5 minutes and cells were removed by centrifugation (12 000 x g, 10 minutes). For membrane protein (CcdA1 and CcdA2) detection, *E. coli* cells were pelleted by centrifugation and

resuspended in 300  $\mu$ l TE buffer. The cells were sonicated (3 x 30 seconds on ice) and centrifuged (15 000 x g, 10 minutes, 4°C). The pellet was then resuspended in 100  $\mu$ l of 1x sample buffer containing 4.5 mM n-dodecylphosphocholine (DPC, Anatrace), warmed at 37°C for 5 minutes, and centrifuged (10 000 x g, 5 minutes).

SDS-PAGE was performed as described by Laemmli (1970). SDS-PAGE gels were stained with Coomassie blue R-250. For western blotting, proteins in SDS-PAGE gels were transferred to nitrocellulose membranes (Bio-Rad) at 200 mA for 60 minutes (Mini Trans-Blot, Bio-Rad) in a transfer buffer (2.9% Tris, 1.45% glycine, and 0.185% SDS; w/v, 20% methanol v/v). After transfer, the membranes were blocked with 1% (w/v) gelatin in PBST (phosphate-buffered saline with 0.1% Tween 20) for 1 hour with gentle rocking at room temperature. The membranes were incubated with primary antibodies in PBST at 4°C. The next day, the membranes were washed 4 times with PBST and incubated with alkaline phosphatase-conjugated secondary antibodies for 1 hour. Membranes were washed and developed with the substrates 5-bromo-4-chloro-3-indolyl-phosphate (BCIP) and 4-nitro blue tetrazolium chloride (NBT) in the alkaline phosphatase buffer (100 mM Tris-HCl, 100 mM NaCl, 10 mM MgCl<sub>2</sub>, pH 9.5).

## **2.8 Protein Alkylation**

### **2.8.1 AtIS**

The redox state of AtIS was determined as described previously (Davey *et al.*, 2013). Proteins were extracted from *S. gordonii* cells with 4% SDS as described for autolysin above. Proteins were precipitated with 9% (w/v) trichloroacetic acid (TCA) on ice for 30 minutes and pelleted by centrifugation (15 000 x g, 10 minutes). The pelleted proteins were washed twice with cold acetone and dissolved in 100 mM Tris-HCl (pH 7.0) containing 1% (w/v) SDS, and 5 mM maleimide-PEG<sub>2</sub>-biotin (525 Da, American Peptide Co.). Proteins in the samples were alkylated by incubation at room temperature for 30 minutes, followed by 10 minutes at 37°C. Excess maleimide-PEG<sub>2</sub>-biotin was then removed by TCA precipitation and acetone wash. The protein pellets were dissolved in



100 mM Tris-HCl (pH 7.0), 1% (w/v) SDS, and 8 M urea. Positive controls were prepared by incubating the samples with 100 mM dithiothreitol (DTT, BioShop) in 10 mM Tris-HCl (pH 8.1) for 30 minutes at room temperature. Proteins were precipitated with TCA on ice for 30 minutes prior to alkylation with maleimide-PEG<sub>2</sub>-biotin. The samples were analyzed by western blotting and reacted with extravidin-alkaline phosphatase (1:60 000; Sigma-Aldrich) to detect biotinylated proteins, and duplicate samples reacted with anti-AtIS antisera (1:2000) (Davey *et al.*, 2013) to determine the total AtIS in the sample. The level of alkylated AtIS was analyzed by densitometry using Image J (Schneider *et al.*, 2012).

### **2.8.2 Anti-CR1 scFv**

The redox state of anti-CR1 scFv was determined as described previously (Davey *et al.*, 2016a). First, anti-CR1 scFv was isolated from *S. gordonii* using affinity chromatography. Cells from a 500 ml overnight culture (HTVG) were pelleted by centrifugation (12 000 x g, 10 minutes) and resuspended in 50 ml Ni-column binding buffer A (50 mM sodium phosphate buffer, 300 mM NaCl, 20 mM imidazole, 8 M urea; pH 7.4). The sample was then incubated overnight at 4°C with slow rotation to extract the anti-CR1 scFv. Cells were then removed by centrifugation (20 000 x g, 15 min), and the clear supernatant was passed through a nickel affinity column (His60 Ni Superflow; Clontech) three times. The column was then washed with 20 ml buffer A followed by 20 ml buffer B (50 mM sodium phosphate buffer, 8 M urea, 300 mM NaCl, 40 mM imidazole; pH 7.4). Anti-CR1 scFv were eluted with 20 ml elution buffer C (50 mM sodium phosphate buffer, 8 M urea, 300 mM NaCl, 300 mM imidazole; pH 7.4) and collected as 1 ml fractions.

To determine the redox state, the anti-CR1 scFv was precipitated with 9% (v/v) TCA plus 0.18% (v/v) sodium deoxycholate, collected by centrifugation (15 000 x g, 10 min, 4°C), washed twice with acetone, and then alkylated with 5 mM maleimide-PEG<sub>2</sub>-biotin as described above. Excess maleimide was removed by TCA precipitation and acetone wash, and the resulting pellets were dissolved in 100 mM Tris (pH 7.0), 1% (v/v)

SDS, and 8 M urea. To prepare positive controls, anti-CR1 scFv were reduced with DTT prior to alkylation. Samples were analyzed by western blotting and reacted with extravidin alkaline phosphatase (Sigma-Aldrich) for detection of alkylated proteins and anti-HA monoclonal antibodies for the detection of total anti-CR1 scFv.

### **2.8.3 SdbA**

Overnight cultures (0.5 ml) of *S. gordonii* grown in HTVG were added to 4.5 ml of pre-warmed HTVG and grown to an OD<sub>600</sub> of 0.8. The cells from a 2 ml culture were collected by centrifugation (4000 x g, 10 minutes) and resuspended in 100 µl of 100 mM sodium phosphate buffer (pH 7.5) containing 2% SDS with 10 mM maleimide-PEG<sub>2</sub>-biotin. Another aliquot of cells was incubated without maleimide-PEG<sub>2</sub>-biotin. The cells were incubated for 30 minutes at room temperature, followed by 10 minutes at 37°C. The cell suspensions were then boiled for 5 minutes and centrifuged (12 000 x g, 10 minutes). The supernatant fluids, which contained the extracted SdbA, were analyzed by western blotting using anti-SdbA (1:1000) as the probe. To prepare for positive control, cells were incubated with 100 mM DTT in 10 mM sodium phosphate buffer (pH 7.5) for 1 hour at room temperature, and excess DTT was removed by centrifugation followed by washing with 10 mM sodium phosphate buffer. The cells were then treated with maleimide-PEG<sub>2</sub>-biotin and processed as above.

## **2.9 DNA Cloning, Protein Expression, and Isolation of Recombinant Proteins**

### **2.9.1 SdbA, SdbB, Sgo\_1177, MsrAB, Trx-2, and TrxB**

The expression vector pQE-30 (Qiagen) was used to express recombinant proteins with an N-terminal His<sub>6</sub>-tag. Briefly, DNA coding for the mature SdbB, Sgo\_1177, and MsrAB was PCR amplified using primers SL1157/SL1158, SL1159/SL1160, and SL1316/SL1319, respectively. The PCR products and pQE30 were digested with BamHI

and HindIII and ligated with T4 DNA ligase. The ligation DNA were transformed into *E. coli* XL1-Blue or M15 (Table 2.1). Recombinant His<sub>6</sub>-SdbB, His<sub>6</sub>-Sgo\_1177, and His<sub>6</sub>-MsrAB represented the portion of proteins without the predicted N-terminal lipoprotein motif and signal sequence. SdbA was produced in *E. coli* XL1-Blue as described previously (Davey *et al.*, 2013). Trx-2 and TrxB were cloned from *Streptococcus pyogenes* M18 into pQE30 and produced in *E. coli* XL1-Blue and were kindly provided by Lee (Unpublished) (Table 2.1). The expression of the recombinant proteins was induced by the addition of 1 mM IPTG and the proteins were purified from cell lysates using affinity chromatography on His<sub>60</sub> Ni Superflow columns (Clontech Laboratories Inc.) following the manufacturer's instructions similar to the purification of anti-CR1 scFv described above.

### 2.9.2 CcdA1 and CcdA2

Recombinant CcdA2 were produced in *E. coli* XL-1 Blue. The DNA coding for the entire CcdA2 was amplified by PCR using primers SL1096/SL1295, and the PCR product was digested with SpeI and ligated to similarly digested pSecCR1 (Knight *et al.*, 2008). The ligation product was amplified using phusion DNA polymerase (New England Biolabs) with the primers SL1096/SL334. The PCR product was digested with BamHI and cloned into the BamHI-EcoRV site of pQEDegP (pQE30 with a *degP* insert, Lee, unpublished) generating pQE30-CcdA2. The cloning placed *ccdA2* behind a His<sub>6</sub> tag and before a second His<sub>6</sub> and an HA tag sequences. The expression of recombinant CcdA2 was induced with 1 mM IPTG, and the protein was found to localize to the cytoplasmic membrane. The isolation of CcdA2 was performed as described previously with modifications (Williamson *et al.*, 2015). Briefly, cells from a 500 ml culture were resuspended in 10 ml of buffer 1 (50 mM sodium phosphate buffer, 300 mM NaCl, pH 8) and were broken by sonication. Intact cells were removed by centrifugation at 5 000 x g for 10 minutes. The cell fragments were subsequently pelleted by centrifugation (29, 000 x g, 1 h, 4°C) and washed once with buffer 1. The resulting pellet was resuspended in buffer 1 containing 1% (w/v) *n*-dodecylphosphocholine and incubated at 4°C for 2 h with

gentle rotation. Insoluble material was removed by centrifugation (27 000 x g, 1 h). The solubilized proteins were applied to a His<sub>60</sub> Ni Superflow column, which was equilibrated with buffer 1 containing 15 mM imidazole and 4.5 mM DPC. Following washing, the recombinant CcdA2 was eluted in 1 ml fractions using buffer 2 (20 mM sodium phosphate buffer, 40 mM NaCl, 200 mM imidazole and 4.5 mM DPC, pH 7.5).

For CcdA1, the DNA coding for the entire CcdA1 was amplified using primers SL1307/SL1308. The PCR product was digested with BglII-SpeI and ligated to BamHI-SpeI digested pQE30-CcdA2. Recombinant CcdA1 was then isolated as described above for CcdA2.

### **2.9.3 DsbC**

DsbC was prepared as described previously with minor modifications (Maskos *et al.*, 2003). Briefly, a 2.5 L culture of *E. coli* JM83/pDsbC was grown at 30°C with shaking to an OD<sub>600</sub> = 1.0, followed by induction with 1 mM IPTG and further grown for 16 hours at 30°C with shaking. Cells were collected by centrifugation (5 000 x g, 10 minutes, 4°C). The pellet was resuspended in 100 ml of cold 150 mM NaCl, 50 mM Tris-HCl (pH 8.0), 5 mM EDTA containing 1 mg/ml polymyxin B and stirred for 90 minutes at 4°C to isolate DsbC. Cells were removed by centrifugation (27 000 x g, 15 minutes, 4°C) and the supernatant was dialyzed against 10 mM 3-(N-morpholino) propanesulfonic acid (MOPS) (pH 7.0). The supernatant was then applied to a diethylaminoethyl (DEAE) sepharose (GE Healthcare) column (50 ml, 1.5 x 30 cm) and DsbC was eluted with a 500 ml linear NaCl gradient (0 mM to 400 mM) collected as 5 ml fractions. Fractions were analyzed by SDS-PAGE.

### **2.10 Antibody Production and Purification**

Purified recombinant SdbB was used to raise an anti-SdbB antibody in mice using a protocol similar to that described for SdbA previously (Davey *et al.*, 2013). Briefly, SdbB was incubated with 10% aluminum hydroxide gel (Sigma) at 4°C for 24 h. The

mixture (10 µg SdbB) was injected into the peritoneal cavity of 4 weeks old, female, BALB/c mice ( $n = 5$ ) on days 1, 14, and 21. On day 48, the animals were euthanized, and blood was collected by cardiac puncture. Blood samples were incubated at 37°C for 1 h and then at 4°C overnight. Samples were centrifuged (10 000 x g, 10 minutes) and serum was collected and stored at -20°C. Anti-Sgo\_1177 and anti-MsrAB were produced using the same protocol.

To prepare the antibody for immuno-precipitation, anti-SdbB antiserum (3 ml) was precipitated with 40% saturation of  $(\text{NH}_4)_2\text{SO}_4$  and the precipitated antibodies were dialyzed against PBS (phosphate buffered saline, pH 7.4). The antibodies were then affinity purified using SdbB-coupled cyanogen bromide (CNBr)-activated Sepharose 4B beads (GE Healthcare, Life Sciences, Mississauga, ON, Canada), which were prepared as follows. Purified recombinant SdbB (5 mg) was coupled to CNBr-activated Sepharose (0.3 g) at 4°C with slow rotation for 18 h. Following coupling, the beads were washed once with coupling buffer (0.1 M  $\text{NaHCO}_3$ , 0.5 M NaCl, pH 8.3) and excess reactive sites were blocked with 0.1 M Tris-HCl, pH 8.0. The beads were then washed five times with 0.1 M acetic acid, 0.5 M NaCl, pH 3.5 followed by another five times with 0.1 M Tris-HCl, 0.5 M NaCl, pH 8.8. The SdbB-Sepharose beads were packed into a 3 ml syringe and used to affinity-purify the anti-SdbB antibodies prepared above (Ed Harlow, 1988). Briefly, anti-SdbB antibodies were passed through the column 3 times followed by two washes each with 20 ml (10 mM Tris-HCl, pH 7.5) and 20 ml (10 mM Tris-HCl, pH 7.5, 0.5 M NaCl). The anti-SdbB antibodies were eluted from the column with 20 ml of 100 mM glycine (pH 2.5) and neutralized immediately with 1 ml of 1 M Tris-HCl (pH 8). The quality and quantity of eluted anti-SdbB antibodies were assessed using SDS-PAGE and showed 95% purity and had a protein concentration of 276 µg/ml.

## **2.11 Preparation of Oxidized and Reduced Recombinant Proteins**

To prepare fully oxidized proteins, samples were incubated in the oxidation buffer (50 mM oxidized glutathione, 100 mM Tris-HCl, pH 8.8, 200 mM KCl, 1 mM EDTA) for 1 hour at room temperature. Samples were then dialyzed against 100 mM sodium

phosphate buffer (pH 7) to remove the unreacted glutathione. CcdA1 and CcdA2 were oxidized similarly but in the presence of 3 mM DPC. Excess glutathione was removed from CcdA1 and CcdA1 using PD-10 desalting columns (Sephadex G-25 column; GE Life Sciences) equilibrated with 50 mM sodium phosphate buffer (pH 7) containing 3 mM DPC.

To fully reduce the purified proteins, samples were incubated with 50 mM DTT for 30 minutes on ice. After incubation, DTT was removed by passing the samples through PD-10 columns (Inaba and Ito, 2002). Reduced CcdA1 and CcdA2 were similarly prepared but in the presence of 3 mM DPC. The complete oxidation and reduction of the recombinant proteins were confirmed by reaction with Ellman's reagent 5,5'-dithio-bis(2-nitrobenzoic acid) (DTNB) (Sigma) and by alkylation with maleimide-PEG<sub>2</sub>-biotin (Winther and Thorpe, 2014).

## **2.12 DTNB Assay**

To test the complete oxidation and reduction of the recombinant proteins and to determine the solvent accessibility of the active site cysteines of SdbB, Ellman's reagent 5,5'-dithio-bis(2-nitrobenzoic acid) (DTNB) was used as described previously (Davey *et al.*, 2016a). Briefly, 1 ml sample containing 15  $\mu$ M recombinant protein in 0.1 M sodium phosphate buffer (pH 8.0), and 200  $\mu$ M DTNB was mixed and the absorbance was recorded at 412 nm. For the denatured SdbB<sub>C81A</sub> sample, the protein was denatured with 6 M guanidine-HCl in 0.1 M sodium phosphate buffer (pH 8.0) at room temperature for 24 h. Guanidine-HCl was removed by PD-10 column chromatography. The recovered denatured SdbB<sub>C81A</sub> was assayed as described above.

## **2.13 Enzyme Assays**

### **2.13.1 Oxidase Assay**

Oxidase activity of TDORs was analyzed in the RNase A refolding assay as

described previously (Daniels *et al.*, 2010; Davey *et al.*, 2013). To prepare the substrate, 5 mg/ml of RNase A (Sigma) was reduced and denatured at room temperature in 100 mM Tris-acetate buffer (pH 8) containing 2 mM EDTA, 6 M guanidine-HCl, and 0.14 M DTT. The next day, DTT and guanidine-HCl were removed using a PD-10 column. Oxidase assay was performed in 1 ml volumes containing 10  $\mu$ M of oxidized recombinant TDORs (SdbA, SdbB, Sgo\_1177, CcdA1, or CcdA2) and 10  $\mu$ M of the reduced, denatured RNase A in a redox buffer (100 mM Tris-acetate pH 8, 20 mM oxidized glutathione, 100 mM reduced glutathione, 2 mM EDTA). The sample was incubated for 2 minutes at room temperature followed by the addition of 4.5 mM cCMP. The cleavage of cCMP by the refolded RNase A was monitored at absorbance 296 nm. A second sample was prepared by omitting the TDORs from the reaction mixtures.

### **2.13.2 Reductase Assay**

Reductase activity of TDORs was assessed using the insulin precipitation assay (Daniels *et al.*, 2010). First, 2 mg/ml of insulin stock was prepared by adding 20 mg of insulin to 7 ml of 100 mM potassium acetate, pH 7.5. The pH was adjusted to 2.5 using 1 M HCl and rapidly titrated to pH 7.5 with 1 M KOH. The volume of the solution was adjusted to 10 ml with potassium acetate and stored in aliquots at -80 °C. Reductase assay was performed in 1 ml volumes containing 10  $\mu$ M of the reduced TDORs (DsbC, SdbA, SdbB, Sgo\_1177, CcdA1, CcdA2) and 1 mg/ml of insulin, 350  $\mu$ M DTT, and 2 mM EDTA. Reductase activity was assayed by monitoring the turbidity of the solution at OD<sub>600</sub> nm due to precipitation of the reduced  $\beta$  chain of insulin. Heat inactivated controls were prepared by boiling the recombinant proteins for 10 minutes before applying them in the assay. A second control sample was prepared by omitting the TDORs from the reaction mixtures.

### 2.13.3 Isomerase Assay

Isomerase activity of TDORs was assessed using scrambled RNase A as the substrate (Hiniker *et al.*, 2005). First, 5 mg/ml of reduced, denatured RNase A (rdRNase A) was prepared as described above. The scrambled RNase A (sRNase A) was prepared by adding 50  $\mu\text{M}$  of rdRNase A to 50  $\mu\text{M}$  copper sulfate in the presence of 2 mM  $\text{H}_2\text{O}_2$  and 50 mM sodium phosphate buffer, pH 7.0. After 30 minutes at room temperature, copper sulfate and  $\text{H}_2\text{O}_2$  were removed using a PD-10 column. Isomerase assay was performed in 1 ml volumes containing 10  $\mu\text{M}$  of the reduced recombinant TDORs and 10  $\mu\text{M}$  of the sRNase A in 100 mM sodium phosphate buffer (pH 8) and 2 mM EDTA. The sample was incubated for 2 minutes at room temperature followed by the addition of 4.5 mM cCMP. The cleavage of cCMP by the refolded RNase A was monitored at absorbance 296 nm. Heat inactivated controls and samples without TDOR were prepared as described above.

### 2.13.4 Methionine Sulfoxide Reductase Assay

Methionine sulfoxide reductase assay was evaluated by monitoring the oxidation of NADPH (Si *et al.*, 2015). Briefly, 10  $\mu\text{M}$  of reduced MsrAB was added to a solution containing 4  $\mu\text{M}$  reduced thioredoxin reductase (TrxB), 250  $\mu\text{M}$  NADPH (Sigma), 100 mM methionine sulfoxide (MetO, Sigma), 1 mM EDTA, 50 mM Tris-HCl (pH 7.5) and 40  $\mu\text{M}$  of the test TDOR. The assays were performed at room temperature in 100  $\mu\text{l}$  volumes in a 96-well plate (model 3635, UV transparent flat bottom microplate, CORNING). NADPH oxidation was monitored at  $A_{340\text{ nm}}$  using a microplate reader (Synergy HT; BioTeK, USA). Samples with no TDORs, no MsrAB, or no MetO were used as controls. The activity of MsrAB with SdbB or Sgo\_1177 was determined by calculating the decrease in  $A_{340\text{ nm}}$  per minute. The amount of oxidized NADPH was calculated using the following equation:  $\text{nmol NADPH}/\text{min}/\text{mg of MsrAB} = (A_{340\text{ nm}}/\text{min})/0.00622$ .



## 2.14 Enzyme Kinetics

### 2.14.1 SdbA

The enzyme kinetics of RNase A refolding by SdbA was performed in 96-well plates (model 3635, UV transparent flat bottom microplate, CORNING). In a 100  $\mu\text{l}$ , the reaction contained 5 to 30  $\mu\text{M}$  of reduced denatured RNase A substrate, 10  $\mu\text{M}$  of oxidized recombinant SdbA, 100 mM Tris-acetate (pH 8), 0.2 mM oxidized glutathione, 1 mM reduced glutathione, 2 mM EDTA, and 4.5 mM cCMP. The reactions were started by the addition of cCMP and monitored over 30 minutes at absorbance 296 nm. The activity was determined after subtracting the readings in control wells in which SdbA was omitted. The concentration of CMP was then calculated using the extinction coefficients ( $\epsilon = 0.38 \text{ mM}^{-1} \text{ cm}^{-1}$ ) at 296 nm, pH 8.0. The concentration of cCMP was obtained by subtracting the calculated CMP from the initial cCMP concentration (4.5 mM). Next, the concentration of active, renatured RNase A ( $E_t$  in  $\mu\text{M}$ ) at each time point was calculated using the equation described by Lyles and Gilbert (1991):  $E_t = vt / \{k_{cat}[cCMP]_t / ([cCMP]_t + K_{mc} (1 + [CMP]_t / K_i))\}$ , where  $vt$  is the reaction velocity at time point  $t$ ,  $k_{cat}$  is the turnover number for fully active RNase A [ $196 \mu\text{mol of cCMP min}^{-1} (\mu\text{mol of RNase})^{-1}$ ],  $K_{mc}$  is the  $K_M$  for cCMP under these conditions ( $8.0 \pm 0.5 \text{ mM}$ ), and  $K_i$  is the inhibition constant for CMP ( $2.1 \pm 0.4 \text{ mM}$ ). The calculated concentration of active, renatured RNase ( $E_t$  in  $\mu\text{M}$ ) was plotted against the time for each substrate concentration (5 to 30  $\mu\text{M}$  of reduced denatured RNase A) and linear regression was performed. The resulting slopes (initial velocity) were plotted against the concentration of substrate and analyzed by the Michaelis Menten analysis using GraphPad Prism 7 (GraphPad Prism Software Inc.).

### 2.14.2 MsrAB

The enzyme kinetics of methionine sulfoxide reductase was also performed in 96-well plates. In a 100  $\mu\text{l}$  reaction, it contained 20 to 160  $\mu\text{M}$  of reduced SdbB or

Sgo\_1177, 10  $\mu\text{M}$  of reduced MsrAB, 4  $\mu\text{M}$  reduced thioredoxin reductase (TrxB), 250  $\mu\text{M}$  NADPH (Sigma), 100 mM MetO (Sigma), 1 mM EDTA, and 50 mM Tris-HCl (pH 7.5) (Si *et al.*, 2015). The reaction was started by the addition of MetO and the oxidation of NADPH was monitored at 340 nm for 30 minutes at room temperature. The activity was determined after subtracting the readings in control wells where MsrAB was omitted. The concentration of NADPH was then calculated using the extinction coefficient ( $\epsilon = 6220 \text{ M}^{-1} \text{ cm}^{-1}$ ) at 340 nm. The concentrations of NADP were obtained by subtracting the calculated NADPH from the initial NADPH concentration (250  $\mu\text{M}$ ) and were plotted against the time for each substrate concentration (20 to 160  $\mu\text{M}$  of reduced TDOR) and linear regression was performed. The resulting slopes (initial velocity) were plotted against the concentration of substrate and analyzed by the Michaelis Menten analysis using GraphPad Prism 7 (GraphPad Prism Software Inc.).

## 2.15 Disulfide Exchange Reactions

Disulfide exchange reactions between proteins were performed as described previously with modifications (Inaba and Ito, 2002). Briefly, oxidized and reduced proteins (10  $\mu\text{M}$  each) were added to 1 ml solutions containing 50 mM sodium phosphate buffer (pH 8.0), 100 mM NaCl, and 0.5 mM EDTA and incubated at room temperature. Aliquots (200  $\mu\text{l}$ ) of the reaction were removed at indicated times and the reaction was terminated by TCA precipitation. Proteins were then alkylated with 5 mM maleimide-PEG<sub>2</sub>-biotin (525 Da) as described above and excess maleimide-PEG<sub>2</sub>-biotin was removed by TCA precipitation and acetone wash. Pellets were then resuspended in 100 mM Tris- HCl (pH 7.0) containing 1% (w/v) SDS and analyzed by western blotting.

Disulfide exchange reactions between CcdA and other TDORs (SdbA, SdbB, and Sgo\_1177) or MsrAB were performed as described above except the protein concentration was decreased to 1  $\mu\text{M}$  and 4.5 mM DPC was included in the reaction.

## 2.16 SdbA-SdbB Complex Formation in *S. gordonii* and Immunoprecipitation

To prepare samples containing the SdbA-SdbB complex, cells from 500 ml HTVG overnight cultures of *S. gordonii* *SdbA<sub>C89A</sub>ΔdegP* mutant (Davey *et al.*, 2016a) were pelleted by centrifugation (12,000 x g, 10 minutes), resuspended in 5 ml of 4% SDS and incubated for 1 h at room temperature with slow rotation. The cell suspension was centrifuged (20,000 x g, 15 minutes) and the clear supernatant was saved. SDS was removed by the addition of 50 mM KCl on ice for 30 minutes followed by centrifugation at 15,000 x g, 15 minutes, 4°C (Zhou *et al.*, 2012). The sample was chromatographed onto a gel filtration column (Sephadex G-50, 2.5 x 100 cm, Life Sciences, Mississauga, ON, Canada) using 10 mM Tris-HCl (pH 7.5) containing 100 mM NaCl as the eluent. Fractions of 5 ml volumes were collected and analyzed by western blotting using anti-SdbA antibodies as the probe. Fractions containing SdbA mixed disulfide complexes were pooled and used as the source for SdbA-SdbB complex analysis and immunoprecipitation (described below).

The affinity purified anti-SdbB antibodies were used to prepare an antibody-protein A magnetic beads (Sure Beads, Bio-Rad Laboratories, Mississauga, ON, Canada) following the manufacturer's instructions with modifications. Briefly, 36 µl of anti-SdbB (10 µg) was rotated with 1 mg of protein A magnetic beads in 200 µl of PBST for 1 hour at room temperature. Beads were magnetized and washed 3 times with PBST. Triton X-100 (1% v/v) and EDTA (1 mM final concentration) were added to 500 µl of the sample containing SdbA-SdbB complex, and the mixture was rotated with the beads at 4°C. The next day, the beads were magnetized and washed. SdbA-SdbB complex was eluted with 20 µl of 20 mM glycine (pH 2.0) at room temperature and neutralized immediately with 2 µl of 1 M sodium phosphate buffer (pH 7.4). The eluted SdbA-SdbB complex was analyzed by SDS-PAGE and immunoblotting.

## 2.17 *In vitro* SdbA-SdbB Complex Formation

An equimolar (10  $\mu$ M) of purified recombinant cysteine point mutant variants of SdbA (SdbA<sub>C86A</sub> or SdbA<sub>C89A</sub>) and SdbB (SdbB<sub>C81A</sub> and SdbB<sub>C84A</sub>) were incubated at 37°C for 30 minutes in 50 mM sodium phosphate buffer (pH 7.5) containing 10 mM K<sub>3</sub>Fe(CN)<sub>6</sub>. SdbA or SdbB variants were also incubated individually as controls. Samples were analyzed by SDS-PAGE.

## 2.18 Sequence Analysis

To identify SdbA redox partners in *S. gordonii*, the *Bacillus subtilis* 168 *ccdA* was used as the query for a BLASTP search in *S. gordonii* Challis DL-1. For promoter analysis, the sequences were analyzed for transcriptional start site using the Neural Network Promoter Prediction tool at the Berkeley Drosophila Genome Project ([http://www.fruitfly.org/seq\\_tools/promoter.html](http://www.fruitfly.org/seq_tools/promoter.html)) (Reese, 2001). Rho-independent terminators were analyzed using TransTermHP prediction tools ([http://transterm.cbcb.umd.edu/tt/Streptococcus\\_gordonii\\_Challis\\_substr\\_CH1.tt](http://transterm.cbcb.umd.edu/tt/Streptococcus_gordonii_Challis_substr_CH1.tt)) (Kingsford *et al.*, 2007).

For prediction of membrane-spanning regions in proteins, the sequences were analyzed using TMHMM 2.0 (<http://www.cbs.dtu.dk/services/TMHMM-2.0/>), and the data were visualized using PROTTTER (<http://wlab.ethz.ch/protter/start/>) (Omasits *et al.*, 2014; Sonnhammer *et al.*, 1998). For prediction of protein subcellular localization, the sequences were analyzed using protein-sorting tools such as LipoP (<http://www.cbs.dtu.dk/services/LipoP/>), SignalP (<http://www.cbs.dtu.dk/services/SignalP/>), and PSORTdb database (<http://db.psort.org>) (Juncker *et al.*, 2003; Nielsen *et al.*, 1997; Peabody *et al.*, 2016). To identify homologs of SdbB, Sgo\_1177, CcdA1, and CcdA2 in other Gram-positive species, a DELTA-BLAST search was carried out using either SdbB (WP\_008808639.1), Sgo\_1177 (WP\_012000580.1), CcdA1 (WP\_012000582.1), or CcdA2 (WP\_012000576.1) as the query sequence. Clustal Omega was used to generate the multiple sequence alignment

data and identity percentage (<https://www.ebi.ac.uk/Tools/msa/clustalo/>) (Sievers *et al.*, 2011).

## **2.19 Statistical Analysis**

The results were analyzed by one-way ANOVA, followed by Tukey post-tests using GraphPad Prism version 7 (GraphPad Software Inc., La Jolla, California).

## Chapter 3. Results

### 3.1 Identification and Characterization of Redox Partners of the Thiol-Disulfide Oxidoreductase SdbA in *S. gordonii*

Previously, our laboratory identified a TDOR in *S. gordonii* named SdbA (*Streptococcus* disulfide bond protein A) that forms disulfide bonds in substrate proteins (Davey *et al.*, 2013). *sdbA* mutants were defective in autolysis, extracellular DNA (eDNA) release, bacteriocin production, and genetic competence, but formed more biofilm (Davey *et al.*, 2013). SdbA shares little sequence homology to DsbA or BdbD. Homologs of SdbA appear to be present in a range of Gram-positive bacteria that lack DsbA (Davey *et al.*, 2013). SdbA is able to introduce a disulfide bond into its natural substrate, the major autolysin AtlS, with a single C-terminal cysteine in its CPDC active site; further suggesting SdbA is quite different from DsbA (Davey *et al.*, 2015a). Interestingly, inactivation of *sdbA* up-regulated the CiaRH two-component regulatory system in *S. gordonii* leading to the repression of the ComDE quorum sensing system, which resulted in the enhanced biofilm formation and the lack of bacteriocin production (Davey *et al.*, 2016a; Davey *et al.*, 2015b).

In the following section, the identification and characterization of the SdbA redox partners SdbB and CcdA2 in *S. gordonii* will be described. The results indicate that SdbB together with CcdA2 constitutes the main pathway for SdbA reoxidation (Jalal *et al.*, 2019).

#### 3.1.1 Identification and Genetic Organization of SdbA Redox Partners

The initial approach to find the redox partner(s) of SdbA was to blast-search the sequenced genome of *S. gordonii* using *E. coli* DsbB and *B. subtilis* BdbC as queries. The search yielded no potential candidates even under low stringency conditions. Because SdbA has homology to ResA in *B. subtilis* and ResA interacts with the integral membrane protein CcdA (Erlendsson *et al.*, 2003), additional search using *B. subtilis* CcdA as the

query was performed. The search found two CcdA proteins, CcdA1 and CcdA2, in *S. gordonii*. CcdA1 and CcdA2 show 23.7% and 27.1% sequence identity to the transmembrane domain of *E. coli* DsbD, respectively (Missiakas *et al.*, 1995). CcdA1 and CcdA2 proteins also show 21.43% and 18.3% sequence identity to the *E. coli* membrane protein DsbB (Missiakas *et al.*, 1993). CcdA1 and CcdA2 are predicted to be integral membrane proteins with six transmembrane regions. CcdA1 and CcdA2 both consist of 236 amino acids and are highly homologous with 69.8% sequence identity (Figures 3.1A, C, and D).

Examination of the genetic locus of *ccdA1* revealed that it has two genes located immediately downstream, namely *sgo\_1177* and *sgo\_1176 (msrAB)*, which are annotated as a TDOR and a methionine sulfoxide reductase (MsrAB), respectively (Figure 3.1E). The *ccdA2* locus contains one gene, *sgo\_1171 (sdbB)*, immediately downstream that is annotated as another TDOR (Figure 3.1E). *Sgo\_1171 (SdbB)* and *Sgo\_1177* was previously identified as homologs of SdbA that contained the characteristic CXXC active site of TDORs and the conserved *cis*-proline residue (Figure 3.1B) (Davey *et al.*, 2013). Both *Sgo\_1171 (SdbB)* and *Sgo\_1177* are predicted to be lipoproteins consisting of 185 and 187 amino acids, respectively, with 41.62% sequence identity (Figure 3.1B).

*In silico* analysis identified predicted promoters and rho-independent transcription terminators on the *ccdA1* and *ccdA2* loci. For the *ccdA1* locus, the promoter and terminator were located upstream of *sgo\_1181* and downstream of *sgo\_1176 (msrAB)*, respectively (Figure 3.1E). The promoter and terminator of the *ccdA2* locus were located upstream and downstream of *sgo\_1175* and *sgo\_1171 (sdbB)*, respectively.

A recent study showed that *sgo\_1180*, *ccdA1*, *sgo\_1177*, and *msrAB* were co-transcribed, suggesting these genes together with *sgo\_1181* form a five-gene operon (Haase *et al.*, 2015). The same study also showed that *sgo\_1175*, *sgo\_1174*, and *ccdA2* were also co-transcribed (Haase *et al.*, 2015). In the current work, transcript analysis confirmed these findings and also showed that *ccdA2* and *sgo\_1171 (sdbB)* were co-transcribed (Figure 3.2), suggesting that the *ccdA2* locus is a four-gene operon. Based on the findings described below, we named *Sgo\_1171* as SdbB (*Streptococcus* disulfide bond protein B).

**Figure 3.1 Genetic organization and amino acid sequences analysis for redox partners of SdbA in *S. gordonii*.**

**A.** Sequence alignment of the integral membrane proteins CcdA1 and CcdA2. **B.** Sequence alignment of the thioredoxin-like lipoproteins Sgo\_1171(SdbB) and Sgo\_1177 of *S. gordonii*. The conserved cysteines and *cis*-proline are indicated in the box, and the six transmembrane regions are underlined. **C** and **D.** A hypothetical topology model of CcdA1 and CcdA2 proteins in *S. gordonii*. The membrane-spanning domain of CcdA1 and CcdA2 proteins from *S. gordonii* is predicted to form six transmembrane segments (TMSs) with three cytoplasmic loops and two extracytoplasmic loops. The conserved cysteine residues located in TMS 1 and 4 (CcdA1: C<sub>32</sub> and C<sub>147</sub>; CcdA2: C<sub>22</sub> and C<sub>147</sub>) as well as the conserved *cis*-proline residue (P<sub>183</sub>) are indicated. The hypothetical topology model was obtained based on the data from TMHMM (<http://www.cbs.dtu.dk/services/TMHMM-2.0>) and visualized using PROTTER (<http://wlab.ethz.ch/protter/start/>). **E.** A schematic diagram describing the genetic locus of the two thioredoxin-like lipoproteins, Sgo\_1171 (SdbB) and Sgo\_1177, and their integral membrane proteins, CcdA1 and CcdA2. Sequence analyses of these two genetic loci indicate two potential promoter-like regions, upstream of *sgo\_1181* and *sgo\_1175* gene, and two rho-independent transcriptional terminator regions downstream of *sgo\_1176* and *sgo\_1171*. Arrowhead indicates the location of the primers used for RT-PCR. HK, histidine kinase; RR, response regulator.



**A.**

```

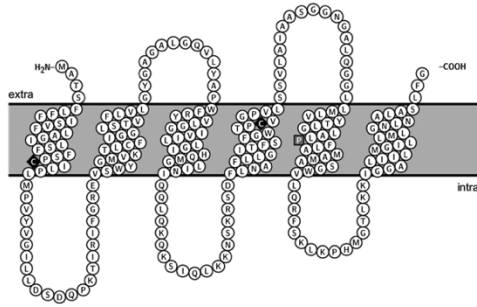
                TM1                                TM2
CcdA1 MATSELFFFISVFLAGLISFFSPELFLMPVYVGLLDS-DQPKTIRIFGREVSKYGMVKT 59
CcdA2 -MESLLFSVSVFLAGVLSFFSPELFPLVPYIGILLDSSEDKPRTVRFLGRELAWYGLVKT 59
      *:* :*****:*****:*:*:*:*:*:*:*:*:*:*:*:*:*:*:*:*:*:*:*:*:*:*
                TM2                                TM3
CcdA1 LCFIGGSTVFLVLVGYGAGALQVLYAPWFRYVLGGVILLGTHQMGLINIQOQKOKSI 119
CcdA2 LCFIAGISCVFFLGPGAGFLGAIINSSWFRYVMGLIIILLGVHQMELINIKPLQMQKNV 119
      *****:*****:*:*:*:*:*:*:*:*:*:*:*:*:*:*:*:*:*:*:*:*:*:*
                TM4                                TM5
CcdA1 QLKNSKRSDFLNAFLLGITFSFGWTFGVGVLSVLAIAASGGNGALQGGLMLVYTLG 179
CcdA2 AFKDKSRNFLSAFVLGITFSFGWTFCGPILSSVLAALAAASGGNGAFQGALTLLYTLG 179
      *:*:*:*:*:*:*:*:*:*:*:*:*:*:*:*:*:*:*:*:*:*:*:*:*:*:*:*:*
                TM5                                TM6
CcdA1 LALPFLAMAMASGWVLRQRFSKLKPHMGLKKIGGALIILMGILLMLGNLNALASLFG 236
CcdA2 MALPFLLALASSFVMQVFNKIKPYMGLLKKIGGATIILMGILLMLGQLNALSGLFG 236
      :*****:*****:*:*:*:*:*:*:*:*:*:*:*:*:*:*:*:*:*:*:*:*:*:*
  
```

**B.**

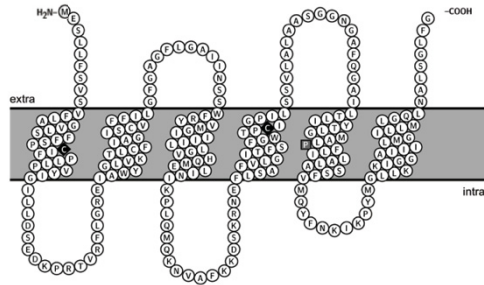
```

SdbB MKKYLTFGVGLLAAVELTACSDEMGMETKSSSNQP-AQNAVQIAVGQEAPDFTLKSMDG 59
Sgo_1177 MKKITVLTLLGLCAGLLGACSNQMESEASTNDKSSMTTKKDSQSSKMAKDFSLQVDG 60
      *** .: :***.* :* ***: . *!::: . . . :* **:..:***
SdbB KTVKLSDYGKKVLKFWASCGPCCKSMPELIELAGK-KDRDFEILSVIAPGIQGEKSE 118
Sgo_1177 KTVKLSDFKGKVVLFWASCSICLSTLGDTNLAKEQEGKDFVVLSVVSPTFNGESA 120
      ** *****:*****.* .: : : * * : : : * * : : * * : : * * *
SdbB TDFPKWFEEQYKDVPVLYDSQATTFQAYQIRSIPFEILLDSQGKIKGIQFGAISNEDAE 178
Sgo_1177 EDFKWYKSLDYKDFPVLMDTKGELLKEYGIRSYPFALFVGSDGLAKTHIGYMSKEDIE 180
      ** *::: . ***** *::: . : * * * * : : : * : * : * : * : * : *
SdbB AAFKEMK 185
Sgo_1177 KTLKEIK 187
      :*:*:*
  
```

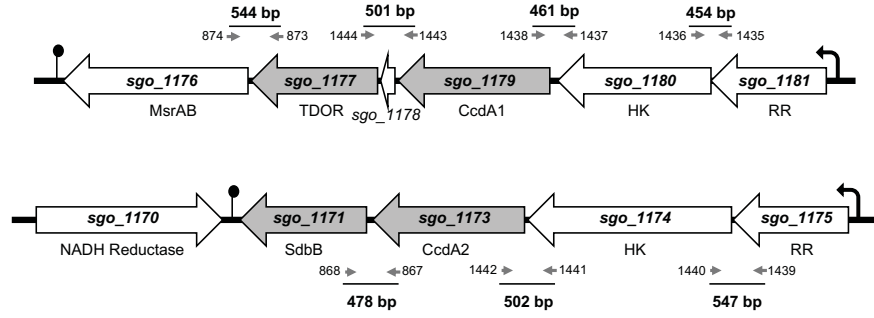
**C.**



**D.**



**E.**



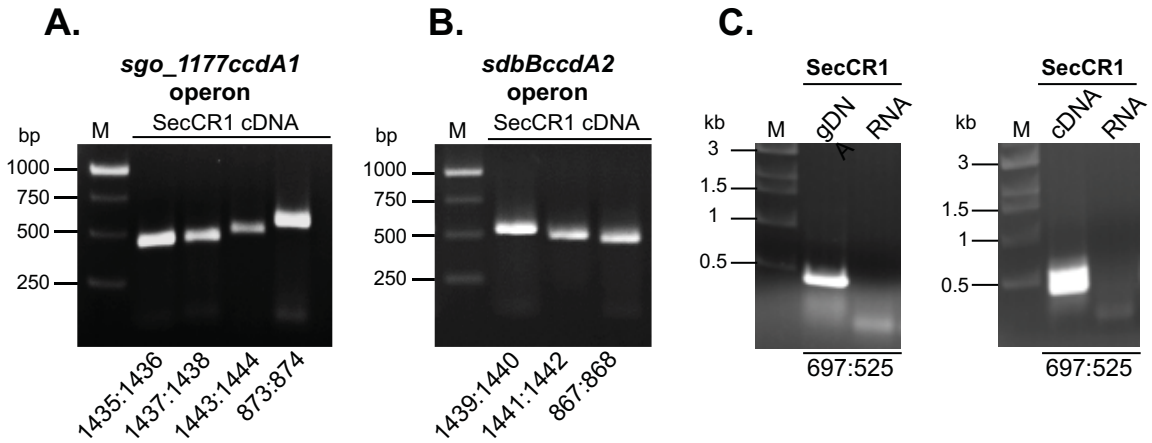


**Figure 3.2 Reverse Transcription (RT)-PCR analysis of *sgo\_1177ccdA1* and *sdbBccdA2* operons in *S. gordonii*.**

**A.** RT-PCR analysis of the *sgo\_1177ccdA1* transcripts. **B.** RT-PCR analysis of the *sdbBccdA2* transcripts. Primers used are indicated at the bottom of the gels and indicated in Figure 3.1E. **C.** Amplification of *16S rRNA*. Primer pairs 679:525, which amplify the *16S rRNA*, was used for the positive control (the genomic (g)DNA), negative control (the DNA-free RNA), and test sample (the complementary (c)DNA). M: 1 kb DNA ladder; bp: base pairs.

### 3.1.2 Confirmation of the Knockout and Complemented Mutant Strains

To help determine whether genes in the *ccdA1* and *ccdA2* loci play a role in disulfide bond formation in *S. gordonii*, single-gene and double-gene inactivation mutants were constructed by insertional inactivation. This method enables the inactivation of a target gene by an antibiotic resistance cassette without interruption of the upstream or downstream genes. These mutants are listed in Table 2.1. The inactivation of *ccdA1*, *ccdA2*, and *ccdA1ccdA2* was verified by PCR or RT-PCR (Figure 3.3). The *ccdA1* mutant was used as the background strain to construct *sdbBccdA1* and *sgo\_1177ccdA1* mutants, and the *ccdA2* mutant was used as a background strain to construct *ccdA1ccdA2*, *sdbBccdA2*, and *sgo\_1177ccdA2* double mutants.

To further confirm gene inactivation, western blotting was performed. The *sdbB*, *sdbBccdA2*, and *sdbBsgo\_1177* mutants showed a complete absence of SdbB protein that was restored in the *sdbBccdA2*-complemented mutant (Figure 3.4). Interestingly, *ccdA2* and *ccdA1ccdA2* mutants produced more SdbB protein compared to the parent strain (Figure 3.5). The *sgo\_1177*, *sdbBsgo\_1177*, and *sgo\_1177ccdA1* mutants also showed a complete loss of Sgo\_1177 production that was restored in the *sgo\_1177ccdA1*-complemented mutant (Figure 3.4). The level of Sgo\_1177 in the *ccdA1* and *ccdA1ccdA2* mutants appeared to be more than that in the parent strain (Figure 3.5).

The production of MsrAB was abolished in the *msrAB* mutant. The production of MsrAB by the *ccdA1* mutant was markedly increased compared to the parent strain (Figure 3.4 and 3.5). The *msrAB* mutant will be studied in section 3.2.

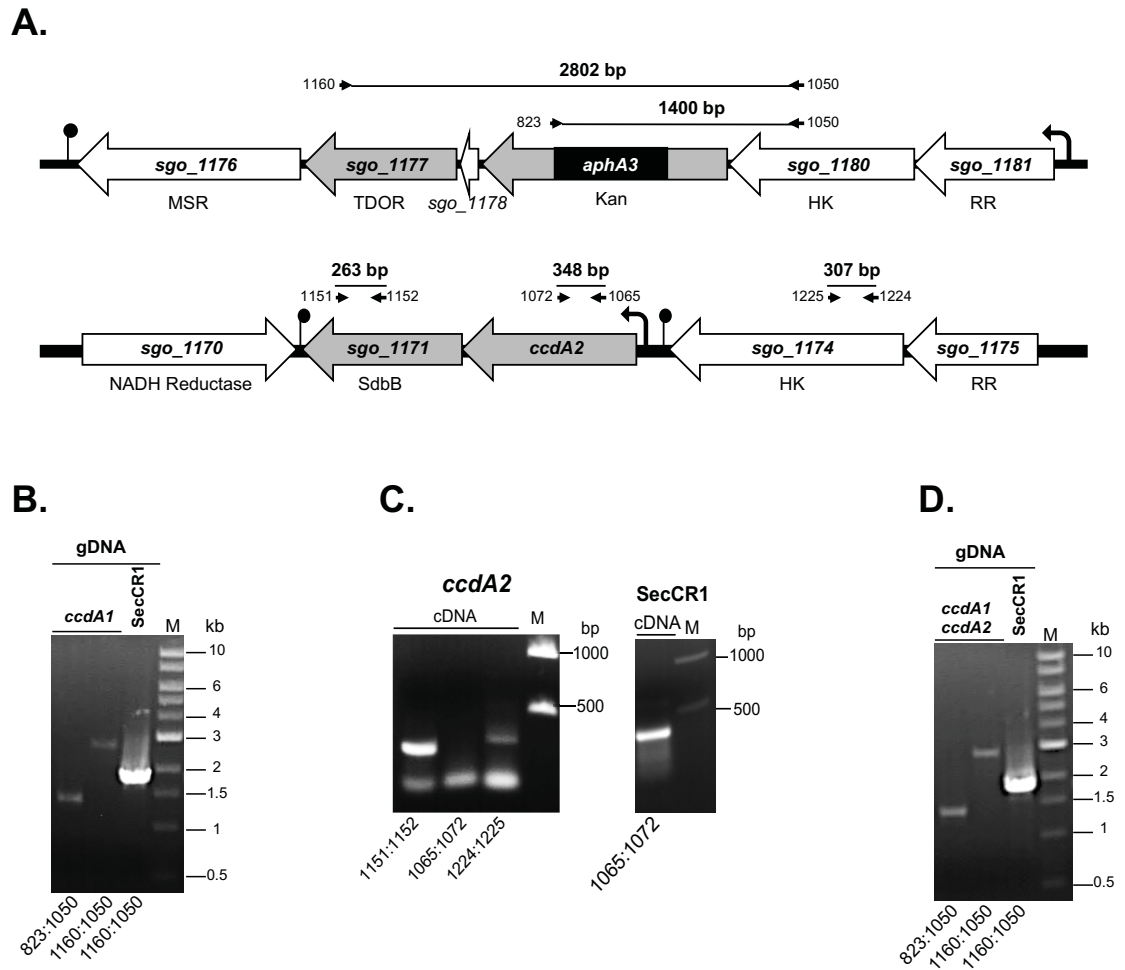


**Figure 3.3 PCR and RT-PCR confirmation of *ccdA* mutants.**

**A.** Schematic diagram depicting the genetic loci of *ccdA1* and *ccdA2*. Arrowheads indicate the location of the primers used for PCR or RT-PCR in B, C, and D. The sizes of the PCR products are shown. The size of the PCR product from primer pair 1160:1050 from the parent strain is 1835 bp. **B.** PCR confirmation of *ccdA1* mutant using templates of DNA from the *ccdA1* mutant and parent SecCR1. **C.** RT-PCR using cDNA from the *ccdA2* mutant and the parent strain SecCR1 as templates. **D.** PCR confirmation of *ccdA1ccdA2* double mutant. M: 1 kb DNA ladder; kb: kilobases.

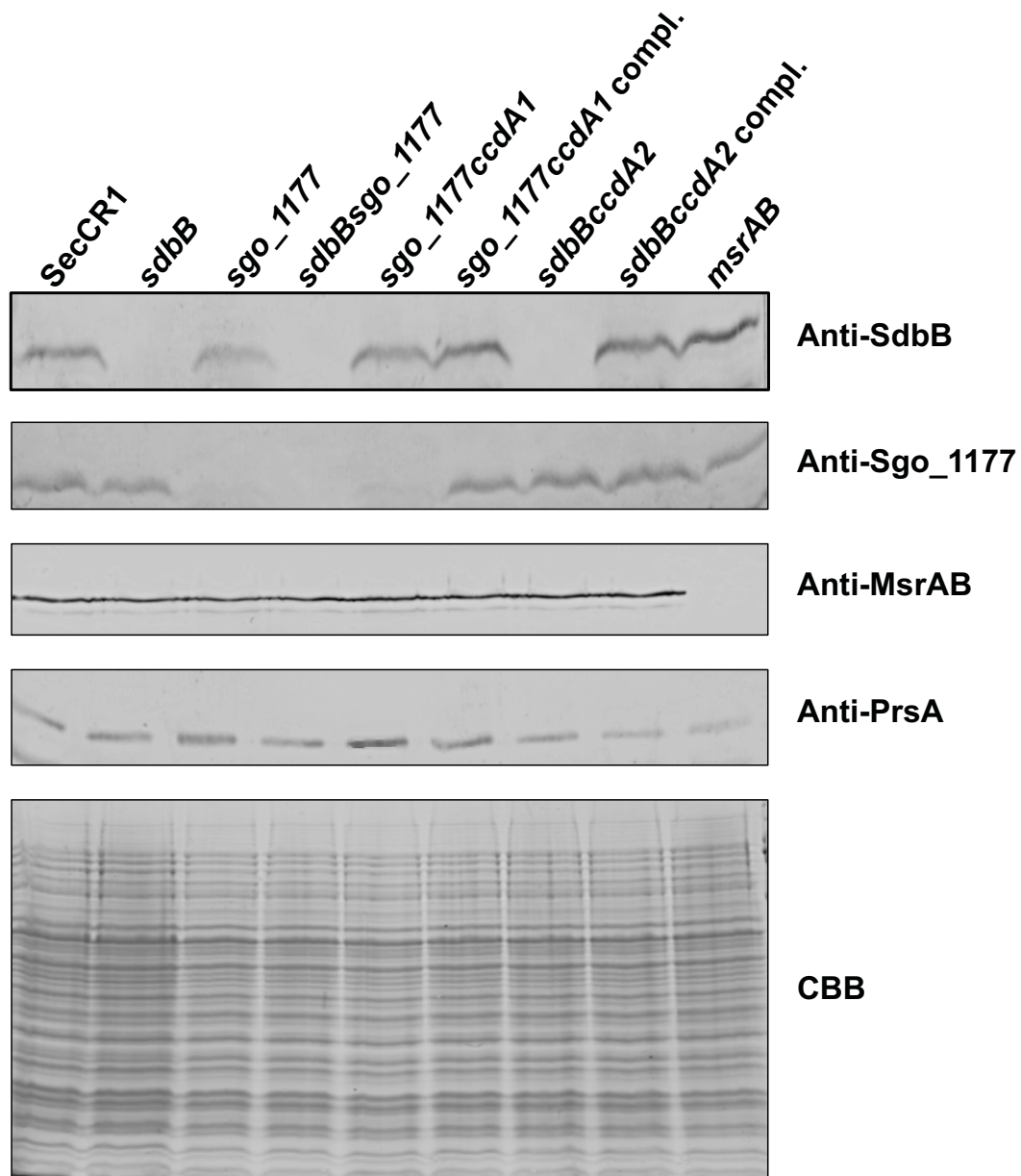


**Figure 3.4 Immunoblot analysis of SdbB, Sgo\_1177, and MsrAB in the parent, knock-out mutant, and complemented mutant strains.**

The production of SdbB, Sgo\_1177, and MsrAB in *S. gordonii* strains was probed with anti-SdbB (1:1000), anti-Sgo\_1177 (1:1000), and anti-MsrAB (1:500) antisera. Duplicate samples were stained with Coomassie brilliant blue (CBB) or reacted with the anti-PrsA antisera (1:4000) to show equal protein loading.

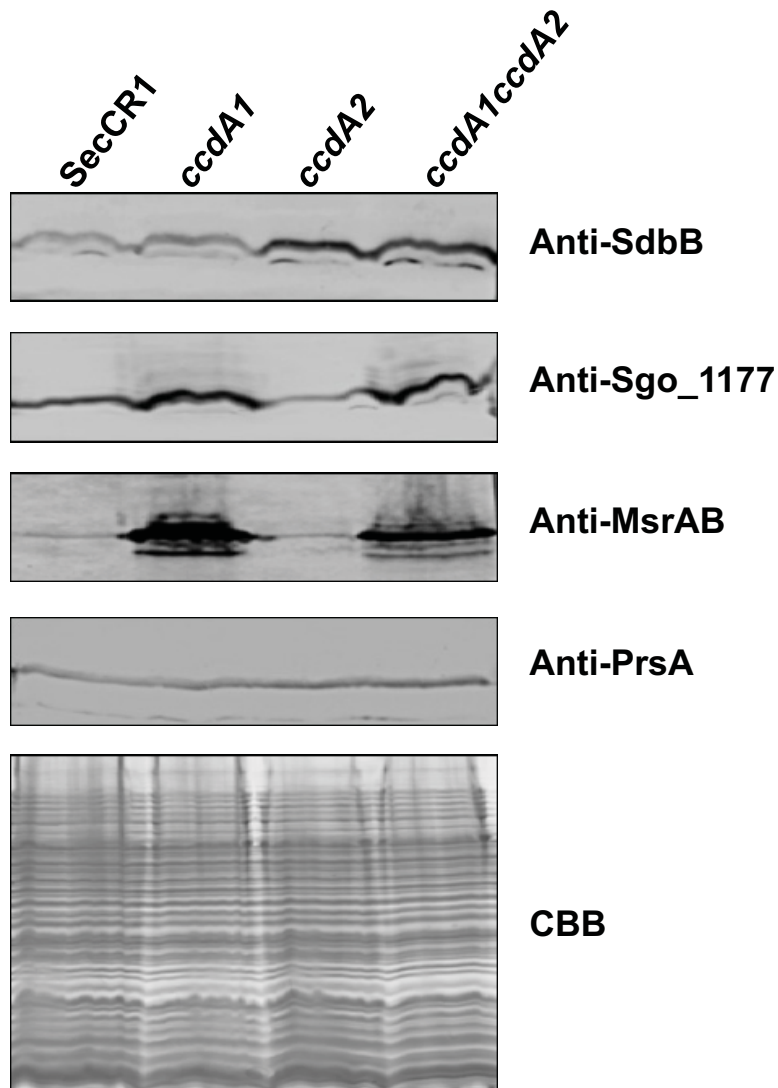


**Figure 3.5 Immunoblot analysis of SdbB, Sgo\_1177, and MsrAB in the parent and *ccdA* mutant strains.**

Detection of SdbB, Sgo\_1177, and MsrAB in the parent and mutant strains of *S. gordonii* using antisera described in Figure 3.4 above. Equal loading of proteins between samples was indicated by the reaction to the anti-PrsA antisera and Coomassie blue (CBB) staining.

### 3.1.3 The *sdbBccdA2* Double-Gene Mutant Exhibits a Pleiotropic Mutant Phenotype Identical to the *sdbA* Mutant

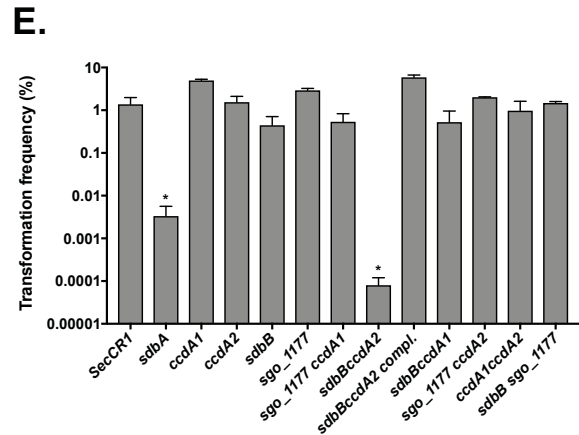
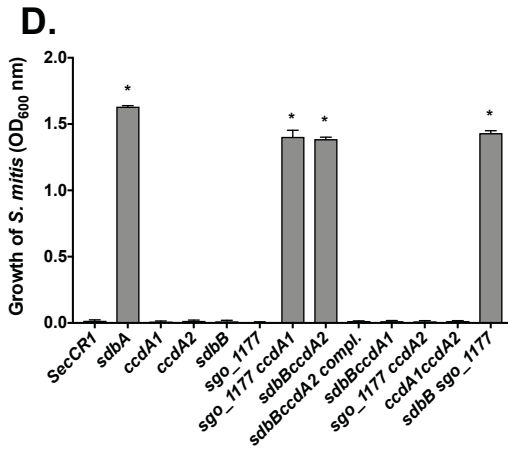
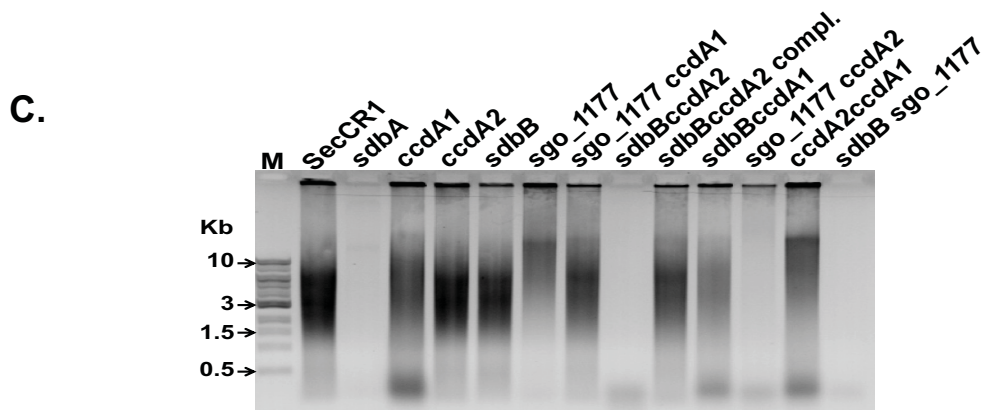
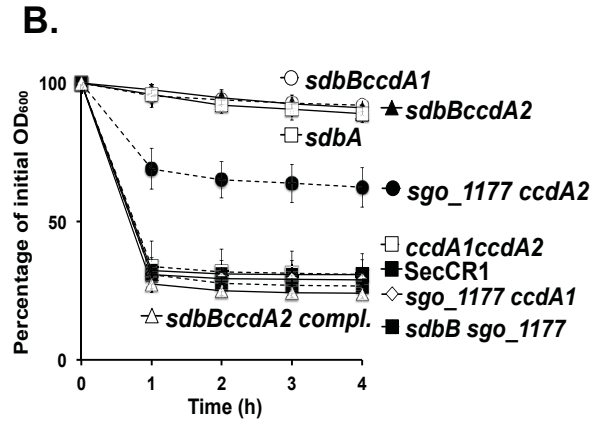
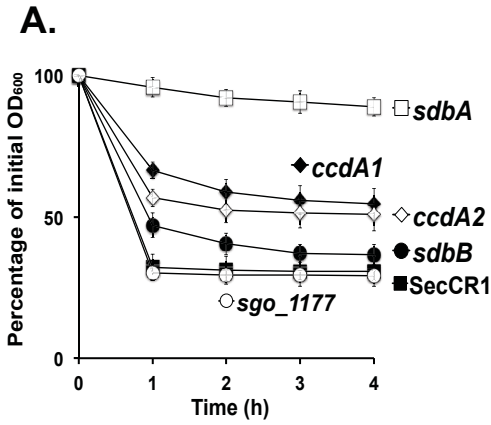
I reasoned that inactivation of the SdbA redox partner would produce mutants with the same phenotypes as the *sdbA* mutant. Thus, the mutants were tested for *sdbA*-associated phenotypes, namely autolysis, eDNA release, bacteriocin production, and genetic competence. None of the single-gene mutants displayed any observable defect in eDNA release, bacteriocin production, and genetic competence with the exception of *ccdA1* and *ccdA2* single-gene mutants, which were partially defective in autolysis, and the *sdbB* mutant, which was slightly defective in autolysis (Figures 3.6). Interestingly, five of the double-gene mutants displayed some phenotypes similar to the *sdbA* mutant. In particular, the *sdbBccdA2* mutant produced all of the phenotypes displayed by the *sdbA* mutant (Figures 3.6).

The *sdbBsgo\_1177* mutant was defective in eDNA release and bacteriocin production but not autolysis and genetic competence (Figures 3.6). The *sdbBccdA1* mutant was defective in autolysis but not eDNA release, bacteriocin production, and genetic competence. RT-PCR analysis showed that the mutation in *sdbBccdA1* was non-polar (Figure 3.7). The *sgo\_1177ccdA2* mutant was partially defective in autolysis but not in other phenotypes. The *ccdA1ccdA2* mutant was only defective in bacteriocin production. Thus, it is clear from the above results that the only mutant that duplicated phenotypes observed in the *sdbA* mutant is the *sdbBccdA2* mutant suggesting that SdbB and CcdA2 may be redox partners of SdbA. The phenotypes exhibited by the *sdbBccdA2* mutant were reversed by *sdbBccdA2* complementation (Figures 3.6). RT-PCR analysis of the *sdbBccdA2* mutant showed that the genes immediately upstream and downstream of the mutated genes were transcribed, indicating that the mutations had no polar effect (Figure 3.7). The above results established that SdbB and CcdA2 are responsible for the *sdbA*-associated phenotypes.

**Figure 3.6 Phenotypic analysis of single- and double-gene mutants of *S. gordonii*.**

**A.** Autolysis of the single-gene mutants. The parent strain and *sdbA* mutant serve as controls. **B.** Autolysis of the double gene mutants compared to the parent and *sdbA* mutant. Autolysis of stationary phase *S. gordonii* cells was monitored by measuring the OD<sub>600</sub> every hour for four hours. Each point represents the mean  $\pm$  SD of three independent experiments. **C.** Extracellular DNA (eDNA) release from stationary phase cultures of the parent and mutant strains analyzed on a 0.8% agarose gel. **D.** Bacteriocin production as assessed by growth inhibition of the target strain *S. mitis*. Filter-sterilized supernatant of *S. gordonii* strains was inoculated with the indicator strain *S. mitis* and the growth of the indicator strain was assessed by measuring the OD<sub>600</sub> after 10 h. **E.** Transformation frequency of *S. gordonii* strains. Transformation frequency was calculated as the percentage of rifampin resistant transformants divided by the total CFU/ml. In panels A, B, D, and E, results are means  $\pm$  SD of three independent experiments. \*:  $P < 0.001$ ; one-way ANOVA. SecCR1: parent strain. *sdbBccdA2* compl.: *sdbBccdA2*-complemented mutant.





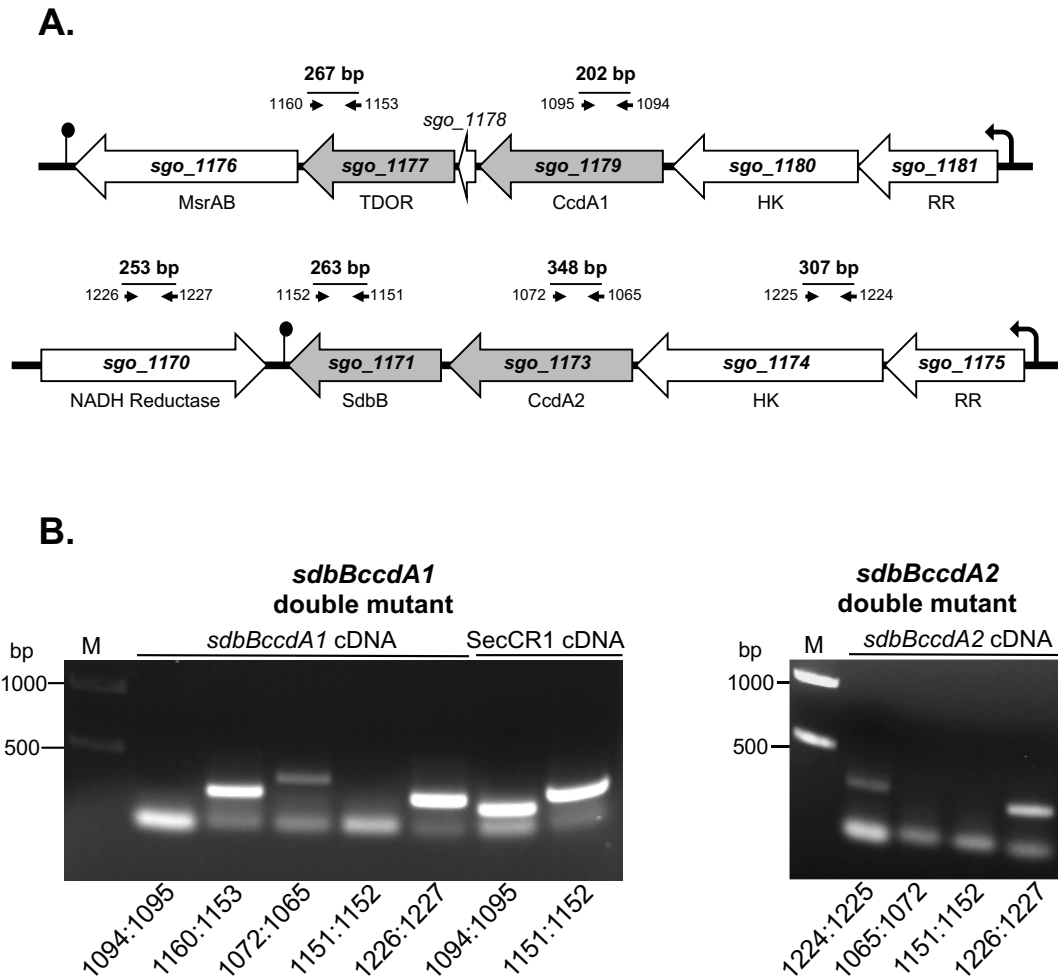


**Figure 3.7 RT-PCR confirmation of *sdbBccdA1* and *sdbBccdA2* mutants.**

**A.** Schematic diagram describing the genetic locus of *sdbB*, *ccdA1*, and *ccdA2* with the upstream and downstream genes. Arrowheads indicate the location of the primers used for RT-PCR. The lengths of PCR products are shown. **B.** Confirmation of *sdbBccdA1* and *sdbBccdA2* mutants by RT-PCR using combinations of primers described in A and templates of cDNA from *sdbBccdA1* and *sdbBccdA2* mutants or the parent strain.

### 3.1.4 AtIS in *sdbBccdA2* Mutant Lacks Activity and a Disulfide Bond

Previously, the major autolysin AtIS was shown to be a natural substrate of SdbA (Davey *et al.*, 2013). SdbA forms an intra-molecular disulfide bond between the two cysteine residues in AtIS that is required for proper folding and autolytic activity (Davey *et al.*, 2013). Thus, examination of the activity and redox state of AtIS would provide evidence of the role of redox partners in protein oxidation by SdbA.

The activity of AtIS was examined by the zymogram assay. The parent strain showed AtIS activity bands at 130 kDa (intact) and 90 kDa (processed), and the *sdbA* mutant showed a much-diminished activity band consistent with previous findings (Davey *et al.*, 2013; Davey *et al.*, 2015a). The *sdbBccdA2* and *sdbBccdA2degP* mutants also showed a reduced activity (Figure 3.8). The reason for including the triple mutant *sdbBccdA2degP* in the analysis was to ensure that the results were not due to the different levels of SdbA in the mutants. My results below (Section 3.1.6; Figure 3.12) showed that the level of SdbA in the *sdbBccdA2* mutant was reduced, and in the *sdbBccdA2degP* mutant, it was comparable to that in the parent strain. Western blotting results confirmed that AtIS was produced by the *sdbBccdA2*, *sdbBccdA2degP*, and *sdbA* mutants. Western blotting results also revealed that the AtIS protein in the *sdbBccdA2* and *sdbBccdA2degP* mutants was not processed similar to that in the *sdbA* mutant (Figure 3.8). When *sdbB* and *ccdA2* were returned to the *sdbBccdA2* mutant, AtIS activity and processing were restored (Figure 3.8). These results confirmed that the lack of autolysis in the *sdbBccdA2* mutant was due to a defect in the activity of AtIS.

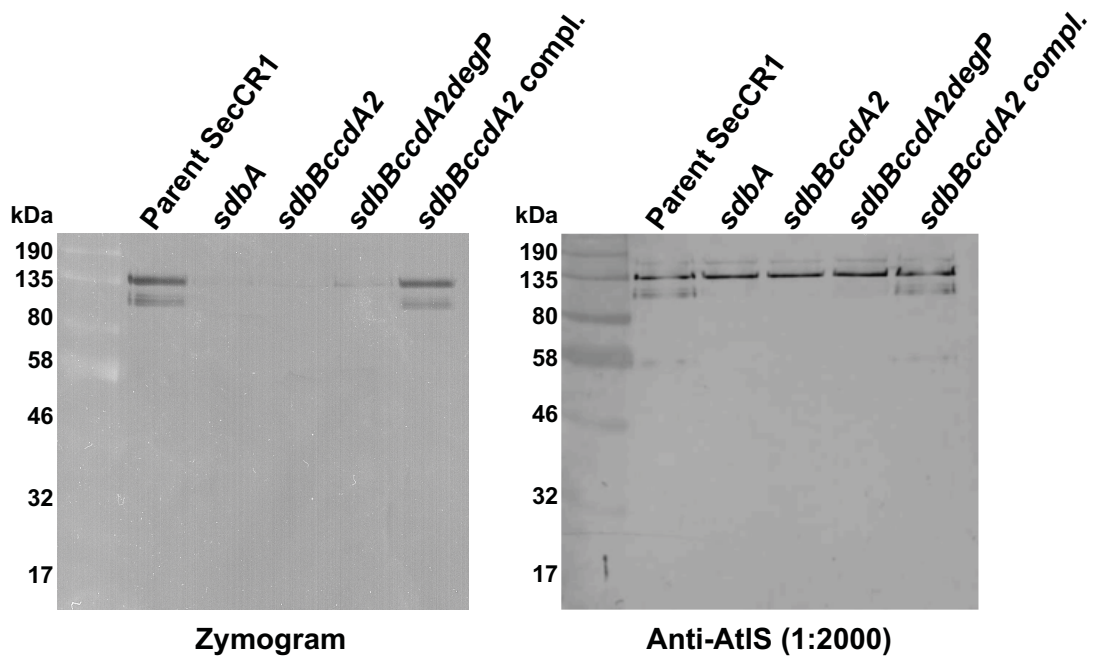


**Figure 3.8 The major autolysin AtIS is inactive in the *sdbBccdA2* and *sdbBccdA2degP* mutants.**

Zymogram analysis (left) of the autolytic activity of the major autolysin AtIS. The zymogram is shown as an inverted image of a digital scan. Western blotting shows the total AtIS in samples used in zymogram analysis. *sdbBccdA2* compl.: *sdbBccdA2*-complemented mutant.

Next, the redox state of AtIS was investigated. AtIS from the parent strain was alkylated by maleimide-PEG<sub>2</sub>-biotin and detected as a 130 kDa protein with either anti-AtIS or extravidin-AP to detect biotinylated proteins. The intensity of the AtIS band detected with extravidin-AP was markedly increased in samples reduced with dithiothreitol (DTT) prior to alkylation indicating that AtIS from the parent strain contains a disulfide bond (Figure 3.9A and B). In contrast, the intensity of the 130 kDa AtIS band from the *sdbBccdA2* and *sdbBccdA2degP* mutants remained the same with or without DTT treatment (Figure 3.9A and B), suggesting that AtIS from these mutants lacked a disulfide bond. The same was observed in the *sdbA* mutant (Figure 3.9A and B). The above results showed that SdbB and CcdA2 are required for disulfide bond formation in AtIS, the natural substrate of SdbA.

### 3.1.5 SdbB and CcdA2 Possess Oxidase Activities

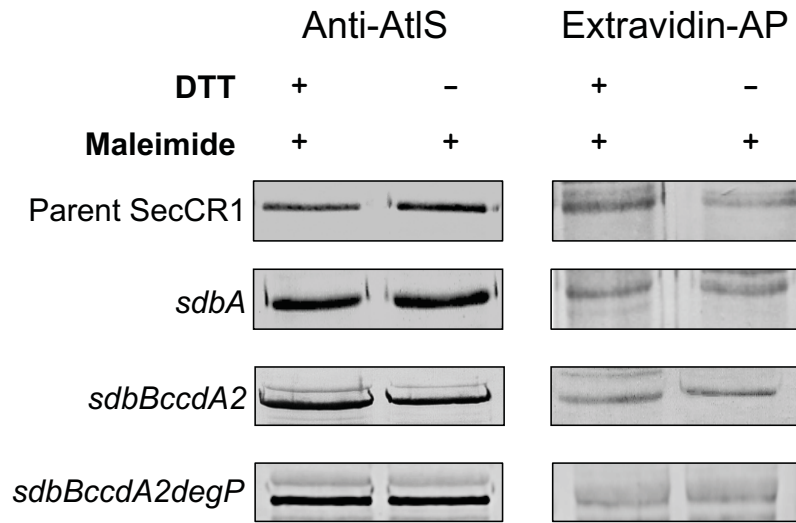
The above results collectively suggest that SdbB and CcdA2 are redox partners of SdbA. For these proteins to function as a redox partner of SdbA, they must possess oxidase activities. To provide support of this notion, recombinant SdbB and CcdA2 were produced and purified from *E. coli* (Figure 3.10A) and assayed in the RNase A refolding assay (Figure 3.10B). Recombinant SdbA was also purified and assayed as a positive control. The results clearly showed that SdbB and CcdA2 were able to refold denatured and reduced RNase A indicating oxidase activities (Figure 3.10B).

The ability of SdbB and CcdA2 to reoxidize SdbA in a disulfide exchange reaction was further examined. The results showed that SdbB could reoxidize reduced SdbA (Figure 3.11A). Similarly, CcdA2 was able to reoxidize SdbA (Figure 3.11B). This reoxidation of SdbA required oxidized SdbB or CcdA2 and was not a result of spontaneous oxidation since reduced SdbA alone (Figure 3.11C) or incubation with reduced SdbB (Figure 3.11D) or reduced CcdA2 (Figure 3.11E) did not result in the reoxidation of SdbA. Collectively, these results indicate that SdbB and CcdA2 possess the enzymatic capability to reoxidize SdbA.

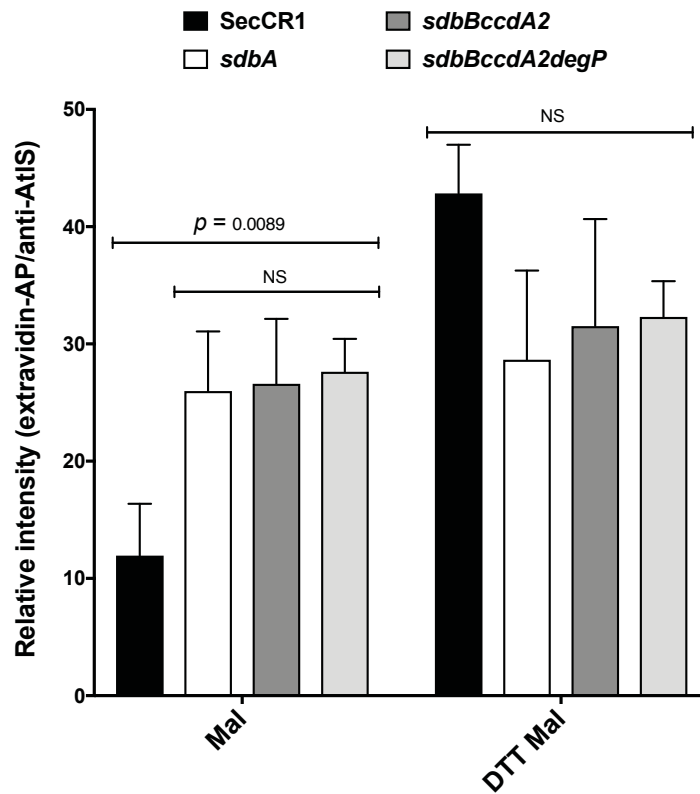
**Figure 3.9 The major autolysin AtlS lacks a disulfide bond in the *sdbBccdA2* and *sdbBccdA2degP* mutants.**

**A.** Alkylation of AtlS. AtlS in samples were alkylated with maleimide-PEG<sub>2</sub>-biotin and detected by either extravidin-alkaline phosphatase (AP) or anti-AtlS for the total amount of AtlS. From each strain, positive control was prepared by reducing the sample with DTT prior to alkylation. **B.** Densitometry analysis of AtlS alkylation using Image J. The intensity of the 130 kDa AtlS band detected by extravidin-AP is divided by that detected by anti-AtlS. Results are means  $\pm$  SD of three independent experiments. NS: not significant;  $P \geq 0.05$ .

**A.**



**B.**



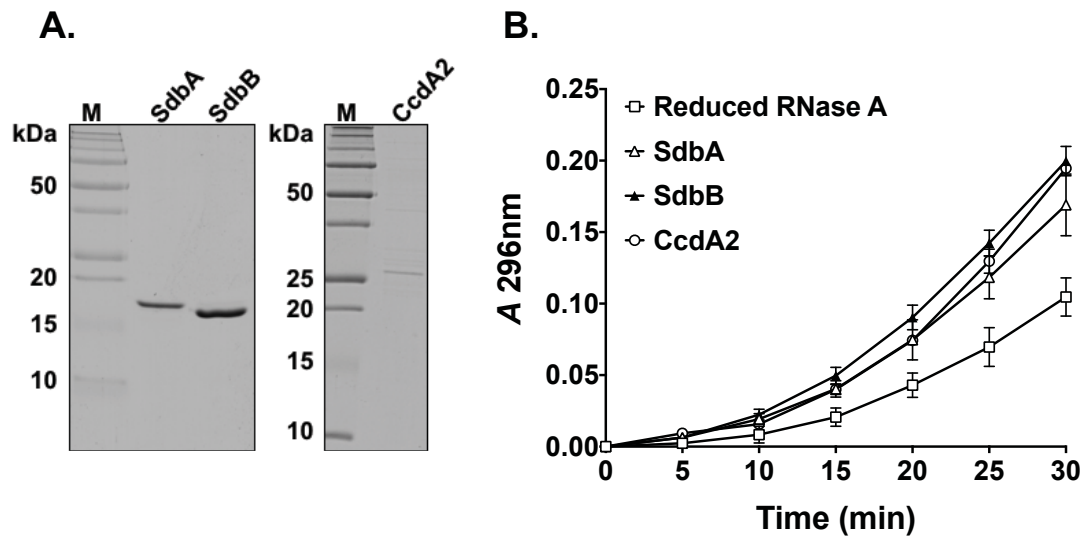


**Figure 3.10 SdbB and CcdA2 exhibit oxidase activity.**

**A.** SDS-PAGE of recombinant SdbA, SdbB, and CcdA2 purified from *E. coli*. M: prestained protein markers. **B.** Oxidative folding of reduced, denatured RNase A by SdbB and CcdA2. SdbA was included as a positive control, and reduced, denatured RNase A alone was used as a negative control. The data are means  $\pm$  SD of three experiments.



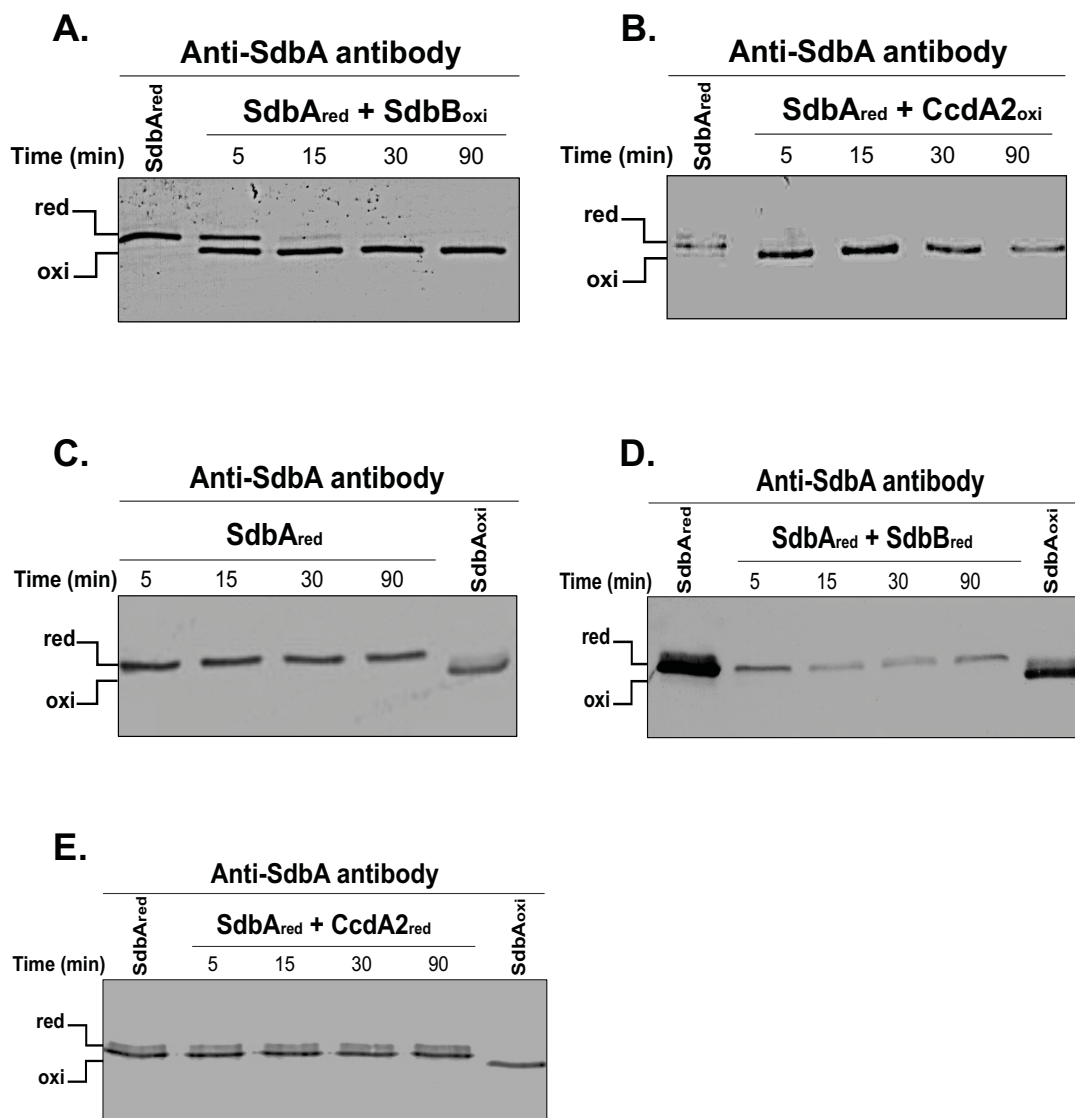


**Figure 3.11 Oxidation of SdbA by oxidized SdbB or CcdA2.**

Disulfide exchange reactions between SdbA and its redox partners, SdbB or CcdA2. Oxidized and reduced proteins were incubated at room temperature and the reaction was terminated at indicated times. Proteins were alkylated with maleimide-PEG<sub>2</sub>-biotin (525 Da) and analyzed by western blotting. **A.** Reoxidation of SdbA by SdbB. **B.** Reoxidation of SdbA by CcdA2. **C.** Lack of reoxidation of reduced SdbA alone. **D.** Lack of reoxidation of reduced SdbA by reduced SdbB. **E.** Lack of reoxidation of reduced SdbA by reduced CcdA2. Reduced and oxidized SdbA alone served as a control.

### 3.1.6 SdbA is in a Reduced State in the *sdbBccdA2* Mutant

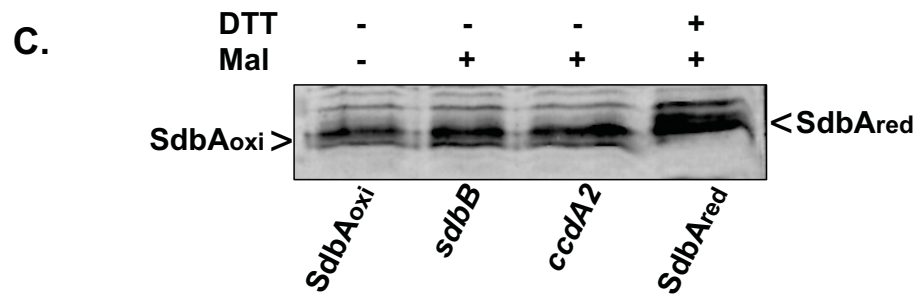
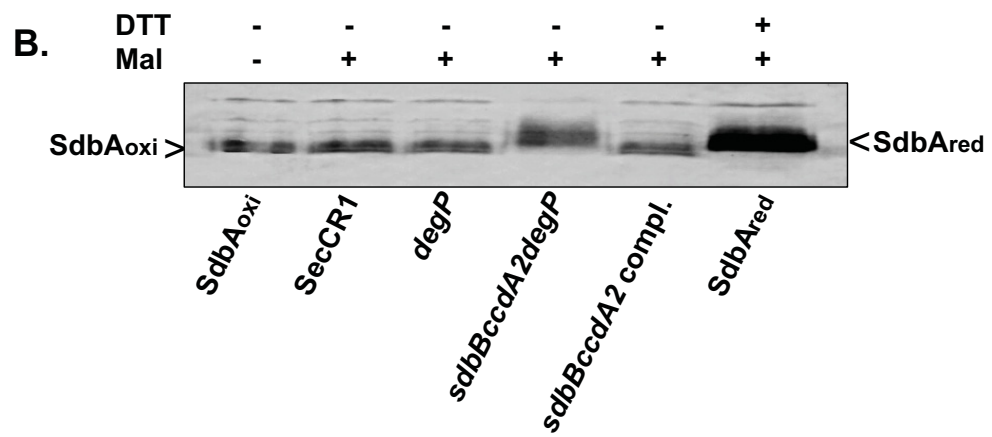
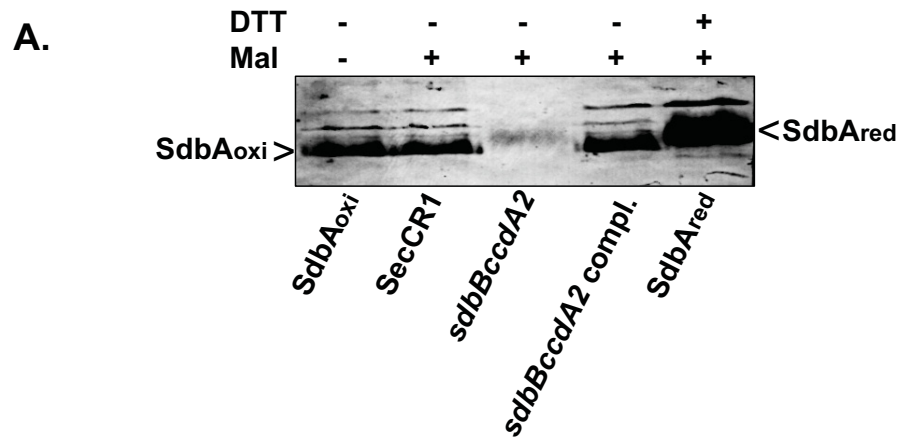
Next, the redox state of SdbA in *S. gordonii* was examined. I reasoned that the inactivation of the redox partners of SdbA would have a direct impact on the redox state of SdbA in the cells. Proteins from the parent and mutant strains were prepared, alkylated, and analyzed in immunoblotting. The results showed that SdbA from the parent strain was present as an oxidized protein and it became reduced after DTT treatment (Figure 3.12A). In contrast, SdbA from the *sdbBccdA2* mutant was present in a reduced form. *sdbBccdA2* complementation restored SdbA to the oxidized form (Figure 3.12A). It was noted that the amount of SdbA in the *sdbBccdA2* mutant was low when compared to the parent and complemented strains. Previous studies showed that the serine protease DegP degraded misfolded anti-CR1 single chain antibody, a protein required two disulfide bonds for stability, in *S. gordonii* (Davey *et al.*, 2013; Davey *et al.*, 2015a). Thus, *degP* was mutated in the *sdbBccdA2* mutant and also in the parent strain as a control. Inactivation of *degP* in the *sdbBccdA2* mutant returned SdbA to a level similar to that in the parent and complemented strains (Figure 3.12B). Importantly, SdbA in the *sdbBccdA2degP* mutant remained reduced. The *degP* mutation in the parent strain did not change the redox state of SdbA, indicating that the alteration of SdbA redox state in the *sdbBccdA2degP* mutant was not due to *degP* mutation (Figure 3.12B). SdbA in the single-gene mutants (*sdbB* and *ccdA2* mutants) was present as an oxidized protein (Figure 3.12C).

### 3.1.7 SdbA<sub>C89A</sub> Variant Forms Mixed Disulfide with SdbB *In vivo*

To provide direct evidence that SdbA and SdbB interacted in *S. gordonii*, the *sdbA<sub>C89A</sub>ΔdegP* mutant was used for the detection of SdbA-SdbB complex. Previous study reported that the single cysteine active site variant, SdbA<sub>C89A</sub>, formed a number of mixed disulfide complexes in this mutant (Davey *et al.*, 2015a). Proteins were extracted from the cells and analyzed by western blotting using anti-SdbA and anti-SdbB antibodies as probes.

**Figure 3.12 The redox state of SdbA in *S. gordonii* parent and mutant strains.**

SdbA in *S. gordonii* strains was alkylated with maleimide-PEG2-biotin (Mal) and analyzed by immunoblotting using anti-SdbA antibody as the probe. Alkylation adds 0.5 kDa per thiol to reduced SdbA, causing an upshift in migration, while oxidized SdbA will not be alkylated and migrated faster during electrophoresis. **A.** The redox state of SdbA in parent strain, *sdbBccdA2* mutant, and *sdbBccdA2*-complemented mutant. **B.** The redox state of SdbA in parent, *degP* mutant of parent, *degP* mutant of *sdbBccdA2*, and *sdbBccdA2*-complemented mutant. **C.** The redox state of SdbA in *sdbB*, and *ccdA2* mutants. SecCR1, parent strain, SdbA<sub>oxi</sub>: oxidized form of SdbA, SdbA<sub>red</sub>: reduced form of SdbA. DTT: dithiothreitol. Arrowheads indicate the position of reduced or oxidized SdbA. Results are representative of three independent experiments.



As shown in Figure 3.13 A, a number of complexes were detected by the antibodies. A band of ~40 kDa, the expected size of the SdbA (21.9 kDa)-SdbB (17.8 kDa) complex, was detected by both antibodies. This 40 kDa band as well as other complexes dissociated under reducing conditions indicating that they were disulfide-linked proteins (Figure 3.13B).

To provide further evidence that the 40 kDa band was a SdbA-SdbB complex, immuno-precipitation using anti-SdbB antibody-coupled beads was performed. The eluate was analyzed by western blotting. The results showed that eluate contained the 40 kDa band that was recognized by both the anti-SdbA and anti-SdbB antibodies (Figure 3.13C). The eluate also contained the SdbB monomer and a weak 37 kDa band, which might be the SdbB homodimer. The blot detected with anti-SdbA showed the 40 kDa band as well as an unknown 28 kDa band. Nonetheless, the recovery of the 40 kDa band by immuno-precipitation strongly indicates that it was a SdbA-SdbB complex.

### **3.1.8 SdbBCcdA2 Homologs Exist in Other Gram-Positive Bacteria**

Homologs of *S. gordonii* SdbA were found in a number of Gram-positive bacteria that lack DsbA (Davey *et al.*, 2013). I speculated that these organisms might also have homologs of SdbBCcdA2. Because SdbB/Sgo\_1177 and CcdA1/CcdA2 share high sequence homology, I searched for homologs of these proteins in Gram-positive bacteria that lack DsbA. Indeed, a blast-search identified homologs of SdbBCcdA2 and Sgo\_1177CcdA1 in other Gram-positive bacteria that lacked a DsbA homolog (Figure 3.14A-C). These bacteria can be placed into two groups, one (for example, *S. pneumoniae*, *S. sanguinis*, and *Clostridium botulinum*) with both SdbBCcdA2 and Sgo\_1177CcdA1, and the other (for example, *S. mutans*, and *S. pyogenes*) with only SdbBCcdA2 or Sgo\_1177CcdA1 underlining diversity among these bacteria. The role of these proteins in these bacteria is largely unknown, except in *S. pneumoniae* where they are involved in a reducing pathway coping with oxidative stress (Saleh *et al.*, 2013).

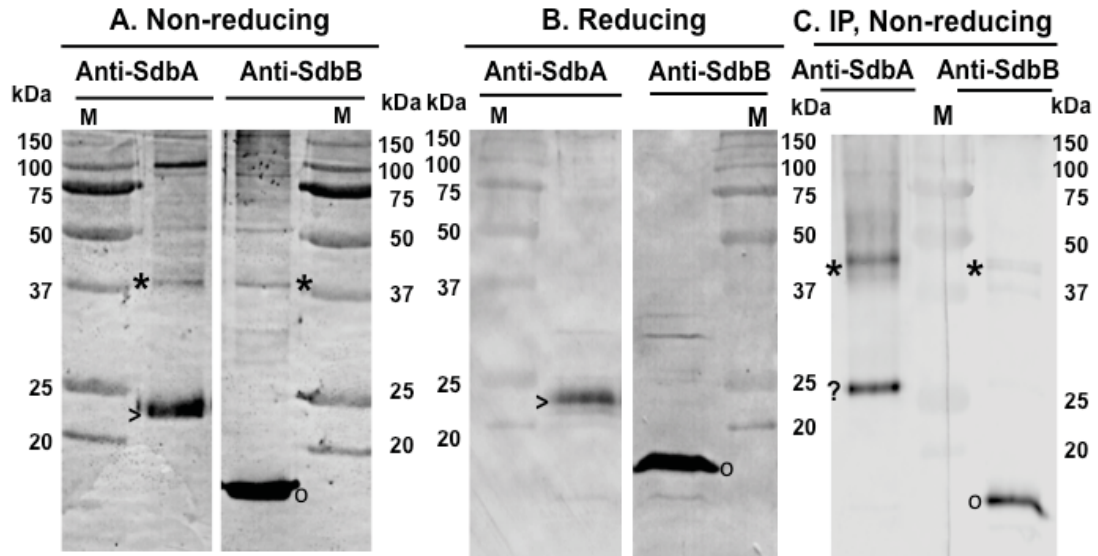


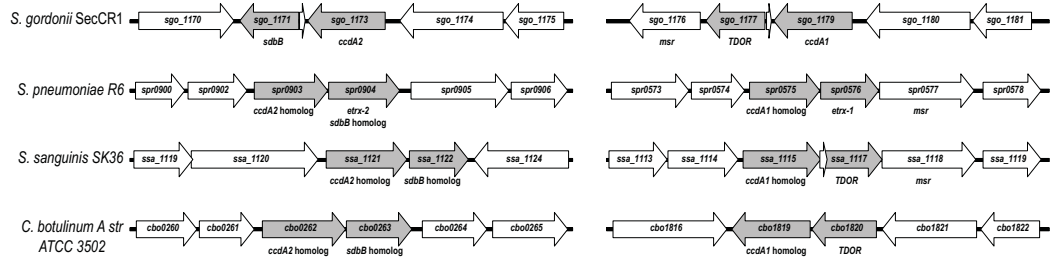
**Figure 3.13 SdbB forms a disulfide-linked complex with SdbA<sub>C89A</sub> in *S. gordonii*.**

**A.** Non-reducing blots of proteins prepared from *S. gordonii* SdbA<sub>C89A</sub> probed with anti-SdbA and anti-SdbB antibodies. **B.** Reducing blots of proteins prepared from *S. gordonii* SdbA<sub>C89A</sub> probed with anti-SdbA and anti-SdbB antibodies. **C.** Proteins recovered from immuno-precipitation (IP) were analyzed by western blotting. M: prestained protein markers. \* : SdbA-SdbB complex. > : SdbA monomer. o: SdbB monomer. ?: unknown protein.

**Figure 3.14 SdbBCcdA2 and Sgo\_1177CcdA1 homologs are present in other Gram-positive bacteria that possess SdbA homolog.**

**A.** Genetic organization of *sdbBccdA2* and *sgo\_1177ccdA1* in *S. gordonii* and other Gram-positive bacteria. **B.** Alignment of homologs to *S. gordonii* SdbB (WP\_008808639) and Sgo\_1177 (WP\_012000580) using Clustal Omega. The CXXC active site and conserved *cis*-proline residue are highlighted. Etrx: *Streptococcus pneumoniae* R6 (NP\_358498, NP\_358170); Ssa: *Streptococcus sanguinis* SK36 (YP\_001035083, YP\_001035078); Cbo: *Clostridium botulinum* ATCC 3502 (YP\_001252806, YP\_001254320). **C.** Alignment of homologs to *S. gordonii* CcdA2 (WP\_012000576) and CcdA1 (WP\_012000582). The two conserved cysteine residues are highlighted. SpCcdA, *Streptococcus pneumoniae* R6 (NP\_358497, NP\_358169); Ssa, *Streptococcus sanguinis* SK36 (YP\_001035082, YP\_001035076); Cbo: *Clostridium botulinum* A str. ATCC 3502 (YP\_001252805, YP\_001254319).

**A.**



**B.**

SdbB	-----MKKYLTFGVLLAAVFLTACSDEMG-----METKSSSNQPAQNAVQGI	45
Sgo_1177	-----MKKITVTLTGLLACAGLLGACSNQKMESE---ASTNDKSS--MTTKKDS	46
Etrx-2	---MNKGGQMKKVMFAGLSLLSLVLMACGEEETKKT-----QAAQQPKQQT	51
Etrx-1	MNKMERNINMKKWQTCVLAGAGSLLCLTACSGKSVTSE---HQTKDEMKT	57
Ssa_1122	-----MKKFVTLAATVSAVFLAACSEQEEKPMTPTSSSSSETPQTSTVTQ	51
Ssa_1117	-----MKKLSILTVSLLCIGLLGACSNQKMNSE---ISKSDKSN--MQTK	46
Cbo0263	---MKNN---KRYIYISVIMLALLVGVKFGY-DY-----LSNNYKSNEA	47
Cbo1820	---MKGKVKL--FIIFILI--VI IAIMAWFK-AVKPK-----EEYS-----	40
.		
SdbB	GQEAPDFTLKSMGDKTVKLSDYKGGKV-YLKFWASWCGPCKKSMPELIELAGK-K	103
Sgo_1177	SKMAKDFSLQGVGDKTYKLSDFKGGKV-YLKFWASWCSICLSTLGDNDLAKEQ	105
Etrx-2	GKDVPDFTLQSMGDKVEKLSDFKGGKV-YLKFWASWCGPCKKSMPELMELAAK-P	109
Etrx-1	GKEVADFELMGVDGKTYRLSDYKGGKV-YLKFWASWCSICLASLPDDEIAKE-AG	115
Ssa_1122	GQEAPDFTLQSMGDKTVKLSDYKGGKA-YLKFWASWCGPCKKSMPELVELAGK-T	109
Ssa_1117	TKMAKDFSLQGVGDKTYKLSDFKGGKV-YLKFWASWCSICLSTLGDNDLAKEQ	105
Cbo0263	FQPAVDFTVYDKDNNEVKLSDYKGGKAI VVNFWASWCSPCKEYMPYQEA	107
Cbo1820	K-----EENIDYEANVGKMPVLELSSPTCGPCRKMTP I I KEVKEKYD	88
	: . ** ::: : * . *	
SdbB	ILSVIAPGIQGEKSETDFPKWFEEQGYKDVPLVYDSQATTFQAYQIRSIPT	163
Sgo_1177	VLSVSPPTFNGEKSAEDFKKWKSLDYKDFPVLMDTKGELLKEYGIRSYPS	165
Etrx-2	ILTVIAPGIQGEKTVEQFPQWFQEQGYKDIPVLYDTKATTFQAYQIRSIPT	169
Etrx-1	VLTVVSPGHKGEQSEADFNWYKGLDYKNLPLVLDPSGKLLLETYGVRSYPT	175
Ssa_1122	ILTVVAPGLQGEKSAEEFPKWFQEQGYKDVPLVLDFTSGEIFQAYQIRSIPT	169
Ssa_1117	VLSVSPPTFNGEKSAEDFKEWYKSLDYKDFPVLIDNKGELLKEYGIRSYPS	165
Cbo0263	ILMVNLTDMRE-TKGS AEGFMKEEGY-DMNV MFDINLDAANKYQLNAP	165
Cbo1820	H-----IIDLTKNPEFGKGYKVSVPVPTQVFLDKEGK	119
	: . : * : *	
SdbB	IGKIQFGAISNEDAEEAFKEMK--	185
Sgo_1177	LAKTHIGYMSKEDIEKTLKEIK--	187
Etrx-2	IGKIQFGAISNADAEEAFKEMN--	191
Etrx-1	LVKTHPGFMEKDAILQTLKELS--	197
Ssa_1122	IGKIQFGAISNADAEEAFKEMK--	191
Ssa_1117	LAKTHIGYMSKEDIEKTLKEIK--	187
Cbo0263	LVYDHVGINKEILDENINKIIN-	188
Cbo1820	VFFRHEGMLTKEEIVDILNKMGVK	143
	: : * : :	



C.

SgCcdA1	-----MATSFLFFISVFLAGILSFFSPC	ILPLMPVYVIGILLDSQ-PKTIRIF	47
SgCcdA2	-----MESLLFSVSVFLAGVLSFFSPC	IFPLLPVYIGILLDSEDKPRTVRF	47
SpCcdA1	-----METIVFLISVFLAGVLSFFSPC	IFPLLPVYAGILLDDQESAKSFSLF	47
SpCcdA2	-----MGHIFFLSVFLAGILSFFSPC	ILPLLPVYTGVLDDKDGQAASS-G	46
Ssa_1115	-----MESHLLFFVSVFLAGILSFFSPC	IFPLLPVYIGILLDDKE-VKTLKVF	46
Ssa_1121	-----MATSFLFFISVFLAGILSFFSPC	ILPLMPVYVIGILLDSQ-PKTVRFM	47
Cbo1819	-----MNYILLFLEGIITFISPC	ILPMIPIYVSYFAGEDIDNKN----	39
Cbo0262	MNEIITKAVSLMGNNVLLALLISFLGGI	ISSFSPCILSSPLIIGYVNKYGRDDK----	55
	. : * * *:: : ** * : : * : . . :		
SgCcdA1	GREVSWYGMVKTLCFIGGLSTVFLVLV	GYGAGALGQVLY--APWFRVYVGGIV	105
SgCcdA2	GREIAWYGLVKTLCFIAGISCVFFILG	FAGFLGAIN--SSWFRYVMGIIILLG	105
SpCcdA1	GRKVLWSGLIRTLCFIAGISLIFFILG	FAGYFGHILY--ANWFRYVMGAIILL	105
SpCcdA2	KFSISVTSLLRTLAFIAGISFIFILLG	YGAGFLGDLLY--ASWFQYLTGAIILL	104
Ssa_1115	GRELAWQGMVRTLFFIAGISTVFLVLL	GYGAGFLGTIIY--SPTFRYVMGGLI	104
Ssa_1121	GKDISWYGLAKTLCFIAGLSTVFLVLV	GYGAGALGQVLY--APWFRVYVGGIV	105
Cbo1819	---YKNRALISSIAFVAGFTFVFTLLG	VAACTVGVIFNKYMRIINIVSGSIMV	96
Cbo0262	----KTAFKYSLFFSLGIIITFTSLGI	ISSLVGKFFTSGGKLWYLLLVVMIFV	110
	. : : * * : * * * . . * . : : * : : . * : :		
SgCcdA1	GLINIQQLQKQKSIQLKKNKR-SDFLN	AFLLGITFSFGWTPC	164
SgCcdA2	ELINIKPLQMKNVAFKKDSKR-NEFLS	AFVLGITFSFGWTPC	164
SpCcdA1	EIFHLKKLEVQKSFTEFKS-DS-NRYW	SFAFLGITFSFGWTPC	163
SpCcdA2	EILHFGLYKELKRLQGGQNGKYSQAF	LLGLTFSFAWTPC	164
Ssa_1115	ELINIRQLQIQKSLTFKKNQK-HHFWS	AFLGITFSFGWTPC	163
Ssa_1121	GIINIQQLQKQKSIQLKKNKR-SDFLN	AFLLGITFSFGWTPC	164
Cbo1819	GIINVGLLHRSEFKINKSA-GHKKSS	IMSTALFGMIFGFGWTPC	154
Cbo0262	GVIESKNK-----CKVPKRRKGLLGA	FFLGILGGVLSSPC	163
	:: . : . * : . . * * * * * . . . .		
SgCcdA1	GALQGGLLMLVYTLGLALPFLAMAMAS	GWVLRQFS--KLKPHMGLTKKIGGALI	222
SgCcdA2	GAFQGAITLIYTLGMALPFLIALASSF	VVMQYFN--KIKPYMGLKKGAIILMGIL	222
SpCcdA1	GAWQGAITYTLIYTLGMALPFLVLA	LASGLVMPYFS--KIKRHMLLKKIGGFLI	221
SpCcdA2	GAWQAGLMLVYTLGLALPFLLLALTSS	YVLKHFR--KLHPYLGLLKKVGGFLI	222
Ssa_1115	GAFQGAITLIYTLGMALPFLIALASSF	VVMQYFN--KIKPYMGLKKGAIILMGIL	221
Ssa_1121	GALQGGLLMLVYTLGLALPFLAMALAS	GWVVRKFA--KLKPYMGLKKGAIILMGIL	222
Cbo1819	NVFMGASMLMIYSLGLGIPFILSALL	IDSLSKTTFD--FIKRYKTNIRISGGLL	212
Cbo0262	-ILLGFLMLLLYSIGHCFVIIISGTS	LGVFESLSGSSKANKINNVLKIIILGII	222
	* : : * * : : : . . : : : * : : * : :		
SgCcdA1	LMLGNLNALASLFG-	236	
SgCcdA2	LMLGQLNALSGLFG-	236	
SpCcdA1	LLLGQVNVLAGIFE-	235	
SpCcdA2	VLFGNASILSQLFE-	236	
Ssa_1115	LMLGQLNALSGVFG-	235	
Ssa_1121	LMLGNLNALASLFG-	236	
Cbo1819	MMTGYNLLLSILTF	227	
Cbo0262	LIYIGI-----	228	
	::		

### 3.1.9 Summary

In summary, the above results showed that SdbA has two redox partners, SdbB and CcdA2. The phenotypic analysis of the single- and double-gene mutants showed that *sdbBccdA2* mutant was able to reproduce *sdbA* mutant phenotypes with a defect in autolysis, bacteriocin production, genetic competence, and extracellular DNA (eDNA) release. Complementation of *sdbBccdA2* mutant restores the parental phenotypes. AtIS, the natural substrate of SdbA, was inactive and lacked a disulfide bond in the *sdbBccdA2* mutant. Both SdbB and CcdA2 possess oxidase activity and were able to reoxidize SdbA *in vitro*. SdbA was in a reduced state in the *sdbBccdA2* mutant and complementation restored the redox state of SdbA to the oxidized state. In *sdbB* or *ccdA2* single-gene mutants, SdbA remains in an oxidized state. Finally, SdbA<sub>C89A</sub> formed a mixed disulfide with SdbB in *S. gordonii*. Collectively, these results strongly support the notion that SdbB and CcdA2 are independent redox partners of SdbA and that SdbA, SdbB, and CcdA2 represent the oxidative protein folding pathway in *S. gordonii*.

### 3.2 Identification and Characterization of a Reducing Pathway in *S. gordonii*

In the dental plaque, *S. gordonii* competes with other bacterial species by producing up to 1.6 mM of hydrogen peroxide (H<sub>2</sub>O<sub>2</sub>) (Barnard and Stinson, 1999; Liu *et al.*, 2011). In addition to *S. gordonii*, other oral bacteria, such as *Streptococcus sanguinis* and *Streptococcus oralis*, also produce H<sub>2</sub>O<sub>2</sub> (Zhu and Kreth, 2012). H<sub>2</sub>O<sub>2</sub> and other reactive oxygen species (ROS) can damage proteins by oxidizing cysteines and methionines (Ezraty *et al.*, 2017). *S. gordonii* has a superoxide dismutase but lacks catalase (Zheng *et al.*, 2011; Jakubovics *et al.*, 2002). Thus, oxidation by H<sub>2</sub>O<sub>2</sub> and other ROS is a problem for *S. gordonii* to deal with. In this section, I will focus on methionine oxidation and repair in *S. gordonii*.

During oxidation, methionine (Met) is converted to methionine sulfoxide (MetO), which can be further oxidized to an irreversible modification methionine sulfone (MetO<sub>2</sub>). Methionine sulfoxide reductase (Msr) is an enzyme that reduces MetO to Met

(Lu and Holmgren, 2014). *S. gordonii* has a methionine sulfoxide reductase A (MsrA) (Lei *et al.*, 2011). MsrA is 36 kDa protein without a predicted signal sequence (Figure 3.15). Western blotting and immunofluorescent analysis showed that only trace amount of MsrA was detected in the cell wall fraction and cell surface, respectively, and the majority of the protein was located in the cytoplasm (Lei *et al.*, 2011). The expression of *msrA* is induced in biofilms and in response to a shift from acidic to neutral pH, and to exogenous H<sub>2</sub>O<sub>2</sub>. *msrA* mutants showed increased sensitivity to H<sub>2</sub>O<sub>2</sub>, and a defect in adhesion and biofilm formation in the presence of exogenous H<sub>2</sub>O<sub>2</sub> (Vriesema *et al.*, 2000; Lei *et al.*, 2011).

In addition to MsrA, the genome of *S. gordonii* also encodes another Msr named MsrAB (SgMsrAB) (Haase *et al.*, 2015). SgMsrAB is a 42.5 kDa protein with a predicted signal sequence and consists of both the MsrA and MsrB domain. MsrAB shares 62% sequence identity to MsrA (Figure 3.15). *msrAB* was down-regulated in mutants lacking amylase-binding protein A (Haase *et al.*, 2015). However, the role of MsrAB in oxidative stress resistance in *S. gordonii* has not been investigated. In addition, little is known about the pathway(s) that catalyzes the regeneration of Msrs in *S. gordonii*. In the following section, the role of MsrAB in protecting *S. gordonii* from oxidative stress is shown and the pathway that regenerates MsrAB is described. This pathway represents a reducing pathway in *S. gordonii*.

### **3.2.1 The Genetic Locus of MsrAB in *S. gordonii***

The extracytoplasmic Msr of *S. pneumoniae* (*SpMsrAB2*) was previously shown to be involved in oxidative stress resistance (Saleh *et al.*, 2013; Kim *et al.*, 2009; Andisi *et al.*, 2012). Therefore, experiments were set forth to determine if *S. gordonii* utilize a similar antioxidation mechanism to *S. pneumoniae*. *In silico* analysis showed that SgMsrAB is highly homologous to *SpMsrAB2* with a 75% sequence identity. Similar to *SpMsrAB*, SgMsrAB appears to be an extracytoplasmic protein with a predicted signal sequence, suggesting a possible role in protecting extracytoplasmic proteins under oxidative stress conditions (Figure 3.15).

SgMsrA	-----	0
SgMsrAB	<u>MESKWKMIMFILAFLLCFGLFLLIRGSM</u> <u>SIDSSHANAEQIKKASMSKTEVVKKKKEDVKE</u>	60
SpMsrAB2	<u>MNDKLIKIFLLLGVFFLATGIFYVLL---</u> <u>IRNAGQTDASQIEKAAVSQGGKAVKKEIFEISKD</u>	57
SgMsrA	--MAEIIYLAGGC FWGLEEYFSRIEGVKKTTVGYANGQVESTNYQLIHQTDHAETVHLLIYD	58
SgMsrAB	ADKRVIYLAGGC FWGVVEEYFSRVPGVIDAESGYANGKGDITTKYELVSQTGHAETVKITYN	120
SpMsrAB2	ADLHEIYLAGGC FWGVVEEYFSRVPGVTDVAVSGYANGRGETTKYELINQTDGHAETVHVITYD	117
	*****:*****: ** .: *****: :*:*:*: **.******: *:	
SgMsrA	EKRVSLEILLYYFRVIDPLSVNKQGNQVGRQYRTGVYYTNQADKAVIEQVFAEQEKQLG	118
SgMsrAB	VKKISLKEILLHYFRIIDPTSKNKQGNQGTQYRTGVYYKDEADLNTINQVFDEVAKKYD	180
SpMsrAB2	AKQISLKEILLHYFRIINPTSKNKQGNQVGTQYRTGVYYTDDKDLEVINQVFDEVAKKYD	177
	*:*:*:*****:***:* * ***** * *****.:*: * .*:*** * *: .	
SgMsrA	QKIAVELEPLRHYVLAEDYHQDYLLKKNPGGY CHINVNDAYQPLVDPGQYKPTDAELKEQ	178
SgMsrAB	KPLAVEKEPLKNYVKAENYHQDYLLKKNPNGY CHIDVNQAAYPVIDANRYTKPSDEEIKSK	240
SpMsrAB2	QPLAVEKENLKNFVVAEDYHQDYLLKKNPNGY CHINVNQAAYPVIDASKYPKPSDEELKKT	237
	: :*** * *:::* **.******.*****:***: * *::* .:* **:* **:	
SgMsrA	LTQEYQVQTQLSATERPFHNAYNATFEEGIYVDVTTGEPFLFFAGDKFESG GWPFSFRPI	238
SgMsrAB	LSPEEYAVTQKNDTERAFSNRYWDKFDAGIYVDVTTGEPFLFSSKDKFDSG GWPFSFRPI	300
SpMsrAB2	LSPEEYAVTQENQTERAFSNRYWDKFDGSIYVDIATGEPFLFSSKDKFESG GWPFSFTQPI	297
	*: *:* *** . *** * * * .*: *****:***** : *****:*****:***	
SgMsrA	AREVLRYYEDKSHGMERIEVRSRSGNAHLGHVFTDGPESAGGLRY INSAAALRFIPKEKM	298
SgMsrAB	SPDVATYKEDKSNMTRTEVRSRVGNHSHLGHVFTDGPDKGGLRY INSLSIKFIPKAEM	360
SpMsrAB2	SPDVVITYKEDKSNMTRMEVRSRVGDSHLGHVFTDGPDKGGLRY INSLSIRFIPKQDM	357
	: * * *****.* * ***** *:*****:*****. ***** :*:***** :*	
SgMsrA	EAEGYAYLLQHMK	311
SgMsrAB	EKGYGYLLDYV-	372
SpMsrAB2	EKGYAYLLDYVD	370
	* :**.****:*	

**Figure 3.15** Sequence alignment of *S. gordonii* MsrA, MsrAB, and *S. pneumoniae* MsrAB2.

Conserved amino acid residues are indicated with an asterisk. Putative catalytic cysteines are boxed. The predicted signal sequences of *S. gordonii* MsrAB and *S. pneumoniae* MsrAB2 are underlined (SignalP).

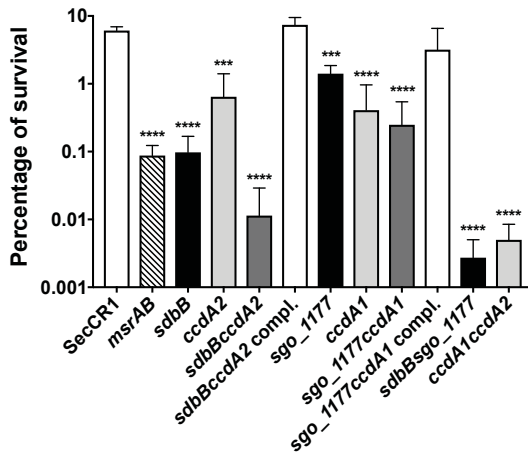
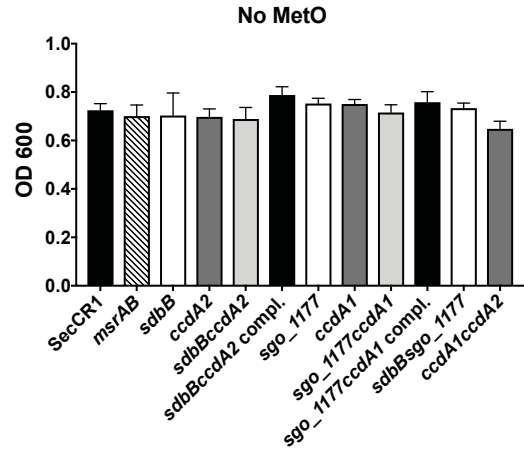
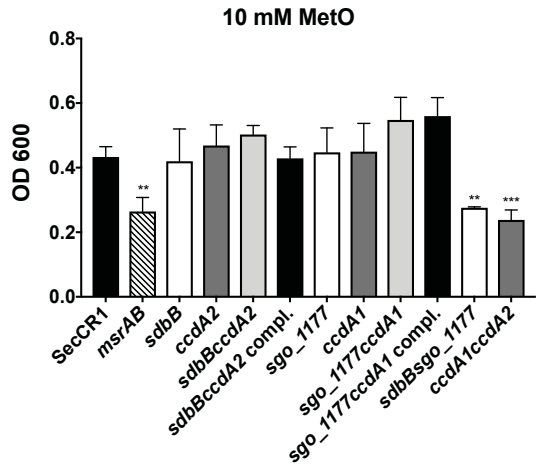
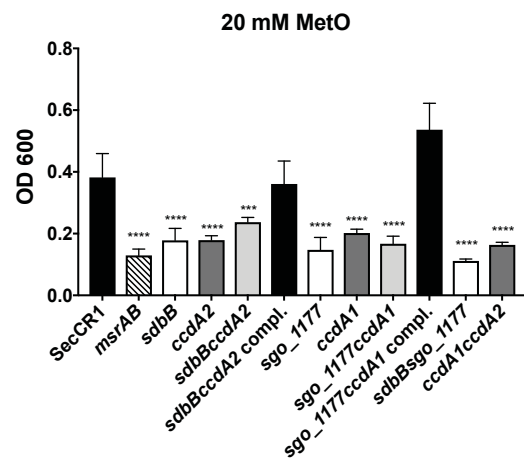
As shown in section 3.1.1, *msrAB* is located in the *ccdA1* locus forming an operon with *ccdA1*, *sgo\_1177*, and a two-component regulatory system (*sgo\_1180* and *sgo\_1181*) (Figure 3.1E and 3.2A) (Haase *et al.*, 2015; Jalal *et al.*, 2019). Further downstream of *msrAB* is the *sdbBccdA2* operon. The genetic organization of these two loci resembles those in *S. pneumoniae* (Saleh *et al.*, 2013). In *S. pneumoniae*, SpMsrAB2 is regenerated by two thioredoxin-like lipoproteins Etrx1 and Etrx2. These lipoproteins were said to acquire electrons from the integral membrane protein SpCcdA1 and SpCcdA2, which receive electrons from the cytoplasmic thioredoxins system (Saleh *et al.*, 2013). CcdA1 and CcdA2 share 57% and 69% sequence identity to SpCcdA1 and SpCcdA2, respectively, while, Sgo\_1177 and SdbB share 53% and 75% sequence identity to Etrx1 and Etrx2, respectively.

### **3.2.2 MsrAB, SdbB, Sgo\_1177, and CcdA Proteins are Involved in Oxidative Stress Resistance**

In both Gram-positive and Gram-negative bacteria, inactivation of *msr* renders the cells more sensitive to oxidative stress (Ezraty *et al.*, 2005a). To assess if *msrAB* and other genes in the *ccdA1* and *ccdA2* loci play a similar role in *S. gordonii*, single- and double-gene mutants were constructed and described in section 3.1.2 (Table 2.1). The mutants were tested for sensitivity to H<sub>2</sub>O<sub>2</sub> by determining the percentage of survival of the strains following exposure to 10 mM H<sub>2</sub>O<sub>2</sub>. The results showed that the *msrAB* mutant was significantly more sensitive to H<sub>2</sub>O<sub>2</sub> compared to the parent strain (Figure 3.16A). Interestingly, the *sdbB*, *sgo\_1177*, *ccdA1*, and *ccdA2* single-gene mutants were also more sensitive to H<sub>2</sub>O<sub>2</sub> compared to the parent strain (Figure 3.16A). Among them, the *msrAB* and *sdbB* mutants were the most sensitive showing a ~100-fold reduction in survival (Figure 3.16A). For the double-gene mutants, *sgo\_1177ccdA1* and *sdbBccdA2* were sensitive to H<sub>2</sub>O<sub>2</sub>. Complementation of *sgo\_1177ccdA1* and *sdbBccdA2* restored the level of sensitivity to that of the parent strain. *sdbBsgo\_1177* and *ccdA1ccdA2* double mutants were the most sensitive showing a ~1000-fold reduction in survival (Figure 3.16A).

**Figure 3.16 Sensitivity to H<sub>2</sub>O<sub>2</sub> and methionine sulfoxide by *S. gordonii*.**

**A.** Sensitivity of *S. gordonii* parent and mutants to H<sub>2</sub>O<sub>2</sub>. *S. gordonii* were challenged with 10 mM H<sub>2</sub>O<sub>2</sub> for 30 minutes and the percentage of survival was determined by CFU counts. Data are means ± SD of three independent experiments with triplicate in each experiment. **B, C, and D.** Sensitivity of *S. gordonii* parent and mutants to methionine sulfoxide. *S. gordonii* were grown for 24 hours in the presence or absence of methionine sulfoxide. Results are means ± SD of two independent experiments with duplicates in each experiment. (\*\*P < 0.01; \*\*\*P < 0.001; \*\*\*\*P < 0.0001; one-way ANOVA).

**A.****B.****C.****D.**

Next, the sensitivity of the mutants to methionine sulfoxide was assessed. All *S. gordonii* strains grew to a similar optical density in media alone (Figure 3.16B), but in the presence of 10 mM methionine sulfoxide, the *msrAB* mutant showed an impaired growth (Figure 3.16C). The *sdbBsgo\_1177* and *ccdA1ccdA2* mutants also showed a defect in growth in the presence of 10 mM methionine sulfoxide compared to the parent strain. At 20 mM methionine sulfoxide, all the single- and double-gene mutants showed reduced growth (Figure 3.16D). Complementation of *sgo\_1177ccdA1* and *sdbBccdA2* restored the sensitivity in the double-gene mutants to that of the parent strain (Figure 3.16D). Collectively, these results indicated that MsrAB, SdbB, CcdA2, Sgo\_1177, and CcdA1 are involved in protection against H<sub>2</sub>O<sub>2</sub> stress and methionine sulfoxide toxicity in *S. gordonii*.

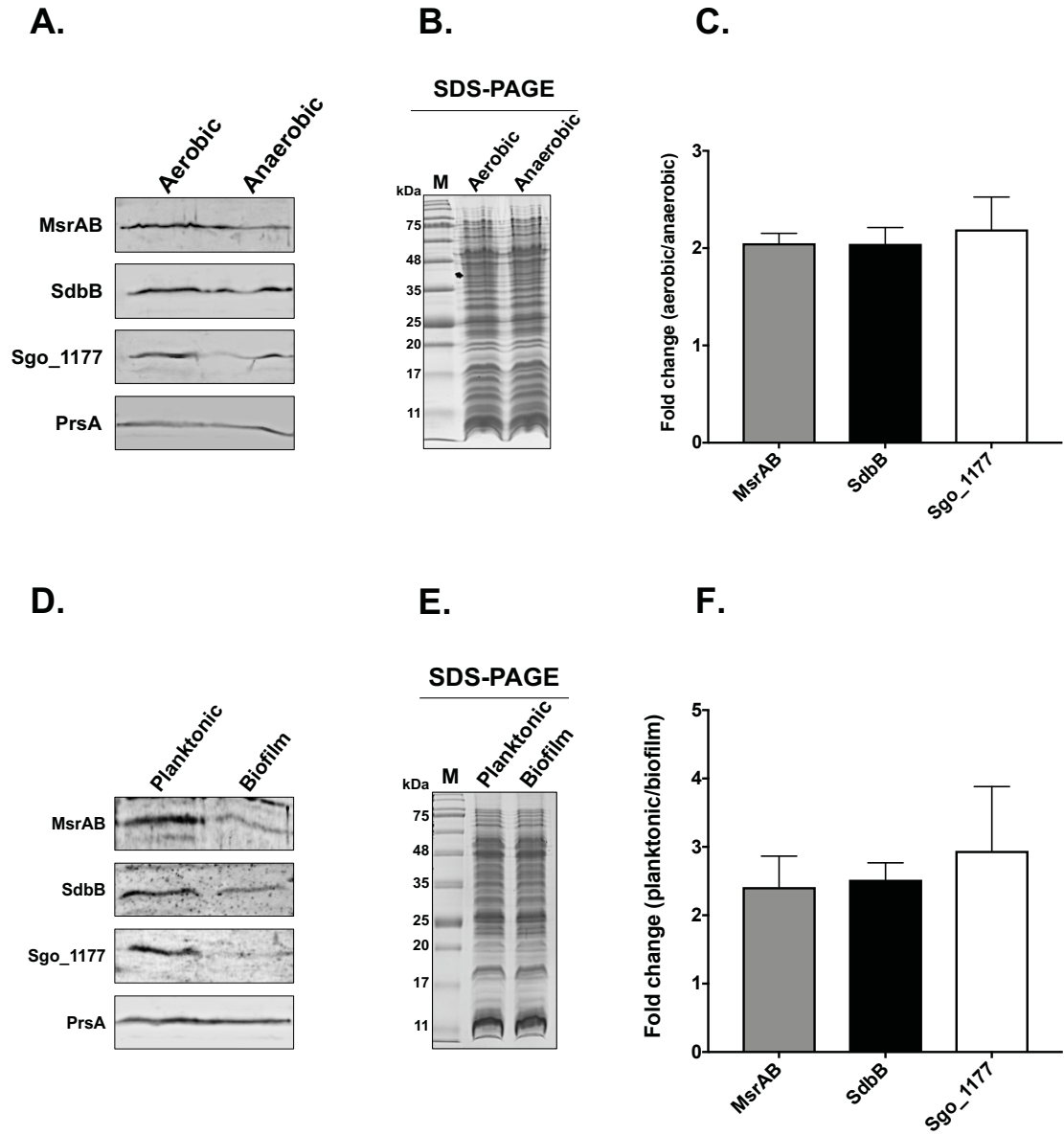
### **3.2.3 MsrAB, SdbB, and Sgo\_1177 Production are Induced by Aeration**

The above results suggest that MsrAB, SdbB, CcdA2, Sgo\_1177, and CcdA1 are involved in resistance to H<sub>2</sub>O<sub>2</sub> and MetO. During aerobic growth, *S. gordonii* produces H<sub>2</sub>O<sub>2</sub> from the conversion of pyruvate to acetyl phosphate (Barnard and Stinson, 1999). Therefore, I hypothesize that the level of MsrAB, SdbB, Sgo\_1177, CcdA1, and CcdA2 are affected by aerobic growth. To test this, *S. gordonii* was grown under aerobic and anaerobic conditions, and the level of MsrAB, SdbB, and Sgo\_1177 was examined by immunoblotting. Due to the lack of antibody to CcdA1 and CcdA2, western blotting of these two proteins were not performed. The results showed that the level of MsrAB was two-fold higher when *S. gordonii* was grown aerobically compared to anaerobically. The same was observed for SdbB and Sgo\_1177 (Figure 3.17A-C).



**Figure 3.17 Immunoblot analysis of the level of MsrAB, SdbB, and Sgo\_1177 in *S. gordonii*.**

**A.** The level of MsrAB, SdbB, and Sgo\_1177 in *S. gordonii* SecCR1 under aerobic and anaerobic growth conditions. Proteins were probed with specific polyclonal antisera. The detection of PrsA was used as a loading control. **B.** SDS-PAGE gel showing equal total protein loading. **C.** Densitometry analysis of the MsrAB, SdbB, and Sgo\_1177 immunoreactive band using Image J. The results are expressed as the intensity of the band from the aerobic sample divided by that from the anaerobic sample. **D.** The level of MsrAB, SdbB, and Sgo\_1177 in *S. gordonii* SecCR1 planktonic and biofilm cells. Proteins were probed with specific polyclonal antisera. The detection of PrsA was used as a loading control. **E.** SDS-PAGE gel showing equal total protein loading. **F.** Densitometry of the MsrAB, SdbB, and Sgo\_1177 immuno-reactive band using Image J. The results are expressed as the intensity of the band from the planktonic sample divided by that from the biofilm sample. Results are means  $\pm$  SD of two independent experiments.



It has been shown in other bacteria that the expression of *msr* is modulated in the biofilm lifestyle (Beloin *et al.*, 2004). Because biofilm and planktonic cells are exposed to different O<sub>2</sub> level, the expression of *msrAB*, *sdbB*, and *sgo\_1177* may be altered in biofilms. To test this, the level of MsrAB, SdbB, and Sgo\_1177 in planktonic and biofilm cells was examined. The results showed that planktonic cells displayed a two-fold increase in the level of MsrAB, SdbB, and Sgo\_1177 compared to the biofilm cells (Figure 3.17D-F).

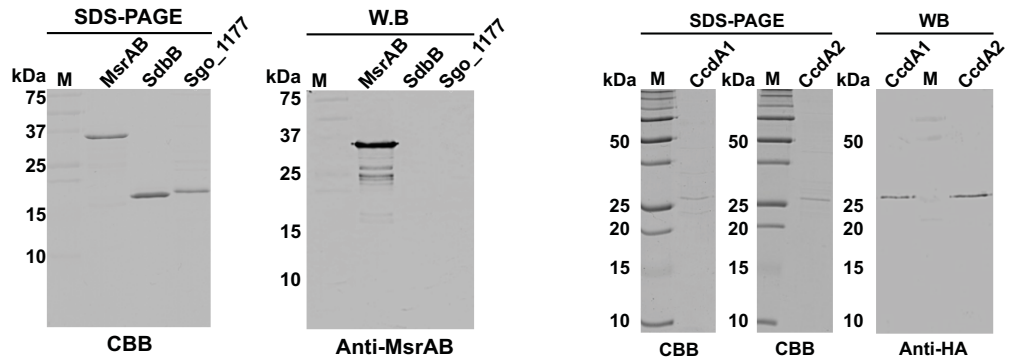
### **3.2.4 SdbB and Sgo\_1177 are Able to Reduce MsrAB**

Following the reduction of MetO, Msr is oxidized with the cysteines in the active site become disulfide bonded (Ezraty *et al.*, 2005a; Lowther *et al.*, 2000). To perform another round of reaction, the oxidized Msr needs to be regenerated to the reduced form, and this is achieved by accepting electrons from its partners in the reducing pathway (Lu and Holmgren, 2014). How MsrAB is regenerated in *S. gordonii* is not known. I hypothesize that electrons are transferred from cytoplasmic thioredoxins to CcdA and then to MsrAB directly or via SdbB or Sgo\_1177. To test this, the ability of CcdA1, CcdA2, SdbB, and Sgo\_1177 to reduce MsrAB in disulfide exchange reactions was examined. In these reactions, recombinant MsrAB, SdbB, Sgo\_1177, CcdA1, and CcdA2 were produced and isolated from *E. coli* (Figure 3.18A). Both the reduced and oxidized forms of MsrAB were detected by the anti-MsrAB antibody, which showed no cross-reaction to SdbB or Sgo\_1177 (Figure 3.18A). When oxidized MsrAB was incubated with reduced SdbB, MsrAB was rapidly reduced (Figure 3.18B). MsrAB was also reduced by Sgo\_1177 (Figure 3.18C). Neither CcdA1 nor CcdA2 were able to reduce MsrAB (Figure 3.18D). These results provided evidence that SdbB and Sgo\_1177 have the enzymatic capability to reduce MsrAB.

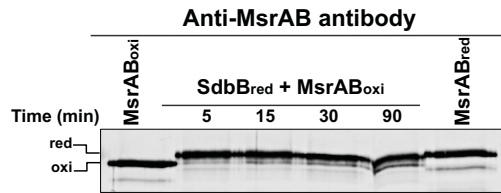
**Figure 3.18 Disulfide exchange between MsrAB, SdbB, Sgo\_1177, CcdA1, and CcdA2.**

**A.** SDS-PAGE gels stained with Coomassie brilliant blue (CBB) and western blots (WB) of purified recombinant MsrAB, SdbB, Sgo\_1177, CcdA1, and CcdA2. M: prestained protein markers. **B.** Reduction of MsrAB by SdbB. **C.** Reduction of MsrAB by Sgo\_1177. **D.** Lack of reduction of MsrAB by CcdA1 or CcdA2. **E.** Reduction of SdbB by CcdA1 or CcdA2. **F.** Reduction of Sgo\_1177 by reduced CcdA1 or CcdA2. In panels **B** to **F**, proteins reduced by DTT or oxidized by glutathione were run alongside to serve as reduced and oxidized protein controls. Disulfide exchange reactions in panels **D**, **E**, and **F** were incubated for 30 minutes.

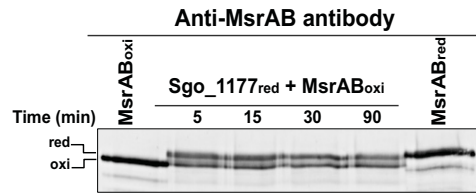
**A.**



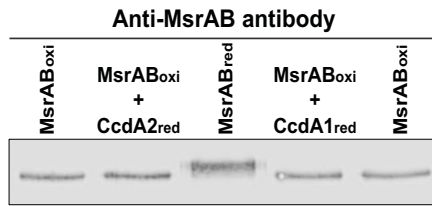
**B.**



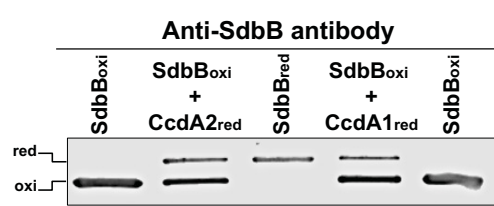
**C.**



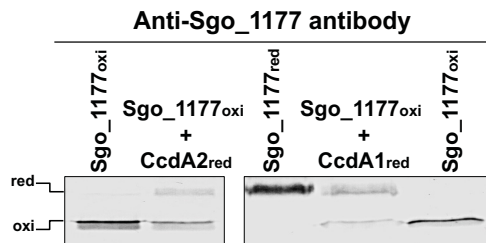
**D.**



**E.**



**F.**



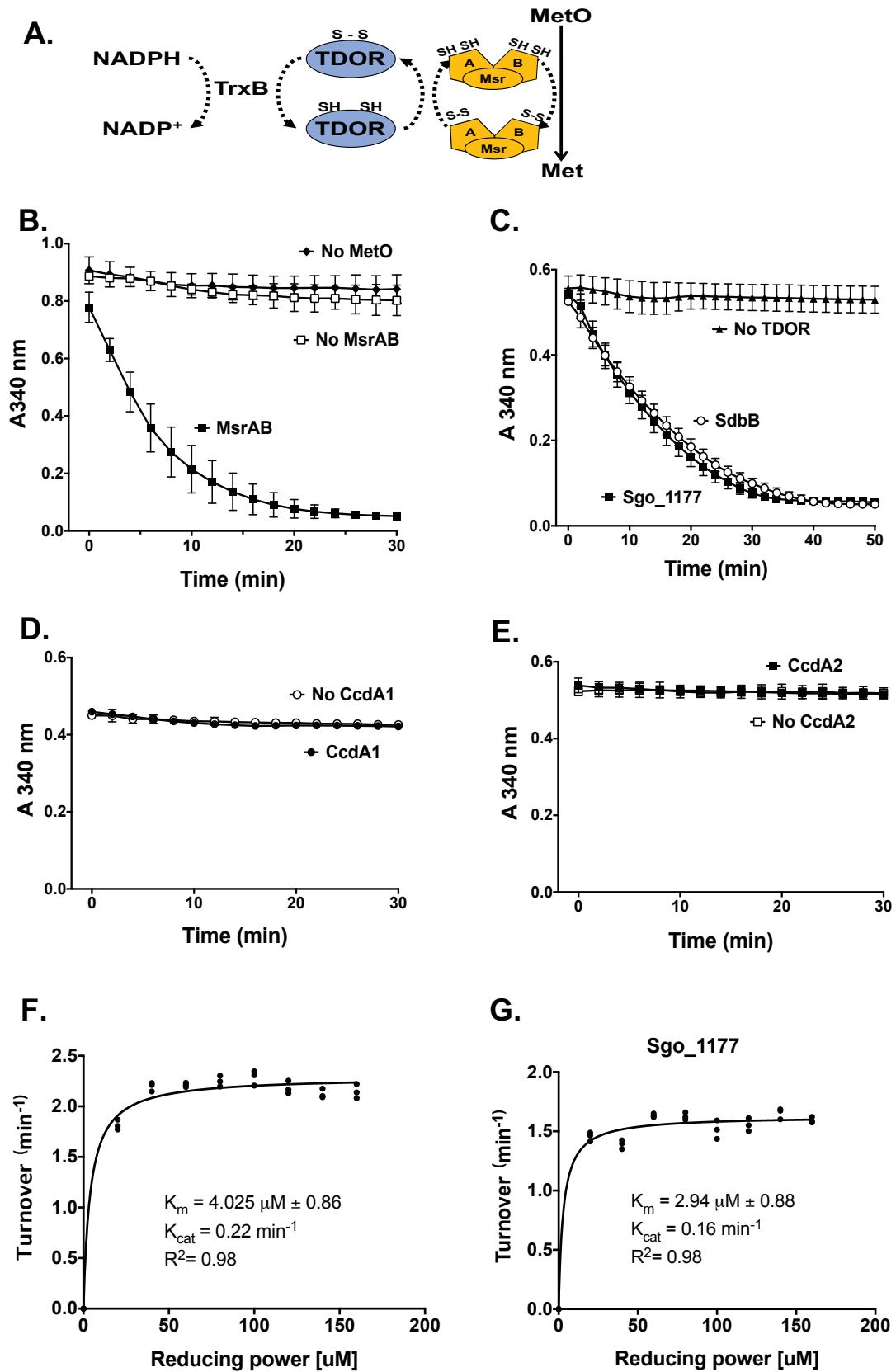
The above results also showed that CcdA1 and CcdA2 were incapable of reducing MsrAB. However, they could play a role in MsrAB regeneration by reducing SdbB and Sgo\_1177. To test this, disulfide exchange reactions were performed between these proteins. The results showed that CcdA1 and CcdA2 could reduce SdbB and Sgo\_1177 (Figure 3.18E and F).

### **3.2.5 Methionine Sulfoxide Reductase Activity of MsrAB with SdbB and Sgo\_1177 as Partners**

The above results suggest that SdbB and Sgo\_1177 play a direct role in MsrAB regeneration. To provide further evidence, methionine sulfoxide reductase assay was conducted. In this assay, MsrAB activity was determined using MetO as a substrate and NADPH as a source of electrons. In the assay, thioredoxin reductase (TrxB) transfer the electrons from NADPH to TDOR (e.g., thioredoxin, SdbB, Sgo\_1177, CcdA1, or CcdA2) and then to MsrAB, which then reduces MetO (Figure 3.19A). First, I tested the validity of the assay by using thioredoxin (Trx-2), a known TDOR in the reaction (Lu and Holmgren, 2014; Si *et al.*, 2015). The results showed that MsrAB was able to reduce MetO. This activity was abolished when MetO or MsrAB was omitted from the reaction (Figure 3.19B). In the presence of SdbB, the reduction of MetO by MsrAB was observed. The same was observed in the presence of Sgo\_1177 (Figure 3.19C). The specific activity of MsrAB with SdbB or Sgo\_1177 was 27.5 and 28.5 nmol NADPH/mg MsrAB/min ( $P = 0.1154$ ), respectively. This activity was not observed when SdbB or Sgo\_1177 was omitted from the reaction indicating the flow of electrons was interrupted (Figure 3.19C). No MsrAB activity was detected when CcdA1 or CcdA2 was used in place of Sgo\_1177 or SdbB (Figure 3.19D and E). This last finding is consistent with the disulfide exchange reaction results (section 3.2.4) where neither CcdA1 nor CcdA2 were able to reduce MsrAB.

**Figure 3.19 Enzymatic activities of MsrAB.**

**A.** Schematic diagram depicting the methionine sulfoxide reductase assay. Electrons are funneled from NADPH to MsrAB by TrxB via TDOR. MsrAB converts MetO to Met. **B.** The reduction of methionine sulfoxide by MsrAB in the presence of thioredoxin (Trx-2), a known TDOR in this assay (Lu and Holmgren, 2014; Si *et al.*, 2015). Reactions without MsrAB or MetO served as controls. **C.** The reduction of methionine sulfoxide by MsrAB in the presence of SdbB or Sgo\_1177. Reactions without SdbB and Sgo\_1177 (no TDOR) served as controls. **D** and **E.** The reduction of methionine sulfoxide by MsrAB in the presence of CcdA1 or CcdA2. Reactions without CcdA1 and CcdA2 (no TDOR) served as controls. Results are mean  $\pm$  SD of three independent experiments with duplicates in each experiment. **F** and **G.** Michaelis-Menten enzyme kinetics of MsrAB activity with SdbB and Sgo\_1177 as a redox partner. The data are representative of three independent experiments.





The above results showed that SdbB and Sgo\_1177 were required for MsrAB activity. To help to determine if the two proteins have different ability to aid MsrAB activity, enzyme kinetics experiments were performed. The  $K_m$ ,  $k_{cat}$ , and catalytic efficiencies of MsrAB with SdbB were  $4.025 \pm 0.861 \mu\text{M}$ ,  $0.22 \pm 0.0035 \text{ min}^{-1}$ , and  $0.057 \pm 0.0023 \mu\text{M}^{-1} \text{ min}^{-1}$ , respectively, while that with Sgo\_1177 were  $2.94 \pm 0.88 \mu\text{M}$ ,  $0.16 \pm 0.0026 \text{ min}^{-1}$ , and  $0.058 \pm 0.0094 \mu\text{M}^{-1} \text{ min}^{-1}$ , respectively (Figure 3.19F and G). The  $K_m$  of MsrAB with SdbB or Sgo\_1177 was similar ( $P = 0.098$ ). Interestingly, the turnover number ( $K_{cat}$ ) between MsrAB with SdbB or Sgo\_1177 was significantly different ( $P = 0.0001$ ). There was no significant difference in the catalytic efficiencies ( $K_{cat}/K_m$ ,  $p = 0.91$ ) between MsrAB with SdbB or Sgo\_1177.

### 3.2.6 Summary

The above results indicated that MsrAB was able to use both SdbB and Sgo\_1177 as a redox partner to reduce MetO. Disulfide exchange reactions showed that both SdbB and Sgo\_1177 were able to reduce MsrAB. CcdA1 and CcdA2 were not able to reduce MsrAB but were able to reduce SdbB and Sgo\_1177. The phenotypic analysis showed that growth of *msrAB*, *sdbBsgo\_1177*, and *ccdA1ccdA2* mutants was impaired in the presence of 10 mM methionine sulfoxide. At 20 mM methionine sulfoxide, the growth of all single- and double-gene mutants were impaired. Similarly, all single-gene mutants, including *msrAB*, *sdbB*, *sgo\_1177*, *ccdA1*, and *ccdA2* were sensitive to exogenous  $\text{H}_2\text{O}_2$ . Among the double-gene mutants, *sdbBsgo\_1177* and *ccdA1ccdA2* showed the highest sensitivity to  $\text{H}_2\text{O}_2$ . Consistent with their role in oxidative stress resistance, the level of MsrAB, SdbB, and Sgo\_1177 was two-fold higher when *S. gordonii* was grown aerobically and in planktonic cells. Collectively, the results indicate that *S. gordonii* has a reducing pathway that consists of MsrAB, SdbB, CcdA2, Sgo\_1177, and CcdA1. In this pathway, electrons from the cytoplasmic thioredoxin flow to CcdA1 or CcdA2 and then to SdbB or Sgo\_1177 and finally to MsrAB. Reduced MsrAB can actively convert MetO to Met. The activity of this pathway in *S. gordonii* protects it from oxidative stress.

### **3.3 SdbB is a Putative Disulfide Bond Isomerase in *S. gordonii***

Disulfide bond formation is not a perfect process, especially for proteins with multiple cysteine residues. In *E. coli*, DsbA is known to preferentially introduce a disulfide bond between two consecutive cysteine residues; thus, it will form incorrect disulfide bonds in proteins with more than 2 cysteines if the native disulfide bond is between two distant cysteines (Kadokura and Beckwith, 2009). In addition, the thiols (-SH) in cysteines are susceptible to oxidation to sulfenic acids (-SOH), which are highly reactive and can react with other cysteines forming incorrect disulfide bonds (Ezraty *et al.*, 2017). To deal with this problem, bacteria are equipped with disulfide bond isomerases to correct these mis-disulfide bonds (Ezraty *et al.*, 2017; Cho and Collet, 2013).

As mentioned earlier, *S. gordonii* is exposed to H<sub>2</sub>O<sub>2</sub> and other oxidative agents that damage proteins (Zheng *et al.*, 2011; Zhu and Kreth, 2012). *S. gordonii* is predicted to produce extracytoplasmic proteins with multiple cysteine residues (Davey *et al.*, 2013). In the following section, the presence of a disulfide bond isomerase in *S. gordonii* was investigated. The results showed that SdbB possesses disulfide isomerase activity and cooperates with CcdA2 to facilitate the production of proteins with multiple disulfide bonds and protect *S. gordonii* from copper stress.

#### **3.3.1 SdbB Exhibits Reductase and Isomerase Activities**

Disulfide bond isomerases possess both oxidase and reductase activity (Gleiter and Bardwell, 2008). As shown earlier in section 3.1.5, SdbB and CcdA2 possess oxidase activity (Figure 3.10). Here, the oxidase activity of Sgo\_1177 and CcdA1 was examined. The RNase A refolding assay showed that Sgo\_1177 and CcdA1 also have oxidase activity (Figure 3.20A).

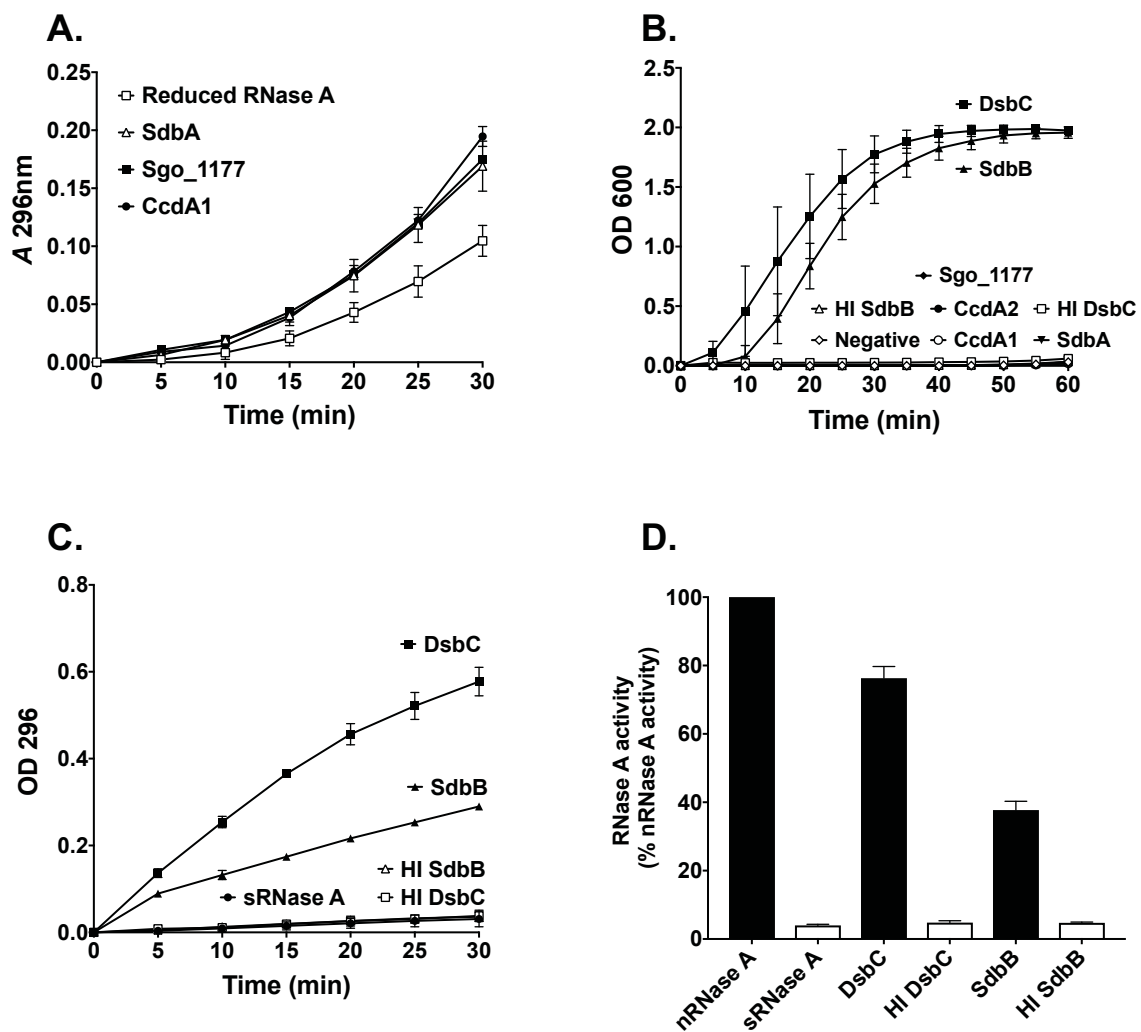


**Figure 3.20 SdbB exhibits isomerase activity.**

**A.** Oxidase activity. Reduced RNase A was used as a negative control, and SdbA was used as a positive control. **B.** Reductase activity. DsbC was used as a positive control and insulin alone was used as a negative control. **C.** Isomerase activity. DsbC was used as a positive control, and scrambled RNase A alone was used as a negative control. **D.** The activity of test samples compared to that of the native RNase A (100%) for the 30 minutes incubation time points. The data are means  $\pm$  SD of three experiments with two replicates in each experiment. Heat inactivation of DsbC (HI DsbC) and SdbB (HI SdbB) were prepared by boiling the protein sample for 10 min prior to the reaction.

Next, the insulin precipitation assay was performed to test if these proteins possess reductase activity. DsbC was included as a positive control because it is known to have reductase activity (Shevchik *et al.*, 1994) and the oxidase SdbA was used as a negative control (Davey *et al.*, 2013). The results showed that SdbB was able to catalyze insulin reduction, and this activity was abolished by heat inactivation (Figure 3.20B). In contrast, Sgo\_1177, CcdA1, and CcdA2 were not able to reduce insulin (Figure 3.20B). As expected, DsbC was able to catalyze insulin reduction, whereas SdbA was not able to reduce insulin (Figure 3.20B). These results showed that SdbB possesses reductase activity.

The finding that SdbB possesses both oxidase and reductase activity suggests that it may act as a disulfide bond isomerase. To investigate this, SdbB was tested in the isomerase assay using scrambled RNase A as the substrate. DsbC was included as a positive control. The results showed that SdbB was able to refold scrambled RNase A (Figure 3.20C). DsbC also rescued the scrambled RNase A (Figure 3.20C). About 76% and 38% of the scrambled RNase A were refolded by DsbC and SdbB, respectively (Figure 3.20D). The above results support the notion that SdbB is a disulfide bond isomerase.

### **3.3.2 SdbBCcdA2 are Required for the Production of Anti-CR1 scFv**

To further investigate SdbB as a disulfide bond isomerase, the production of a protein with multiple disulfide bonds was examined in *S. gordonii*. Due to the lack of a known natural substrate of SdbB, the anti-CR1 single-chain variable fragment antibody (scFv) was chosen as the target protein. Anti-CR1 scFv secreted by *S. gordonii* contains two intramolecular disulfide bonds that are essential for proper folding and stability (Knight *et al.*, 2008; Davey *et al.*, 2013). Previous studies showed that the level of anti-CR1 scFv production is a good indicator of the cell's ability to produce disulfide-bonded proteins (Davey *et al.*, 2013; Davey *et al.*, 2015a). Inactivation of *sdbA* leads to the misfolding and degradation of anti-CR1 scFv (Davey *et al.*, 2013).

Western blotting analysis showed that anti-CR1 scFv produced by the *sdbB* mutant contained many smaller size bands suggesting extensive degradation due to misfolding (Figure 3.21A). These smaller size bands were absent in the sample from the parent strain. Inactivation of the serine protease gene *degP* reduced the number of smaller size bands of anti-CR1 scFv in the *sdbB* mutant (Figure 3.21A).

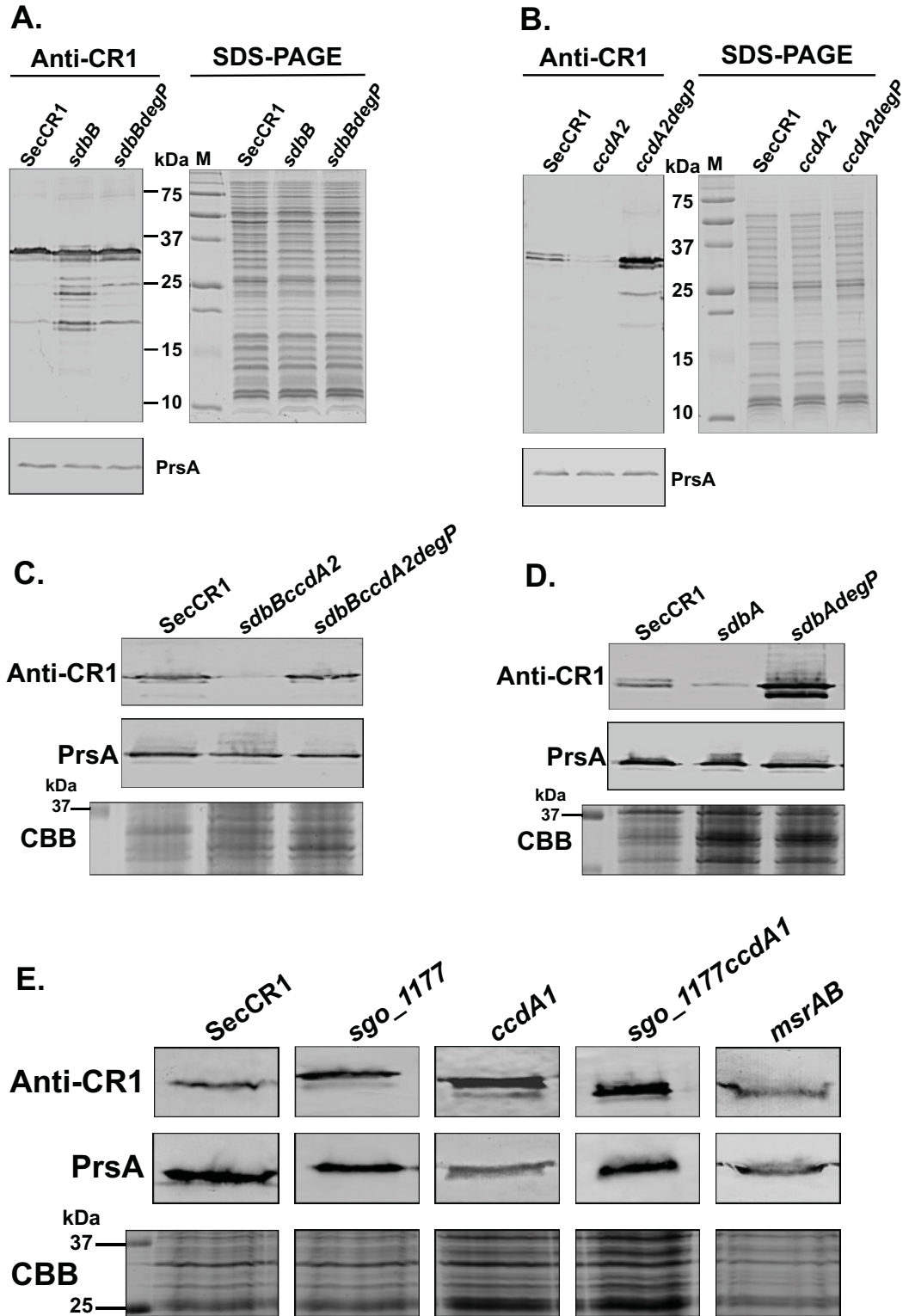
Interestingly, the level of anti-CR1 scFv produced by the *ccdA2* mutant was almost undetectable and was restored by *degP* mutation (Figure 3.21B). Similar results were observed in the *sdbBccdA2* mutant (Figure 3.21C). Consistent with previous reports, the *sdbA* mutant showed a marked reduction in anti-CR1 scFv production and the level was restored in the *sdbAdegP* mutant (Davey *et al.*, 2013; Davey *et al.*, 2015a) (Figure 3.21D). Other mutants, namely *sgo\_1177*, *ccdA1*, *sgo\_1177ccdA1*, and *msrAB*, showed no reduction in anti-CR1 scFv production (Figure 3.21E).

To exclude the possibility that inactivation of *sdbBccdA2* might have affected the general *sec* pathway that led to the reduction in the anti-CR1 scFv production, the level of production of the extracytoplasmic peptidyl-prolyl *cis-trans* isomerase PrsA that lacks a disulfide bond was examined (Davey *et al.*, 2015a). The results showed that the level of PrsA was similar between the parent strain and mutants, suggesting that the *sec* pathway was functional in all these mutants (Figure 3.21).

Taken together, these results suggested that SdbB and CcdA2 are required for the proper folding and production of anti-CR1 scFv, a protein with two disulfide bonds, in *S. gordonii*.

**Figure 3.21 SdbB and CcdA2 are required for the production of anti-CR1 scFv protein in *S. gordonii*.**

**A.** Production of the 33-kDa anti-CR1 scFv protein from the parent strain SecCR1, *sdbB*, and *sdbBdegP*. **B.** Anti-CR1 scFv from SecCR1, *ccdA2*, and *ccdA2degP*. **C.** Anti-CR1 scFv from SecCR1, *sdbBccdA2*, and *sdbBccdA2degP*. **D.** Anti-CR1 scFv from SecCR1, *sdbA*, and *sdbAdegP*. **E.** Anti-CR1 scFv from SecCR1, *sgo\_1177*, *ccdA1*, *sgo\_1177ccdA1*, and *msrAB*. Duplicate samples were stained with Coomassie brilliant blue (CBB) and probed with anti-PrsA to show equal protein loading.



### 3.3.3 Anti-CR1 is Oxidized and Misfolded in *sdbBccdA2* Mutant

Because inactivation of *degP* stabilized the anti-CR1 scFv in the *sdbB* and *ccdA2* mutants, the *degP* mutants were used for the determination of the redox state of scFv. Previous studies showed that the inactivation of *degP* has no effect on the redox state of anti-CR1 scFv (Davey *et al.*, 2015a). Anti-CR1 scFv was isolated from the parent strain (properly folded oxidized control), *sdbAdegP* mutant (unfolded reduced control), *sdbB*, *sdbBdegP*, *ccdA2degP*, and *sdbBccdA2degP* mutants. The free thiols in the scFv protein were alkylated with maleimide-PEG<sub>2</sub>-biotin before or after dithiothreitol (DTT) treatment.

As expected, the results showed that anti-CR1 scFv from the parent strain was fully oxidized. Free thiols were only detected when the sample was reduced with DTT prior to alkylation. The total amount of anti-CR1 in the samples was detected with the anti-HA antibody, and the results indicated equal loading between the DTT treated and untreated samples (Figure 3.22). Anti-CR1 scFv from the *sdbAdegP* mutant was in a reduced state, whereas that from the *sdbB*, *sdbBdegP*, *ccdA2degP*, and *sdbBccdA2degP* mutants were fully oxidized (Figure 3.22). These results suggest that anti-CR1 scFv in these mutants were oxidized but mis-disulfide bonded and thus susceptible to degradation by DegP.

Collectively, these data suggest that SdbB and CcdA2 are needed for the proper folding and stability of protein with multiple disulfide bonds and DegP is responsible for the degradation of the misfolded protein in the *sdbBccdA2* mutant.



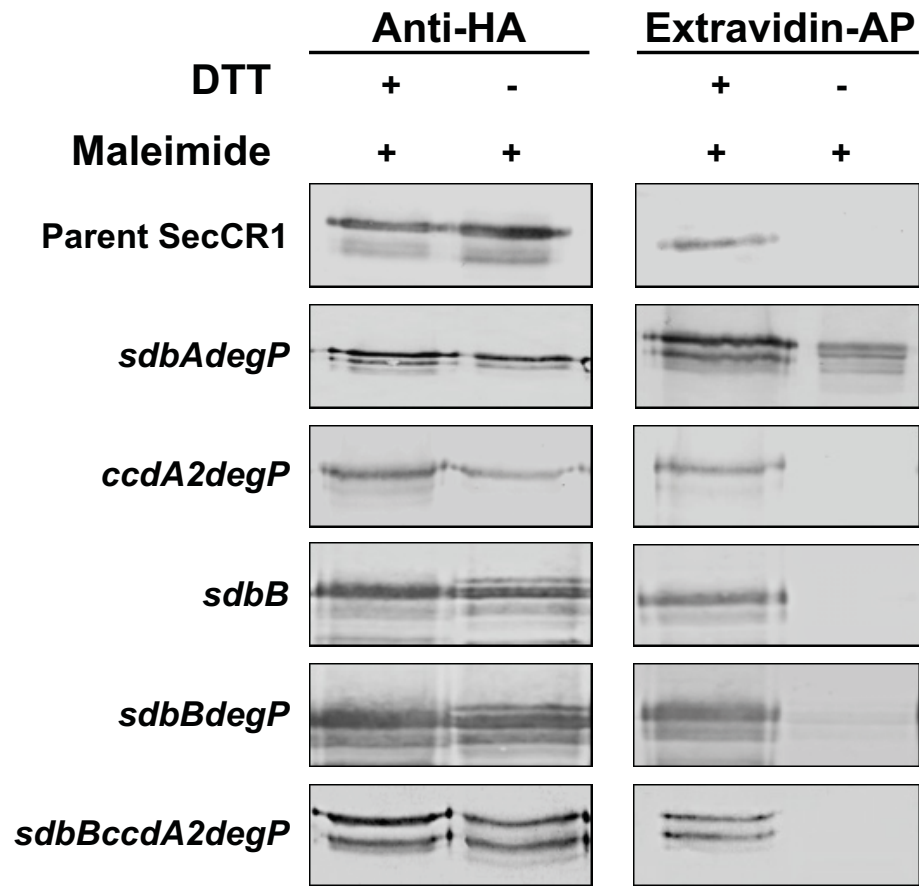


**Figure 3.22 SdbB and CcdA2 are required for the proper folding of anti-CR1 scFv in *S. gordonii*.**

The redox state of anti-CR1 scFv from the parent strain SecCR1, *sdbAdegP*, *ccdA2degP*, *sdbB*, *sdbBdegP*, and *sdbBccdA2degP* mutants were determined by alkylation with maleimide-PEG2-biotin and detected using extravidin alkaline phosphatase (Extravidin-AP). Duplicate samples were reacted with anti-HA to detect the total anti-CR1 scFv protein as a loading control.

### 3.3.4 SdbB and CcdA2 are Involved in Copper Resistance in *S. gordonii*

In bacteria, disulfide bond isomerization systems are known to play a role in protection against copper stress. This is because copper catalyzes the formation of non-native disulfide bonds in proteins. In *E. coli*, inactivation of the disulfide bond isomerase DsbC or its redox partner DsbD renders the bacterium more sensitive to copper (Denoncin *et al.*, 2014; Hiniker *et al.*, 2005). Thus, I hypothesized that SdbB and CcdA2 play a similar role in copper stress resistance in *S. gordonii*. To test this hypothesis, the effect of inactivation of *sdbB*, *ccdA2*, and *sdbBccdA2* in *S. gordonii* on copper sensitivity was investigated. The results showed that the *sdbB*, *ccdA2*, and *sdbBccdA2* mutants were more sensitive to CuSO<sub>4</sub> than the parent (Figure 3.23). Complementation of *sdbBccdA2* restored the level of sensitivity to that of the parent strain (Figure 3.23B). The colonies of *sdbB*, *ccdA2*, and *sdbBccdA2* mutants were slightly smaller than the parent strain colonies when grown in the presence of 2.5 mM CuSO<sub>4</sub>. The effect was more dramatic for the *ccdA2* and *sdbBccdA2* mutant, which failed to grow at 3.5 mM CuSO<sub>4</sub> (Figure 3.23). These results suggest that SdbB and CcdA2 are involved in protection against copper stress in *S. gordonii* and support the notion that SdbBCcdA2 is a potential disulfide bond isomerization system in *S. gordonii*.

### 3.3.5 Summary

The above results showed that SdbB possesses disulfide bond isomerization activity. *In vitro*, SdbB was able to refold mis-disulfide bonded RNase A (sRNase A). In the cells, SdbB plays a role in the stability and production of anti-CR1 scFv. The results showed that CcdA2 is also needed for the production of anti-CR1 scFv. Anti-CR1 scFv from the *sdbB*, *sdbBdegP*, *ccdA2degP*, and *sdbBccdA2degP* mutants were fully oxidized, suggesting that anti-CR1 scFv in these mutants were mis-disulfide bonded. In addition, SdbB and CcdA2 protect *S. gordonii* from copper-induced oxidative stress and mis-disulfide bond formation. Collectively, the results suggest that SdbB is a disulfide bond isomerase and CcdA2 is likely the redox partner.

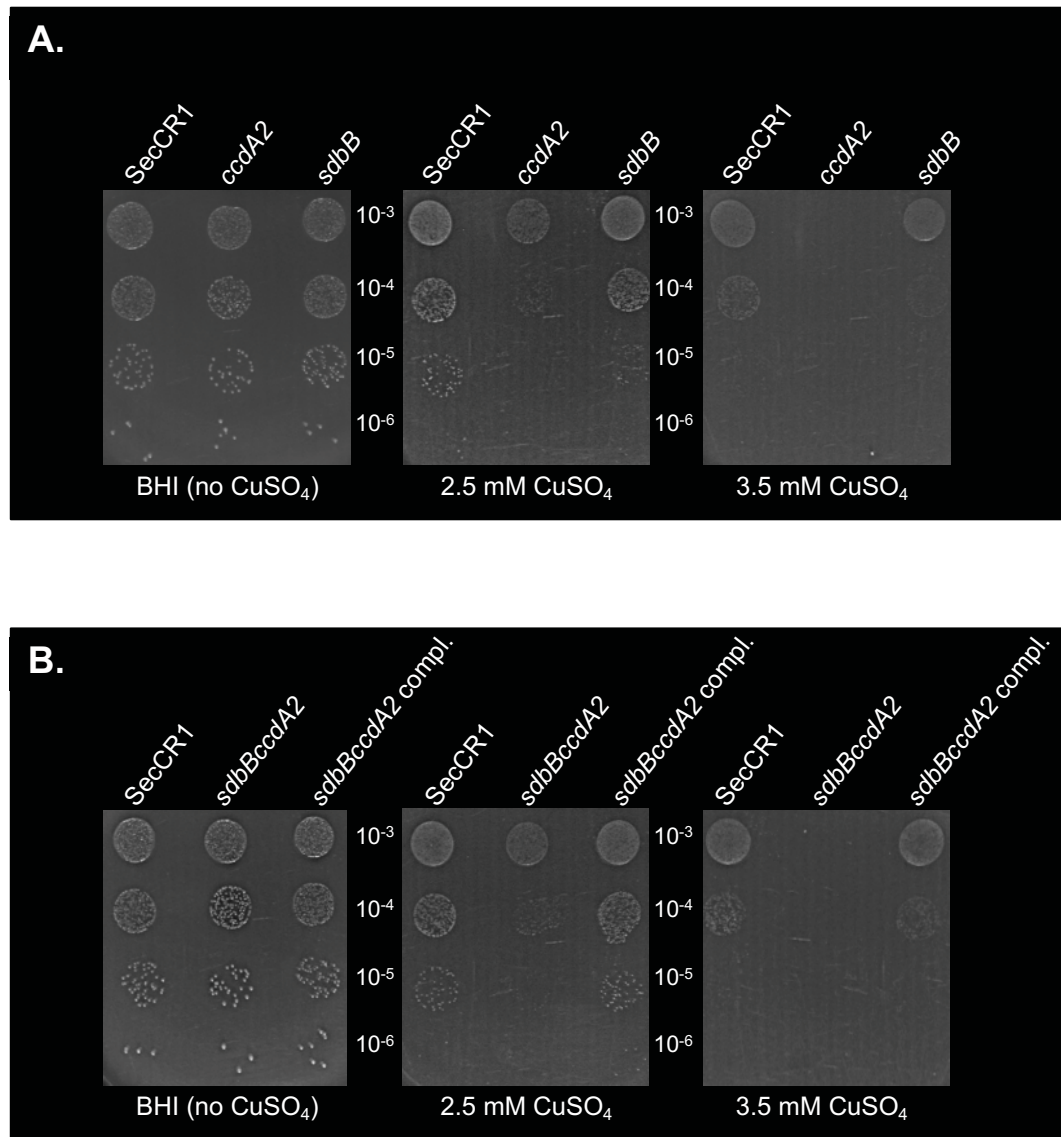


**Figure 3.23 Growth of *S. gordonii* strains in the presence of CuSO<sub>4</sub>.**

**A.** Growth of *S. gordonii* parent strain SecCR1, *ccdA2*, and *sdbB* in the presence or absence of CuSO<sub>4</sub>. **B.** Growth of *S. gordonii* SecCR1, *sdbBccdA2*, and *sdbBccdA2* complemented mutant in the presence or absence of CuSO<sub>4</sub>.

## 3.4 Preliminary Investigations of Structure and Function of SdbA

### 3.4.1 Role of the Active-Site Cysteines in SdbA-SdbB Interaction

Thiol-disulfide oxidoreductases (TDORs) are known to interact with their redox partners through the active site cysteines (Kishigami *et al.*, 1995b). Typically, these TDORs have a CXXC active site motif where the N-terminal cysteine is solvent-exposed and the C-terminal cysteine is buried (Zapun *et al.*, 1994). The reoxidation of TDORs by their redox partners involves the formation of a mixed disulfide bond between the solvent-exposed cysteines on the TDOR and the redox partner (Inaba *et al.*, 2006). SdbA also has a solvent-exposed N-terminal cysteine C<sub>86</sub> and a buried C-terminal cysteine C<sub>89</sub> (Davey *et al.*, 2015a; Stogios and Savchenko, 2015). To determine if SdbB has a solvent-exposed N-terminal cysteine and a buried C-terminal cysteine, single cysteine point mutants (SdbB<sub>C81A</sub> and SdbB<sub>C84A</sub>) were constructed, produced, and purified from *E. coli*. The reactivity to dithionitrobenzoic acid (DTNB) by the single cysteine mutants was tested. The result showed that the parent SdbB (SdbB WT) reacted strongly to DTNB (Figure 3.24) whereas SdbB<sub>C84A</sub> gave about half the reactivity compared to the parent SdbA. In contrast, SdbB<sub>C81A</sub> did not react with DTNB. When SdbB<sub>C81A</sub> was denatured, the protein reacted rapidly with DTNB, indicating that C<sub>84</sub> is buried in the structure of SdbB (Figure 3.24). It is notable that the reactivity of SdbB<sub>C84A</sub> was a bit higher than that of denatured SdbB<sub>C81A</sub>, which was likely due to the amounts of proteins were a bit off from estimation.

To investigate the mechanism of interaction, SdbA and SdbB active-site variants were tested in complex formation. The results showed that when SdbA<sub>C86A</sub> was incubated with either SdbB<sub>C81A</sub> or SdbB<sub>C84A</sub>, no hetero-complex was detected and only SdbB<sub>C84A</sub> homodimer was observed (Figure 3.25A). Similarly, no complex was detected between SdbA<sub>C89A</sub> and SdbB<sub>C81A</sub>. However, SdbA<sub>C89A</sub> formed a complex with SdbB<sub>C84A</sub>, SdbB<sub>C84A</sub> homodimer was also detected (Figure 3.25B). Collectively, these results suggest that SdbA-SdbB interacts through their solvent-exposed N-terminal cysteines.

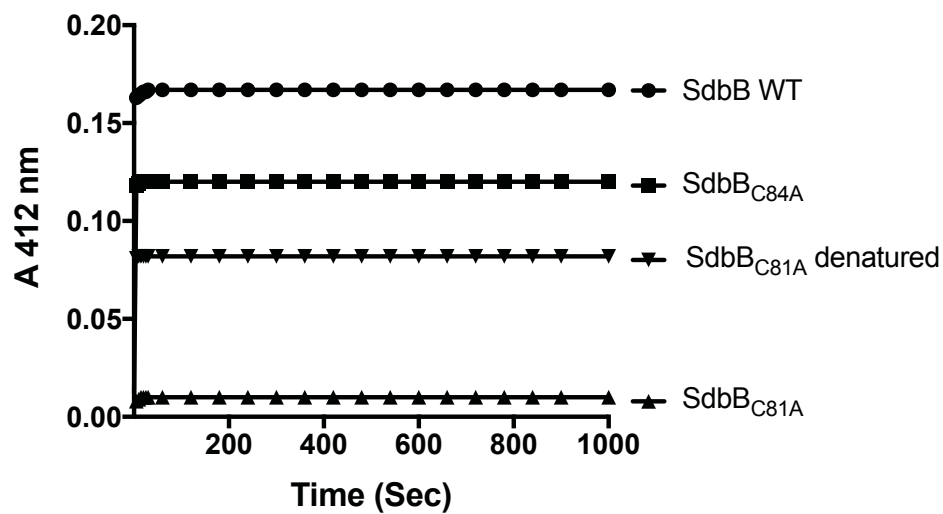


**Figure 3.24 Reactivity of SdbB cysteines with DTNB.**

Reduced SdbB, SdbB single cysteine point mutants (SdbB<sub>C81A</sub> and SdbB<sub>C84A</sub>) and denatured SdbB<sub>C81A</sub> were reacted with excess DTNB, and the absorbance was monitored at 412 nm.

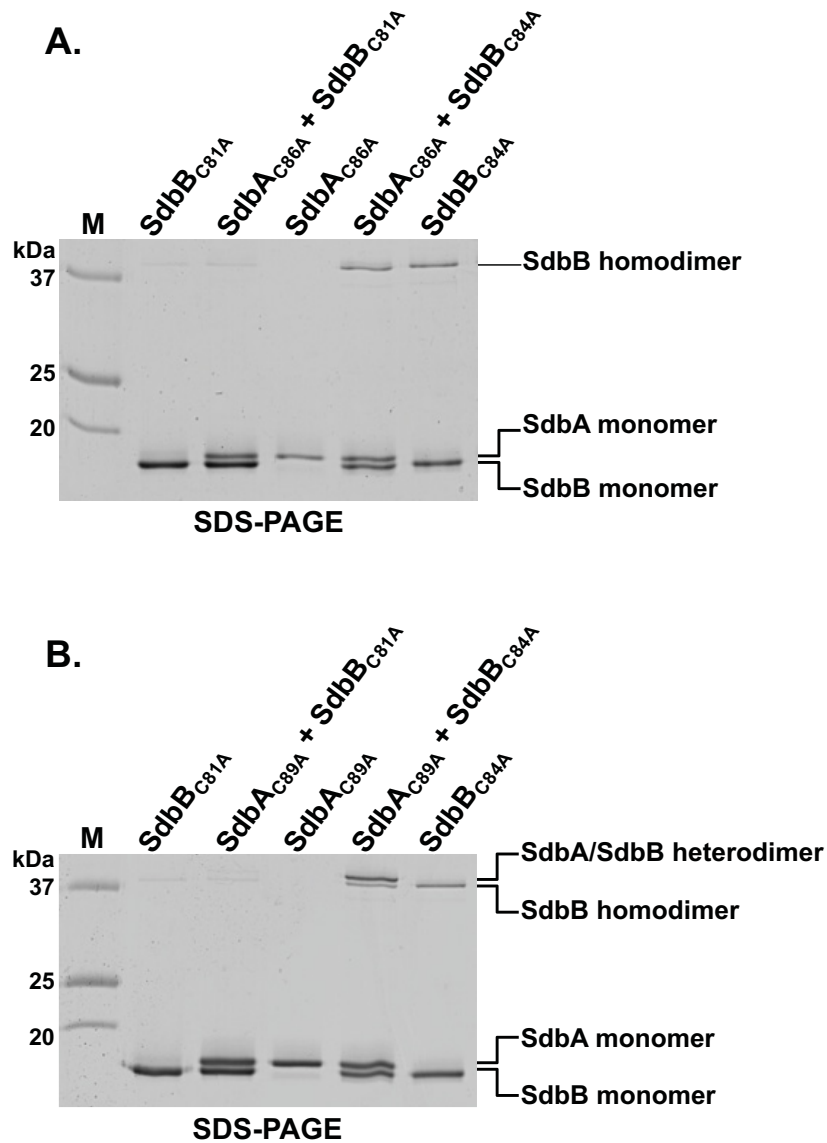


**Figure 3.25 SdbA-SdbB complex formation.**

**A.** SdbA<sub>C86A</sub> with cysteine point mutant variants of SdbB (SdbB<sub>C81A</sub> and SdbB<sub>C84A</sub>). **B.** SdbA<sub>C89A</sub> with cysteine point mutant variants of SdbB (SdbB<sub>C81A</sub> and SdbB<sub>C84A</sub>). SdbA and SdbB point mutant variant alone was used as a control for homodimer detection. All samples were incubated for 30 minutes at 37°C with 10 mM K<sub>3</sub>Fe(CN)<sub>6</sub>.

### 3.4.2 Role of Surface-Exposed Amino Acid Residues in SdbA Enzyme Kinetics

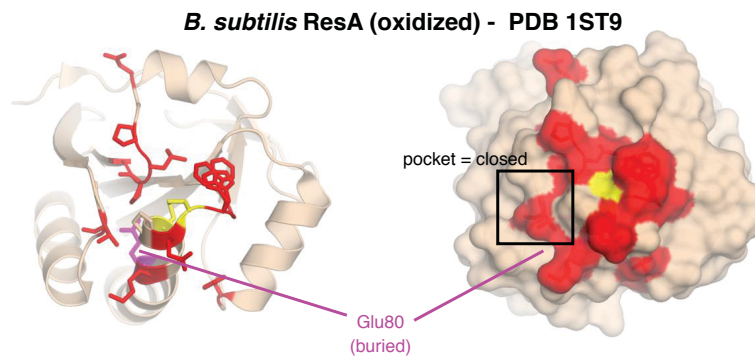
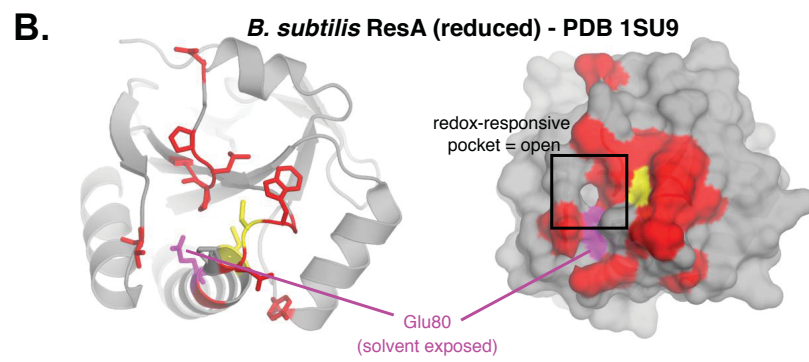
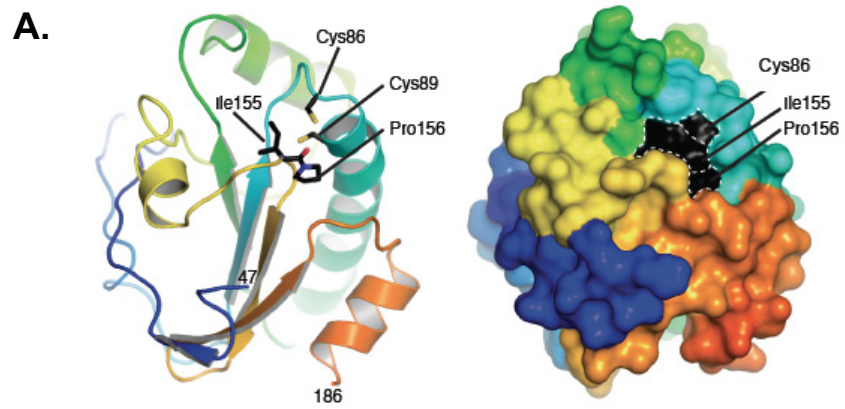
The crystal structure of SdbA showed that it has a thioredoxin fold and the conserved *cis*-proline (P<sub>156</sub>) residue is in close proximity to the C<sub>86</sub>PDC<sub>89</sub> active site (Stogios and Savchenko, 2015). Similar to other thioredoxin enzymes, the structure of SdbA has four-stranded  $\beta$ -sheet with three flanking  $\alpha$ -helices in  $\beta$ - $\alpha$ - $\beta$ - $\alpha$ - $\beta$ - $\alpha$  configuration and an isoleucine residue closed to the active site (Figure 3.26A). It is known in other TDOR that the conserved *cis*-proline affects the interactions of TDOR with its substrates and redox partners, whereas the isoleucine adjacent to the *cis*-proline has been reported to influence enzymatic activity (Ren *et al.*, 2009; Kadokura *et al.*, 2004; Kadokura *et al.*, 2005). The structure of SdbA also showed that the C<sub>86</sub> is surface-exposed, whereas C<sub>89</sub> is buried (Figure 3.26A). However, SdbA was shown to be active with the single buried C<sub>89</sub> (Davey *et al.*, 2015a). This suggests that SdbA might undergo a conformational change that allows access to the buried C<sub>89</sub> upon binding to its substrate.

This notion of conformational change has been reported in ResA (Crow *et al.*, 2004; Colbert *et al.*, 2006), a TDOR from *B. subtilis* that is structurally similar to SdbA. In ResA, the reduction of the active site resulted in a movement of the buried C<sub>77</sub>. This is accompanied by the formation of a cavity close to the active site with E<sub>80</sub> at its base. The E<sub>80</sub> residue in ResA alters between buried, when the protein is oxidized, to surface-exposed, when the protein is reduced. Other amino acids such as E<sub>75</sub>, K<sub>79</sub>, D<sub>136</sub>, P<sub>139</sub>, L<sub>140</sub>, P<sub>141</sub>, and T<sub>159</sub> also rearranged during the conformational change to line the cavity in reduced ResA (Figure 3.26B and C) (Crow *et al.*, 2004; Hodson *et al.*, 2008; Lewin *et al.*, 2006).

**Figure 3.26 Crystal structure and sequence alignment of SdbA and ResA.**

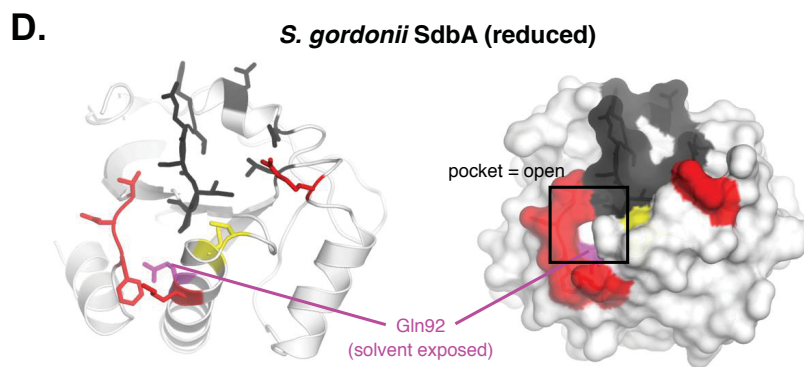
**A.** Left, SdbA structure showing the active site. Right, the surface representation showing the surface-exposed amino acids, including the N-terminal cysteine (C<sub>86</sub>) of the active site. The conserved *cis*-proline (P<sub>156</sub>) and adjacent isoleucine (I<sub>155</sub>) localize adjacent to the active site (Stogios and Savchenko, 2015). **B.** Structure of reduced and oxidized ResA from *B. subtilis*. The structures show the active site (yellow) and the key Glu<sub>80</sub> (purple) located within the substrate-binding pocket. Positions involved in substrate interaction are labeled in red (Colbert *et al.*, 2006). **C.** Sequence alignment of *S. gordonii* SdbA and *B. subtilis* ResA. The active site CXXC motif is indicated in the box. In ResA, amino acids involved in substrate interaction are highlighted in red. In SdbA, amino acids that are mutated are highlighted in red. **D.** The structure of reduced SdbA shows the active site cysteines (yellow), and the solvent-exposed Gln<sub>92</sub> (purple). Highlighted in red are the amino acids that showed changes in  $K_m$  ( $p < 0.1$ ). Amino acids that showed no change in  $K_m$  or  $K_{cat}$  ( $p > 0.1$ ) are highlighted in black (Stogios and Savchenko, 2015).





**C.**

SdbA	MLKEKWLPFLT VGVILVAVFALFYIAGPNRHNKGSTQKDGSSAVEHELTGQQLPEFEMV	60
ResA	--MKKRRLFIRTGILLVLICALGYTIYNAVFA-----GKESISEGSDAPNFVLE	48
	:* *: .:*** : ** * . * *: ** :	
	<b>Active site</b>	
SdbA	DQAGYQKKS AEFY NK PMLVVEWASWCPDCQKQLPEIQKVYEKYKGIHFV-MLDMLDSKR	119
ResA	DTNGKRIELSDLKGGVFLNFWGTWCEPCKKEFPYMANQYKHFKSQGVEIVAVNV---G	104
	* * : : : : . * : : : * . : * * * * : * : * : * : : * : : : * : : :	
SdbA	ETKERADQYISEKDYTFPYYDTERAADILHVQSIPTIYLVDKNQKVKVMTDFHDEAA	179
ResA	ESKIAVHNFMKSYGVNFPVVLDTDRQVLDAYDVSPLPTTFLINPEGKVVKVVTGTMTESM	164
	* : * . . : : . . . * * * . . . * . * . : * * : : : : * * * * . * :	
SdbA	LEKQLEEI-----	187
ResA	IHDYMNLIKPGETSG	179
	:.. : : *	



The structure of SdbA suggests the presence of a similar substrate binding pocket that is formed by a number of surface-exposed amino acids (Figure 3.26C and D). Using this information, I attempt to explore the structural basis of SdbA-substrate interaction. Variants of SdbA with single or double amino acid substitution to the surface-exposed amino acids that line and surround the suspected substrate-binding pocket of SdbA were constructed. These were P87A, D88K, K91E, Q92E, Q92A, L115D, R119E, E144K, D148K, H151E, V152A, Q153K, S154E, I155A, P156T, T172E, F174E, Q92E/S154E, and Q92A/S154E (Lee *et al.*, Unpublished). Recombinant SdbA variants were expressed and purified from *E. coli* XL-1. Through the help of a summer student (C. Guinard), 15 SdbA variants (P87A, D88K, K91E, L115D, R119E, E144K, D148K, H151E, V152A, Q153K, S154E, I155A, P156T, T172E, F174E) were screened for activity using the RNase A refolding assay. Seven SdbA variants (K91E, R119E, V152A, S154E, P156T, T172E, and F174E) showed an altered oxidase activity (Guinard *et al.*, Unpublished). K91E, T172E, and R119E showed an increase in oxidase activity, whereas V152A, S154E, P156T, and F174E showed a decrease in oxidase activity. To further investigate the findings, enzyme kinetics of RNase A refolding were performed for the seven SdbA variants and additional four variants (Q92E, Q92A, Q92E/S154E, and Q92A/S154E). The  $K_m$ ,  $K_{cat}$ ,  $V_{max}$ , and catalytic efficiencies of SdbA were determined (Table 3.1).

The results showed that five of the mutants, namely K91E, R119E, S154E, T172E, and F174E, showed an increase in  $K_m$  values compared to the parent SdbA, indicating a reduction in the affinity of SdbA to RNase A (Table 3.1). None of the point mutants showed a change in the  $K_{cat}$ ,  $V_{max}$ , or the catalytic efficiencies. Interestingly, when the mutation (Q92A or Q92E) was introduced into SdbA<sub>S154E</sub>, the  $K_m$  of these double point mutants (S154E/Q91A or S154E/Q91E) returned to values similar to that of the parent SdbA (Table 3.1). Collectively, these results suggest that five surface-exposed amino acids, namely K91E, R119E, S154E, T172E, and F174E, play a role in SdbA-substrate interaction.

**Table 3.1 Kinetic parameters of parent SdbA and SdbA point mutants**

Enzyme	$K_m$ ( $\mu\text{M}$ )	$K_{cat} \times 10^{-3}$ ( $\text{min}^{-1}$ )	$K_{cat}/K_m \times 10^{-3}$ ( $\mu\text{M}^{-1} \text{min}^{-1}$ )	$V_{max}$ ( $\text{nmol min}^{-1}$ )
Parent	$13.2 \pm 3.97^a$	$17.7 \pm 9.45^a$	$1.34 \pm 0.66^a$	$177 \pm 94.55^a$
K91E	$20.51 \pm 3.56^b$ ( $P=0.012$ ) <sup>c</sup>	$22.65 \pm 1.63^b$ ( $P=0.14$ ) <sup>c</sup>	$1.18 \pm 0.22^b$ ( $P=0.78$ ) <sup>c</sup>	$215.1 \pm 33.0^b$ ( $P=0.22$ ) <sup>c</sup>
R119E	$18.49 \pm 1.90^b$ ( $P=0.03$ ) <sup>c</sup>	$9.20 \pm 1.41^b$ ( $P=0.38$ ) <sup>c</sup>	$0.52 \pm 0.01^b$ ( $P=0.06$ ) <sup>c</sup>	$91.7 \pm 14.4^b$ ( $P=0.59$ ) <sup>c</sup>
V152A	$14.85 \pm 0.55^b$ ( $P=0.29$ ) <sup>c</sup>	$8.95 \pm 2.90^b$ ( $P=0.36$ ) <sup>c</sup>	$0.63 \pm 0.23^b$ ( $P=0.12$ ) <sup>c</sup>	$89.5 \pm 28.9^b$ ( $P=0.52$ ) <sup>c</sup>
P156T	$10.75 \pm 1.50^b$ ( $P=0.49$ ) <sup>c</sup>	$8.6 \pm 0.21^b$ ( $P=0.33$ ) <sup>c</sup>	$0.83 \pm 0.13^b$ ( $P=0.34$ ) <sup>c</sup>	$86.5 \pm 1.5^b$ ( $P=0.29$ ) <sup>c</sup>
T172E	$27.59 \pm 1.54^b$ ( $P=0.0002$ ) <sup>c</sup>	$23.50 \pm 6.22^b$ ( $P=0.13$ ) <sup>c</sup>	$0.89 \pm 0.26^b$ ( $P=0.45$ ) <sup>c</sup>	$147.2 \pm 62.2^b$ ( $P=0.81$ ) <sup>c</sup>
S154E	$24.88 \pm 5.52^b$ ( $P=0.0026$ ) <sup>c</sup>	$24.95 \pm 2.19^b$ ( $P=0.076$ ) <sup>c</sup>	$1.09 \pm 0.36^b$ ( $P=0.96$ ) <sup>c</sup>	$249.5 \pm 22.1^b$ ( $P=0.10$ ) <sup>c</sup>
F174E	$18.84 \pm 4.87^b$ ( $P=0.043$ ) <sup>c</sup>	$18.00 \pm 6.08^b$ ( $P=0.50$ ) <sup>c</sup>	$0.95 \pm 0.06^b$ ( $P=0.58$ ) <sup>c</sup>	$223.0 \pm 120.8^b$ ( $P=0.24$ ) <sup>c</sup>
Q92A	$14.44 \pm 7.63^b$ ( $P=0.089$ ) <sup>c</sup>	$29.2 \pm 0.8^b$ ( $P=0.5$ ) <sup>c</sup>	$2.2 \pm 1.4^b$ ( $P=0.99$ ) <sup>c</sup>	$291.9 \pm 8.4^b$ ( $P=0.5$ ) <sup>c</sup>
Q92A/S154E	$16.15 \pm 9.27^b$ ( $P=0.99$ ) <sup>c</sup>	$33.6 \pm 3.7^b$ ( $P=0.34$ ) <sup>c</sup>	$2.6 \pm 1.7^b$ ( $P=0.55$ ) <sup>c</sup>	$336 \pm 36.7^b$ ( $P=0.34$ ) <sup>c</sup>
Q92E	$18.59 \pm 2.01^b$ ( $P=0.63$ ) <sup>c</sup>	$30.7 \pm 12.2^b$ ( $P=0.99$ ) <sup>c</sup>	$1.7 \pm 0.8^b$ ( $P=0.166$ ) <sup>c</sup>	$306.8 \pm 121.6^b$ ( $P=0.99$ ) <sup>c</sup>
Q92E/S154E	$16.17 \pm 12.04^b$ ( $P=0.99$ ) <sup>c</sup>	$30.1 \pm 0.6^b$ ( $P=0.4$ ) <sup>c</sup>	$2.6 \pm 2^b$ ( $P=0.64$ ) <sup>c</sup>	$300.9 \pm 5.9^b$ ( $P=0.4$ ) <sup>c</sup>

<sup>a</sup> Mean  $\pm$  SD of nine independent experiments of parent SdbA with triplicate in each experiment.

<sup>b</sup> Mean  $\pm$  SD of two independent experiments of point mutant with triplicate in each experiment.

<sup>c</sup> Student *t*'s test between parent and point mutant.

### **3.4.3 Role of Surface-Exposed Amino Acid Residues in SdbA-SdbB Interaction**

Next, I explored the structural basis of SdbA-redox partner interaction. The interaction of seven SdbA variants (K91E, L115D, R119E, H151E, V152A, Q153K, and S154E) with SdbB was examined. The ability of SdbB to reoxidize SdbA variants was examined in disulfide exchange reactions. The results showed that SdbA<sub>S154E</sub> exhibited a delay in reoxidation by SdbB after 10 minutes of interaction. However, after 20 minutes, the majority of both parent SdbA and SdbA<sub>S154E</sub> was reoxidized by SdbB (Figure 3.27A). Other SdbA variants, including K91E, L115D, R119E, H151E, V152A, and Q153K showed no difference in reoxidation by SdbB compared to the parent SdbA (Figure 3.27B-G). However, K91E, L115D, R119E, and Q153K were tested at different time points (15 min and 30 min), which might be too late to detect any differences. Collectively, these results suggest that S154E plays a role in SdbA-redox partner interaction, but further in-depth investigations should be performed.

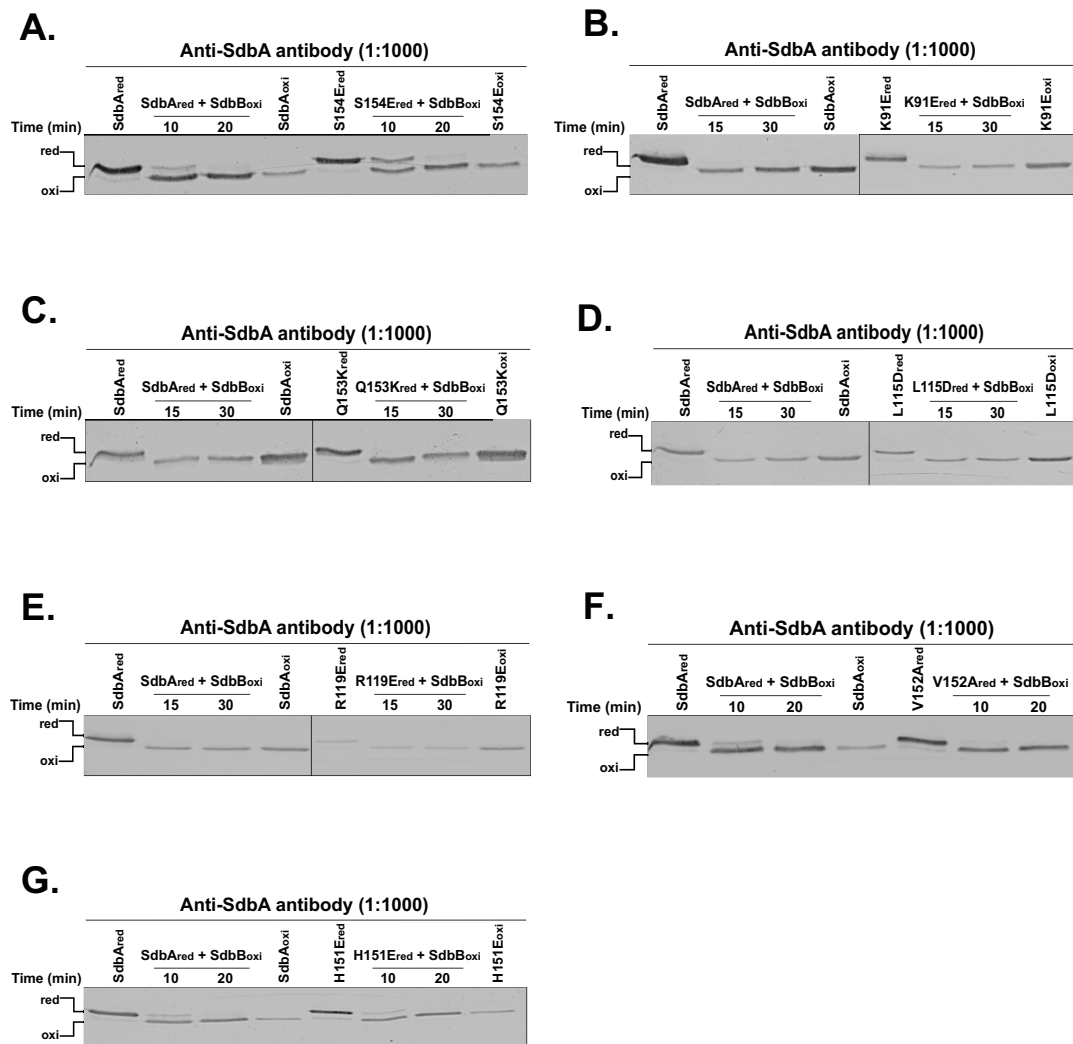


**Figure 3.27 Oxidation of parent SdbA and SdbA variants by SdbB.**

**A.** Oxidation of reduced parent SdbA and SdbA<sub>S154E</sub> by oxidized SdbB. **B.** Oxidation of reduced parent SdbA and SdbA<sub>K91E</sub> by oxidized SdbB. **C.** Oxidation of reduced parent SdbA and SdbA<sub>Q153K</sub> by oxidized SdbB. **D.** Oxidation of reduced parent SdbA and SdbA<sub>L115D</sub> by oxidized SdbB. **E.** Oxidation of reduced parent SdbA and SdbA<sub>R119E</sub> by oxidized SdbB. **F.** Oxidation of reduced parent SdbA and SdbA<sub>V152A</sub> by oxidized SdbB. **G.** Oxidation of reduced parent SdbA and SdbA<sub>H151E</sub> by oxidized SdbB. Reduced and oxidized parent SdbA and SdbA variants alone was used as a control.

## Chapter 4. Discussion

Despite several TDORs having now been identified in a number of Gram-positive species (Davey *et al.*, 2016b; Reardon-Robinson and Ton-That, 2015), the pathways of disulfide bond formation and reduction in Gram-positive bacteria remain poorly understood. To date, no disulfide isomerization pathway has been identified in Gram-positive organisms.

*S. gordonii* is a good model organism for studying disulfide bond formation, reduction, and isomerization because *S. gordonii* produces disulfide bonded proteins and has many testable phenotypes (Davey *et al.*, 2013). The recent discovery of SdbA, a TDOR that introduces disulfide bonds in substrate proteins and plays a role in multiple phenotypes, indicates that this organism has a disulfide bond formation pathway (Davey *et al.*, 2013). Despite these advances, there are still many questions surrounding the mechanisms of disulfide bond formation in this organism. In addition, nothing is known about the disulfide bond reduction and isomerization pathways in *S. gordonii*.

### 4.1 Oxidative Protein-Folding Pathway in *S. gordonii*

In the first part of this study, the redox partners of SdbA were identified (Jalal *et al.*, 2019). The results show that SdbB and CcdA2 are the primary redox partners of SdbA. Several lines of evidence support this statement. First, mutational results showed that the *sdbBccdA2* mutant duplicated phenotypes exhibited by the *sdbA* mutant, and *sdbBccdA2*-complemented mutant restored the parental phenotypes. Second, SdbA was locked in a reduced state when *sdbB* and *ccdA2* were inactivated, and complementation returned SdbA to the oxidized state as in the parent strain. Third, SdbB formed a mixed disulfide with SdbA<sub>C89A</sub> in the cells. Fourth, AtIS, the natural substrate of SdbA, was in a reduced state in the *sdbBccdA2* mutant. Fifth, SdbB and CcdA2 possess oxidase activities capable of refolding RNase A and reoxidizing SdbA *in vitro*. Collectively, these results strongly support that SdbB and CcdA2 are the redox partners of SdbA.

The results showed that mutation of *sdbB* or *ccdA2* alone did not result in *sdbA* mutant phenotypes; mutation of both genes is needed to reproduce the *sdbA* mutant phenotypes. This suggests that SdbB and CcdA2 can both serve as independent redox partners of SdbA. Accordingly, SdbA remains in an oxidized state in the *sdbB* and *ccdA2* single-gene mutants. *In vitro*, both SdbB and CcdA2 could reoxidize SdbA independently, supporting the notion that SdbB and CcdA2 are independent redox partners of SdbA. These results indicate that the protein-folding pathway in *S. gordonii* is quite complex and very different from the two-protein pathway (DsbA-DsbB) of *E. coli* (Landeta *et al.*, 2018) or the MdbA-VKOR pathway of *A. oris* (Reardon-Robinson *et al.*, 2015a). A similar complex protein-folding pathway was reported previously in *L. pneumophila*, where DsbA2 interacts with multiple redox partners, including DsbB1/2 and DsbD1/2 (Jameson-Lee *et al.*, 2011; Kpadeh *et al.*, 2015).

It is interesting that the second set of proteins, Sgo\_1177 and CcdA1, which are homologous to SdbB and CcdA2, respectively, appear to have limited ability to serve as redox partners of SdbA. The *sgo\_1177ccdA1* mutant fails to reproduce the *sdbA* mutant phenotypes except for bacteriocin production. However, it remains possible that Sgo\_1177 and CcdA1 can serve as minor partners of SdbA in the absence of SdbB or CcdA2. Because of this cross-interaction, the phenotypes of some of the cross-operon mutants are difficult to explain.

SdbB and Sgo\_1177 are predicted to belong to the thioredoxin family of redox proteins with a typical active site CXXC motif. As demonstrated in this study, SdbB exhibited oxidase activity and the ability to reoxidize SdbA. Sgo\_1177 also has the ability to refold denatured and reduced RNase A, however, it seems to play a minor role in SdbA reoxidation. The genetic organization of the *sgo\_1177* operon closely resembles the recently characterized *ccdA1-etrx1* (*sgo\_1177* homolog)-*msrAB2* operon in *S. pneumoniae*. In *S. pneumoniae*, the *etrx1* operon plays an important role in oxidative stress resistance (Saleh *et al.*, 2013).

CcdA1 and CcdA2 are annotated as cytochrome *c* biogenesis protein A. In *B. subtilis*, CcdA was part of the reducing pathway required for cytochrome *c* maturation and sporulation (Schiott *et al.*, 1997b; Schiott and Hederstedt, 2000). Given that



streptococci lack cytochrome *c* and do not sporulate (Brooijmans *et al.*, 2009), it is unlikely that they play a role in these two processes. Both CcdA1 and CcdA2 contain two conserved cysteines separated by two transmembrane domains, a feature that is similar to the  $\beta$  domain of the *E. coli* DsbD. In *E. coli*, electrons from thioredoxin flow to the  $\beta$  domain of DsbD initially during the reduction of DsbC in the isomerization pathway (Gleiter and Bardwell, 2008; Landeta *et al.*, 2018). Recent studies showed that CcdA from the archaea *Archaeoglobus fulgidus* (*AfCcdA*) and the Gram-negative bacteria *Thermus thermophilus* (*TtCcdA*) is capable of relaying electrons from thioredoxins across the cytoplasmic membrane (Williamson *et al.*, 2015; Zhou and Bushweller, 2018). Unlike *AfCcdA* and *TtCcdA* that act as a reductase, *S. gordonii* CcdA2 acts as an oxidase and has, in addition to the two conserved cysteines (C<sub>22</sub> and C<sub>147</sub>), a second pair of cysteines (C<sub>61</sub> and C<sub>68</sub>) in its second transmembrane domain. Hence, it is conceivable that CcdA2 is capable of receiving electrons from SdbA or SdbB, although these are extracytoplasmic proteins. In agreement with this notion, the results showed that CcdA2 is able to reoxidize reduced SdbA. The novelty of these results is the oxidase activity possessed by CcdA2. To the best of my knowledge, this is the first report of such an activity displayed by CcdA-like proteins. This suggests a potential role of CcdA proteins as interchangeable modules in different disulfide exchange pathways connecting the oxidation and the reduction pathways.

The role of SdbB and CcdA2 in oxidative protein folding is further demonstrated in the examination of the redox state and activity of AtIS, the natural substrate of SdbA. The results showed that AtIS from the *sdbBccdA2* mutant lacked a disulfide bond and was inactive. These results suggest that SdbB and CcdA2 play a critical role in working with SdbA in the oxidative folding of AtIS. The results showed that SdbB and CcdA2 are required to maintain SdbA in an oxidized state in the cell. This statement is supported by the findings that inactivation of *sdbB* and *ccdA2* resulted in a reduced SdbA, and SdbA was restored to the oxidized form upon the return of *sdbB* and *ccdA2* genes back into the mutant. The conversion of SdbA from an oxidized to a reduced state is only achieved by the inactivation of *sdbB* and *ccdA2* simultaneously, but not individually, lends support to the notion that SdbB and CcdA2 are independent redox partners of SdbA. It is

interesting to note that the level of SdbA was lowered in the *sdbBccdA2* mutant than in the parent and complemented mutant strains. Inactivation of the serine protease DegP restored SdbA level in the *sdbBccdA2* mutant to a level similar to that of the parent and complemented mutant strains. These results suggest that the reduced form of SdbA is unstable and prone to degradation in the cell and may explain why only oxidized SdbA was detected in the parent strain. This stability issue helps to explain the need for multiple redox partners to ensure SdbA is maintained in the most stable (i.e., oxidized) form in *S. gordonii*.

To provide further evidence that SdbB is a redox partner, the formation of disulfide-linked complexes between SdbB and the active site variant SdbA<sub>C89A</sub> in the cell was investigated. Previous study showed that SdbA<sub>C89A</sub> formed mixed disulfide complexes, and one of the complexes was SdbA<sub>C89A</sub> and its natural substrate AtIS (Davey *et al.*, 2015a). Here the results show that SdbA<sub>C89A</sub> formed a disulfide-linked complex with SdbB. Oxidoreductases with mutations to the C-terminal cysteine of the CXXC motif, including DsbA (Kishigami *et al.*, 1995b; Guilhot *et al.*, 1995), protein disulfide isomerase PDI (Walker *et al.*, 1996) and thioredoxin (Balmer *et al.*, 2003), can form disulfide-linked complexes with their redox partners and substrates respectively. Thus, the results are consistent with the literature. I was not able to investigate complex formation between CcdA2 and SdbA because of the lack of a specific anti-CcdA2 antibody. CcdA2 and CcdA1 share high sequence homology and to distinguish reactions to CcdA2, not CcdA1, would require a highly specific antibody such as a monoclonal antibody.

A question remained is where electrons are flown to from SdbB and CcdA2 after SdbA reoxidation. *S. gordonii* lacks a respiratory chain, cytochrome *c*, quinone, menaquinone, and fumarate reductase (Brooijmans *et al.*, 2009; Kakinuma, 1998; Vickerman *et al.*, 2007). This means that the mechanism of CcdA2 and SdbB reoxidation is different from DsbB in *E. coli* (Bader *et al.*, 1999). One possibility is that CcdA2 and SdbB shuttle electrons to the reducing pathway in *S. gordonii*. It is also possible that a yet to be identified downstream redox partner(s) is present in SdbB and CcdA2 reoxidation.

Homologs of SdbBCcdA2 and Sgo\_1177CcdA1 are found in other Gram-positive bacteria (*S. pneumoniae*, *S. sanguinis*, and *C. botulinum*) that lacked a DsbA homolog. The role of these proteins in these bacteria is largely unknown, except in *S. pneumoniae* where they are involved in a reducing pathway coping with oxidative stress (Saleh *et al.*, 2013).

In conclusion, the results showed that SdbA has multiple redox partners forming a complex oxidative protein-folding pathway in *S. gordonii* (Figure 4.1). I propose that SdbA is the oxidase that introduces disulfide bonds in protein substrates. This results in a disulfide-bonded substrate protein (e.g., AtIS) and a reduced SdbA. SdbB pairs up with CcdA2 to reoxidize SdbA, allowing SdbA to continue its function. The SdbA-SdbB and SdbA-CcdA2 pathways represent the main oxidative pathway affecting autolysis, bacteriocin production, genetic competence, and eDNA release.

## 4.2 The Reducing Pathway in *S. gordonii*

The exposure of bacterial cells to ROS can damage DNA, lipid, and proteins. Thus, bacteria are equipped with specialized enzymes such as catalase and superoxide dismutase to neutralize ROS (Cho and Collet, 2013; Ezraty *et al.*, 2017). In proteins, cysteine and methionine are vulnerable to oxidation by ROS, which can lead to misfolding and even degradation. Therefore, enzymes such as disulfide bond reductase, disulfide bond isomerase, and methionine sulfoxide reductase are important in oxidative stress resistance in bacteria (Cho and Collet, 2013; Gleiter and Bardwell, 2008; Ezraty *et al.*, 2017). Methionine sulfoxide reductases are enzymes that reduce MetO to Met and, by doing so, alleviates damages caused by oxidation (Ezraty *et al.*, 2005a). In the second part of this study, I identified and characterized MsrAB and related proteins as a reducing pathway in *S. gordonii*. The results showed that MsrAB possesses the enzymatic capability to reduce MetO. Accordingly, inactivation of *msrAB* lead to impaired growth of *S. gordonii* in the presence of MetO. This is consistent with that reported in *S. pneumoniae*, where the loss of MsrAB2 resulted in impaired growth in the presence of exogenous MetO (Saleh *et al.*, 2013).

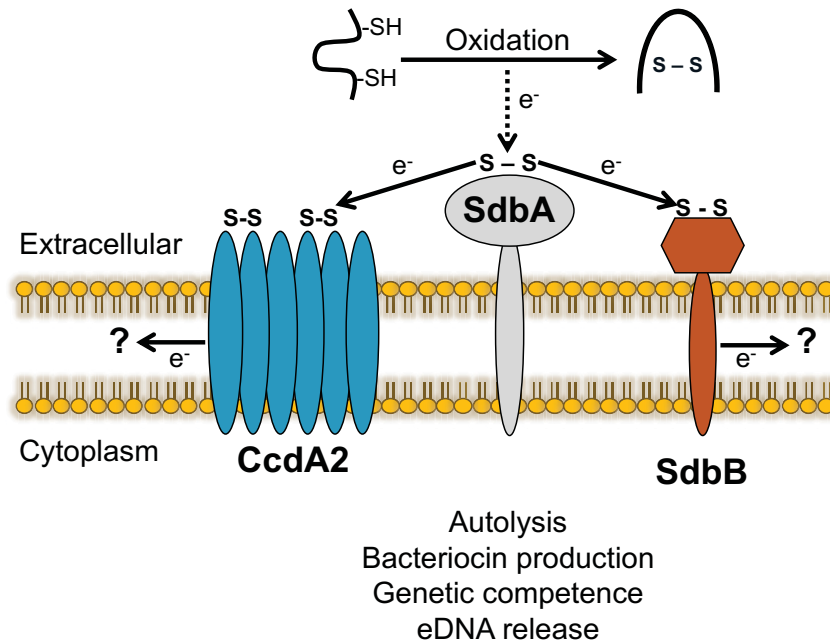


**Figure 4.1 A proposed model for oxidative protein-folding pathway in *S. gordonii*.**

SdbA is the oxidase that introduces a disulfide bond in substrate proteins. The reduced SdbA can be oxidized by CcdA2 or SdbB. This SdbA-CcdA2 or SdbA-SdbB pathway is the main oxidative pathway affecting autolysis, bacteriocin production, genetic competence, and eDNA release. The downstream partner of CcdA2 and SdbB is unknown and is depicted as question marks.

The phenotypic analysis showed that inactivation of *msrAB* increased the susceptibility of *S. gordonii* to H<sub>2</sub>O<sub>2</sub>. This is also consistent with the literature that *msr* mutants are sensitive to ROS. For example, inactivation of *msrA* in *E. coli* and *Corynebacterium glutamicum* lead to increase sensitivity to H<sub>2</sub>O<sub>2</sub> (Si *et al.*, 2015; Moskovitz *et al.*, 1995). Collectively, these results support the notion that MsrAB is a methionine sulfoxide reductase that reduces MetO and protects *S. gordonii* from oxidative damages.

Bacteria are known to have more than one Msr to reduce the two isoforms of MetO (Met-S-O and Met-R-O) and to protect cytoplasmic and extracytoplasmic proteins from oxidation (Ezraty *et al.*, 2005a; Ezraty *et al.*, 2017). *S. gordonii* has, in addition to MsrAB, a second Msr named MsrA. Previous report showed that MsrA reduces MetO and protects *S. gordonii* from oxidative damage (Lei *et al.*, 2011). However, unlike MsrAB, MsrA lacks a signal sequence and thus, the majority of the protein localized in the cytoplasm (Lei *et al.*, 2011), suggesting that MsrA protects cytoplasmic proteins, whereas MsrAB reduces MetO in extracytoplasmic proteins.

The reduction of MetO results in the formation of a disulfide bond within the active site of Msr (Ezraty *et al.*, 2005a; Lowther *et al.*, 2000). To perform another round of reaction, Msr needs to be reduced by a reducing pathway such as the thioredoxin/ thioredoxin reductase/ NADPH (Lu and Holmgren, 2014). For extracytoplasmic Msr, electrons need to cross the cytoplasmic membrane to an extracytoplasmic TDOR and then to Msr (Cho and Collet, 2013; Saleh *et al.*, 2013; Quinternet *et al.*, 2009). The results presented here suggested that SdbB and Sgo\_1177 are independent redox partners of MsrAB. This statement is supported by the findings that showed both SdbB and Sgo\_1177 are able to reduce MsrAB in disulfide exchange reactions and the results of the methionine sulfoxide reductase assay. The enzyme kinetic data showed that SdbB and Sgo\_1177 have the same ability to reduce MsrAB. In *S. pneumoniae*, Etrx1 (Sgo\_1177 homolog) preferentially reduces the A2 domain of *Sp*MsrAB2, whereas Etrx2 (SdbB homolog) is able to reduce both MsrA2 and MsrB2 domains. Thus, further investigation is required to determine if SdbB or Sgo\_1177 has a preferential partner as well.

In bacteria, it is known that extracytoplasmic TDORs can receive electrons from the cytoplasm via membrane proteins, such as DsbD and CcdA (Cho and Collet, 2013; Williamson *et al.*, 2015; Zhou and Bushweller, 2018). Here, the disulfide exchange results showed that CcdA1 and CcdA2 are able to reduce SdbB and Sgo\_1177, suggesting that the two CcdA proteins can functionally replace each other in reducing SdbB and Sgo\_1177. This finding is consistent with the previously reported role of CcdA protein in bacteria (Williamson *et al.*, 2015; Zhou and Bushweller, 2018; Saleh *et al.*, 2013). The two CcdA proteins were unable to reduce MsrAB as shown in the methionine sulfoxide reductase assay and disulfide exchange reactions. Collectively, these results suggest a sequential flow of electrons from CcdA1 or CcdA2 to SdbB or Sgo\_1177 and finally to MsrAB. In bacteria, the cytoplasmic thioredoxin system fuels electrons to the reducing pathway. In this system, thioredoxin donates the electrons to the membrane associated TDOR such as CcdA or DsbD, which funnel the electrons to the extracytoplasmic TDORs. Oxidized thioredoxin is then reduced at the expense of NADPH by the thioredoxin reductase (Lu and Holmgren, 2014; Cho and Collet, 2013; Gleiter and Bardwell, 2008). Recent studies showed that CcdA protein is able to transfer electrons from thioredoxins across the cytoplasmic membrane (Williamson *et al.*, 2015; Zhou and Bushweller, 2018). To do so, CcdA undergoes an outward-to-inward conformational change to transfer electrons across the cytoplasmic membrane. This conformational change allows the reactive cysteines to shuttle across the cytoplasmic membrane in an elevator-type movement (Williamson *et al.*, 2015; Zhou and Bushweller, 2018). Thus, it is feasible that the thioredoxin system donates the electrons to CcdA1 and CcdA2 in *S. gordonii*, which then funnel the electrons to MsrAB via SdbB or Sgo\_1177. However, further investigation is required to address the interaction between CcdA1 or CcdA2 and thioredoxin in *S. gordonii*.

It is interesting that the single *sdbB*, *sgo\_1177*, *ccdA1*, or *ccdA2* mutants did not display an impaired growth in the presence of 10 mM MetO, compared to the double *sdbBsgo\_1177* and *ccdA1ccdA2* mutants. These double gene mutants had a similar growth defect phenotype like the *msrAB* mutant. Therefore, only the deficiency of both SdbB and Sgo\_1177 or both CcdA1 and CcdA2 or MsrAB significantly impaired the

growth of *S. gordonii* in the presence of 10 mM MetO. This result further suggests that SdbB/Sgo1177 and CcdA1/CcdA2 proteins can functionally replace each other in MsrAB regeneration and that the two pathways (SdbBCcdA2 and Sgo\_1177CcdA1) are interconnected with SdbB interacting with CcdA1 and Sgo\_1177 with CcdA2. At 20 mM MetO, all the single- and double-gene mutants showed impaired growth compared to the parent strain, suggesting that MsrAB, SdbBCcdA2, and Sgo\_1177CcdA1 are required for optimal protection from oxidative stress.

In agreement with their role in the reducing pathway, *sdbB*, *sgo\_1177*, *ccdA1*, and *ccdA2* single gene mutants exhibited higher sensitivity to H<sub>2</sub>O<sub>2</sub> compared to the parent strain. *sdbBccdA2* and *sgo\_1177ccdA1* double mutants were even more sensitive to H<sub>2</sub>O<sub>2</sub> than the single gene mutants. *sdbBsgo\_1177* and *ccdA1ccdA2* double mutants were the most sensitive to H<sub>2</sub>O<sub>2</sub>. This is consistent with previous reports from *S. pneumoniae* and *N. meningitidis*, where the loss of Msr redox partner increases the susceptibility to H<sub>2</sub>O<sub>2</sub> (Kumar *et al.*, 2011; Saleh *et al.*, 2013).

The level of MsrAB, SdbB, and Sgo\_1177 under different growth conditions was examined. The results showed that the level of MsrAB, SdbB, and Sgo\_1177 increased under aerobic growth condition and planktonic lifestyle, which is in agreement with findings reported in other bacteria (Moskovitz *et al.*, 1995; Beloin *et al.*, 2004; Si *et al.*, 2015; Lei *et al.*, 2011). Because H<sub>2</sub>O<sub>2</sub> is produced under aerobic conditions (Barnard and Stinson, 1999), it is logical that *S. gordonii* produces more MsrAB, SdbB, and Sgo\_1177 to help to resist oxidative stress. In *S. gordonii*, *msrAB* is part of a five-gene operon including *ccdA1*, *Sgo\_1177* and a two-component system *sgo\_1180* (histidine kinase) and *sgo\_1181* (response regulator), whereas *sdbB* is part of a four-gene operon including *ccdA2*, and a two-component system *sgo\_1174* (histidine kinase) and *sgo\_1175* (response regulator). The results showed that the level of MsrAB and Sgo\_1177 was markedly increased in the *ccdA1* mutant, whereas the level of SdbB was increased in the *ccdA2* mutant, suggesting an active regulation of these two operons in response to oxidative stress or defect in the reducing pathway. In *E. coli*, the expression of *msrPQ* operon is regulated by the two-component system YedVW in response to oxidative stress such as exogenous H<sub>2</sub>O<sub>2</sub> (Gennaris *et al.*, 2015; Urano *et al.*, 2015). Thus, it is possible that the

expression of these operons in *S. gordonii* is regulated by the two-component system located within each operon; however, further investigation is required to confirm this.

In conclusion, the data suggest that *S. gordonii* possesses reducing pathways and one of these pathways consists of MsrAB, two thioredoxin-like lipoproteins (SdbB and Sgo\_1177), and two integral membrane proteins (CcdA1 and CcdA2). The results highlight the important role of MsrAB and other components of the pathway in resistance to oxidative stress. I propose that CcdA1 and CcdA2 funnel electrons to SdbB and Sgo\_1177, which in turn reduce MsrAB. MsrAB reduces MetO to Met (Figure 4.2).

### **4.3 Disulfide Bond Isomerization Pathway in *S. gordonii***

Disulfide bond isomerase can serve two functions for the cell: corrects non-native disulfide bonds and protects the cell from oxidative damage (Cho and Collet, 2013). To date, no disulfide-isomerization pathway has been identified in Gram-positive organisms despite Gram-positive bacteria face oxidative stress during their life cycle and produce extracytoplasmic proteins with more than one disulfide bond (Baker *et al.*, 2004; Davey *et al.*, 2016b; Landeta *et al.*, 2018; Ezraty *et al.*, 2017). In the third part of this study, the results showed that SdbB can function as a disulfide bond isomerase. One of the hallmarks of disulfide bond isomerases is that they have oxidase and reductase activity (Rietsch *et al.*, 1996; Darby *et al.*, 1996). The results showed that of all the tested TDORs from *S. gordonii*, SdbB is the only TDOR that showed reductase activity in addition to oxidase activity. Although Sgo\_1177, CcdA1, and CcdA2 did not exhibit reductase activity in the insulin precipitation assay, these proteins were able to act as a reductase in the disulfide exchange reaction. For example, CcdA1 and CcdA2 are able to reduce SdbB and Sgo\_1177, whereas Sgo\_1177 is able to reduce MsrAB. This could be due to the narrow substrate specificity for these proteins, such as its redox partner(s) not insulin. Collectively, these results suggest that SdbB can act as a disulfide bond isomerase. In agreement with this notion, the results showed that SdbB was able to rescue the scrambled RNase A in the isomerase assay.



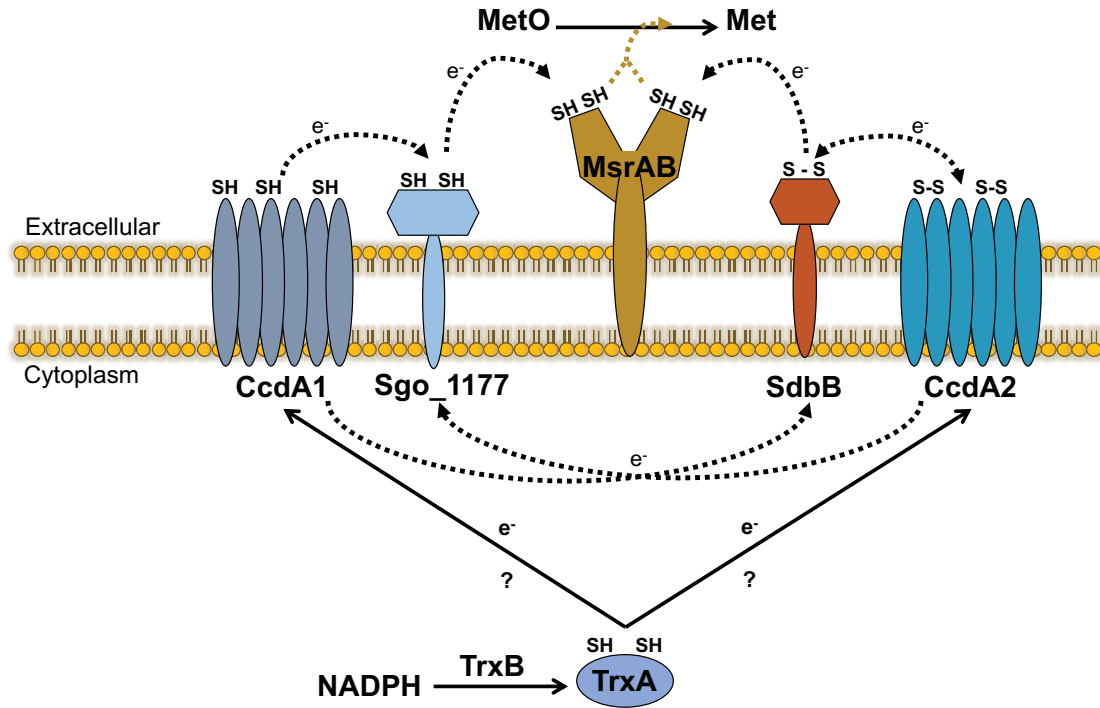


**Figure 4.2 A proposed model for the reducing pathway in *S. gordonii*.**

MsrAB reduces MetO to Met. Next, SdbB and Sgo\_1177 reduce MsrAB, allowing MsrAB to perform another round of reaction. CcdA1 and CcdA2 reduce SdbB and Sgo\_1177. The electrons likely come from the thioredoxin system in the cytoplasm, which is depicted as question marks.

In bacteria, disulfide bond isomerase plays an important role in the proper folding and stability of many extracytoplasmic proteins by correcting the non-native disulfide bonds. Consequently, loss of this isomerase results in accumulation of mis-disulfide bonded proteins and subsequent degradation of these proteins (Rietsch *et al.*, 1996; Sone *et al.*, 1997). DsbC is known to be required for the proper folding of periplasmic proteins with multiple disulfide bonds such as RNase I (contains four disulfide bonds) and murein endopeptidase (contains three disulfide bonds) (Hiniker and Bardwell, 2004; Denoncin *et al.*, 2010). Here, the notion of SdbB is a disulfide bond isomerase in *S. gordonii* was investigated for the production of anti-CR1 scFv, a protein with two disulfide bonds. The results showed that the anti-CR1 scFv was degraded in the *sdbB* mutant. Interestingly, the anti-CR1 scFv was also degraded in the *ccdA2* mutant. The level of anti-CR1 scFv produced by the *sdbB* and *ccdA2* mutant was restored to the parental level by *degP* mutation, indicating that anti-CR1 scFv is misfolded and degraded by DegP. In the *sdbA* mutant, anti-CR1 scFv is misfolded and degraded by DegP due to the lack of a disulfide bond (Davey *et al.*, 2015a). The alkylation experiments showed that anti-CR1 scFv isolated from *sdbB*, *sdbBdegP*, and *ccdA2degP* were fully oxidized. Collectively, these results support that SdbB is a disulfide bond isomerase. In addition, these results also suggest that CcdA2 may be a redox partner of SdbB in the disulfide bond isomerization pathway. In agreement with this notion, the disulfide exchange results showed that CcdA2 is able to reduce SdbB.

The role of SdbB and CcdA2 in the disulfide bond isomerization pathway was further demonstrated by investigating their role in copper stress resistance in *S. gordonii*. Copper is an oxidant that can catalyze the formation of non-native disulfide bonds, which lead to protein misfolding and degradation. In bacteria, disulfide bond isomerization systems are known to counteract copper toxicity by correcting these non-native disulfide bonds (Kachur *et al.*, 1999; Hiniker *et al.*, 2005). This study revealed that SdbB and CcdA2 are crucial for protecting *S. gordonii* from copper toxicity. The *sdbB*, *ccdA2*, and *sdbBccdA2* were more sensitive to CuSO<sub>4</sub> than the parent. This sensitivity is consistent with that reported for the *E. coli dsbC* and *dsbD* mutants that showed an increased sensitivity to copper (Denoncin *et al.*, 2014; Hiniker *et al.*, 2005).

It is important to identify the natural substrates of the SdbB in order to understand the role of the disulfide bond isomerization pathway in *S. gordonii*. Previous study identified 20 potential extracytoplasmic proteins with more than two cysteines in *S. gordonii* (Davey *et al.*, 2013), which could be potential natural substrates for SdbB. These proteins include transporters, protease, hydrolase, and some with unknown function (Davey *et al.*, 2013). In addition, proteomics analysis could be used to identify possible SdbB substrates as described previously for BdbCD in *B. subtilis* (Goosens *et al.*, 2013).

In conclusion, the data suggest that SdbB is a disulfide bond isomerase that corrects the non-native disulfide bonds and protects *S. gordonii* from oxidative damage. The results also suggest that CcdA2 is a redox partner of SdbB in the disulfide bond isomerization pathway. I propose that SdbB corrects the non-native disulfide bonds, which results from cysteine oxidation by ROS, copper, or as a result of incorrect disulfide bond formation by SdbA or other TDORs. SdbB can isomerize the non-native disulfide bonds or can reduce these bonds and give SdbA another chance to introduce the correct disulfide bonds to facilitate protein folding and prevent protein degradation. Preliminary results suggest that CcdA2 is a redox partner of SdbB (Figure 4.3).

#### **4.4 Structural Determinants of SdbA Protein and Evidence of SdbA-SdbB Interaction Through their Active Site Cysteines**

The role of the active-site cysteines in SdbA-SdbB interaction was investigated to explore the mechanism of SdbA reoxidation. The results showed that SdbA-SdbB interacts through their active site cysteines. The initial interaction between SdbA and SdbB involved the solvent-exposed N-terminal cysteine. Previous studies showed that the N-terminal cysteine of SdbA (C<sub>86</sub>) of the active site is solvent-exposed (Davey *et al.*, 2015a; Stogios and Savchenko, 2015). Here the results suggest that the N-terminal cysteine of SdbB (C<sub>81</sub>) is also solvent exposed. SdbA<sub>C89A</sub> forms a disulfide complex with SdbB *in vivo* (Figure 3.13). This finding is supported by the *in vitro* interaction between SdbA and SdbB active site variants. The results showed that SdbA<sub>C89A</sub> formed a stable complex with SdbB<sub>C84A</sub>.

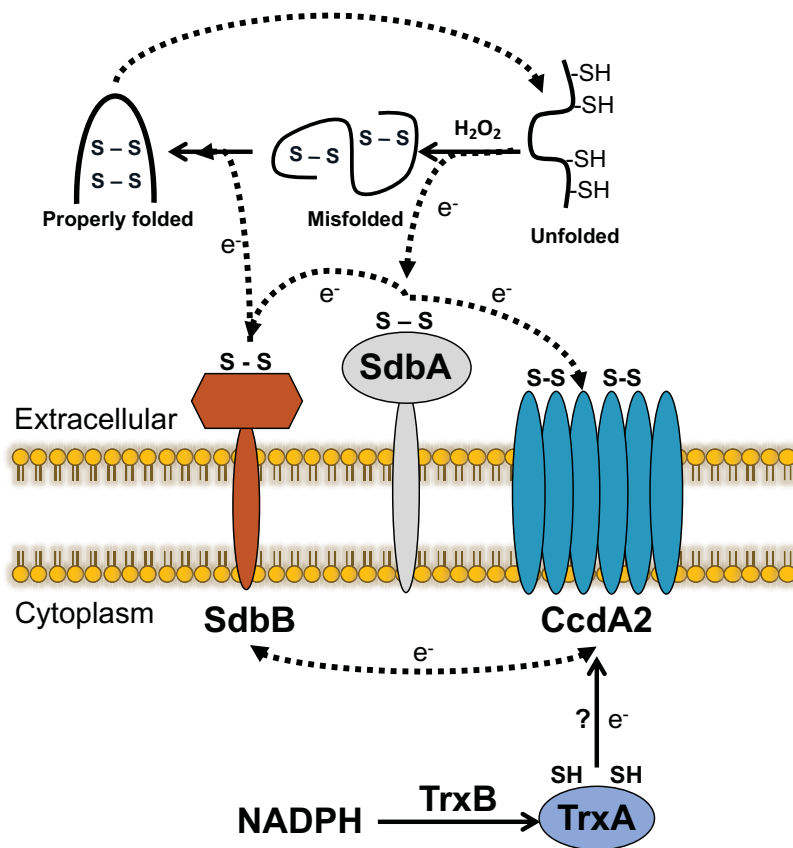


**Figure 4.3 A proposed model for the disulfide bond isomerase pathway in *S. gordonii*.**

Disulfide bond oxidase such as SdbA and ROS can form mis-disulfide bonds in the extracytoplasmic proteins, which, if not corrected, can cause protein degradation. SdbB is the disulfide bond isomerase that corrects these non-native disulfide bonds either directly or by reducing the disulfide bonds and give SdbA another chance to introduce the correct disulfide bonds in the target protein. CcdA2 acts as a redox partner of SdbB. The electrons may come from the thioredoxin system in the cytoplasm, which is depicted as question marks or from the oxidation pathway after SdbA reoxidation.

This is in agreement with the mechanism of DsbA reoxidation that involves the formation of a mixed disulfide bond (DsbA<sub>C30</sub>–DsbB<sub>C104</sub>) between the two solvent exposed cysteines (Inaba *et al.*, 2006; Kishigami *et al.*, 1995b). Collectively, the results suggest that SdbA-SdbB interacts through their solvent-exposed N-terminal cysteines. I propose that during SdbA reoxidation, C<sub>86</sub> of the reduced SdbA attack C<sub>81</sub> in the C<sub>81</sub>-C<sub>84</sub> disulfide bond of SdbB. This resulted in a mixed disulfide complex between SdbA C<sub>86</sub> and C<sub>81</sub> of SdbB. This is followed by the attack of SdbA C<sub>89</sub> to SdbA<sub>C86</sub>–SdbB<sub>C81</sub> disulfide bond. This results in the release of oxidized SdbA from the complex and SdbB is reduced (Figure 4.4).

The structural basis of SdbA-substrate interaction was explored using the information provided from the crystal structure of SdbA (Stogios and Savchenko, 2015). The SdbA structure showed a thioredoxin fold containing a conserved active site C<sub>86</sub>PDC<sub>89</sub> and a *cis*-proline (P<sub>156</sub>) residue in close proximity to the active site. Interestingly, the enzyme kinetic results showed that the point mutation of the P<sub>156</sub>T did not cause a change to the enzyme activity. This was unexpected since similar mutants in other TDOR displayed defects in TDOR-substrate interaction (Kadokura *et al.*, 2004; Kadokura *et al.*, 2005). However, it was reported previously in *E. coli* DsbA that only P<sub>151</sub>T cause an accumulation of DsbA-substrate complexes, whereas P<sub>151</sub>S or P<sub>151</sub>H cause an accumulation of DsbA-DsbB complex. Thus, further investigation is required, including testing the effect of multiple P<sub>156</sub> point mutants before excluding the role of P<sub>156</sub> in SdbA-substrate interaction.

SdbA is highly similar in structure to ResA of *B. subtilis*. ResA is known to undergo a redox-dependent conformational change that is accompanied by a rearrangement of multiple surface-exposed amino acids (Crow *et al.*, 2004; Colbert *et al.*, 2006). The enzyme kinetic results of SdbA showed that point mutations in three-surface exposed amino acids K<sub>91</sub>, S<sub>154</sub>, and F<sub>174</sub>, which correspond to K<sub>79</sub>, P<sub>139</sub>, and T<sub>159</sub> in *B. subtilis* ResA, causes a significant increase in the K<sub>m</sub> value of SdbA compared to the parent enzyme. The results suggest a role for K<sub>91</sub>, S<sub>154</sub>, and F<sub>174</sub> in SdbA-substrate interaction.

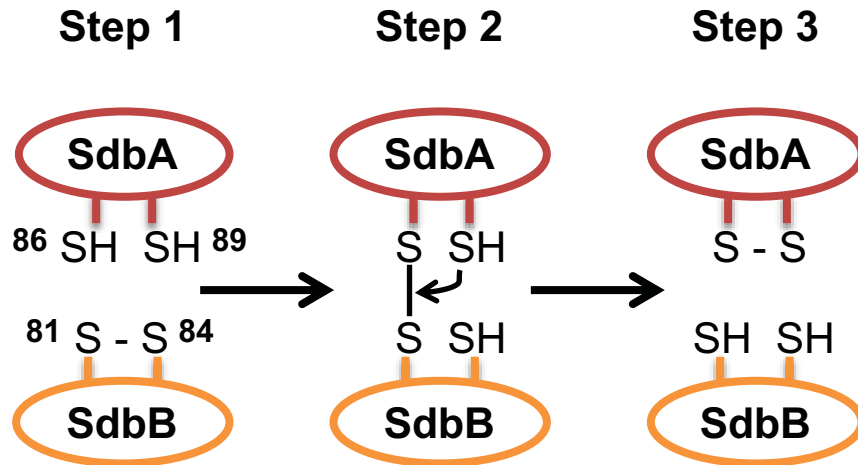


**Figure 4.4 A proposed model for SdbA reoxidation by SdbB.**

The process starts with oxidized SdbB with a C<sub>81</sub>-C<sub>84</sub> disulfide bond in the resting state and a reduced SdbA (step 1). C<sub>86</sub> of SdbA attacks C<sub>81</sub> of SdbB forming SdbA-SdbB mixed disulfide complex (step 2). C<sub>89</sub> of SdbA attacks the intermolecular SdbA<sub>C86</sub>-SdbB<sub>C81</sub> disulfide bond resulting in an oxidized SdbA and a reduced SdbB (Step 3).

It is worthy to note that K<sub>79</sub>, P<sub>139</sub>, and T<sub>159</sub> in *B. subtilis* ResA undergo redox-dependent rearrangement, which is essential for ResA-substrate interaction (Crow *et al.*, 2004; Colbert *et al.*, 2006). The enzyme kinetic results further suggest that R<sub>119</sub> and T<sub>172</sub> may also play a role in SdbA-substrate interaction. It is interesting to note that mutation of Q<sub>92</sub> in SdbA, which correspond to E<sub>80</sub> in *B. subtilis* ResA, did not affect the enzyme's kinetic properties. E<sub>80</sub> in *B. subtilis* ResA alters between buried, when the protein is oxidized, to surface exposed, when the protein is reduced, and located at the base of the substrate binding cavity close to the active site (Crow *et al.*, 2004; Colbert *et al.*, 2006). Surprisingly, when Q<sub>92</sub>A or Q<sub>92</sub>E was introduced into SdbA<sub>S154E</sub>, the K<sub>m</sub> of these double point mutants (S154E/Q91A or S154E/Q91E) returned to values similar to that of the parent SdbA.

In addition to its effect on SdbA-substrate interaction, S<sub>154</sub> appears to play a role in SdbA-redox partner interaction. The disulfide exchange results showed that SdbA<sub>S154E</sub> exhibited a delay in reoxidation by SdbB. However, further in-depth investigations should be performed to fully examine the role of this amino acid and to explore the role of other surface exposed amino acids in SdbA-SdbB interaction.

## 4.5 General Conclusion

The work presented in this study provides new insight into the oxidation, reduction, and isomerization pathways in *S. gordonii*. In the oxidation pathway, the results of this study indicate that SdbB and CcdA2 are the independent redox partners of the disulfide bond catalyst SdbA (Figure 4.5). In the reduction pathway, the results indicated that MsrAB, the two thioredoxin-like lipoproteins (SdbB and Sgo\_1177), and the two integral membrane proteins (CcdA1 and CcdA2) form a reducing pathway that is important in protecting *S. gordonii* from oxidative stress. The results suggest that the activity of MsrAB depends on the presence of its redox partners, SdbB and Sgo\_1177. Both SdbB and Sgo\_1177 may receive the electrons from the integral membrane proteins CcdA1 and CcdA2 (Figure 4.5).

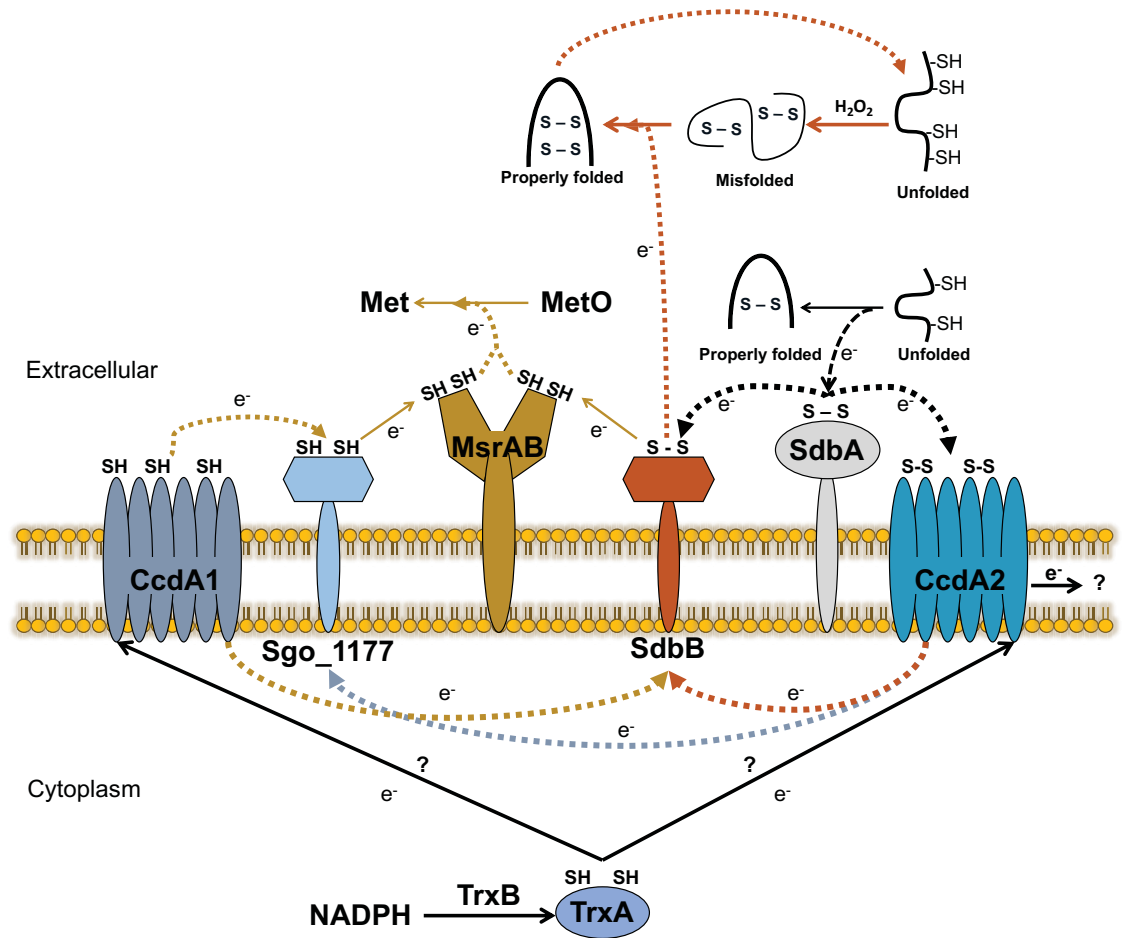


**Figure 4.5 A proposed model for the oxidation, reduction, and isomerization pathways in *S. gordonii*.**

SdbA is the oxidase that introduces the disulfide bonds into substrate proteins. SdbB and CcdA2 reoxidize the reduced SdbA. SdbA and ROS may form non-native disulfide bonds in the extracytoplasmic proteins, which can be corrected by the disulfide bond isomerase SdbB. For the reducing pathway, electrons likely come from the thioredoxin system in the cytoplasm and via the CcdA proteins to SdbB or Sgo\_1177. Both SdbB and Sgo\_1177 can reduce MsrAB, which in turn reduces MetO.



Finally, the results suggest that *S. gordonii* has a disulfide bond isomerization pathway that corrects the non-native disulfide bonds and protects *S. gordonii* from oxidative damage. This isomerization pathway consists of SdbB as a disulfide bond isomerase and CcdA2 as the redox partner (Figure 4.5). Collectively, these findings significantly advanced the knowledge of disulfide bond formation, methionine sulfoxide reduction, and disulfide bond isomerization in Gram-positive bacteria.

## 4.6 Future Direction

The work presented here answered a number of questions about the oxidation, reduction, and isomerization pathways in *S. gordonii*. At the same time, many questions remained, which require further investigation.

In the disulfide bond formation pathway, the results indicated that SdbB and CcdA2 are independent redox partners of SdbA. However, it is still unknown how electrons flow from SdbB and CcdA2 after SdbA reoxidation. Given that *S. gordonii* lacks in a respiratory chain, cytochrome *c*, quinone, menaquinone, and fumarate reductase (Brooijmans *et al.*, 2009; Kakinuma, 1998; Vickerman *et al.*, 2007), suggesting that the mechanism of CcdA2 and SdbB reoxidation is different from DsbB in *E. coli* (Bader *et al.*, 1999). One possibility is that SdbB and CcdA2 channel electrons to the disulfide bond reduction or isomerization pathway. However, it is also possible that downstream redox partners are involved in SdbB and CcdA2 reoxidation. One approach for finding the downstream components of the SdbA oxidative pathway is to screen a transposon mutant library for *sdbA*-associated phenotype (Loo *et al.*, 2000). Mutants that reproduce the *sdbA*-associated phenotype can be further examined to determine its effect on the oxidative protein folding pathway and the redox state of SdbA and its redox partners. Another question in the disulfide bond formation pathway is, does SdbA has other natural substrates. Previous study identified a list of potential substrates for SdbA that can be used as a starting point to identify additional natural substrates (Davey *et al.*, 2013).

A key question in the MetO reducing pathway is how electrons are funneled to the CcdA proteins. One possibility is that the cytoplasmic thioredoxin funnels electrons to

SdbB or Sgo\_1177 via the CcdA proteins. Thus, investigating the CcdA-thioredoxin interaction in *S. gordonii* may elucidate the source of electrons for this pathway.

A second question in the MetO reducing pathway is what are the natural substrates of MsrAB in *S. gordonii*. Previous study showed that MsrA could reduce MetO in adhesins SspB (Lei *et al.*, 2011). However, MsrA occurs mainly in the cytoplasm and SspB is a surface protein (Kerrigan *et al.*, 2007; Lei *et al.*, 2011); thus it is likely that MsrAB also involves in the reduction of MetO in SspB. In addition, screening for other Met-rich cell envelope-associated proteins (e.g., amylase-binding protein B) may yield a new substrate for MsrAB. The results from this study indicated that SdbB and Sgo\_1177 are the immediate redox partners of MsrAB and CcdA1 and CcdA2 are a part of the pathways. Thus, it is important to determine the redox state of MsrAB in the parent and TDORs mutant strains. This will shed light on the role of each TDOR in the reducing pathway.

In the isomerization pathway, one of the key questions remained is the identity of the natural substrate of SdbB. The previously identified list of 20 potential extracytoplasmic proteins with more than two cysteines in *S. gordonii* (Davey *et al.*, 2013) may have potential natural substrates for SdbB. In addition, because SdbB plays a role in oxidative stress and copper stress resistance, one cannot rule out the possibility that SdbB may also involve in protecting single cysteine residues from oxidation. Therefore, it will be prudent to include all extracytoplasmic protein with one or more cysteine residues during the search for natural substrates of SdbB, which can be performed using proteomics analysis as described previously for BdbCD in *B. subtilis* (Goosens *et al.*, 2013).

One of the most interesting findings of this study is the role played by SdbB and CcdA2 as interchangeable modules in different thiol-disulfide exchange pathways in *S. gordonii*. The results of this study suggest that SdbB acts as an electron hub, connecting the oxidation, reduction, and isomerization pathway in *S. gordonii*. This makes SdbB a unique TDOR; however, further investigations are required to understand how SdbB is able to perform this multifunction. In Gram-negative bacteria, TDOR with multifunction is maintained in a mixture of reduced and oxidized form by multiple redox

partners (Jameson-Lee *et al.*, 2011; Kpadeh *et al.*, 2015). Thus, determining the redox state of SdbB is important to understand how SdbB is able to perform these multifunctions.

## Reference

- Ahn, S. J. and Burne, R. A. 2007. Effects of oxygen on biofilm formation and the AtIA autolysin of *Streptococcus mutans*. *Journal of Bacteriology*, 189, 6293-6302.
- Alanen, H. I., Salo, K. E., Pekkala, M., Siekkinen, H. M., Pirneskoski, A. and Ruddock, L. W. 2003. Defining the domain boundaries of the human protein disulfide isomerases. *Antioxid Redox Signal*, 5, 367-74.
- Andisi, V. F., Hinojosa, C. A., De Jong, A., Kuipers, O. P., Orihuela, C. J. and Bijlsma, J. J. 2012. Pneumococcal gene complex involved in resistance to extracellular oxidative stress. *Infect Immun*, 80, 1037-49.
- Appenzeller-Herzog, C. and Ellgaard, L. 2008. *In vivo* reduction-oxidation state of protein disulfide isomerase: the two active sites independently occur in the reduced and oxidized forms. *Antioxid Redox Signal*, 10, 55-64.
- Bader, M., Muse, W., Ballou, D. P., Gassner, C. and Bardwell, J. C. 1999. Oxidative protein folding is driven by the electron transport system. *Cell*, 98, 217-27.
- Bader, M. W., Hiniker, A., Regeimbal, J., Goldstone, D., Haebel, P. W., Riemer, J., Metcalf, P. and Bardwell, J. C. 2001. Turning a disulfide isomerase into an oxidase: DsbC mutants that imitate DsbA. *EMBO J*, 20, 1555-62.
- Baker, M. D., Gendlina, I., Collins, C. M. and Acharya, K. R. 2004. Crystal structure of a dimeric form of streptococcal pyrogenic exotoxin A (SpeA1). *Protein Sci*, 13, 2285-90.
- Balmer, Y., Koller, A., Del Val, G., Manieri, W., Schurmann, P. and Buchanan, B. B. 2003. Proteomics gives insight into the regulatory function of chloroplast thioredoxins. *Proc Natl Acad Sci U S A*, 100, 370-5.
- Banci, L., Bertini, I., Cefaro, C., Ciofi-Baffoni, S., Gallo, A., Martinelli, M., Sideris, D. P., Katrakili, N. and Tokatlidis, K. 2009. MIA40 is an oxidoreductase that catalyzes oxidative protein folding in mitochondria. *Nat Struct Mol Biol*, 16, 198-206.
- Bardwell, J. C., Lee, J. O., Jander, G., Martin, N., Belin, D. and Beckwith, J. 1993. A pathway for disulfide bond formation *in vivo*. *Proceedings of the National Academy of Sciences of the United States of America*, 90, 1038-1042.
- Bardwell, J. C., McGovern, K. and Beckwith, J. 1991. Identification of a protein required for disulfide bond formation *in vivo*. *Cell*, 67, 581-589.
- Barnard, J. P. and Stinson, M. W. 1999. Influence of environmental conditions on hydrogen peroxide formation by *Streptococcus gordonii*. *Infect Immun*, 67, 6558-64.
- Beeby, M., O'connor, B. D., Ryttersgaard, C., Boutz, D. R., Perry, L. J. and Yeates, T. O. 2005. The genomics of disulfide bonding and protein stabilization in thermophiles. *PLoS Biol*, 3, e309.
- Beloin, C., Valle, J., Latour-Lambert, P., Faure, P., Kzreminski, M., Balestrino, D., Haagensen, J. A., Molin, S., Prensier, G., Arbeille, B. and Ghigo, J. M. 2004. Global impact of mature biofilm lifestyle on *Escherichia coli* K-12 gene expression. *Mol Microbiol*, 51, 659-74.

- Bessette, P. H., Cotto, J. J., Gilbert, H. F. and Georgiou, G. 1999. In vivo and in vitro function of the *Escherichia coli* periplasmic cysteine oxidoreductase DsbG. *J Biol Chem*, 274, 7784-92.
- Bihlmaier, K., Mesecke, N., Terziyska, N., Bien, M., Hell, K. and Herrmann, J. M. 2007. The disulfide relay system of mitochondria is connected to the respiratory chain. *J Cell Biol*, 179, 389-95.
- Birnboim, H. C. and Doly, J. 1979. A rapid alkaline extraction procedure for screening recombinant plasmid DNA. *Nucleic Acids Res*, 7, 1513-23.
- Bocian-Ostrzycka, K. M., Lasica, A. M., Dunin-Horkawicz, S., Grzeszczuk, M. J., Drabik, K., Dobosz, A. M., Godlewska, R., Nowak, E., Collet, J. F. and Jagusztyn-Krynicka, E. K. 2015. Functional and evolutionary analyses of *Helicobacter pylori* HP0231 (DsbK) protein with strong oxidative and chaperone activity characterized by a highly diverged dimerization domain. *Front Microbiol*, 6, 1065.
- Bolhuis, A., Venema, G., Quax, W. J., Bron, S. and Van Dijl, J. M. 1999. Functional analysis of paralogous thiol-disulfide oxidoreductases in *Bacillus subtilis*. *The Journal of biological chemistry*, 274, 24531-24538.
- Bos, J., Duverger, Y., Thouvenot, B., Chiaruttini, C., Branlant, C., Springer, M., Charpentier, B. and Barras, F. 2013. The sRNA RyhB regulates the synthesis of the *Escherichia coli* methionine sulfoxide reductase MsrB but not MsrA. *PLoS One*, 8, e63647.
- Boschi-Muller, S., Azza, S., Sanglier-Cianferani, S., Talfournier, F., Van Dorsselear, A. and Branlant, G. 2000. A sulfenic acid enzyme intermediate is involved in the catalytic mechanism of peptide methionine sulfoxide reductase from *Escherichia coli*. *J Biol Chem*, 275, 35908-13.
- Bouwman, C. W., Kohli, M., Killoran, A., Touchie, G. A., Kadner, R. J. and Martin, N. L. 2003. Characterization of SrgA, a *Salmonella enterica* serovar Typhimurium virulence plasmid-encoded paralogue of the disulfide oxidoreductase DsbA, essential for biogenesis of plasmid-encoded fimbriae. *J Bacteriol*, 185, 991-1000.
- Brooijmans, R., Smit, B., Santos, F., Van Riel, J., De Vos, W. M. and Hugenholtz, J. 2009. Heme and menaquinone induced electron transport in lactic acid bacteria. *Microb Cell Fact*, 8, 28.
- Brot, N., Weissbach, L., Werth, J. and Weissbach, H. 1981. Enzymatic reduction of protein-bound methionine sulfoxide. *Proc Natl Acad Sci U S A*, 78, 2155-8.
- Bukowska-Faniband, E. and Hederstedt, L. 2017. Transpeptidase activity of penicillin-binding protein SpoVD in peptidoglycan synthesis conditionally depends on the disulfide reductase StoA. *Mol Microbiol*, 105, 98-114.
- Burne, R. A., Wen, Z. T., Chen, Y. Y. and Penders, J. E. 1999. Regulation of expression of the fructan hydrolase gene of *Streptococcus mutans* GS-5 by induction and carbon catabolite repression. *Journal of Bacteriology*, 181, 2863-2871.
- Chim, N., Harmston, C. A., Guzman, D. J. and Goulding, C. W. 2013. Structural and biochemical characterization of the essential DsbA-like disulfide bond forming protein from *Mycobacterium tuberculosis*. *BMC Struct Biol*, 13, 23.

- Chim, N., Riley, R., The, J., Im, S., Segelke, B., Lekin, T., Yu, M., Hung, L. W., Terwilliger, T., Whitelegge, J. P. and Goulding, C. W. 2010. An extracellular disulfide bond forming protein (DsbF) from *Mycobacterium tuberculosis*: structural, biochemical, and gene expression analysis. *J Mol Biol*, 396, 1211-26.
- Cho, S. H. and Collet, J. F. 2013. Many roles of the bacterial envelope reducing pathways. *Antioxid Redox Signal*, 18, 1690-8.
- Choe, S., Bennett, M. J., Fujii, G., Curmi, P. M., Kantardjieff, K. A., Collier, R. J. and Eisenberg, D. 1992. The crystal structure of diphtheria toxin. *Nature*, 357, 216-22.
- Chung, J., Chen, T. and Missiakas, D. 2000. Transfer of electrons across the cytoplasmic membrane by DsbD, a membrane protein involved in thiol-disulphide exchange and protein folding in the bacterial periplasm. *Mol Microbiol*, 35, 1099-109.
- Claverys, J. P., Dintilhac, A., Pestova, E. V., Martin, B. and Morrison, D. A. 1995. Construction and evaluation of new drug-resistance cassettes for gene disruption mutagenesis in *Streptococcus pneumoniae*, using an ami test platform. *Gene*, 164, 123-128.
- Colbert, C. L., Wu, Q., Erbel, P. J., Gardner, K. H. and Deisenhofer, J. 2006. Mechanism of substrate specificity in *Bacillus subtilis* ResA, a thioredoxin-like protein involved in cytochrome c maturation. *Proc Natl Acad Sci U S A*, 103, 4410-5.
- Crow, A., Acheson, R. M., Le Brun, N. E. and Oubrie, A. 2004. Structural basis of Redox-coupled protein substrate selection by the cytochrome c biosynthesis protein ResA. *J Biol Chem*, 279, 23654-60.
- Crow, A., Lewin, A., Hecht, O., Carlsson Moller, M., Moore, G. R., Hederstedt, L. and Le Brun, N. E. 2009a. Crystal structure and biophysical properties of *Bacillus subtilis* BdbD. An oxidizing thiol:disulfide oxidoreductase containing a novel metal site. *J Biol Chem*, 284, 23719-33.
- Crow, A., Liu, Y., Moller, M. C., Le Brun, N. E. and Hederstedt, L. 2009b. Structure and functional properties of *Bacillus subtilis* endospore biogenesis factor StoA. *J Biol Chem*, 284, 10056-66.
- Dailey, F. E. and Berg, H. C. 1993. Mutants in disulfide bond formation that disrupt flagellar assembly in *Escherichia coli*. *Proc Natl Acad Sci U S A*, 90, 1043-7.
- Daniels, R., Mellroth, P., Bernsel, A., Neiers, F., Normark, S., Von Heijne, G. and Henriques-Normark, B. 2010. Disulfide bond formation and cysteine exclusion in gram-positive bacteria. *The Journal of biological chemistry*, 285, 3300-3309.
- Darby, N. J. and Creighton, T. E. 1995. Functional properties of the individual thioredoxin-like domains of protein disulfide isomerase. *Biochemistry*, 34, 11725-35.
- Darby, N. J., Kemmink, J. and Creighton, T. E. 1996. Identifying and characterizing a structural domain of protein disulfide isomerase. *Biochemistry*, 35, 10517-28.
- Darmon, E., Dorenbos, R., Meens, J., Freudl, R., Antelmann, H., Hecker, M., Kuipers, O. P., Bron, S., Quax, W. J., Dubois, J. Y. and Van Dijl, J. M. 2006. A disulfide bond-containing alkaline phosphatase triggers a BdbC-dependent secretion stress response in *Bacillus subtilis*. *Appl Environ Microbiol*, 72, 6876-85.
- Davey, L., Cohen, A., Leblanc, J., Halperin, S. A. and Lee, S. F. 2015a. The disulfide oxidoreductase SdbA is active in *Streptococcus gordonii* using a single C-terminal cysteine of the CXXC motif. *Molecular microbiology*.

- Davey, L., Halperin, S. A. and Lee, S. F. 2015b. Mutation of the thiol-disulfide oxidoreductase SdbA activates the CiaRH two-component system leading to bacteriocin expression shutdown in *Streptococcus gordonii*. *Journal of Bacteriology*.
- Davey, L., Halperin, S. A. and Lee, S. F. 2016a. Mutation of the *Streptococcus gordonii* Thiol-Disulfide Oxidoreductase SdbA Leads to Enhanced Biofilm Formation Mediated by the CiaRH Two-Component Signaling System. *PloS one*, 11, e0166656.
- Davey, L., Halperin, S. A. and Lee, S. F. 2016b. Thiol-Disulfide Exchange in Gram-Positive Firmicutes. *Trends in microbiology*, 24, 902-915.
- Davey, L., Ng, C. K., Halperin, S. A. and Lee, S. F. 2013. Functional analysis of paralogous thiol-disulfide oxidoreductases in *Streptococcus gordonii*. *The Journal of biological chemistry*, 288, 16416-16429.
- Denoncin, K. and Collet, J. F. 2013. Disulfide bond formation in the bacterial periplasm: major achievements and challenges ahead. *Antioxidants & redox signaling*, 19, 63-71.
- Denoncin, K., Vertommen, D., Arts, I. S., Goemans, C. V., Rahuel-Clermont, S., Messens, J. and Collet, J. F. 2014. A new role for *Escherichia coli* DsbC protein in protection against oxidative stress. *J Biol Chem*, 289, 12356-64.
- Denoncin, K., Vertommen, D., Paek, E. and Collet, J. F. 2010. The protein-disulfide isomerase DsbC cooperates with SurA and DsbA in the assembly of the essential beta-barrel protein LptD. *J Biol Chem*, 285, 29425-33.
- Depuydt, M., Leonard, S. E., Vertommen, D., Denoncin, K., Morsomme, P., Wahni, K., Messens, J., Carroll, K. S. and Collet, J. F. 2009. A periplasmic reducing system protects single cysteine residues from oxidation. *Science*, 326, 1109-11.
- Depuydt, M., Messens, J. and Collet, J. F. 2011. How proteins form disulfide bonds. *Antioxidants & redox signaling*, 15, 49-66.
- Dorenbos, R., Stein, T., Kabel, J., Bruand, C., Bolhuis, A., Bron, S., Quax, W. J. and Van Dijl, J. M. 2002. Thiol-disulfide oxidoreductases are essential for the production of the lantibiotic sublancin 168. *The Journal of biological chemistry*, 277, 16682-16688.
- Dumoulin, A., Grauschopf, U., Bischoff, M., Thony-Meyer, L. and Berger-Bachi, B. 2005. *Staphylococcus aureus* DsbA is a membrane-bound lipoprotein with thiol-disulfide oxidoreductase activity. *Archives of Microbiology*, 184, 117-128.
- Dunny, G. M., Lee, L. N. and Leblanc, D. J. 1991. Improved electroporation and cloning vector system for gram-positive bacteria. *Applied and Environmental Microbiology*, 57, 1194-1201.
- Dutton, R. J., Boyd, D., Berkmen, M. and Beckwith, J. 2008. Bacterial species exhibit diversity in their mechanisms and capacity for protein disulfide bond formation. *Proc Natl Acad Sci U S A*, 105, 11933-8.
- Dutton, R. J., Wayman, A., Wei, J. R., Rubin, E. J., Beckwith, J. and Boyd, D. 2010. Inhibition of bacterial disulfide bond formation by the anticoagulant warfarin. *Proc Natl Acad Sci U S A*, 107, 297-301.
- Ed Harlow, D. L. 1988. *Antibodies: A Laboratory Manual.*, USA, Cold Spring Harbor Laboratory.

- Erlendsson, L. S., Acheson, R. M., Hederstedt, L. and Le Brun, N. E. 2003. *Bacillus subtilis* ResA is a thiol-disulfide oxidoreductase involved in cytochrome c synthesis. *The Journal of biological chemistry*, 278, 17852-17858.
- Erlendsson, L. S. and Hederstedt, L. 2002. Mutations in the thiol-disulfide oxidoreductases BdbC and BdbD can suppress cytochrome c deficiency of CcdA-defective *Bacillus subtilis* cells. *J Bacteriol*, 184, 1423-9.
- Erlendsson, L. S., Moller, M. and Hederstedt, L. 2004. *Bacillus subtilis* StoA Is a thiol-disulfide oxidoreductase important for spore cortex synthesis. *Journal of Bacteriology*, 186, 6230-6238.
- Etienne, F., Spector, D., Brot, N. and Weissbach, H. 2003. A methionine sulfoxide reductase in *Escherichia coli* that reduces the R enantiomer of methionine sulfoxide. *Biochem Biophys Res Commun*, 300, 378-82.
- Ezraty, B., Aussel, L. and Barras, F. 2005a. Methionine sulfoxide reductases in prokaryotes. *Biochim Biophys Acta*, 1703, 221-9.
- Ezraty, B., Bos, J., Barras, F. and Aussel, L. 2005b. Methionine sulfoxide reduction and assimilation in *Escherichia coli*: new role for the biotin sulfoxide reductase BisC. *J Bacteriol*, 187, 231-7.
- Ezraty, B., Gennaris, A., Barras, F. and Collet, J. F. 2017. Oxidative stress, protein damage and repair in bacteria. *Nat Rev Microbiol*, 15, 385-396.
- Fabianek, R. A., Hennecke, H. and Thony-Meyer, L. 1998. The active-site cysteines of the periplasmic thioredoxin-like protein CcmG of *Escherichia coli* are important but not essential for cytochrome c maturation *in vivo*. *J Bacteriol*, 180, 1947-50.
- Feng, W. K., Wang, L., Lu, Y. and Wang, X. Y. 2011. A protein oxidase catalysing disulfide bond formation is localized to the chloroplast thylakoids. *FEBS J*, 278, 3419-30.
- Fernandes, A. P. and Holmgren, A. 2004. Glutaredoxins: glutathione-dependent redox enzymes with functions far beyond a simple thioredoxin backup system. *Antioxid Redox Signal*, 6, 63-74.
- Fontaine, L. and Hols, P. 2008. The inhibitory spectrum of thermophilin 9 from *Streptococcus thermophilus* LMD-9 depends on the production of multiple peptides and the activity of BlpG(St), a thiol-disulfide oxidase. *Appl Environ Microbiol*, 74, 1102-10.
- Genevaux, P., Bauda, P., Dubow, M. S. and Oudega, B. 1999. Identification of Tn10 insertions in the *dsbA* gene affecting *Escherichia coli* biofilm formation. *FEMS Microbiol Lett*, 173, 403-9.
- Gennaris, A., Ezraty, B., Henry, C., Agrebi, R., Vergnes, A., Oheix, E., Bos, J., Leverrier, P., Espinosa, L., Szewczyk, J., Vertommen, D., Iranzo, O., Collet, J. F. and Barras, F. 2015. Repairing oxidized proteins in the bacterial envelope using respiratory chain electrons. *Nature*, 528, 409-412.
- Gleiter, S. and Bardwell, J. C. 2008. Disulfide bond isomerization in prokaryotes. *Biochim Biophys Acta*, 1783, 530-4.
- Goldberger, R. F., Epstein, C. J. and Anfinsen, C. B. 1963. Acceleration of reactivation of reduced bovine pancreatic ribonuclease by a microsomal system from rat liver. *J Biol Chem*, 238, 628-35.



- Goosens, V. J., Mars, R. A., Akeroyd, M., Vente, A., Dreisbach, A., Denham, E. L., Kouwen, T. R., Van Rij, T., Olsthoorn, M. and Van Dijk, J. M. 2013. Is proteomics a reliable tool to probe the oxidative folding of bacterial membrane proteins? *Antioxidants & redox signaling*, 18, 1159-1164.
- Goulding, C. W., Apostol, M. I., Gleiter, S., Parseghian, A., Bardwell, J., Gennaro, M. and Eisenberg, D. 2004. Gram-positive DsbE proteins function differently from Gram-negative DsbE homologs. A structure to function analysis of DsbE from *Mycobacterium tuberculosis*. *J Biol Chem*, 279, 3516-24.
- Grimaud, R., Ezraty, B., Mitchell, J. K., Lafitte, D., Briand, C., Derrick, P. J. and Barras, F. 2001. Repair of oxidized proteins. Identification of a new methionine sulfoxide reductase. *J Biol Chem*, 276, 48915-20.
- Gross, E., Sevier, C. S., Heldman, N., Vitu, E., Bentzur, M., Kaiser, C. A., Thorpe, C. and Fass, D. 2006. Generating disulfides enzymatically: reaction products and electron acceptors of the endoplasmic reticulum thiol oxidase Ero1p. *Proc Natl Acad Sci U S A*, 103, 299-304.
- Gross, E. L., Leys, E. J., Gasparovich, S. R., Firestone, N. D., Schwartzbaum, J. A., Janies, D. A., Asnani, K. and Griffen, A. L. 2010. Bacterial 16S sequence analysis of severe caries in young permanent teeth. *J Clin Microbiol*, 48, 4121-8.
- Guilhot, C., Jander, G., Martin, N. L. and Beckwith, J. 1995. Evidence that the pathway of disulfide bond formation in *Escherichia coli* involves interactions between the cysteines of DsbB and DsbA. *Proc Natl Acad Sci U S A*, 92, 9895-9.
- Haase, E. M., Feng, X., Pan, J., Miecznikowski, J. C. and Scannapieco, F. A. 2015. Dynamics of the *Streptococcus gordonii* Transcriptome in Response to Medium, Salivary alpha-Amylase, and Starch. *Applied and Environmental Microbiology*, 81, 5363-5374.
- Han, H. and Wilson, A. C. 2013. The two CcdA proteins of *Bacillus anthracis* differentially affect virulence gene expression and sporulation. *Journal of Bacteriology*, 195, 5242-5249.
- Hatahet, F. and Ruddock, L. W. 2009. Protein disulfide isomerase: a critical evaluation of its function in disulfide bond formation. *Antioxid Redox Signal*, 11, 2807-50.
- Hendrickson, E. L., Wang, T., Dickinson, B. C., Whitmore, S. E., Wright, C. J., Lamont, R. J. and Hackett, M. 2012. Proteomics of *Streptococcus gordonii* within a model developing oral microbial community. *BMC Microbiol*, 12, 211.
- Heng, N. C., Tagg, J. R. and Tompkins, G. R. 2006. Identification and characterization of the loci encoding the competence-associated alternative sigma factor of *Streptococcus gordonii*. *FEMS Microbiol Lett*, 259, 27-34.
- Heng, N. C., Tagg, J. R. and Tompkins, G. R. 2007. Competence-dependent bacteriocin production by *Streptococcus gordonii* DL1 (Challis). *Journal of Bacteriology*, 189, 1468-1472.
- Heras, B., Edeling, M. A., Schirra, H. J., Raina, S. and Martin, J. L. 2004. Crystal structures of the DsbG disulfide isomerase reveal an unstable disulfide. *Proc Natl Acad Sci U S A*, 101, 8876-81.
- Heras, B., Kurz, M., Jarrott, R., Byriel, K. A., Jones, A., Thony-Meyer, L. and Martin, J. L. 2007. Expression and crystallization of DsbA from *Staphylococcus aureus*. *Acta Crystallogr Sect F Struct Biol Cryst Commun*, 63, 953-6.

- Heras, B., Kurz, M., Jarrott, R., Shouldice, S. R., Frei, P., Robin, G., Cemazar, M., Thony-Meyer, L., Glockshuber, R. and Martin, J. L. 2008. *Staphylococcus aureus* DsbA does not have a destabilizing disulfide. A new paradigm for bacterial oxidative folding. *The Journal of biological chemistry*, 283, 4261-4271.
- Heras, B., Shouldice, S. R., Totsika, M., Scanlon, M. J., Schembri, M. A. and Martin, J. L. 2009. DSB proteins and bacterial pathogenicity. *Nature reviews.Microbiology*, 7, 215-225.
- Hiniker, A. and Bardwell, J. C. 2004. *In vivo* substrate specificity of periplasmic disulfide oxidoreductases. *J Biol Chem*, 279, 12967-73.
- Hiniker, A., Collet, J. F. and Bardwell, J. C. 2005. Copper stress causes an *in vivo* requirement for the *Escherichia coli* disulfide isomerase DsbC. *J Biol Chem*, 280, 33785-91.
- Hodson, C. T., Lewin, A., Hederstedt, L. and Le Brun, N. E. 2008. The active-site cysteinyls and hydrophobic cavity residues of ResA are important for cytochrome *c* maturation in *Bacillus subtilis*. *J Bacteriol*, 190, 4697-705.
- Hudson, D. A. and Thorpe, C. 2015. Mia40 is a facile oxidant of unfolded reduced proteins but shows minimal isomerase activity. *Arch Biochem Biophys*, 579, 1-7.
- Inaba, K. and Ito, K. 2002. Paradoxical redox properties of DsbB and DsbA in the protein disulfide-introducing reaction cascade. *The EMBO journal*, 21, 2646-2654.
- Inaba, K., Murakami, S., Suzuki, M., Nakagawa, A., Yamashita, E., Okada, K. and Ito, K. 2006. Crystal structure of the DsbB-DsbA complex reveals a mechanism of disulfide bond generation. *Cell*, 127, 789-801.
- Itzek, A., Zheng, L., Chen, Z., Merritt, J. and Kreth, J. 2011. Hydrogen peroxide-dependent DNA release and transfer of antibiotic resistance genes in *Streptococcus gordonii*. *J Bacteriol*, 193, 6912-22.
- Jakubovics, N. S., Brittan, J. L., Dutton, L. C. and Jenkinson, H. F. 2009. Multiple adhesin proteins on the cell surface of *Streptococcus gordonii* are involved in adhesion to human fibronectin. *Microbiology*, 155, 3572-80.
- Jakubovics, N. S., Kerrigan, S. W., Nobbs, A. H., Stromberg, N., Van Dolleweerd, C. J., Cox, D. M., Kelly, C. G. and Jenkinson, H. F. 2005. Functions of cell surface-anchored antigen I/II family and Hsa polypeptides in interactions of *Streptococcus gordonii* with host receptors. *Infect Immun*, 73, 6629-38.
- Jakubovics, N. S., Smith, A. W. and Jenkinson, H. F. 2002. Oxidative stress tolerance is manganese (Mn(2+)) regulated in *Streptococcus gordonii*. *Microbiology*, 148, 3255-63.
- Jalal, N. A., Davey, L., Halperin, S. A. and Lee, S. F. 2019. Identification of redox partners of the thiol-disulfide oxidoreductase SdbA in *Streptococcus gordonii*. *J Bacteriol*.
- Jameson-Lee, M., Garduno, R. A. and Hoffman, P. S. 2011. DsbA2 (27 kDa Com1-like protein) of *Legionella pneumophila* catalyses extracytoplasmic disulphide-bond formation in proteins including the Dot/Icm type IV secretion system. *Mol Microbiol*, 80, 835-52.
- Joly, J. C. and Swartz, J. R. 1997. *In vitro* and *in vivo* redox states of the *Escherichia coli* periplasmic oxidoreductases DsbA and DsbC. *Biochemistry*, 36, 10067-72.

- Juillan-Binard, C., Picciocchi, A., Andrieu, J. P., Dupuy, J., Petit-Hartlein, I., Caux-Thang, C., Vives, C., Niviere, V. and Fieschi, F. 2017. A Two-component NADPH Oxidase (NOX)-like System in Bacteria Is Involved in the Electron Transfer Chain to the Methionine Sulfoxide Reductase MsrP. *J Biol Chem*, 292, 2485-2494.
- Juncker, A. S., Willenbrock, H., Von Heijne, G., Brunak, S., Nielsen, H. and Krogh, A. 2003. Prediction of lipoprotein signal peptides in Gram-negative bacteria. *Protein Sci*, 12, 1652-62.
- Kachur, A. V., Koch, C. J. and Biaglow, J. E. 1999. Mechanism of copper-catalyzed autoxidation of cysteine. *Free Radic Res*, 31, 23-34.
- Kadokura, H. and Beckwith, J. 2009. Detecting folding intermediates of a protein as it passes through the bacterial translocation channel. *Cell*, 138, 1164-73.
- Kadokura, H. and Beckwith, J. 2010. Mechanisms of oxidative protein folding in the bacterial cell envelope. *Antioxidants & redox signaling*, 13, 1231-1246.
- Kadokura, H., Katzen, F. and Beckwith, J. 2003. Protein disulfide bond formation in prokaryotes. *Annual Review of Biochemistry*, 72, 111-135.
- Kadokura, H., Nichols, L., 2nd and Beckwith, J. 2005. Mutational alterations of the key *cis* proline residue that cause accumulation of enzymatic reaction intermediates of DsbA, a member of the thioredoxin superfamily. *J Bacteriol*, 187, 1519-22.
- Kadokura, H., Tian, H., Zander, T., Bardwell, J. C. and Beckwith, J. 2004. Snapshots of DsbA in action: detection of proteins in the process of oxidative folding. *Science (New York, N.Y.)*, 303, 534-537.
- Kakinuma, Y. 1998. Inorganic cation transport and energy transduction in *Enterococcus hirae* and other streptococci. *Microbiol Mol Biol Rev*, 62, 1021-45.
- Kang, H. J., Paterson, N. G., Gaspar, A. H., Ton-That, H. and Baker, E. N. 2009. The *Corynebacterium diphtheriae* shaft pilin SpaA is built of tandem Ig-like modules with stabilizing isopeptide and disulfide bonds. *Proc Natl Acad Sci U S A*, 106, 16967-71.
- Katzen, F. and Beckwith, J. 2000. Transmembrane electron transfer by the membrane protein DsbD occurs via a disulfide bond cascade. *Cell*, 103, 769-79.
- Ke, N., Landeta, C., Wang, X., Boyd, D., Eser, M. and Beckwith, J. 2018. Identification of the Thioredoxin Partner of Vitamin K Epoxide Reductase in Mycobacterial Disulfide Bond Formation. *J Bacteriol*, 200.
- Kerrigan, S. W., Jakubovics, N. S., Keane, C., Maguire, P., Wynne, K., Jenkinson, H. F. and Cox, D. 2007. Role of *Streptococcus gordonii* surface proteins SspA/SspB and Hsa in platelet function. *Infect Immun*, 75, 5740-7.
- Kim, Y. K., Shin, Y. J., Lee, W. H., Kim, H. Y. and Hwang, K. Y. 2009. Structural and kinetic analysis of an MsrA-MsrB fusion protein from *Streptococcus pneumoniae*. *Mol Microbiol*, 72, 699-709.
- Kingsford, C. L., Ayanbule, K. and Salzberg, S. L. 2007. Rapid, accurate, computational discovery of Rho-independent transcription terminators illuminates their relationship to DNA uptake. *Genome Biol*, 8, R22.
- Kishigami, S., Akiyama, Y. and Ito, K. 1995a. Redox states of DsbA in the periplasm of *Escherichia coli*. *FEBS Lett*, 364, 55-8.

- Kishigami, S., Kanaya, E., Kikuchi, M. and Ito, K. 1995b. DsbA-DsbB interaction through their active site cysteines. Evidence from an odd cysteine mutant of DsbA. *J Biol Chem*, 270, 17072-4.
- Knight, J. B., Halperin, S. A., West, K. A. and Lee, S. F. 2008. Expression of a functional single-chain variable-fragment antibody against complement receptor 1 in *Streptococcus gordonii*. *Clinical and vaccine immunology : CVI*, 15, 925-931.
- Koch, J. R. and Schmid, F. X. 2014. Mia40 combines thiol oxidase and disulfide isomerase activity to efficiently catalyze oxidative folding in mitochondria. *J Mol Biol*, 426, 4087-4098.
- Kosuri, P., Alegre-Cebollada, J., Feng, J., Kaplan, A., Ingles-Prieto, A., Badilla, C. L., Stockwell, B. R., Sanchez-Ruiz, J. M., Holmgren, A. and Fernandez, J. M. 2012. Protein folding drives disulfide formation. *Cell*, 151, 794-806.
- Kouwen, T. R., Dubois, J. Y., Freudl, R., Quax, W. J. and Van Dijl, J. M. 2008. Modulation of thiol-disulfide oxidoreductases for increased production of disulfide-bond-containing proteins in *Bacillus subtilis*. *Appl Environ Microbiol*, 74, 7536-45.
- Kouwen, T. R., Van Der Goot, A., Dorenbos, R., Winter, T., Antelmann, H., Plaisier, M. C., Quax, W. J., Van Dijl, J. M. and Dubois, J. Y. 2007. Thiol-disulphide oxidoreductase modules in the low-GC Gram-positive bacteria. *Mol Microbiol*, 64, 984-99.
- Kouwen, T. R. and Van Dijl, J. M. 2009a. Applications of thiol-disulfide oxidoreductases for optimized in vivo production of functionally active proteins in *Bacillus*. *Appl Microbiol Biotechnol*, 85, 45-52.
- Kouwen, T. R. and Van Dijl, J. M. 2009b. Interchangeable modules in bacterial thiol-disulfide exchange pathways. *Trends Microbiol*, 17, 6-12.
- Kpadeh, Z. Z., Day, S. R., Mills, B. W. and Hoffman, P. S. 2015. *Legionella pneumophila* utilizes a single-player disulfide-bond oxidoreductase system to manage disulfide bond formation and isomerization. *Mol Microbiol*, 95, 1054-69.
- Kreth, J., Vu, H., Zhang, Y. and Herzberg, M. C. 2009. Characterization of hydrogen peroxide-induced DNA release by *Streptococcus sanguinis* and *Streptococcus gordonii*. *Journal of Bacteriology*, 191, 6281-6291.
- Kreth, J., Zhang, Y. and Herzberg, M. C. 2008. Streptococcal antagonism in oral biofilms: *Streptococcus sanguinis* and *Streptococcus gordonii* interference with *Streptococcus mutans*. *J Bacteriol*, 190, 4632-40.
- Krupp, R., Chan, C. and Missiakas, D. 2001. DsbD-catalyzed transport of electrons across the membrane of *Escherichia coli*. *J Biol Chem*, 276, 3696-701.
- Kumar, P., Sannigrahi, S., Scoullar, J., Kahler, C. M. and Tzeng, Y. L. 2011. Characterization of DsbD in *Neisseria meningitidis*. *Mol Microbiol*, 79, 1557-73.
- Kuramitsu, H. K., He, X., Lux, R., Anderson, M. H. and Shi, W. 2007. Interspecies interactions within oral microbial communities. *Microbiol Mol Biol Rev*, 71, 653-70.
- Laemmli, U. K. 1970. Cleavage of structural proteins during the assembly of the head of bacteriophage T4. *Nature*, 227, 680-5.

- Lafaye, C., Iwema, T., Carpentier, P., Jullian-Binard, C., Kroll, J. S., Collet, J. F. and Serre, L. 2009. Biochemical and structural study of the homologues of the thiol-disulfide oxidoreductase DsbA in *Neisseria meningitidis*. *J Mol Biol*, 392, 952-66.
- Landeta, C., Boyd, D. and Beckwith, J. 2018. Disulfide bond formation in prokaryotes. *Nat Microbiol*, 3, 270-280.
- Lappi, A. K. and Ruddock, L. W. 2011. Reexamination of the role of interplay between glutathione and protein disulfide isomerase. *J Mol Biol*, 409, 238-49.
- Le Brun, N. E., Bengtsson, J. and Hederstedt, L. 2000. Genes required for cytochrome *c* synthesis in *Bacillus subtilis*. *Mol Microbiol*, 36, 638-50.
- Lei, Y., Zhang, Y., Guenther, B. D., Kreth, J. and Herzberg, M. C. 2011. Mechanism of adhesion maintenance by methionine sulfoxide reductase in *Streptococcus gordonii*. *Mol Microbiol*, 80, 726-38.
- Lester, J., Kichler, S., Oickle, B., Fairweather, S., Oberc, A., Chahal, J., Ratnayake, D. and Creuzenet, C. 2015. Characterization of *Helicobacter pylori* HP0231 (DsbK): role in disulfide bond formation, redox homeostasis and production of *Helicobacter* cystein-rich protein HcpE. *Mol Microbiol*, 96, 110-33.
- Lewin, A., Crow, A., Hodson, C. T., Hederstedt, L. and Le Brun, N. E. 2008. Effects of substitutions in the CXXC active-site motif of the extracytoplasmic thioredoxin ResA. *Biochem J*, 414, 81-91.
- Lewin, A., Crow, A., Oubrie, A. and Le Brun, N. E. 2006. Molecular basis for specificity of the extracytoplasmic thioredoxin ResA. *J Biol Chem*, 281, 35467-77.
- Lin, D., Kim, B. and Slauch, J. M. 2009. DsbL and DsbI contribute to periplasmic disulfide bond formation in *Salmonella enterica* serovar Typhimurium. *Microbiology*, 155, 4014-24.
- Liu, X., Ramsey, M. M., Chen, X., Koley, D., Whiteley, M. and Bard, A. J. 2011. Real-time mapping of a hydrogen peroxide concentration profile across a polymicrobial bacterial biofilm using scanning electrochemical microscopy. *Proc Natl Acad Sci U S A*, 108, 2668-73.
- Liu, Y. and Burne, R. A. 2011. The major autolysin of *Streptococcus gordonii* is subject to complex regulation and modulates stress tolerance, biofilm formation, and extracellular-DNA release. *Journal of Bacteriology*, 193, 2826-2837.
- Liu, Y., Carlsson Moller, M., Petersen, L., Soderberg, C. A. and Hederstedt, L. 2010. Penicillin-binding protein SpoVD disulphide is a target for StoA in *Bacillus subtilis* forespores. *Mol Microbiol*, 75, 46-60.
- Loo, C. Y., Corliss, D. A. and Ganeshkumar, N. 2000. *Streptococcus gordonii* biofilm formation: identification of genes that code for biofilm phenotypes. *J Bacteriol*, 182, 1374-82.
- Lowther, W. T., Brot, N., Weissbach, H., Honek, J. F. and Matthews, B. W. 2000. Thiol-disulfide exchange is involved in the catalytic mechanism of peptide methionine sulfoxide reductase. *Proc Natl Acad Sci U S A*, 97, 6463-8.
- Lu, J. and Holmgren, A. 2014. The thioredoxin antioxidant system. *Free Radic Biol Med*, 66, 75-87.
- Lunsford, R. D. and London, J. 1996. Natural genetic transformation in *Streptococcus gordonii*: comX imparts spontaneous competence on strain wicky. *J Bacteriol*, 178, 5831-5.

- Luong, T. T., Reardon-Robinson, M. E., Siegel, S. D. and Ton-That, H. 2017. Reoxidation of the Thiol-Disulfide Oxidoreductase MdbA by a Bacterial Vitamin K Epoxide Reductase in the Biofilm-Forming Actinobacterium *Actinomyces oris*. *J Bacteriol*, 199.
- Lyles, M. M. and Gilbert, H. F. 1991. Catalysis of the oxidative folding of ribonuclease A by protein disulfide isomerase: pre-steady-state kinetics and the utilization of the oxidizing equivalents of the isomerase. *Biochemistry*, 30, 619-25.
- Mallick, P., Boutz, D. R., Eisenberg, D. and Yeates, T. O. 2002. Genomic evidence that the intracellular proteins of archaeal microbes contain disulfide bonds. *Proc Natl Acad Sci U S A*, 99, 9679-84.
- Martin, J. L., Bardwell, J. C. and Kuriyan, J. 1993. Crystal structure of the DsbA protein required for disulphide bond formation *in vivo*. *Nature*, 365, 464-8.
- Maskos, K., Huber-Wunderlich, M. and Glockshuber, R. 2003. DsbA and DsbC-catalyzed oxidative folding of proteins with complex disulfide bridge patterns *in vitro* and *in vivo*. *J Mol Biol*, 325, 495-513.
- Mccarthy, A. A., Haebel, P. W., Torronen, A., Rybin, V., Baker, E. N. and Metcalf, P. 2000. Crystal structure of the protein disulfide bond isomerase, DsbC, from *Escherichia coli*. *Nat Struct Biol*, 7, 196-9.
- Meima, R., Eschevins, C., Fillinger, S., Bolhuis, A., Hamoen, L. W., Dorenbos, R., Quax, W. J., Van Dijl, J. M., Provvedi, R., Chen, I., Dubnau, D. and Bron, S. 2002. The *bdbDC* operon of *Bacillus subtilis* encodes thiol-disulfide oxidoreductases required for competence development. *The Journal of biological chemistry*, 277, 6994-7001.
- Mesecke, N., Terziyska, N., Kozany, C., Baumann, F., Neupert, W., Hell, K. and Herrmann, J. M. 2005. A disulfide relay system in the intermembrane space of mitochondria that mediates protein import. *Cell*, 121, 1059-69.
- Mezghrani, A., Fassio, A., Benham, A., Simmen, T., Braakman, I. and Sitia, R. 2001. Manipulation of oxidative protein folding and PDI redox state in mammalian cells. *EMBO J*, 20, 6288-96.
- Miki, T., Okada, N. and Danbara, H. 2004. Two periplasmic disulfide oxidoreductases, DsbA and SrgA, target outer membrane protein SpiA, a component of the Salmonella pathogenicity island 2 type III secretion system. *J Biol Chem*, 279, 34631-42.
- Missiakas, D., Georgopoulos, C. and Raina, S. 1993. Identification and characterization of the *Escherichia coli* gene *dsbB*, whose product is involved in the formation of disulfide bonds *in vivo*. *Proc Natl Acad Sci U S A*, 90, 7084-8.
- Missiakas, D., Georgopoulos, C. and Raina, S. 1994. The *Escherichia coli dsbC* (*xprA*) gene encodes a periplasmic protein involved in disulfide bond formation. *EMBO J*, 13, 2013-20.
- Missiakas, D., Schwager, F. and Raina, S. 1995. Identification and characterization of a new disulfide isomerase-like protein (DsbD) in *Escherichia coli*. *The EMBO journal*, 14, 3415-3424.

- Moskovitz, J., Rahman, M. A., Strassman, J., Yancey, S. O., Kushner, S. R., Brot, N. and Weissbach, H. 1995. *Escherichia coli* peptide methionine sulfoxide reductase gene: regulation of expression and role in protecting against oxidative damage. *J Bacteriol*, 177, 502-7.
- Nelson, J. W. and Creighton, T. E. 1994. Reactivity and ionization of the active site cysteine residues of DsbA, a protein required for disulfide bond formation *in vivo*. *Biochemistry*, 33, 5974-83.
- Nielsen, H., Engelbrecht, J., Brunak, S. and Von Heijne, G. 1997. Identification of prokaryotic and eukaryotic signal peptides and prediction of their cleavage sites. *Protein Eng*, 10, 1-6.
- Nobbs, A. H., Shearer, B. H., Drobni, M., Jepson, M. A. and Jenkinson, H. F. 2007. Adherence and internalization of *Streptococcus gordonii* by epithelial cells involves beta1 integrin recognition by SspA and SspB (antigen I/II family) polypeptides. *Cell Microbiol*, 9, 65-83.
- Ohba, H., Harano, T. and Omura, T. 1977. Presence of two different types of protein-disulfide isomerase on cytoplasmic and luminal surfaces of endoplasmic reticulum of rat liver cells. *Biochem Biophys Res Commun*, 77, 830-6.
- Olry, A., Boschi-Muller, S., Marraud, M., Sanglier-Cianferani, S., Van Dorsselaar, A. and Branlant, G. 2002. Characterization of the methionine sulfoxide reductase activities of PILB, a probable virulence factor from *Neisseria meningitidis*. *J Biol Chem*, 277, 12016-22.
- Omasits, U., Ahrens, C. H., Muller, S. and Wollscheid, B. 2014. Protter: interactive protein feature visualization and integration with experimental proteomic data. *Bioinformatics (Oxford, England)*, 30, 884-886.
- Paxman, J. J., Borg, N. A., Horne, J., Thompson, P. E., Chin, Y., Sharma, P., Simpson, J. S., Wielens, J., Piek, S., Kahler, C. M., Sakellaris, H., Pearce, M., Bottomley, S. P., Rossjohn, J. and Scanlon, M. J. 2009. The structure of the bacterial oxidoreductase enzyme DsbA in complex with a peptide reveals a basis for substrate specificity in the catalytic cycle of DsbA enzymes. *The Journal of biological chemistry*, 284, 17835-17845.
- Peabody, M. A., Laird, M. R., Vlasschaert, C., Lo, R. and Brinkman, F. S. 2016. PSORTdb: expanding the bacteria and archaea protein subcellular localization database to better reflect diversity in cell envelope structures. *Nucleic Acids Res*, 44, D663-8.
- Perry, D. and Kuramitsu, H. K. 1981. Genetic transformation of *Streptococcus mutans*. *Infect Immun*, 32, 1295-7.
- Persson, K., Esberg, A., Claesson, R. and Stromberg, N. 2012. The pilin protein FimP from *Actinomyces oris*: crystal structure and sequence analyses. *PLoS One*, 7, e48364.
- Potamitou, A., Holmgren, A. and Vlamis-Gardikas, A. 2002. Protein levels of *Escherichia coli* thioredoxins and glutaredoxins and their relation to null mutants, growth phase, and function. *J Biol Chem*, 277, 18561-7.

- Premkumar, L., Heras, B., Duprez, W., Walden, P., Halili, M., Kurth, F., Fairlie, D. P. and Martin, J. L. 2013. Rv2969c, essential for optimal growth in *Mycobacterium tuberculosis*, is a DsbA-like enzyme that interacts with VKOR-derived peptides and has atypical features of DsbA-like disulfide oxidases. *Acta Crystallogr D Biol Crystallogr*, 69, 1981-94.
- Quinternet, M., Tsan, P., Selme-Roussel, L., Jacob, C., Boschi-Muller, S., Branlant, G. and Cung, M. T. 2009. Formation of the complex between DsbD and PilB N-terminal domains from *Neisseria meningitidis* necessitates an adaptability of nDsbD. *Structure*, 17, 1024-33.
- Reardon-Robinson, M. E., Osipiuk, J., Chang, C., Wu, C., Jooya, N., Joachimiak, A., Das, A. and Ton-That, H. 2015a. A Disulfide Bond-forming Machine Is Linked to the Sortase-mediated Pilus Assembly Pathway in the Gram-positive Bacterium *Actinomyces oris*. *The Journal of biological chemistry*, 290, 21393-21405.
- Reardon-Robinson, M. E., Osipiuk, J., Jooya, N., Chang, C., Joachimiak, A., Das, A. and Ton-That, H. 2015b. A thiol-disulfide oxidoreductase of the Gram-positive pathogen *Corynebacterium diphtheriae* is essential for viability, pilus assembly, toxin production and virulence. *Molecular microbiology*.
- Reardon-Robinson, M. E. and Ton-That, H. 2015. Disulfide-Bond-Forming Pathways in Gram-Positive Bacteria. *J Bacteriol*, 198, 746-54.
- Reese, M. G. 2001. Application of a time-delay neural network to promoter annotation in the *Drosophila melanogaster* genome. *Comput Chem*, 26, 51-6.
- Reid, E., Cole, J. and Eaves, D. J. 2001. The *Escherichia coli* CcmG protein fulfils a specific role in cytochrome *c* assembly. *Biochem J*, 355, 51-8.
- Ren, G., Stephan, D., Xu, Z., Zheng, Y., Tang, D., Harrison, R. S., Kurz, M., Jarrott, R., Shouldice, S. R., Hiniker, A., Martin, J. L., Heras, B. and Bardwell, J. C. 2009. Properties of the thioredoxin fold superfamily are modulated by a single amino acid residue. *J Biol Chem*, 284, 10150-9.
- Rietsch, A. and Beckwith, J. 1998. The genetics of disulfide bond metabolism. *Annu Rev Genet*, 32, 163-84.
- Rietsch, A., Belin, D., Martin, N. and Beckwith, J. 1996. An *in vivo* pathway for disulfide bond isomerization in *Escherichia coli*. *Proceedings of the National Academy of Sciences of the United States of America*, 93, 13048-13053.
- Rietsch, A., Bessette, P., Georgiou, G. and Beckwith, J. 1997. Reduction of the periplasmic disulfide bond isomerase, DsbC, occurs by passage of electrons from cytoplasmic thioredoxin. *J Bacteriol*, 179, 6602-8.
- Rissler, M., Wiedemann, N., Pfannschmidt, S., Gabriel, K., Guiard, B., Pfanner, N. and Chacinska, A. 2005. The essential mitochondrial protein Erv1 cooperates with Mia40 in biogenesis of intermembrane space proteins. *J Mol Biol*, 353, 485-92.
- Ritz, D., Patel, H., Doan, B., Zheng, M., Aslund, F., Storz, G. and Beckwith, J. 2000. Thioredoxin 2 is involved in the oxidative stress response in *Escherichia coli*. *J Biol Chem*, 275, 2505-12.
- Rogers, J. D., Palmer, R. J., Jr., Kolenbrander, P. E. and Scannapieco, F. A. 2001. Role of *Streptococcus gordonii* amylase-binding protein A in adhesion to hydroxyapatite, starch metabolism, and biofilm formation. *Infect Immun*, 69, 7046-56.



- Rutkevich, L. A. and Williams, D. B. 2012. Vitamin K epoxide reductase contributes to protein disulfide formation and redox homeostasis within the endoplasmic reticulum. *Mol Biol Cell*, 23, 2017-27.
- Saleh, M., Bartual, S. G., Abdullah, M. R., Jensch, I., Asmat, T. M., Petruschka, L., Pribyl, T., Gellert, M., Lillig, C. H., Antelmann, H., Hermoso, J. A. and Hammerschmidt, S. 2013. Molecular architecture of *Streptococcus pneumoniae* surface thioredoxin-fold lipoproteins crucial for extracellular oxidative stress resistance and maintenance of virulence. *EMBO molecular medicine*, 5, 1852-1870.
- Sambrook, J., Maniatis, T. and Fritsch, E. F. 1989. *Molecular cloning: A laboratory manual*. (2ed ed.). New York, NY, Cold Spring Harbor Laboratory Press.
- Sanchez, B. C., Chang, C., Wu, C., Tran, B. and Ton-That, H. 2017. Electron Transport Chain Is Biochemically Linked to Pilus Assembly Required for Polymicrobial Interactions and Biofilm Formation in the Gram-Positive Actinobacterium *Actinomyces oris*. *MBio*, 8.
- Schiavo, G., Papini, E., Genna, G. and Montecucco, C. 1990. An intact interchain disulfide bond is required for the neurotoxicity of tetanus toxin. *Infect Immun*, 58, 4136-41.
- Schiott, T. and Hederstedt, L. 2000. Efficient spore synthesis in *Bacillus subtilis* depends on the CcdA protein. *Journal of Bacteriology*, 182, 2845-2854.
- Schiott, T., Throne-Holst, M. and Hederstedt, L. 1997a. *Bacillus subtilis* CcdA-defective mutants are blocked in a late step of cytochrome *c* biogenesis. *J Bacteriol*, 179, 4523-9.
- Schiott, T., Von Wachenfeldt, C. and Hederstedt, L. 1997b. Identification and characterization of the *ccdA* gene, required for cytochrome *c* synthesis in *Bacillus subtilis*. *Journal of Bacteriology*, 179, 1962-1973.
- Schirra, H. J., Renner, C., Czisch, M., Huber-Wunderlich, M., Holak, T. A. and Glockshuber, R. 1998. Structure of reduced DsbA from *Escherichia coli* in solution. *Biochemistry*, 37, 6263-76.
- Schneider, C. A., Rasband, W. S. and Eliceiri, K. W. 2012. NIH Image to ImageJ: 25 years of image analysis. *Nat Methods*, 9, 671-5.
- Sengupta, R. and Holmgren, A. 2014. Thioredoxin and glutaredoxin-mediated redox regulation of ribonucleotide reductase. *World J Biol Chem*, 5, 68-74.
- Shevchik, V. E., Condemine, G. and Robert-Baudouy, J. 1994. Characterization of DsbC, a periplasmic protein of *Erwinia chrysanthemi* and *Escherichia coli* with disulfide isomerase activity. *EMBO J*, 13, 2007-12.
- Shouldice, S. R., Cho, S. H., Boyd, D., Heras, B., Eser, M., Beckwith, J., Riggs, P., Martin, J. L. and Berkmen, M. 2010. *In vivo* oxidative protein folding can be facilitated by oxidation-reduction cycling. *Mol Microbiol*, 75, 13-28.
- Si, M., Feng, Y., Chen, K., Kang, Y., Chen, C., Wang, Y. and Shen, X. 2017. Functional comparison of methionine sulphoxide reductase A and B in *Corynebacterium glutamicum*. *J Gen Appl Microbiol*, 63, 280-286.

- Si, M., Zhang, L., Chaudhry, M. T., Ding, W., Xu, Y., Chen, C., Akbar, A., Shen, X. and Liu, S. J. 2015. *Corynebacterium glutamicum* methionine sulfoxide reductase A uses both mycoredoxin and thioredoxin for regeneration and oxidative stress resistance. *Appl Environ Microbiol*, 81, 2781-96.
- Sievers, F., Wilm, A., Dineen, D., Gibson, T. J., Karplus, K., Li, W., Lopez, R., McWilliam, H., Remmert, M., Soding, J., Thompson, J. D. and Higgins, D. G. 2011. Fast, scalable generation of high-quality protein multiple sequence alignments using Clustal Omega. *Molecular systems biology*, 7, 539.
- Simpson, L. L., Maksymowych, A. B., Park, J. B. and Bora, R. S. 2004. The role of the interchain disulfide bond in governing the pharmacological actions of botulinum toxin. *J Pharmacol Exp Ther*, 308, 857-64.
- Sinha, S., Ambur, O. H., Langford, P. R., Tonjum, T. and Kroll, J. S. 2008. Reduced DNA binding and uptake in the absence of DsbA1 and DsbA2 of *Neisseria meningitidis* due to inefficient folding of the outer-membrane secretin PilQ. *Microbiology*, 154, 217-25.
- Smith, R. P., Paxman, J. J., Scanlon, M. J. and Heras, B. 2016. Targeting Bacterial Dsb Proteins for the Development of Anti-Virulence Agents. *Molecules*, 21.
- Sone, M., Akiyama, Y. and Ito, K. 1997. Differential *in vivo* roles played by DsbA and DsbC in the formation of protein disulfide bonds. *J Biol Chem*, 272, 10349-52.
- Sonnhammer, E. L., Von Heijne, G. and Krogh, A. 1998. A hidden Markov model for predicting transmembrane helices in protein sequences. *Proc Int Conf Intell Syst Mol Biol*, 6, 175-82.
- Stewart, E. J., Katzen, F. and Beckwith, J. 1999. Six conserved cysteines of the membrane protein DsbD are required for the transfer of electrons from the cytoplasm to the periplasm of *Escherichia coli*. *EMBO J*, 18, 5963-71.
- Stirnemann, C. U., Rozhkova, A., Grauschopf, U., Grutter, M. G., Glockshuber, R. and Capitani, G. 2005. Structural basis and kinetics of DsbD-dependent cytochrome *c* maturation. *Structure*, 13, 985-93.
- Stogios, P. and Savchenko, A. 2015. Crystal structure of SdbA. Unpublished.
- Tanaka, R., Araki, Y., Mizukami, M., Miyauchi, A., Ishibashi, M., Tokunaga, H. and Tokunaga, M. 2004. Expression and purification of the *Bacillus subtilis* thioredoxin superfamily protein YkvV. *Biosci Biotechnol Biochem*, 68, 1801-4.
- Throne-Holst, M., Thony-Meyer, L. and Hederstedt, L. 1997. *Escherichia coli ccm* in-frame deletion mutants can produce periplasmic cytochrome *b* but not cytochrome *c*. *FEBS Lett*, 410, 351-5.
- Tinsley, C. R., Voulhoux, R., Beretti, J. L., Tommassen, J. and Nassif, X. 2004. Three homologues, including two membrane-bound proteins, of the disulfide oxidoreductase DsbA in *Neisseria meningitidis*: effects on bacterial growth and biogenesis of functional type IV pili. *J Biol Chem*, 279, 27078-87.
- Tompkins, G. R., Peavey, M. A., Birchmeier, K. R. and Tagg, J. R. 1997. Bacteriocin production and sensitivity among coaggregating and noncoaggregating oral streptococci. *Oral Microbiol Immunol*, 12, 98-105.
- Tossounian, M. A., Pedre, B., Wahni, K., Erdogan, H., Vertommen, D., Van Molle, I. and Messens, J. 2015. *Corynebacterium diphtheriae* methionine sulfoxide reductase a exploits a unique mycothiol redox relay mechanism. *J Biol Chem*, 290, 11365-75.

- Um, S. H., Kim, J. S., Lee, K. and Ha, N. C. 2014. Structure of a DsbF homologue from *Corynebacterium diphtheriae*. *Acta Crystallogr F Struct Biol Commun*, 70, 1167-72.
- Um, S. H., Kim, J. S., Song, S., Kim, N. A., Jeong, S. H. and Ha, N. C. 2015. Crystal Structure of DsbA from *Corynebacterium diphtheriae* and Its Functional Implications for CueP in Gram-Positive Bacteria. *Molecules and cells*, 38, 715-722.
- Urano, H., Umezawa, Y., Yamamoto, K., Ishihama, A. and Ogasawara, H. 2015. Cooperative regulation of the common target genes between H(2)O(2)-sensing YedVW and Cu(2)(+)-sensing CusSR in *Escherichia coli*. *Microbiology*, 161, 729-38.
- Van Der Kooi-Pol, M. M., Reilman, E., Sibbald, M. J., Veenstra-Kyuchukova, Y. K., Kouwen, T. R., Buist, G. and Van Dijl, J. M. 2012. Requirement of signal peptidase ComC and thiol-disulfide oxidoreductase DsbA for optimal cell surface display of pseudopilin ComGC in *Staphylococcus aureus*. *Applied and Environmental Microbiology*, 78, 7124-7127.
- Vats, N. and Lee, S. F. 2001. Characterization of a copper-transport operon, copYAZ, from *Streptococcus mutans*. *Microbiology (Reading, England)*, 147, 653-662.
- Vickerman, M. M., Iobst, S., Jesionowski, A. M. and Gill, S. R. 2007. Genome-wide transcriptional changes in *Streptococcus gordonii* in response to competence signaling peptide. *J Bacteriol*, 189, 7799-807.
- Vriesema, A. J., Dankert, J. and Zaat, S. A. 2000. A shift from oral to blood pH is a stimulus for adaptive gene expression of *Streptococcus gordonii* CH1 and induces protection against oxidative stress and enhanced bacterial growth by expression of *msrA*. *Infect Immun*, 68, 1061-8.
- Walker, K. W. and Gilbert, H. F. 1997. Scanning and escape during protein-disulfide isomerase-assisted protein folding. *J Biol Chem*, 272, 8845-8.
- Walker, K. W., Lyles, M. M. and Gilbert, H. F. 1996. Catalysis of oxidative protein folding by mutants of protein disulfide isomerase with a single active-site cysteine. *Biochemistry*, 35, 1972-80.
- Wang, L., Li, J., Wang, X., Liu, W., Zhang, X. C., Li, X. and Rao, Z. 2013. Structure analysis of the extracellular domain reveals disulfide bond forming-protein properties of *Mycobacterium tuberculosis* Rv2969c. *Protein Cell*, 4, 628-40.
- Wang, L., Zhang, L., Niu, Y., Sitia, R. and Wang, C. C. 2014. Glutathione peroxidase 7 utilizes hydrogen peroxide generated by Ero1alpha to promote oxidative protein folding. *Antioxid Redox Signal*, 20, 545-56.
- Wang, X., Dutton, R. J., Beckwith, J. and Boyd, D. 2011. Membrane topology and mutational analysis of *Mycobacterium tuberculosis* VKOR, a protein involved in disulfide bond formation and a homologue of human vitamin K epoxide reductase. *Antioxid Redox Signal*, 14, 1413-20.
- Williamson, J. A., Cho, S. H., Ye, J., Collet, J. F., Beckwith, J. R. and Chou, J. J. 2015. Structure and multistate function of the transmembrane electron transporter CcdA. *Nature structural & molecular biology*, 22, 809-814.
- Winther, J. R. and Thorpe, C. 2014. Quantification of thiols and disulfides. *Biochim Biophys Acta*, 1840, 838-46.

- Wizemann, T. M., Moskovitz, J., Pearce, B. J., Cundell, D., Arvidson, C. G., So, M., Weissbach, H., Brot, N. and Masure, H. R. 1996. Peptide methionine sulfoxide reductase contributes to the maintenance of adhesins in three major pathogens. *Proc Natl Acad Sci U S A*, 93, 7985-90.
- Xu, Y. and Kreth, J. 2013. Role of LytF and AtlS in eDNA release by *Streptococcus gordonii*. *PloS one*, 8, e62339.
- Zapun, A., Cooper, L. and Creighton, T. E. 1994. Replacement of the active-site cysteine residues of DsbA, a protein required for disulfide bond formation *in vivo*. *Biochemistry*, 33, 1907-14.
- Zapun, A., Missiakas, D., Raina, S. and Creighton, T. E. 1995. Structural and functional characterization of DsbC, a protein involved in disulfide bond formation in *Escherichia coli*. *Biochemistry*, 34, 5075-5089.
- Zheng, L., Itzek, A., Chen, Z. and Kreth, J. 2011. Environmental influences on competitive hydrogen peroxide production in *Streptococcus gordonii*. *Appl Environ Microbiol*, 77, 4318-28.
- Zhong, Y., Anderl, F., Kruse, T., Schindele, F., Jagusztyn-Krynicka, E. K., Fischer, W., Gerhard, M. and Mejias-Luque, R. 2016. *Helicobacter pylori* HP0231 Influences Bacterial Virulence and Is Essential for Gastric Colonization. *PLoS One*, 11, e0154643.
- Zhou, J. Y., Dann, G. P., Shi, T., Wang, L., Gao, X., Su, D., Nicora, C. D., Shukla, A. K., Moore, R. J., Liu, T., Camp, D. G., 2nd, Smith, R. D. and Qian, W. J. 2012. Simple sodium dodecyl sulfate-assisted sample preparation method for LC-MS-based proteomics applications. *Anal Chem*, 84, 2862-7.
- Zhou, Y. and Bushweller, J. H. 2018. Solution structure and elevator mechanism of the membrane electron transporter CcdA. *Nat Struct Mol Biol*, 25, 163-169.
- Zhou, Y., Cierpicki, T., Jimenez, R. H., Lukasik, S. M., Ellena, J. F., Cafiso, D. S., Kadokura, H., Beckwith, J. and Bushweller, J. H. 2008. NMR solution structure of the integral membrane enzyme DsbB: functional insights into DsbB-catalyzed disulfide bond formation. *Mol Cell*, 31, 896-908.
- Zhu, L. and Kreth, J. 2012. The role of hydrogen peroxide in environmental adaptation of oral microbial communities. *Oxid Med Cell Longev*, 2012, 717843.
- Zito, E., Melo, E. P., Yang, Y., Wahlander, A., Neubert, T. A. and Ron, D. 2010. Oxidative protein folding by an endoplasmic reticulum-localized peroxiredoxin. *Mol Cell*, 40, 787-97.

## Appendix: Copyright Release for Published Material



RightsLink®

Home

Account Info

Help



AMERICAN  
SOCIETY FOR  
MICROBIOLOGY

**Title:** Identification of Redox Partners of the Thiol-Disulfide Oxidoreductase SdbA in *Streptococcus gordonii*

**Author:** Naif A. Jalal, Lauren Davey, Scott A. Halperin, Song F. Lee

**Publication:** Journal of Bacteriology

**Publisher:** American Society for Microbiology

**Date:** Apr 24, 2019

Copyright © 2019, American Society for Microbiology

Logged in as:

Naif Jalal

LOGOUT

### Permissions Request

Authors in ASM journals retain the right to republish discrete portions of his/her article in any other publication (including print, CD-ROM, and other electronic formats) of which he or she is author or editor, provided that proper credit is given to the original ASM publication. ASM authors also retain the right to reuse the full article in his/her dissertation or thesis. For a full list of author rights, please see: [http://journals.asm.org/site/misc/ASM\\_Author\\_Statement.xhtml](http://journals.asm.org/site/misc/ASM_Author_Statement.xhtml)

BACK

CLOSE WINDOW

Copyright © 2019 Copyright Clearance Center, Inc. All Rights Reserved. [Privacy statement](#). [Terms and Conditions](#).  
Comments? We would like to hear from you. E-mail us at [customercare@copyright.com](mailto:customercare@copyright.com)